OPTIMIZED ACCUMULATION OF ALGAL LIPIDS FOR BIO-JET FUEL PRODUCTION

by

Emren Borhan

B.Sc. in Molecular Biology and Genetics, Boğaziçi University, 2018

Submitted to the Institute of Environmental Sciences

in partial fulfillment of the requirements for the degree of

Master of Science

in

Environmental Sciences

Boğaziçi University

2022

ACKNOWLEDGEMENTS

As with all unique stories, the journey means nothing without those who accompanied it on the way. I would like to express my sincere thanks to my thesis advisor Assist. Prof. Dr. Berat Zeki Haznedaroğlu, who has always been a guiding light in my academic journey. It was his endurance to show us how to overcome the challenges despite all the difficulties, not how to watch them. In these difficult days, sustaining a place where we can do science with such opportunities requires a great love and dedication to science. I am grateful to Assoc. Prof. Dr. Ulaş Tezel for everything he showed me, including being the living proof that my passion for music can continue alongside academia. I would like to thank the jury members of my thesis, Prof. Dr. Bahar İnce and Assoc. Prof. Dr. Alper Uzun, for their valuable insights.

There is no word to describe the value of Prof. Dr. M. Levent Kurnaz and Gülin Yücel's support for me, who advised me to use the means at my disposal to make the world a better place and introduced the principles of sustainability, when even I did not know what I wanted to do.

I am proud to be a member of the IMBIYOTAB family. I need to write more theses to fully explain what each of them have contributed to me. I am deeply grateful to our post-doctoral researchers Dr. Engin Bayram and Dr. İrem Karamollaoğlu for their unwavering support. I want to thank my friends F. Koray Sakarya, Dila Hocaoğlu, Duygu Özçelik, Arca Yılmaz, Zeynep Şahin, Tuna Sürmeli and Aslıhan Yesir who worked with me in the lab and shared with me in the mind. I would like to thank Elifcan Çalışkan, Sevda Avcı, Derya Gelgör, Gizem Çetin and Begüm Erdinçler who gave meaning to my journey in the lab and always supported me. I would like to remember and thank all my intern friends who contributed to the study. Everyone on this team has a special place in me.

This study was partially funded by The Scientific and Technological Research Council of Turkey (TÜBİTAK), 1003 Primary Subjects R&D Funding Program (Award No: 218M857), The Ministry of Industry and Technology & Directorate General for EU and Foreign Affairs Department of EU Financial Programmes, Competitiveness and Innovation Sector Operational Programme (Award ID: EuropeAid/140111/IH/SUP/TR).

Special thanks to my family, Işın Borhan and Muzaffer Borhan, who always make me feel that they are by my side and support me no matter what. If I manage to continue on these paths, it is thanks to their limitless love.

I would like to thank all my friends for their patience during the thesis.

I want to give the most precious thanks to my dear Yağmur Ersoy. She is the one who gives warm serenity to my heart and soul, lifts me up and gives me immense strength in my darkest hours.

ABSTRACT

OPTIMIZED ACCUMULATION OF ALGAL LIPIDS FOR BIO-JET FUEL PRODUCTION

Civil aviation sector faces the enormous challenge of becoming carbon neutral by 2050, while the sector is rapidly growing despite the drawbacks of COVID-19. The sector aims to reduce its carbon emissions and encourages sustainable aviation fuels. Microalgae stands out as a third-generation biobased feedstock for an alternative sustainable jet-fuel production as microalgae cultivation does not need arable area, produce respectable amounts of biomass in limited time periods and does not compete with other food and energy crops. In this study, three different oleaginous green microalgae species were cultivated under 23 different conditions, and their biomass, lipid, and fatty acid methyl ester (FAME) productivities were evaluated to optimize microalgal lipids suitable for bio-jet fuel. Changes in biomass and lipid contents were observed by applying nitrogen deprivation in different culture media. *Nannochloropsis gaditana* grown in Algal medium and *Ettlia oleoabundans* in MB3N medium were scaled-up to 15000L cultures under nitrogen-replete conditions to observe the changes in biomass and lipid content in outdoor open ponds respectively. *N. gaditana* reached the highest biomass (1.53 g/L) and lipid productivity (0.72 g/L) in Algal medium. *Nannochloropsis sp.* had the highest FAME productivity (363.2 mg/L), transesterifiable lipid percentage (67.7% of lipid dry weight) and FAME percentage in biomass (35.1% of dried biomass) in f/2 medium under nitrogen deprivation. Lipid extraction efficiency and FAME profile changes of different pretreatment and cell disruption methods were compared. *N. gaditana* in Algal medium produced eicosapentaenoic acid equivalent to 2.86% dry weight, considered as a biorefinery side product.

ÖZET

BİYO-JET YAKIT ÜRETİMİ İÇİN OPTİMİZE MİKROYOSUN YAĞI ÜRETİMİ

Sivil havacılık sektörü, 2050'de karbon nötr olma hedefi ile zorlu bir imtihan içerisindeyken, COVID-19 etkisinin dezavantajlarını arkasında bırakarak hızla büyümeye devam etmektedir. Sektör karbon emisyonları düşürmek istemekte ve sürdürülebilir havacılık yakıtlarını teşvik etmektedir. Mikroyosunlar, sürdürülebilir jet yakıtı üretimi için üçüncü nesil organik hammadde stoku olarak alternatifleri arasında tarım arazisine ihtiyaç duymama, kısa sürede dikkate değer miktarda biyokütle üretme ve gıda mahsulleriyle rekabet etmemesiyle öne çıkmaktadır. Bu çalışmada, 3 farklı yağlı yeşil mikroyosun türü 23 farklı koşulda yetiştirilmiş ve biyo-jet yakıtı dönüşümüne uygun lipitlerin optimizasyonu için tüm koşulların biyokütle, lipit ve yağ asidi metil ester (FAME) üretkenlikleri değerlendirilmiştir. Küçük ölçekte farklı besiyerlerinde azot yoksunluğu uygulanarak biyokütle ve lipit içeriğindeki değişiklikler gözlemlenmiştir. Algal besiyerindeki *Nannochloropsis gaditana* ve MB3N besiyerindeki *Ettlia oleoabundans* türlerinin yetiştirilme ölçeği azot yeterli koşullar altında 15000L açık havuzlarda büyütülecek kadar arttırılmış ve tüm evrelerdeki biyokütle ve lipit içeriğindeki değişimler gözlemlenmiştir. Algal besiyerinde büyütülen *N. gaditana* en fazla biyokütle (1,53 g/L) ve lipit üretkenliğine (0,72 g/L) ulaşmıştır. f/2 besiyerinde azot yoksunluğun büyütülen Nannochloropsis sp., en yüksek FAME üretkenliğine (363.2 mg/L), transesterlenebilir lipit yüzdesine (lipit kuru ağırlığının %67.7'si) ve biyokütledeki FAME konsantrasyonuna (kurutulmuş biyokütlenin %35.1'i) ulaşmıştır. Farklı PBR tasarımlarında aynı kültivasyon hacminde yetiştirilen mikroyosunlar arasındaki farklılıklardan bahsedilmiştir. Farklı ön muamele ve hücre parçalama yöntemlerinin lipit ekstraksiyon verimliliği ve FAME profil değişiklikleri karşılaştırılmıştır. Algal besiyerinde büyütülen *N. gaditana*, biyorafineri yan ürünü olarak kabul edilen kuru ağırlığının %2.86'sına eşdeğer eikosapentaenoik asit üretmiştir.

TABLE OF CONTENTS

LIST OF FIGURES

LIST OF TABLES

LIST OF SYMBOLS/ABBREVIATIONS

Symbol	**Explanation**
%	Percent
%DW	Percentage Dry Weight
°C	Degrees Celsius
µM	Micromolar
µm	Micrometer

Abbreviations	**Explanation**
ACCase	Acetyl-CoA Carboxylase
ACS	Acetyl-CoA Synthetase
APR	Aqueous Phase Reforming
ASTM	American Society for Testing and Materials
ATJ	Alcohol to Jet
ATP	Adenosine Triphosphate
C15:0	Pentadocanoic Acid
CAAFI	Commercial Aviation Alternative Fuels Initiative
cc/g	Cubic Centimeter/Gram
cm	Centimeter
COVID-19	Coronavirus Disease of 2019
DC	Direct Current
DCM	Dichloromethane
DGAT	Diacylglycerol Acyltransferase
DHA	Docosahexaenoic Acid
DME	Dimethyl Ether
DNA	Deoxyribonucleic Acid
DSHC	Direct Sugar to Hydrocarbons
E. oleoabundans	*Ettlia oleoabundans*
EDTA	Ethylenediamine Tetraacetic Acid
EPA	Eicosapentaenoic Acid
etc.	Et Cetera
FA	Fatty Acid
FAME	Fatty Acid Methyl Ester

FAS	Fatty Acid Synthetase
FRL	Fuel Readiness Level
FT	Fischer – Tropsch
FT-SPK	Fischer-Tropsch- Synthetic Paraffinic Kerosene
g	Gram
g	Standard gravity
GC	Gas Chromatography
GC/MS	Gas Chromatography Mass Spectrometry
GC-FID	Gas Chromatography with Flame Ionization Detector
GDP	Gross Domestic Product
GHG	Greenhouse Gas
HDCJ	Hydrotreated Depolymerized Cellulosic Jet
HEFA	Hydroprocessed Esters and Fatty Acids
HPH	High Pressure Homogenizer
h	Hour
HTL	Hydrothermal Liquefaction
IATA	International Air Transport Association
İMBİYOTAB	İstanbul Microalgae Biotechnologies Research and Development Center
kHz	Kilohertz
L	Liter
LCA	Life Cycle Assessment
LED	Light-emitting Diode
M&M	Mann&Myers
max	Maximum
MB3N	Modified Bold 3N
mg	Milligram
min	Minute
min	Minimum
MJ	Megajoule
mL	Milliliter
mM	Millimolar
MTBE	Methyl-butyl ether
MUFA	Monounsaturated Fatty Acid
MVA	Mevalonate

N-	Nitrate Deplete
N. gaditana	*Nannochloropsis gaditana*
N+	Nitrate Replete
nm	Nanometer
OD_{680}	Optical Density at 680 Nanometer Wavelength
PBR	Photobioreactor
PEF	Pulsed Electric Field
PP	Polypropylene
ppt	Parts Per Thousand
PUFA	Polyunsaturated Fatty Acids
RNA	Ribonucleic Acid
rpm	Revolutions per Minute
s	Second
SAF	Sustainable Aviation Fuel
SCF	Supercritical Fluid Extraction
SDBS	Surfactants like Dodecyl Benzene Sulfonate
sec	Second
SIP	Iso-paraffinic
SPK	Synthetic Paraffinic Kerosene
TAG	Triacylglyceride
TÜİK	Türkiye İstatistik Kurumu
UFA	Unsaturated Fatty Acid
UPH_2O	Ultra-Pure Water
UV	Ultraviolet
v/v	Volume to Volume
w/w	Weight to Weight

1. INTRODUCTION

1.1. Latest Trends in Global Climate Change and Carbon Footprint

With the Great Acceleration starting from the 1950s, a simultaneous increase in all human activities and the amount of energy needed for human civilization's economic activities has risen astronomically (Figure 1.1). The increasing demand for fossil energy sources, seen as cheap, easily available, and reliable baseload suppliers for long periods of time, has accelerated the greenhouse gas (GHG) concentration in the world's atmosphere (Neagu and Teodoru, 2019). Fossil energy usage corresponds to 83.2% (Oil: 31.2%; Coal: 27.2; Natural Gas: 24.7%) of all primary energy demand in 2020 (BP Statistical Review of World Energy, 2021). As anthropogenic activities increased primary energy demand 5.67 times compared to the 1950s, carbon dioxide concentration in Earth's atmosphere has increased by 30% in the last 60 years (Figure 1.1).

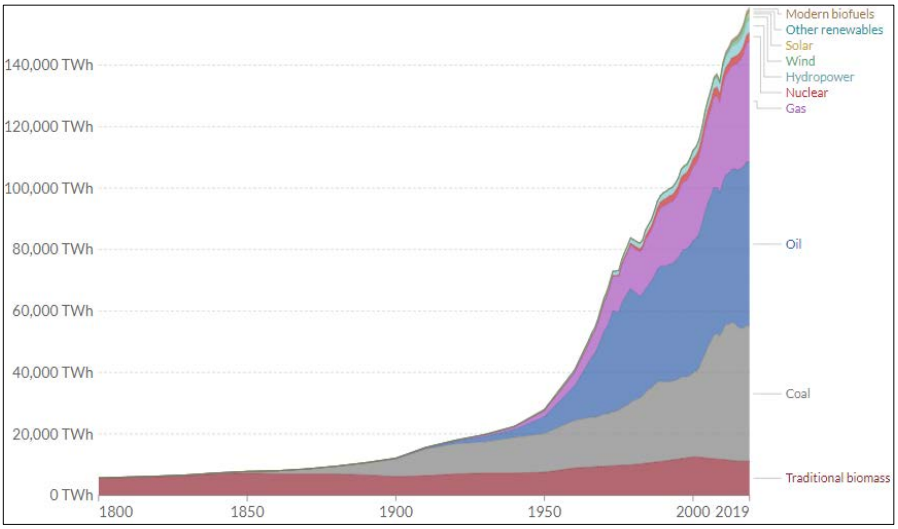

Figure 1.1. Global primary energy consumption from 1800 to 2019 (BP Statistical Review of World Energy, 2020).

Despite the suppressive effect of COVID-19 pandemic, global fossil-induced carbon emissions in 2021 was 36.4 billion tons, which is 0.8% behind the pre-COVID industry peak (36.7-billion-ton CO_2-equivalent) (Quéré et al., 2020; Figure 1.3), and it is expected to be increased in 2022. With increasing concentrations of greenhouse gases, such as methane, nitrous oxide, fluorinated gases etc., the average global temperature has so far increased by 0.87±0.12°C compared to the pre-industrial (1850-1900) average (IPCC, 2018). If the increase in GHG emissions continues as "business-as-usual", average global temperature increase of 1.5°C is expected by 2040 (IPCC,2018). In accordance

with the Paris Agreement (2015), which was ratified by 196 countries among which Turkey recently rejoined, all countries have pledged to tackle climate change and to reduce their greenhouse gas emissions.

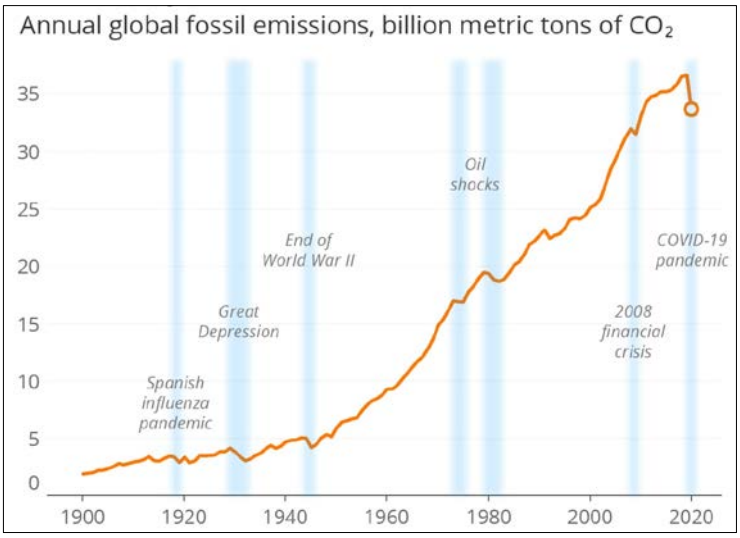

Figure 1.2. Global carbon footprint from 1900's to 2020 (Global Carbon Project, 2021).

Thanks to awareness-raising campaigns which also apply economic incentives to GHG emission reduction, such as the European Green Deal, industries have initiated concrete steps to decouple economic growth from GHG emissions and other adverse environmental impacts. Although the pledges made and the actions done are not enough for present goals (UNEP, 2021), every economic sector has started to adopt the principles of sustainability and circular economy and redefine their activities in this direction. Among all, the energy sector contributes to three-quarters of all emissions and is the most responsible for GHG emissions causing climate change (Figure 1.4).

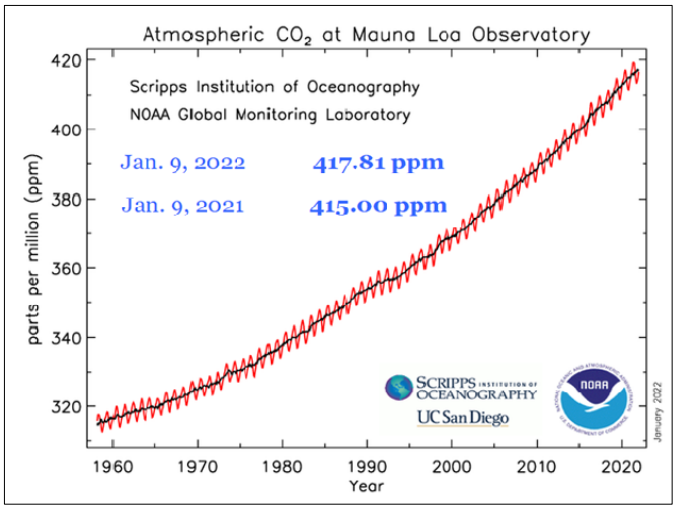

Figure 1.3. Carbon dioxide concentration in the Earth's atmosphere by years (NOAA, 2022).

Largest contributors of energy use are industrial applications (24.2%), buildings (17.5%) and transportation activities (16.2%). An understanding which will protect the environment, increase energy efficiency, and strengthen the independence from fossil fuels, which will be adopted under three energy sections, will be one of the most valuable progresses which will contribute to humanity in the global fight against climate change.

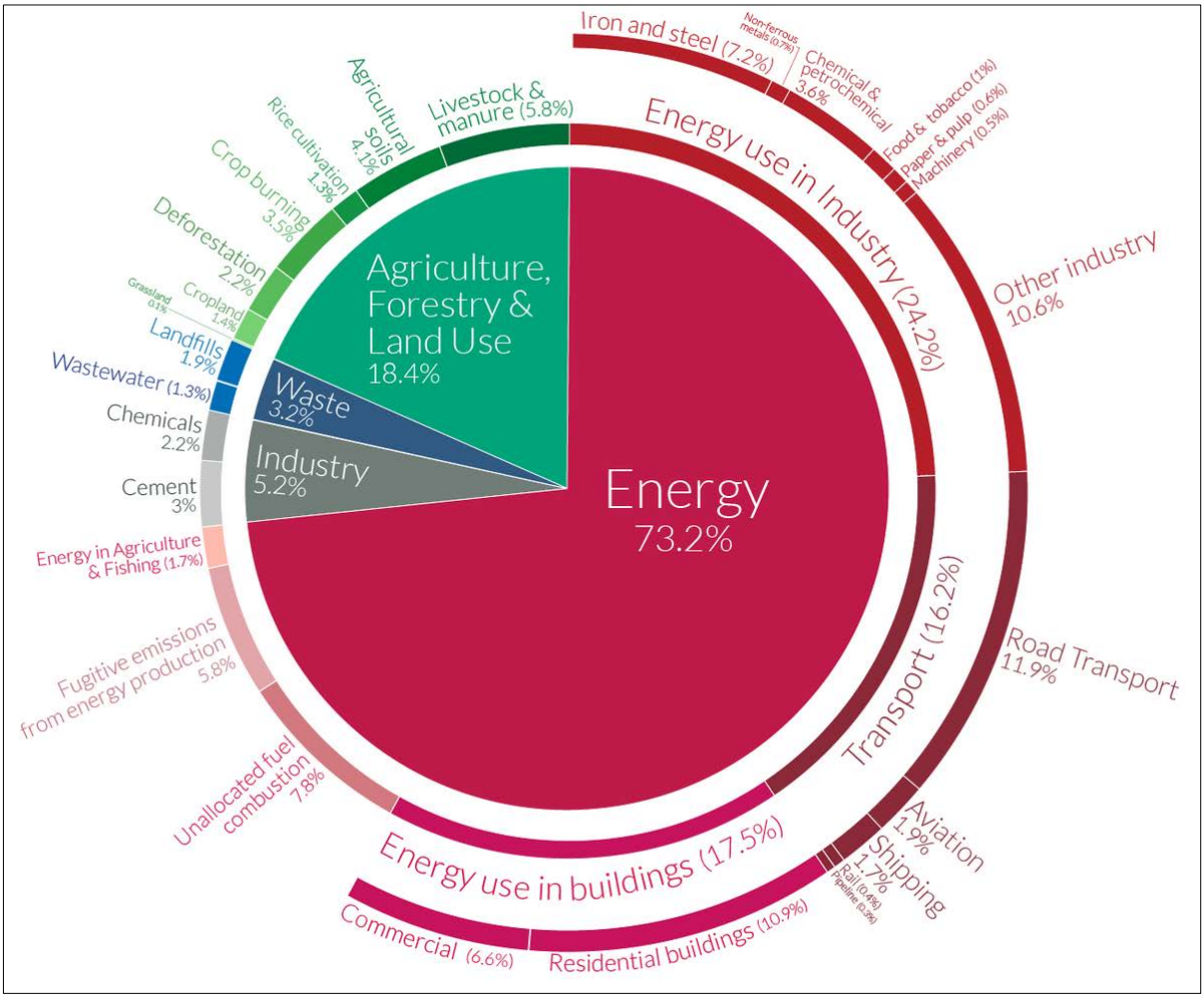

Figure 1.4. Global greenhouse gas emissions by sector (Climate Watch, the World Resources Institute, 2020).

1.2. Sustainability Activities in the Civil Aviation Sector

Civil aviation industry is a transportation sector that has been ambitiously increasing its contribution to global GDP (Gross Domestic Product) and GHG emissions since the 1960's (Figure 1.5). The sector, which provided 65.5 million jobs in the pre-COVID period, contributed 2.7 trillion dollars to the world GDP, which corresponds to 3.6% of the world GDP (equivalent to Switzerland or Argentina's GDP) (Forbes, 2020). In addition, the sector which is currently responsible for approximately 2% of global GHG emissions (1.04 billion tons CO_2-eq in 2018), is expected to be

responsible for 3% of global GHG emission in 2050 if current forecasts for its economic growth are considered (ATAG, 2020).

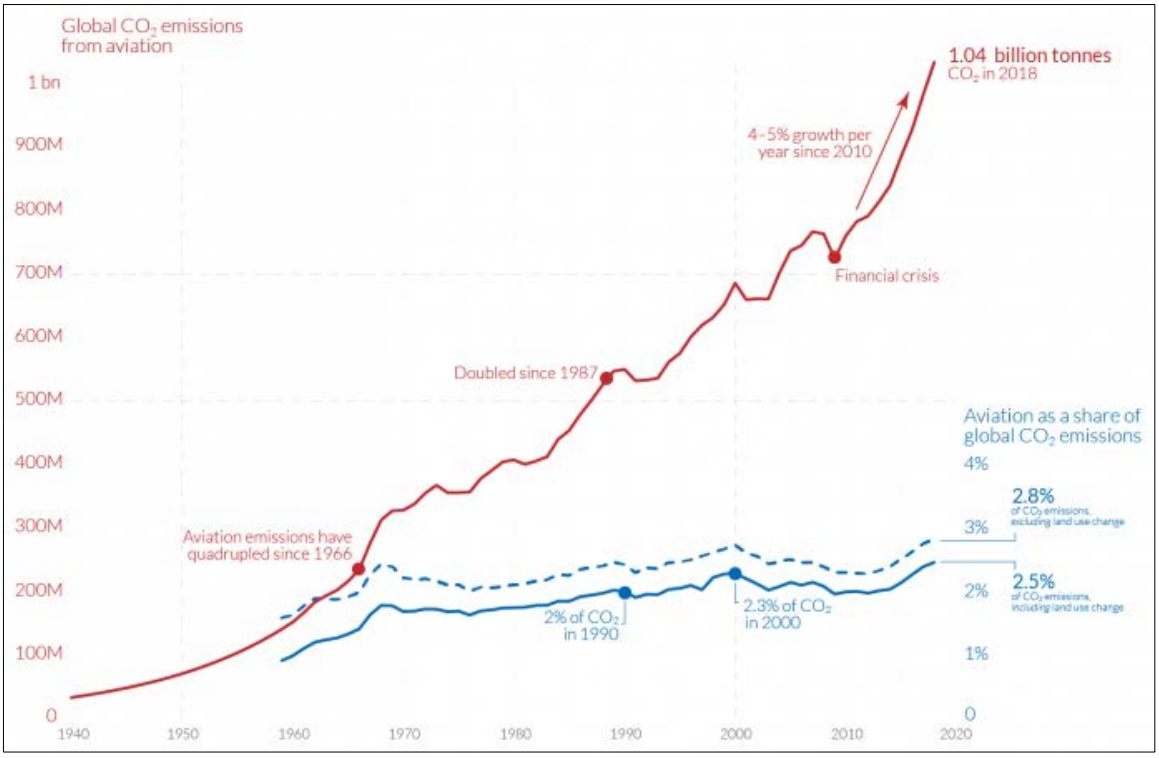

Figure 1.5. Global carbon dioxide emission from aviation sector by year (Lee et al., 2020).

At its 77th annual meeting on October 4th 2021, International Air Transport Association (IATA) declared that all their affiliated airlines companies should aim to make all civilian flights with zero carbon emissions by 2050 (IATA, 2021). Pledging such a massive carbon mitigation for the civil aviation industry, which is predicted to host around 10 billion passengers and emit 21.2 billion tons of net carbon dioxide by 2050, is ‘an enormous technology challenge’ and ‘to be successful, combined effort of entire industry and significant government support is must’, as IATA report dictates (IATA, 2021). The most competent institution of the aviation industry has four key strategies, in which it adopts sustainable principles, in order for the industry to enter 2050 with carbon neutrality. These are:

1) Use of Sustainable Aviation Fuel (SAF) (65%)
2) Investment in New Aircraft Technology (13%)
3) Improvement in Infrastructure/Operations (3%)
4) Use of Carbon Capture & Storage Technology (19%)

Declaring how it will mitigate carbon emissions with its detailed roadmap, the sector aims to eliminate carbon emissions caused by jet fuels, with priority given to fuels obtained from more sustainable resources.

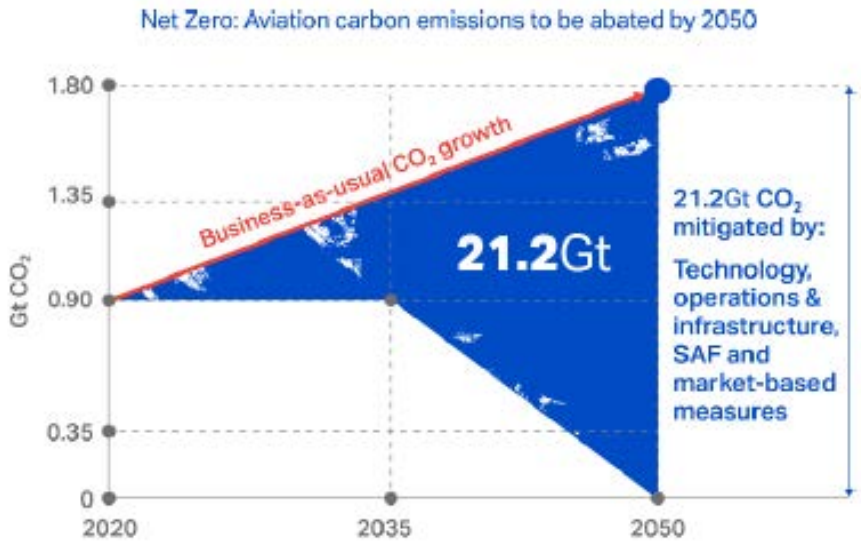

Figure 1.6. Civil aviation mitigation of carbon emission chart by IATA (IATA, 2021).

1.3. Sustainable Aviation Fuels and Classification of Biomass Feedstock

Civil aviation industry relies heavily on sustainable aviation fuels (SAFs) to achieve its ambitious goal of becoming carbon neutral (IATA,2021). Sustainable aviation fuels (SAFs) can be defined as aviation fuels produced from raw materials (biofeedstocks) grown in sustainable conditions, instead of using fossil resources (Bauen, 2020).

Table 1.1. Comparison of main features of conventional jet A-1 fuel, SAF and their blend. (ref. Berat Haznedaroğlu – personal communication).

Specifications	**Standard Jet A -1** (According to ASTM D1655 standards)	**50% Jet A-1 50% Bio-jet Fuel (v/v)**	**100% Bio-jet Fuel**
Flash point (°C)	Min 38	46	45
Freezing point (°C)	Max -47	-57	-57
Energy density (MJ/kg)	Min 42.8	43.6	43.9
Density (kg/m^3@15 °C)	Min 775 Max 840	778	761
Thermal Stability	Standard	Excellent	Excellent
Aromatics	Min8 Max 25	8.5	0

Chemical composition of SAFs obtained from different types of biofeedstocks is similar to traditional jet fuels and they can be used ‘drop-in’ today without changing the engine system (Rye et al., 2010). In addition, SAFs have lower aromatic content, low sulfur ratios and low freezing point than required by ASTM D1655 (Standard Specification for Aviation Turbine Fuel) and provide advantages to the jet engine (Yılmaz and Atmanlı, 2017). With the use of SAF, up to 80% GHG emissions have been reduced compared to conventional jet fuel (Siew Ng et al., 2021). Although current SAF production accounts for less than 0.05% of global jet fuel production (O’Mallet et al., 2021), the demand for sustainable jet fuel alternatives is expected to increase with the appropriate biofeedstock availability and sustainability-promoting regulations of the decision makers like carbon tax (White House, 2021).

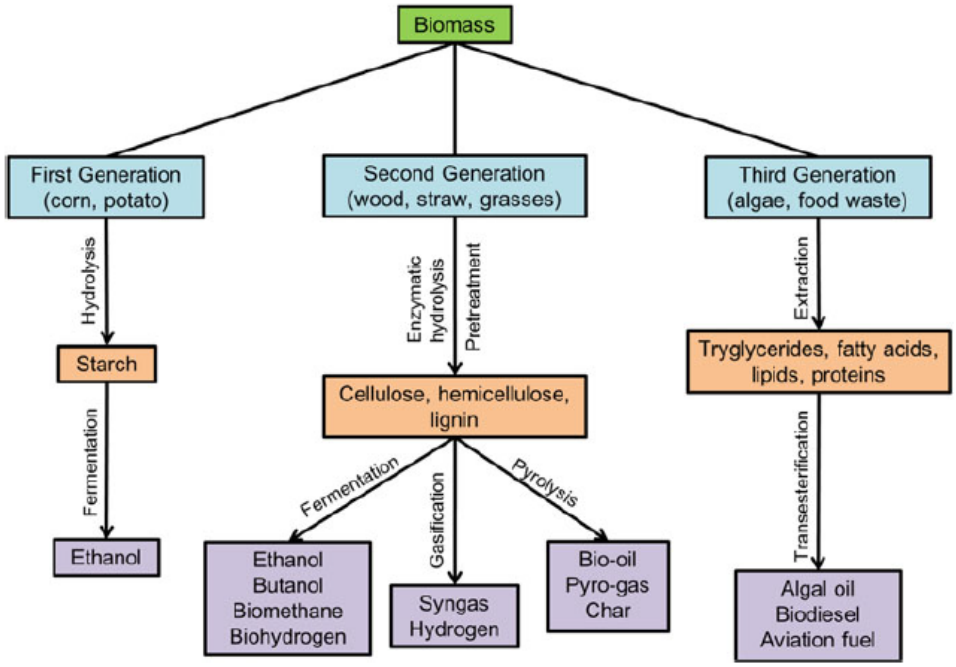

Figure 1.7. Overview of feedstock generations for biofuel (Nanda et al., 2018).

Sustainable aviation fuel can be produced from many biomass and waste sources, called feedstocks. Feedstocks can be classified under three categories according to their origin and the way they are obtained (Figure 1.7). First generation biofeedstocks are edible crops like wheat, maize, palm oil and sugarcane, and their production needs many requirements such as arable land, freshwater use, fertilizers etc. Their use for biofuel is a controversial topic in terms of Food vs. Fuel debate (Thompson et al., 2012). Instead, second generation biofeedstocks which are inedible, do not require arable land and have low production costs, are used for biofuel (Singh et al., 2020). Examples of second generation biofeedstocks are some inedible energy crops (Jatropha, camelina, rubber seed tree) and wastes or unused parts of edible crops (wood, straw, bran, grass, cob). However, the

conversion of lignocellulosic material in second generation biofeedstocks to biofuel complicates the operation and increases operational costs, and cultivation of these raw materials in arable lands to meet global fuel demand pose socioeconomic problems. All conclusions lead to the search for a third generation biofeedstock which does not conflict with food and can supply raw material in sufficient quantities to meet the global fuel demand (Neto et al., 2019). Biofuel production from waste oils and microalgae is in this category, and they offer promising raw material production opportunities compared to other biofeedstocks.

1.4. Advantages of Microalgae Cultivation for Bio Jet-Fuel Production

Microalgae species are remarkable in all biofeedstocks for having high biomass productivity and high lipid ratio (up to 70% of dry weight) at the same time. In terms of biomass productivity, microalgae cultivation produces 10 times more biomass/day than closest terrestrial energy crop alternative, which is oil palm (Bošnjakovic and Sinaga, 2020), and they can accumulate lipid up to 70% of their biomass (Hawrot-Paw et al., 2021). Combination of high biomass productivity and high lipid content makes microalgae a unique source for biofuel production (Figure 1.8).

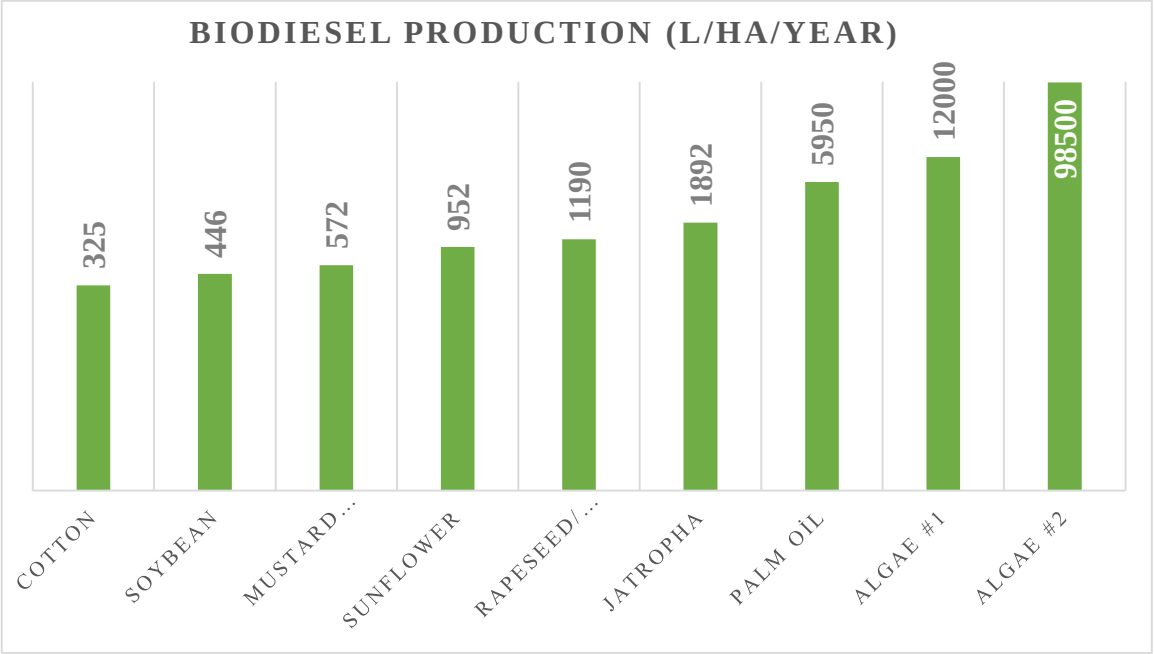

Algae #1: Microalgae cultivation with 10 g/m^2/day at 30% TAG condition

Algae #2: Microalgae cultivation with 50 g/m^2/day at 50% TAG condition

Figure 1.8. Biodiesel productivity of different biofeedstocks in log scale (Schenk et al., 2008).

Microalgae do not need arable land to be cultivated. According to theoretical calculations, microalgae cultivation on an area of 49 million hectares may be sufficient to meet global oil demand, which corresponds to 0.3% of landmass in the world and 2.5% of global arable land (Figure 1.9).

Marine microalgae species can grow without using freshwater, which is a limited resource and is more vulnerable due to climate crisis (Merlo et al., 2021). Novel chemistry products such as artificial fertilizers and pesticides which may adversely affect the environment and public health do not need to be used for microalgae cultivation.

Jet fuels obtained from microalgae make an enormous contribution to the goal of reducing GHG emissions, which is one of the most important motivations of SAF use, by causing 56% less GHG emissions than conventional jet fuel, when the whole life cycles of both products are considered (Prussi et al., 2021; Kolosz et al., 2020). On the other hand, GHG emission of microalgal biofuel is in seriously divergent range as -41.7 to 103.0 gCO_2-eq/MJ, considering the used LCA methodology and operational differences (Mentel et al., 2013).

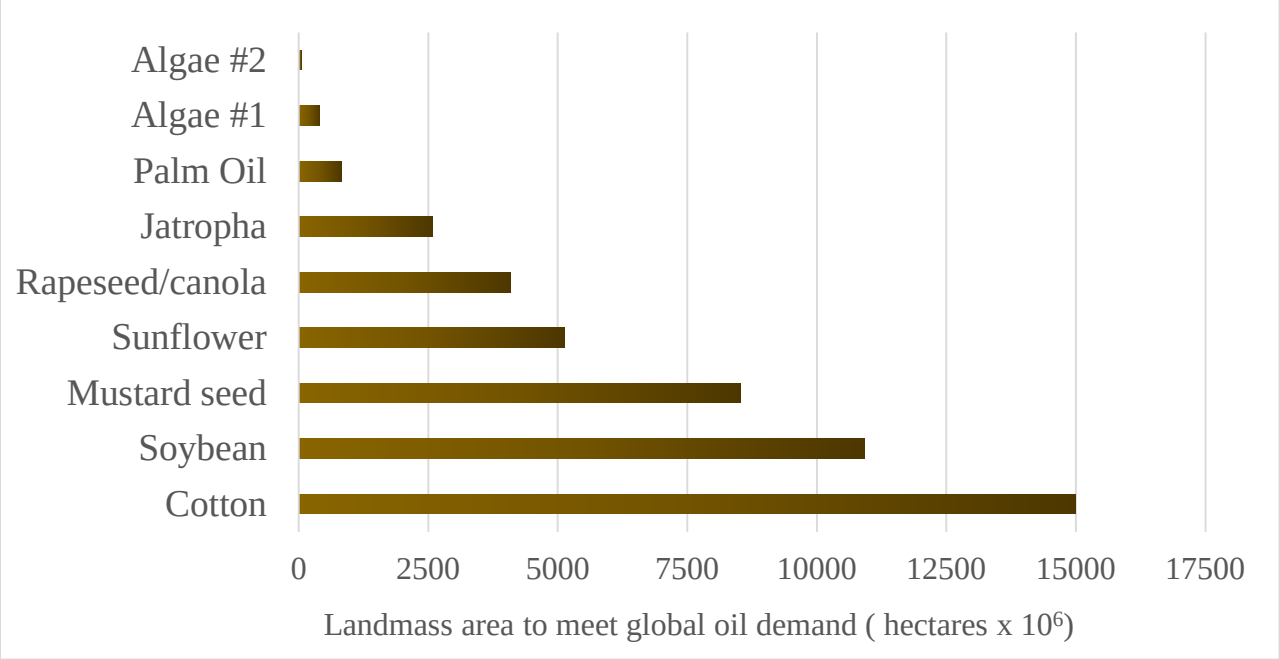

Algae #1: Microalgae cultivation with 10 g/m^2/day at 30% TAG condition

Algae #2: Microalgae cultivation with 50 g/m^2/day at 50% TAG condition

Figure 1.9. Landmass area needs of different plant sources to meet global oil demand (Schenk et al., 2008).

Ultimately, in addition to the biofuel made from microalgae lipids, converting the remaining compounds of the microalgae biomass into value-added products like pharmaceuticals, pigments, organic fertilizer supplements, animal feed etc. in other words, multivalorization of microalgae biomass, is a sustainable biorefinery approach with high market potential (Zhu ,2015). In times of high volatility of oil price, biofuels to be produced from microalgae cultivation in accordance with

local geography conditions support energy security/independence and employment (Sharma and Singh, 2017).

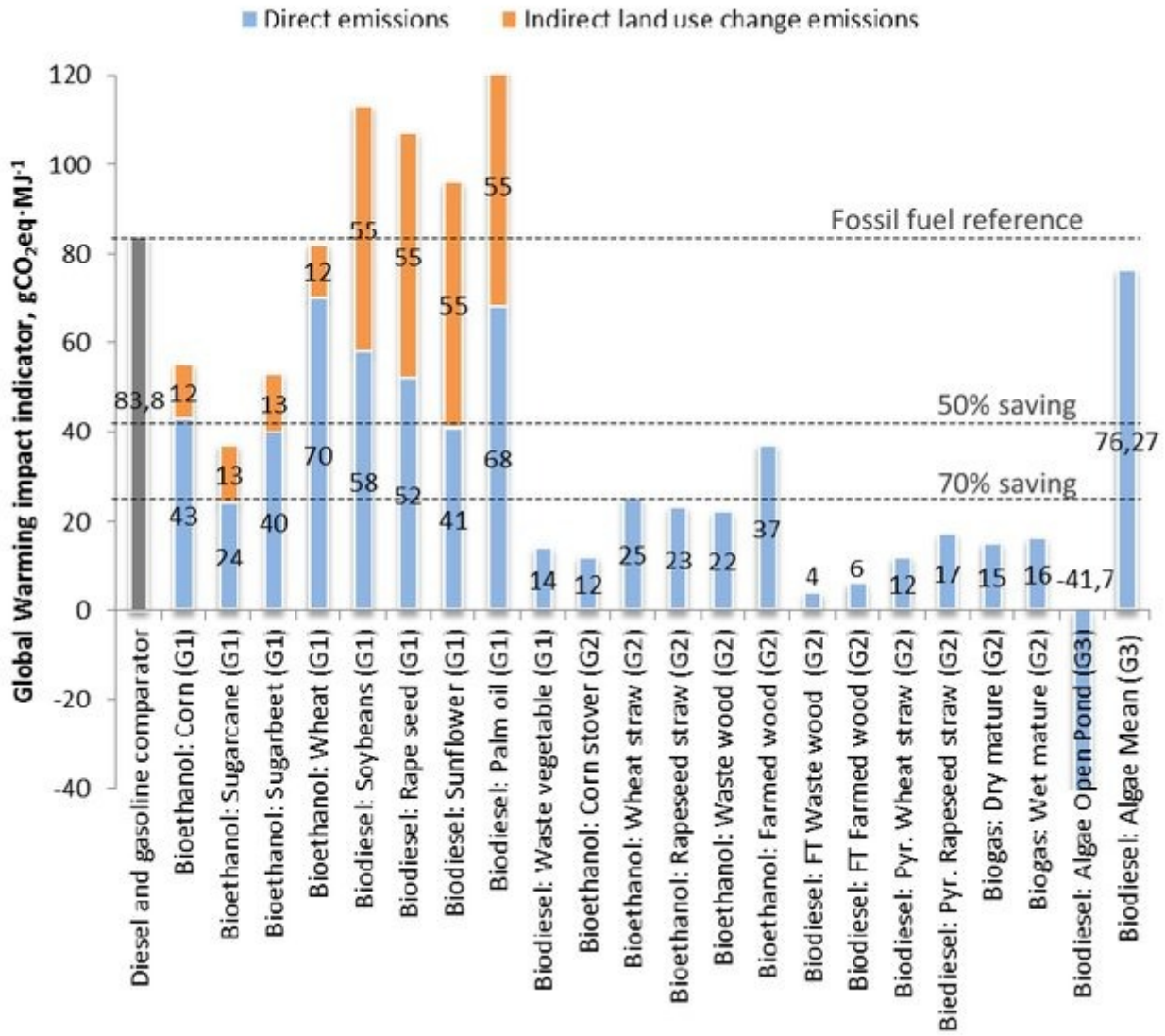

Figure 1.10. Global warming impact comparison of different biofeedstocks (Algae: First & Second from rightmost).

1.5. Objective of the Thesis

The primary motivation of this study is to sustain the thriving civil aviation sector in meeting its jet fuel demand from more eco-friendly resources by cultivating different microalgae species and optimizing the lipid amount and profile to be produced from microalgae. In the context of the energy sector, which has Turkey's largest current account deficit (TUIK, 2021), the bio-jet fuel from microalgae project includes another significant motivation in order to reduce dependence on imported fossil resources and strengthen the energy resiliency of Turkey. To ensure that bio-jet fuel production is environmentally friendly and affordable, it is aimed to establish a microalgae cultivation and lipid

extraction design in which all raw materials from the cradle to the grave were evaluated and multiple end products were obtained within the integrated biorefinery approach (Figure 1.11)

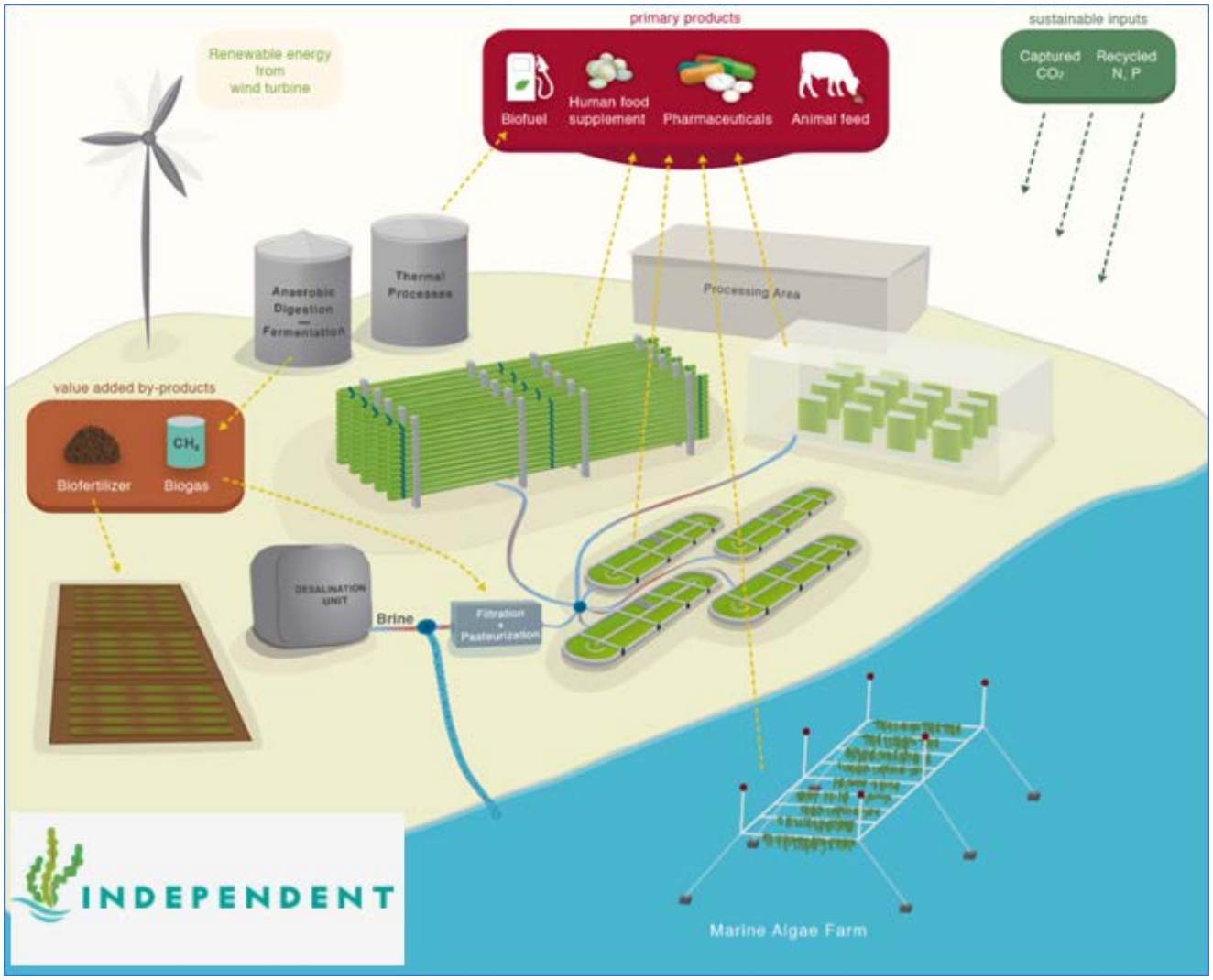

Figure 1.11. Integrated biorefinery design at IMBIYOTAB, Boğaziçi University (Design by Duygu Koldere).

The next section will focus on the technical elaboration of bio-jet fuel production from microalgae and the discussion of considerations when determining the roadmap of this study.

2. LITERATURE REVIEW

In this part of the study, different pathways of bio-jet fuel production from microalgae were explained and physicochemical elements which play a key role in microalgae cultivation were mentioned. After explaining how these elements affect lipid accumulation in microalgae, a summary of lipid extraction methods from microalgae was given. An overview of the microalgae lipid metabolism was followed by explaining the necessity and types of the transesterification step. Analytical chemistry instruments and methods which can be used for the quantification and qualification of optimized fatty acid methyl esters (FAMEs) were briefed. This section was divided into six subsections to facilitate traceability.

2.1. Six Different Pathways to Produce Bio-Jet Fuel from Algal Biomass

There are six different renewable jet fuel production techniques suitable for large-scale production. These pathways are ordered as follows according to their Fuel Readiness Level (FRL) determined by CAAFI (Commercial Aviation Alternative Fuels Initiative) standards (Figure 2.1):

1) Hydroprocessed Esters and Fatty Acids (HEFA) (Full-scale commercial)
2) Fischer – Tropsch (FT) (Full-scale commercial)
3) Direct Sugar to Hydrocarbons (DSHC) (Certification/ Fuel approval)
4) Hydrotreated Depolymerized Cellulosic Jet (HDCJ) (Full-scale technical evaluation)
5) Alcohol to Jet (ATJ) (Preliminary tech. evaluation)
6) Aqueous Phase Reforming (APR) (Process validation)

Technical certification of ‘drop-in’ SAFs is evaluated according to ASTM D7566 standards and produced bio-jet fuel is approved for use by blending up to 50% with conventional jet fuel, regardless of the pathways it is produced (IATA, 2021).

Bio-jet fuel production via Fischer-Tropsch- Synthetic Paraffinic Kerosene (FT-SPK) was approved in 2009; followed by HEFA (2011), HDCJ (2014) and ATJ (2016) receiving technical certifications (IATA, 2021). In addition, the catalytic hydrothermal process, also known as hydrothermal liquefaction process, was approved for large-scale bio-jet fuel production in 2020 (IATA, 2021). All conversion pathways were explained respectively in the relevant subsections.

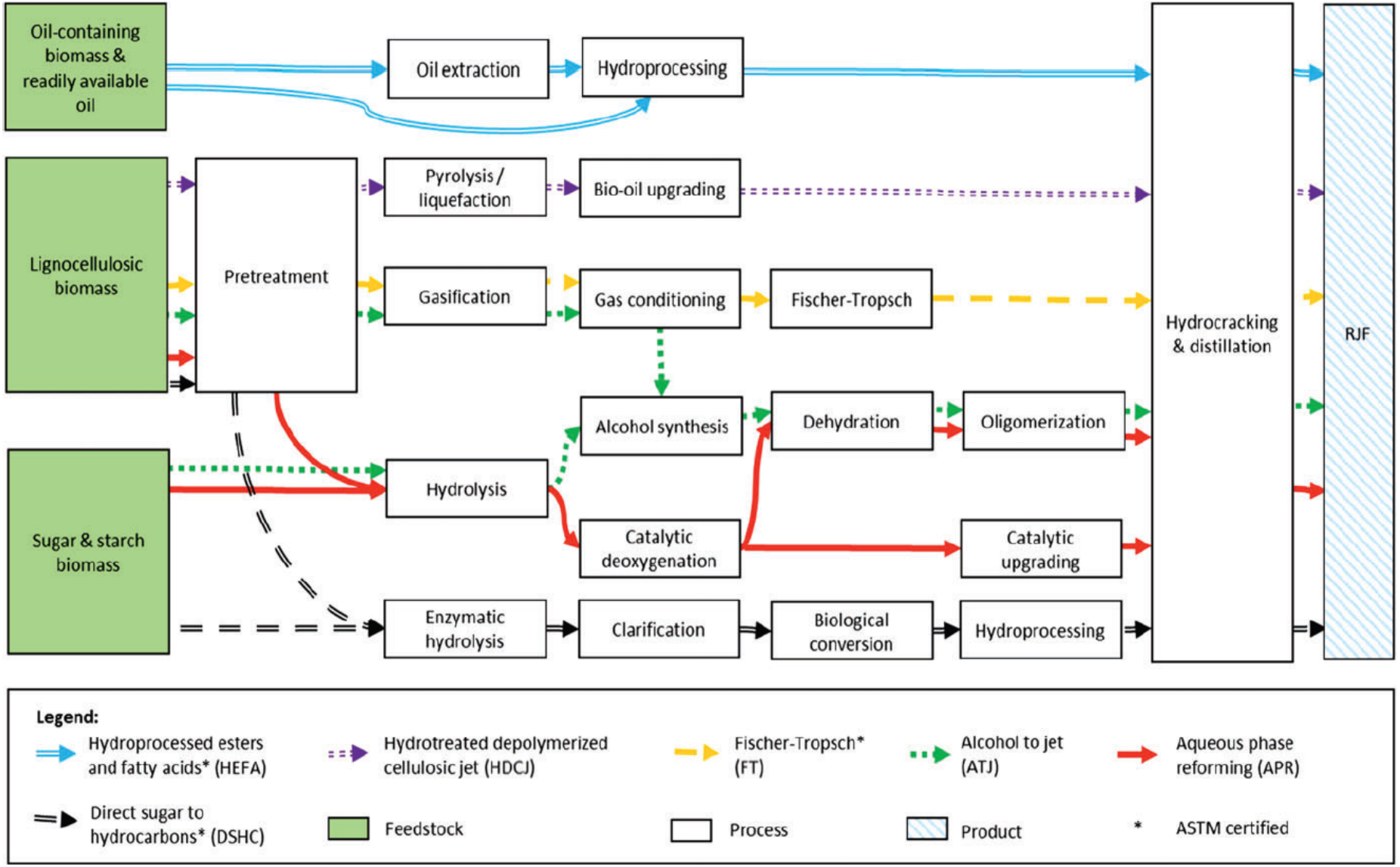

Figure 2.1. Alternative pathways and preferred biofeedstocks for renewable jet fuel production (Mawhood et al., 2016).

2.1.1. Hydroprocessed Esters and Fatty Acids (HEFA)

HEFA is a hydrotreatment method used to produce jet-fuel from readily available oil. This method, which demands a high percentage of oleaginous raw materials, is extremely suitable for the conversion of vegetable lipid extracts, microalgae lipids and waste oils into bio-jet fuel (Doliente et al., 2020). Extracted lipids are transesterified to liberate fatty acids (FAs) from triacylglycerides (TAGs), lipid storage unit of the cell, and to get rid of glycerol linkage. It is aimed to convert esterified FAs to the desired hydrocarbon profile by hydrotreating and catalytic cracking in the presence of high pressure and temperature (~ 350 °C) (Robota et al., 2013).

The catalysts to be used for hydrodeoxygenation and hydrocracking may vary according to desired hydrocarbon profile. For example, *Botryococcus braunii* lipids were converted with the use of Pt-Re/SiO_2-Al_2O_3 bifunctional catalyst to jet-fuel hydrocarbons (50.2%) and diesel hydrocarbon profile (16.7%) (Murata et al., 2014). Bifunctional catalysts are used to efficiently convert the lipids other than the fatty acids, like terpenes. Bio-jet fuel hydrocarbons were obtained from 52% of *Botryococcus braunii* lipid extract which contains mostly C_{29}-C_{34} terpenes, as a result of hydrocracking performed with NiMo/Al_{13}-Mont catalyst at 300 °C for 6 h (Liu et al., 2019). According to the results seen in most studies, hydrocarbon fraction obtained from microalgae lipids by HEFA method is more suitable for biodiesel production, and additional treatments are required for bio-jet fuel production. Over 2L algal triglyceride was hydrocracked with 3% Pd/C catalyst at 350 °C and 800 psig of H_2 and products were hydrocracked again with 0.5% Pt/US-Y zeolite catalyst to observe HEFA bio-jet fuel fraction (Robota et al., 2013).

Another example of modified HEFA conversion of algal lipids was shown in Poddar et al. study. *Nannochloropsis sp.* lipid was hydroprocessed with CoMoP/ Al_2O_3 catalyst at 300–375 °C with H_2 at 50–120 bar and 35-50% (w/w) biokerosene and 87% alkanes were produced (Poddar et al., 2018). Examples of high jet fuel conversion rate from algal lipids can be found in the literature. 76% bio-jet fuel yield was modeled using *Chlorella sp*. bio-oil at 410 °C and 5 MPa with the help of mesoporous zeolite 5% NiO, 18% MoO_3/H-ZSM-5 (Cruz et al., 2017). According to the study of Sundara et al., it was observed that bio-jet fuel from Jatropha oil produced using HEFA method has high viscosity, sulfur-free and low aromatic content, higher calorific value, and low emission (Sundara et al., 2019). It is aimed to convert a significant part of algal lipids produced from this thesis study to jet-fuel hydrocarbon profile by HEFA process.

2.1.2. Fischer – Tropsch

Microalgae with low lipid content and other biofeedstocks can be used to produce synthetic paraffinic kerosene (SPK) by Fischer-Tropsch (FT) synthesis. In terms of technical applicability and commercialization, FT-SPK and HEFA jet fuel are known as the two most successful and reliable pathways (Mawhood et al., 2016). Significant advantage of FT synthesis for SPK production is that almost any biofeedstocks can be used in FT reaction to produce syngas (SWAFEA, 2011). Before FT reaction, biomass undergoes gasification at above 700°C and syngas is produced, which is carbon monoxide, hydrogen, small amounts of carbon dioxide and methane. In summary, syngas is purified and FT-SPK is produced by going through hydrotreatment, hydrocracking, hydroisomerization and fractionation processes (Yang et al., 2016).

As an example, from the literature, lignocellulosic biomass gasified around 900 °C was purified from 95% of CO_2. After hydrocracking and isomerization, 77% of the end product was at the range of jet fuel whereas 23% of it was naphtha (Figure 2.2). In FT studies with *Spirulina* species, the highest theoretical methanol yield (0.64 g methanol/ 1 g biomass) was achieved using 1000 °C gasification (Hirana et al., 1998). It is known that catalysts have an important role in FT synthesis, especially in carbon monoxide hydrogenation. While ruthenium is quite efficient, active and expensive; iron catalysts are frequently used in FT synthesis plants with their high olefin yield and cheap alternatives (Hall et al., 1957). It should be noted that there is a possibility to produce bio-hydrogen from algal biomass via gasification, as Duman et al. shows 413 cc/g *Nannochloropsis oculata* hydrogen yield using Fe_2O_3-CeO_2 catalyst (Duman et al., 2014).

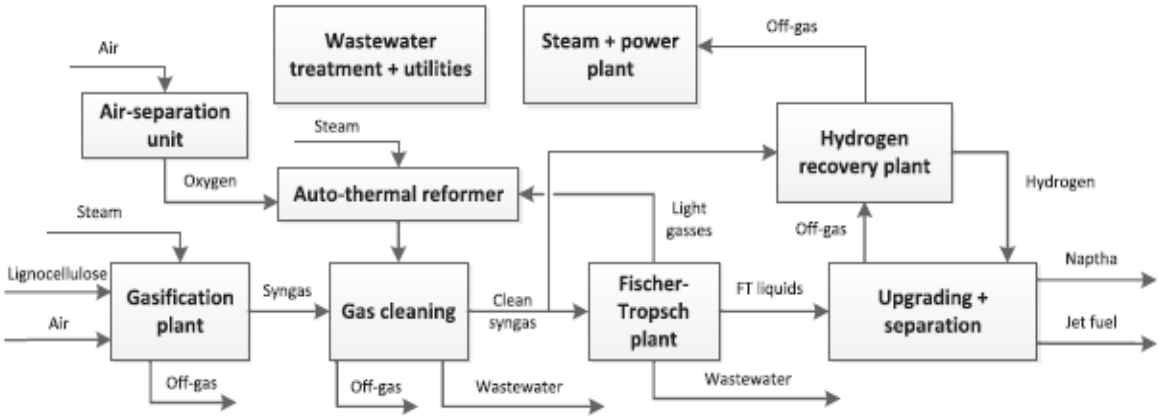

Figure 2.2. Flow diagram of lignocellulosic biomass to bio-jet fuel operation (Diederichs et al., 2016).

2.1.3. Direct Sugar to Hydrocarbons (DSHC)

Direct sugar to hydrocarbons pathway, also known as sugar-to-jet, aims to convert sugars in biomass directly to hydrocarbons without producing alcohol intermediates (Wang et al., 2016). This route potentially targets lignocellulosic biomass or sugarcane, and hydrolyzes hemicellulosic sugars in an anaerobic environment to form hydrocarbon intermediates (Mawhood et al., 2016). In direct sugar to jet mevalonic (MVA) pathway which produces xylose from glucose, there are studies of jet fuel production using corn stoves through MVA pathway (Lloyd et al., 2005). There is a facility of Amyris & Total's facility in Brazil which uses sugarcane and molasses to produce 40000-ton biofuels annually, with the partnership of Airbus, Safran and Air France (Mawhood et al., 2016).

2.1.4. Hydrotreated Depolymerized Cellulosic Jet (HDCJ)

Main rationale of the HDCJ pathway, which includes pyrolysis and hydrothermal liquefaction (HTL), is to convert lignocellulosic biomass to bio-oil and to produce jet-fuel by hydrotreatment of bio-oil. Pyrolysis can be divided into slow, fast and flash pyrolysis and due to high bio-oil yield, fast pyrolysis is used for biofuel production (Lim et al., 2021). Pyrolysis can also be used as pretreatment of hydrotreatments, as in the study of *Chlorella vulgaris* biofuel intermediate, it was pyrolyzed at 850 °C and hydrotreated with NiOx-CoOx-MoOx-zeolite catalyst (Asiedu et al., 2020). As a result, 41% of iso-alkanes and 35% of cyclo-alkanes were produced. Main difference of hydrothermal liquefaction from pyrolysis is that it can produce bio-oil with low oxygen content and without the need to dry biomass (Chiaramonti et al., 2017). Chiaramonti et al. showed that *Nannochloropsis sp*. can both be pyrolyzed and hydrothermally liquified by around 36% (w/w) of total biomass (Chiaramonti et al., 2017). In the studies, it has been observed that biocrude produced by applying pyrolysis and HTL to the microalgae needs to be upgraded by hydrotreatment applications (Li et al., 2018). Bio-jet fuel from microalgae with HTL has a promising market and research potential (Sahoo et al., 2021; Brindhadevi et al., 2021). Some of the microalgae cultivated under the scope of this thesis were also used for studies of biokerosene production via hydrothermal liquefaction.

2.1.5. Alcohol to Jet (ATJ)

Similar to DSHC, the rationale of alcohol-to-jet includes sugar fermentation to produce alcohol intermediates and convert alcohols to hydrocarbons using hydrotreatments (Bwapwa et al., 2017). This process is also known as synthesized iso-paraffinic (SIP) fuel from fermented hydroprocessed sugar. Dehydration to generate olefins (as it is relatively hard to directly convert alcohol into paraffin),

oligomerization, hydrogenation and fractionation were used to convert alcohol to bio-jet fuel pathway, respectively (Wei et al., 2019). For example, biofeedstocks were converted to isobutanol with 98.8% selectivity and to isobutylene with 95.5% using γ-Al_2O_3 catalyst at 325 °C and 60 psig (Taylor et al., 2010). Among all conversion methods, ATJ is known as the most energy efficient method with 91% average efficiency (Jong et al., 2015). Possibility to produce 23.5% bioethanol (w/w) from *Chlamydomonas reinhardtii* biomass by enzymatic treatments offers an alternative to producing bio-jet fuel by alcohol-to-jet pathway through microalgae (Choi et al., 2010).

2.1.6. Aqueous Phase Reforming (APR)

Aqueous phase reforming pathway enables soluble plant sugars to be converted into oxygenated hydrocarbons, and hydrocarbons into bio-jet fuel via catalytic conversion (Wei et al. 2019). It is one of the less preferred, long route pathways, and is in the trial phase in pilot scale. Virent™ company uses various biofeedstocks containing cellulose and starch, such as corn stove, and produces 19000 liters of biodiesel/ year with APR pathway (Mawhood et al., 2016). Commercialization of APR jet fuel is at ASTM technical certification stage.

Since oleaginous green algae species were used in this study, it is expected that HEFA and HTL pathways are expected to be applied after microalgal lipid extraction was performed.

2.2. Lipid Accumulation in Microalgae and Its Dependence on Intracellular and Extracellular Factors

In this section, in order to discuss lipid accumulation, i.e. lipid boosting, in microalgae cultivation, basic information about microalgae cultivation and lipid metabolism was given, and both internal and external factors affecting lipid metabolism and related studies were discussed. This section was divided into 7 subsections to facilitate traceability.

2.2.1. Basic Information on Microalgae Cultivation and Lipid Metabolism

Microalgae are unicellular phytoplankton which grow in fresh and marine water (Suganya et al., 2016). In this respect, they should not be confused with macroalgae (seaweed), which can reach 40 meters in size (Barnabe, 2007). Today, there are 164,800 registered species and infraspecific names of algae, the majority of which are microalgae species (AlgaeBase, 2022). It is estimated that there may be more than 1 million algae species with undiscovered ones (Guiry et al., 2012). 164 thousand

species of algae are very differentiated within themselves, and microalgae have become a community that can show various features inside. Taxonomically, microalgae can be classified into five main phyla: *Chlorophyta* (Green algae), *Rhodophyta* (Red algae), *Haptophyta*, *Stramenopiles* (Brown algae/kelp) and *Dinophyta* (Dinoflagellates) (Heimann et al., 2015).

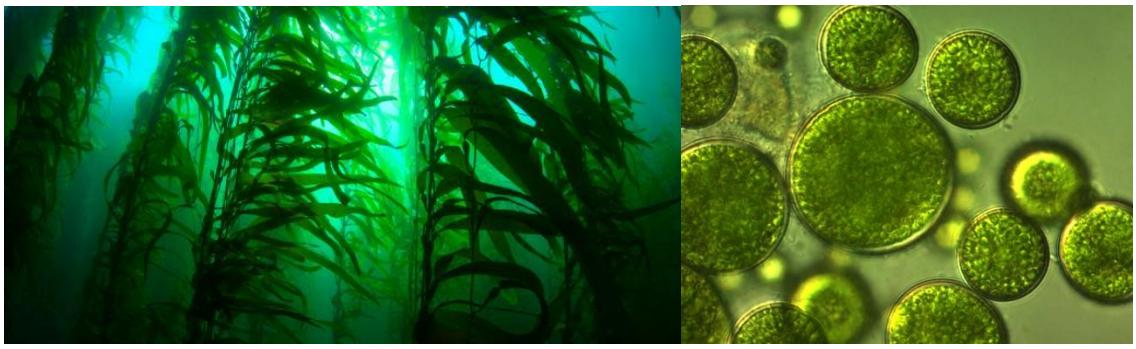

Figure 2.3. Macroalgae and microalgae (copyright with Techexplorist and Feedipedia).

Microalgae can be grown in autotrophic, heterotrophic or mixotrophic conditions (Jaeronsin and Pumas, 2021). Although microalgae cultivation in heterotrophic conditions is remarkable with its high biomass productivity and suitable conditions for some phytochemicals, autotrophic growing conditions are often preferred due to unique photosynthetic efficiency of algae and its opportunities to provide more eco-friendly and affordable conditions (Cupo et al., 2021). Microalgae are responsible for more than 50% of global primary photosynthetic activity. Their high photosynthetic efficiency, which is up to 10 times higher than terrestrial plants, turns them into robust “cell factories” enabling the production of several compounds (Santos et al., 2019).

Algae cultivation design can be roughly divided into closed photobioreactors (PBRs) and open ponds (Figure 2.5). PBRs are closed, controlled cultivation systems and has higher biomass productivity ratio (both areal and volumetric) (Haznedaroğlu et al., 2021). PBR systems are less susceptible to contamination (Yakoob et al., 2014). Design of PBRs is more elaborate than open ponds: more conventional PBRs like tubular, tank, flat panel, airlift etc. or recent PBR designs like biofilm-based, twin-layer immobilized, liquid foam-bed, mesh ultra-thin layer systems etc. (Olaizola and Grewe, 2019). Microalgae cultivation using PBRs, especially for value-added products, has been already commercialized (Chang et al., 2017).

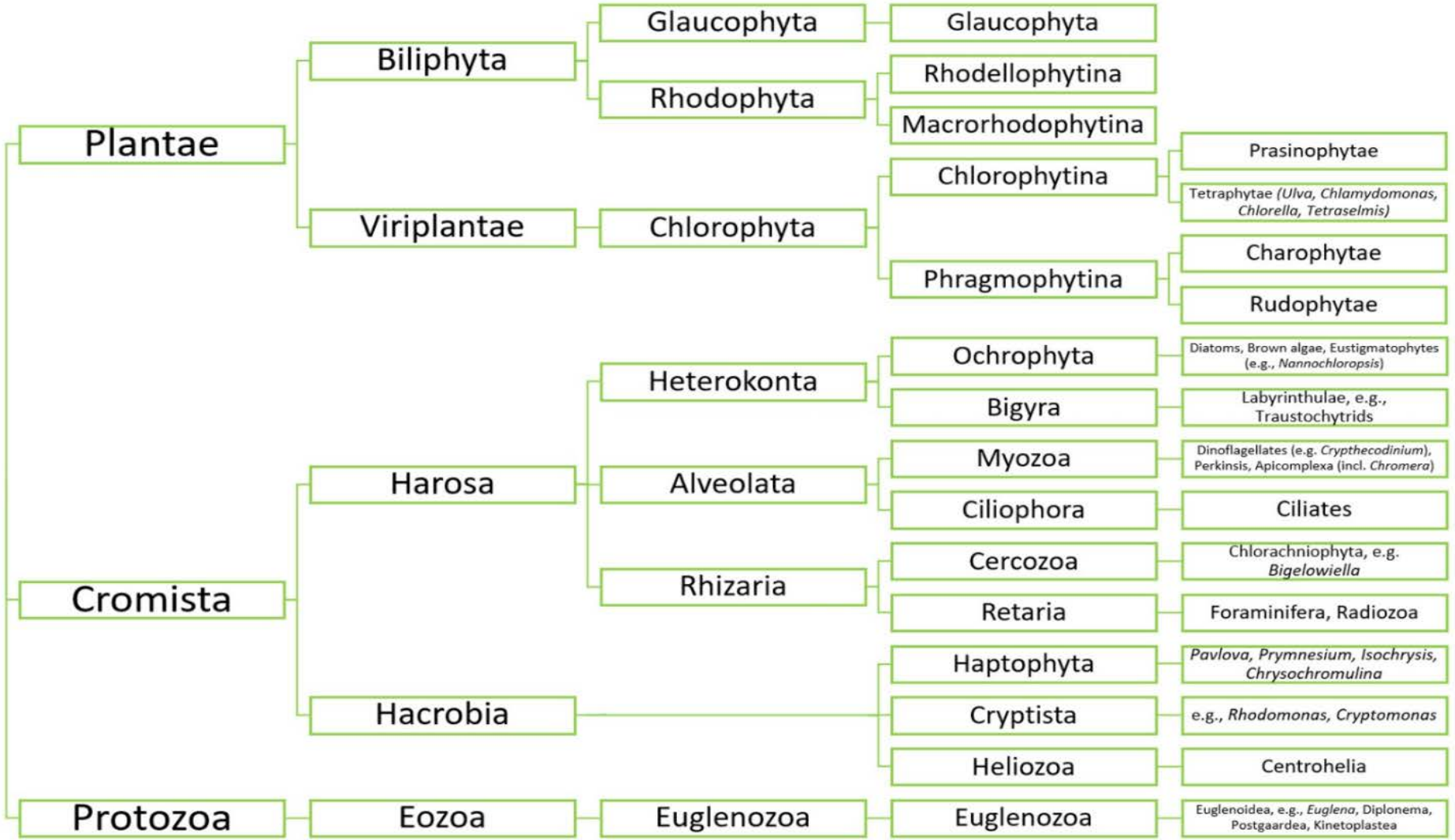

Figure 2.4. Algae phyla classification (Heimann et al., 2015).

Figure 2.5. Closed tubular PBRs (left) and open raceway pond (right) available at IMBIYOTAB facilities.

Open ponds are frequently used in microalgae cultivation for commodity products (fuel, feed etc.). In open ponds which can easily access high cultivation volumes with operational ease. Drawbacks of open pond cultivation are their biomass production is low (0.5-2 g/L), land use is demanding, and they are more susceptible to contamination and stress factors (rain, wind, dust, animals etc.) due to direct contact of ambient air (Aratboni et al., 2019).

Both cultivation systems can operate in batch, semi-continuous or continuous conditions and the amount and quality of biomass and final product from microalgae cultivation varies depending on the operational conditions (Benvenuti et al., 2016).

In this thesis, autotrophic oleaginous green algae were grown firstly in closed PBRs and then scale-up of microalgae cultivation was performed by using open ponds in batch mode.

Lipid synthesis and storage pathway of microalgae are similar to that of terrestrial plants (Figure 2.6). According to past research experience, lipid profile of algal oil is similar to vegetable oils such as olive oil and sunflower oil, but differs from animal fats such as butter, especially in terms of light fatty acids. Fatty acids (FAs) and Acetyl-CoA plays a key role in FA production (Chalima et al., 2017). In microalgae, sixteen and eighteen carbon (C16- C18) free fatty acids are synthesized by the combination of two-carbon FAs with the help of Acetyl-CoA (Figure 2.7). Like in vegetable oils, microalgal lipids have a high percentage of unsaturated fatty acids (UFAs) (Gustafsson and Boberg,

1992), which means one or more double/triple carbon-carbon bonds in FA, that provides a lubricity advantage in bio-jet fuel production. Lipid storage unit in microalgae is triacylglyceride (TAG), which is composed of three FA and one glycerol molecule (Figure 2.8). FAs are 'packaged' as TAGs to store energy in more compact form, and lipid droplets can form in algae as a result of high TAG accumulation (Reza et al., 2020).

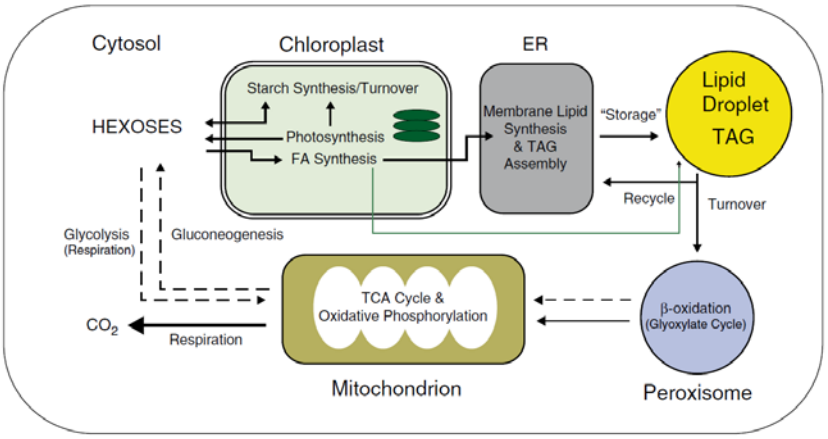

Figure 2.6. Carbon flow pathway for triacylglyceride (TAG) accumulation in microalgae (Chapman and Ohlrogge, 2012).

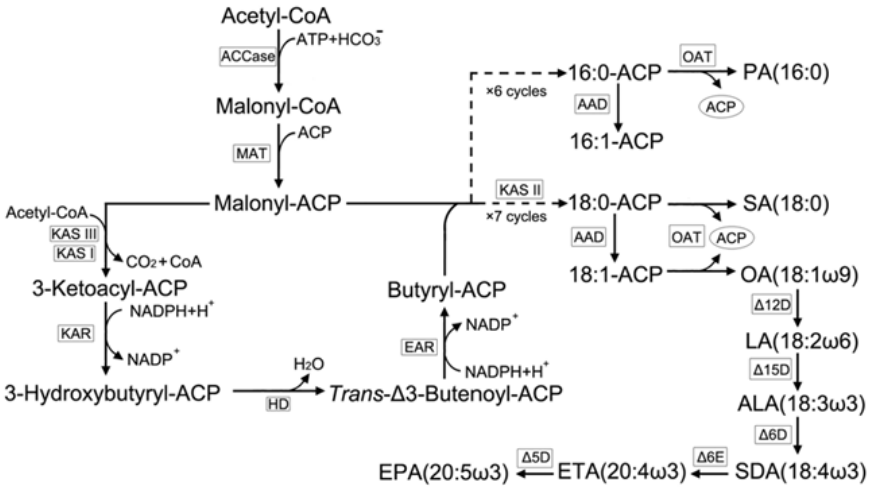

Figure 2.7. *De novo* fatty acid biosynthesis pathway of *Eustigmatos* cf. *polyphem* (Wan et al., 2012).

Aim of this study is to optimize free FA and TAG production by manipulating lipid metabolism of microalgae. While FA in microalgae consist of generally from 16 and 18 carbon, hydrocarbon profile required for jet fuel varies between 9 and 15 carbons (Yang et al., 2016). Starting from the next subsection, extracellular factors used in the literature to manipulate algal lipid metabolism were discussed.

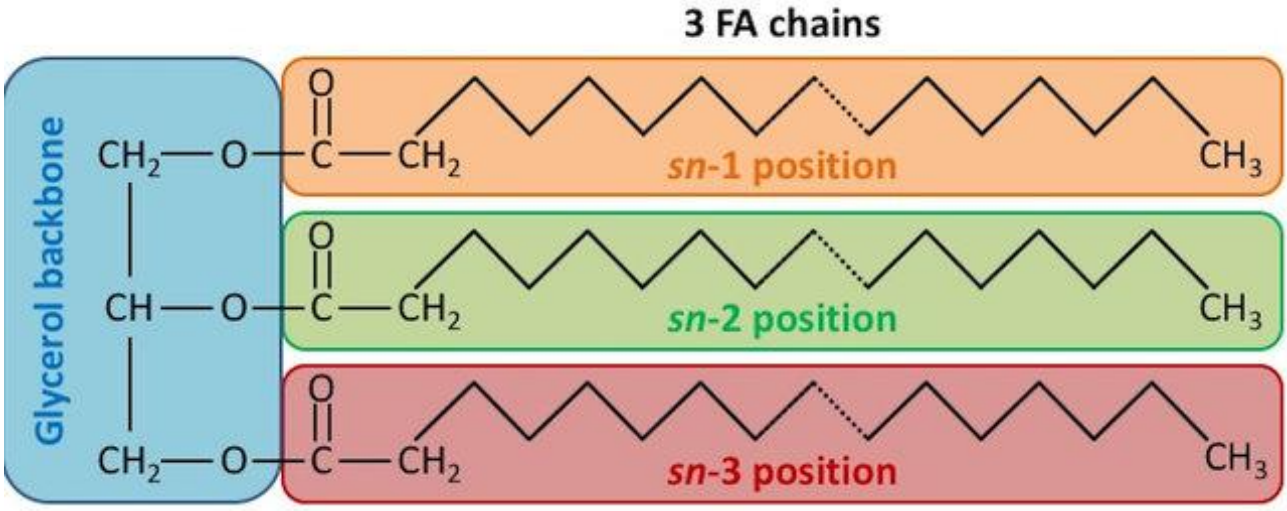

Figure 2.8. Triacylglycerol as storage unit of algal lipids (Alfieri et al., 2017).

2.2.2. Nutrient

One of the most important factors triggering lipid accumulation is nutrient content and concentration in algae media. Related nutrients in microalgae cultivation can be categorized in macronutrient and micronutrients. Nitrogen, phosphorus, sulfur, potassium, chlorine can be counted as macronutrient, which are essential compounds to sustain metabolic activity (Fox and Zimba, 2018). Micronutrients are required elements in trace amounts to catalyze homeostasis. Iron, manganese, zinc, copper, cobalt, and molybdenum are micronutrient examples of microalgae (Quigg, 2016).

Nitrogen has a key role in protein synthesis and energy metabolism, and it is a bottleneck for plant growth (Weber and Burow, 2018). Nitrogen concentration is one of the most impactful factors to manipulate lipid metabolism. Nitrogen deprivation regulates lipid synthesis to accumulate TAG (Yap et al., 2016). There are studies which increase lipid productivity in six different microalgae (*C. sorokiniana, C. vulgaris, C. oleofaciens, E. oleoabundans, S. dimorphus, S. naegleii*) to 222-358% by reducing nitrogen concentration in media by up to 60% (Adams et al., 2013). Same study also addressed biomass productivity loss under nitrogen deprivation. Inverse relationship between biomass productivity and lipid accumulation reveals that further studies are needed for optimal conditions for lipid production. For example, 75% nitrogen decrease in media increases the lipid content of *Nannochloropsis oculata* from 5.90% to 15.31% (Converti et al., 2009). Severity of nitrogen deprivation may change by increasing duration of nitrogen starvation in microalgae cultures. For example, maximum lipid content in *Scenedesmus obliquus* (22.4%) was achieved in 5-day nitrogen starvation (Hsin Ho et al., 2012). Lipid percentage in microalgae cells is almost virtually

increased with nitrogen deprivation, but their lipid productivities ($g_{lipid}/m_2/day$) does not always increase under the same conditions (Rodolfi et al., 2008).

Phosphorus is an element found in DNA, RNA, and ATP which is "energy currency" of life (Karl, 2000). Decrease in phosphorus concentration in algae culture also creates external stress, and forces algae to accumulate lipids. Adenan et al. showed that total lipid in *Chlorella sp.* and *Chaetoceros calcitrans* was increased to around 40% (from 25% to 35%) by reducing phosphate concentration by 75% (Adenan et al., 2016). Phosphorus can be uptaken by microalgae cells as phosphate salts, and studies confirmed that reduction of phosphate salt molarity results in shifting the metabolites in cells to lipid metabolism. Lipid productivity in *Chlorella sp.* was increased 6 mg/L/day to 15.67 mg/L/day by reducing K_2HPO_4 molarity from 240 μM to 32 μM (Liang et al., 2013). Another study showed that *Botryococcus braunii* KMITL2 increased its lipid content from 22% to 54% in 30 days by reducing phosphorus concentration by half (Ruangsomboon, 2012). On the other hand, there are several studies in literature showing that change in phosphorus concentration does not affect or reduce the lipid productivity (Praveenkumar et al., 2012; Chen et al., 2011).

Concentration changes of other macro- and micronutrients affect biomass and lipid productivity in microalgae (Sajjadi et al., 2018). Micronutrients such as iron and nickel play vital parts to catalyze metabolic activities in microalgae and change in iron and nickel concentration affect lipid metabolism. Lipid content in *Botryococcus* was more than doubled in iron-deficient and nickel-deficient media (Yeesang and Cheirsilp et al., 2011). El Baky et al. showed that addition of 20 mg/L $FeCl_3$ in medium increased the lipid productivity of *Scenedesmus obliquus* more than four times, from 20.1 mg/L/d to 95.35 mg/L/d (El Baky et al., 2012). Other micronutrient metals also participate in anabolic and catabolic reactions in the cell and change in the concentration of these metals may promote or inhibit the lipid accumulation in algae cells. The lipid content of *Dunaliella teriolecta* was at least doubled with the increase of manganese, zinc and molybdenum concentrations (Chen et al., 2011).

2.2.3. Light

Light intensity (irradiance), light:dark cycle and wavelength spectrum of light affect biomass and lipid productivity of microalgae cultivation (Nagappan et al., 2019). Lipid productivity was increased 42% in *Nannochloropsis oculata* by changing light intensity from 200 to 400 μmol photons/m^2/s with nitrogen deprivation at the same time (Hung Su et al., 2011). Another study showed that lipid content of *Scenedesmus sp.* strain CCNM 1077 increased 35.34% to 42.58% by changing

light intensity from 30 to 150 μmol photons/m^2/s (Pacha et al., 2015). Biomass productivity and lipid productivity of microalgae are affected from different patterns in light:dark cycle. In computational fluid dynamics study, 3 seconds of light:dark cycle period increases biomass yield by 22% (Yang et al., 2016). Effect of light wavelength on growth rate of microalgae is also studied, many of microalgae species have high growth rate with red light (Park et al., 2012), and also some green and blue light conditions are found to improve biomass productivity (Das et al., 2011). *Nannochloropsis* sp. was observed to have the highest growth rate in 18:6 h light:dark cycle, and shortening light duration reduced lipid ratio of the biomass (Wahidin et al., 2012).

2.2.4. Temperature

Microalgae cultivation under suboptimal temperatures alters metabolic activity and affects all macromolecular content, including lipids. Most of the studies in this field show that increase in temperatures stressed the algae out and lipids were accumulated as stress response. For example, with 24-hour 40°C temperature increase of *Scenedesmus quadricauda* batch, lipid productivity increased to 33.5% (23.2 mg/L/day), 39.6% better yield compared to the control group (Han et al., 2016). Another study indicated that mixotrophic algae cultivation induced by 30 °C stress had improved lipid productivity (+24.5% total lipid, +10.2% neutral lipid) (Subhash et al., 2014). Different microalgae species triggered different mechanisms in their lipid metabolisms when temperature stress was applied on them. *Nannochloropsis oculata* had higher lipid yield with a temperature increase from 20°C to 25°C, where *C. vulgaris* lipid decreased from 25°C to 30 °C (Converti et al., 2009).

2.2.5. pH

Culture pH, which is of particular importance for freshwater (pH 6-9) and marine (7.5-8.6) microalgae, tends to increase during growth due to CO_2 assimilation unless there is a pH buffer. pH and CO_2 solubility are also bidirectionally important in autotrophic cultivation to maintain available inorganic carbon source and photosynthetic efficiency. Shifting pH of the culture to suboptimal values change the balance between biomass and lipid productivity. For example, *Ettlia oleoabundans* (*E. oleoabundans*) UTEX 1185 accumulated more lipid when pH 10 and salinity is higher than normal (Santos et al., 2012) and *Scenedesmus sp*. had higher growth and lipid rate under more alkali (pH>9) conditions (Gardner et al., 2010). Another study showed that *Nannochloropsis sp.* strain MASCC 11 had highest lipid content (108.2 mg/L) at pH 6 and 35°C, whereas their highest biomass yield was at pH 9 and 35°C (Xiaoling et al., 2020). Change in pH manipulates the lipid metabolism to store FA with different saturation levels. Saturated FA of *Chlamydomonas sp.* significantly increased at pH 1,

suggesting that it was due to decrease the membrane fluidity to be protected from harmful conditions (Tatsuzawa and Takizawa, 1996).

2.2.6. Other External Factors

Salinity, presence of organic carbon, airflow rate, shear resistance, heavy metal presence and other microbial competitors can be included as potential stress factors for microalgae cultivation. Several studies showed the effect of stress factors mentioned above on lipid accumulation in microalgae. As an example of lipid metabolism selectivity under salinity change, *Chlamydomonas sp.* JSC4 prefers lipid metabolism to starch under high salinity due to induction of lipid synthesis related genes (Hsin Ho et al., 2017). Freshwater microalgae *Chlamydomonas mexicana* and *Scenedesmus obliquus* had the highest biomass and lipid productivity under 25 mM NaCl stress (Salama et al., 2013). In terms of organic source presence, addition of sugars in the media changed the lipid content in the microalgae. Chiranjeevi and Mohan observed that 30 g/L glucose addition with mild temperature stress (20°C) increased lipid productivity (55%) of mixed microalgae culture (Chiranjeevi and Mohan, 2016).

Microalgae cultivation can be used for both lipid production and elimination of heavy metal presence from water. For heavy metal presence, *Nannochloropsis gaditana* (*N. gaditana)* and *Chaetoceros muelleri* had promising lipid contents when cultivated with wastewater for heavy metals bioremediation (Richards and Mullins, 2013). CO_2 aeration percentage was shown to have an inverse relationship with total lipid productivity in *Nannochloropsis oculata* strain NCTU-3 cultivation (Chiu et al., 2009). Apart from these, mechanical stress can be applied to some microalgae species to accumulate lipids. Shear stress is less effective against green algae, but it can be used for lipid accumulation in red algae and dinoflagellates (Wang and Lan, 2018). Ultimately, oxidative stress can be applied to microalgae to achieve higher polyunsaturated fatty acids (PUFAs), as in Sun et al. study for docosahexaenoic acid (DHA) boosting, however overall lipid accumulation was slightly reduced (Sun et al., 2016).

2.2.7. Internal Factors: Lipid Boosting with Metabolic Engineering

Idea of lipid boosting through metabolic engineering practices to microalgae has led to the emergence of the ‘fourth generation biofuel’ concept with specific genetically modified microalgae (Shokravi et al., 2019). Review of Sun et al. categorized the strategies for lipid boosting in microalgae using genetic tools (Sun et al., 2019):

- Regulation of acetyl-CoA carboxylase expression (ACCase)
- Fatty acid synthetase (FAS) pathway alteration
- TAG biosynthesis pathway improvements
- Desaturase/ elongase pathway modification
- Acetyl-CoA synthetase gene (ACS) overexpression
- Knock down of key genes in carbohydrate metabolism (Bypass approach)

Diacylglycerol acyltransferase (DGAT) enzyme is terminal enzyme to synthesize triacylglyceride (TAG). Overexpression of related genes increased the TAG accumulation and neutral lipid content of microalgae species like *Nannochloropsis oceanica* (Wei et al., 2017). Overexpression of *DGAT2* in *Phaeodactylum tricornutum* resulted in 35% neutral lipid increase (Niu et al., 2013). Other genes responsible for activities in lipid metabolism can be edited with genetic tools to achieve higher lipid productivities in microalgae cells. As an example for that statement, random mutation by *Tn5* transposome insertion provided 21.95% total lipid/biomass ratio increase in *N. oceanica* cultivation and 71.13% total lipid in high-lipid mutant clones (Osorio et al., 2019). Desaturase/elongase pathway modification is effective strategy to boost PUFAs like eicosapentaenoic acid (EPA) and DHA, as in Peng et al. study showed that Δ5 desaturase *PtD5b* gene overexpression in *P. tricornutum* increased PUFA yield by 75% (Peng et al., 2014). Transcription factors are emerging properties to regulate lipid metabolism, and Kwon et al. performed that NsbZIP1 transcription factor can improve both lipid and biomass productivity, up to 88% and 39%, respectively (Kwon et al., 2017).

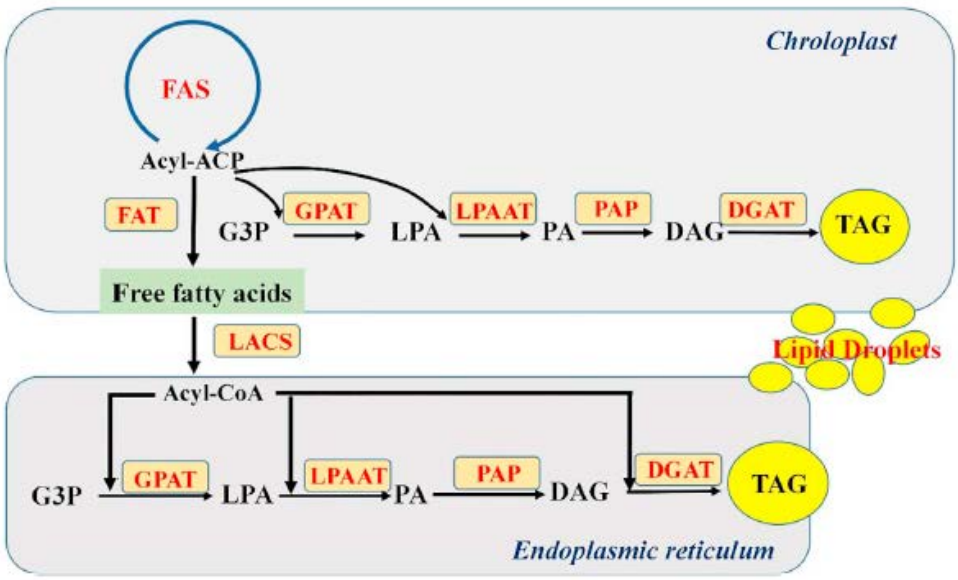

Figure 2.9. Triacylglyceride synthesis pathway in microalgae (Sun et al., 2019).

2.3. Lipid Extraction Methods

For bio-jet fuel production from microalgal lipids, cell disruption of microalgae is required to release the metabolites to the extracellular environment. Afterwards, lipids of the cell extract should be separated from carbohydrates, proteins and other metabolites and collected in one place. In this section, cell disruption strategies and methods to efficiently extract lipids in the environment were discussed.

Diverse microalgae species have differently complex cell wall compositions. It is necessary to analyze the chemical composition of microalgae cell walls to assess which cell disruption method would be more efficient (Gerken et al., 2013). For example, *Chlorella vulgaris* is known to have a cell wall embedded with a plastic polymeric matrix which contains arabinose, uronic acid, fucose, xylose, mannose, galactose, and glucose (Takeda, 1991). On the other hand, eustagmataceae *N. gaditana* strain CCMP526 cell wall in Scholz et al. study had more rigid cell wall structure, which consists of bilayer hydrophobic algaenan layers and heavy cellulosic inner wall between the algaenan layers (Scholz et al., 2014). Since the compositions of the cell walls are different from each other, Gerken et al. showed that enzymatic lysis is also possible using different enzymes for different cell wall composition, which showed that different cell disruption approaches are needed to optimize the lysis of selected microalgae species specifically (Gerken et al., 2013).

Most of the lipid extraction processes have three broad steps: Disruption of microalgae cells, separation using solvents with different polarities, and nonpolar solvent evaporation to obtain algal lipid extract. Meanwhile, cell disruption methods applied to microalgae can be divided as mechanical and non-mechanical methods (Figure 2.10). Bead milling is one of the most widely used mechanical cell disruption methods, especially on small-scale. With its simple definition, glass beads and algae samples are vigorously agitated in the same container, so that the collisions between beads and algae would result in mechanical disruption of cells (Nemer et al., 2021). Material and size of the beads, agitation rate and shear resistance of microalgae affect bead milling performance. Simultaneous cooling processes are also required as rapidly colliding beads increase the temperature in the sample environment.

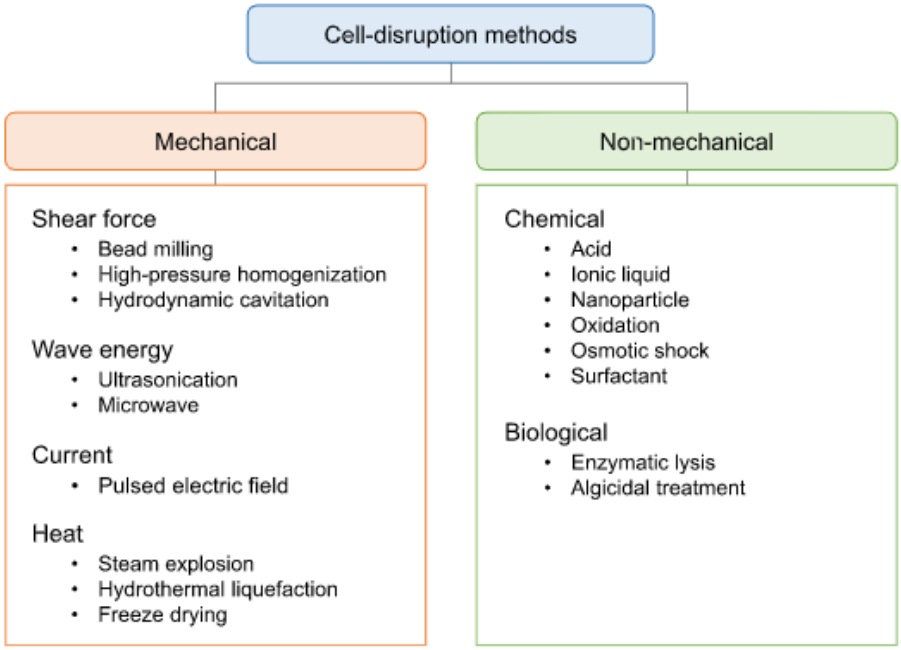

Figure 2.10. Different microalgae cell disruption methods (Lee et al., 2017).

High pressure homogenizer (HPH) is another mechanical cell rupture method by forcing the cells to pass through very narrow nozzle at high pressure up to 2000 bar (Barnaerts et al., 2019), and HPH is widely used in cell disruption of energy crops at industrial scale. *Nannochloropsis oculata* was successfully lyzed, and protein and carbohydrate extraction rates were increased using HPH (Shene et al., 2016). Hydrodynamic cavitation is a relatively novel disruption method by which microalgae slurry is passed through a point with smallest diameter and maximum fluid velocity. The rapid pressure drop creates microbubbles, and their explosion results in the disruption of microalgae cells (Waghmare et al., 2019). Ultrasonication acoustically blasts microalgae cells using soundwaves with high-frequency (>20 kHz). Burst efficiency in microalgae cells using ultrasonication depends on amplitude of sound and on/off pattern (Zang et al., 2019). This method is highly efficient in many microalgae species, but it is energy-intensive and has a high initial capital cost (Kumar et al., 2015). Microwave-assisted cell disruption is frequently used in microalgae disruption, and it may result in a higher lipid yield than other disruption methods (McMillan et al., 2013). Ultimately, microalgal lipids can be mechanically extracted using oil expeller, like olive oil extraction (Topare et al., 2011).

Pulsed electric field (PEF) uses high intensity electric field pulses to rupture cell membranes and facilitate the solubilization of metabolites (Goettel et al.,2013). Electroporation and cell disruption efficiencies depend on cell membrane structure of microalgae, pulse intensity and frequency (Frey et al., 2013).

Non-mechanical cell disruption methods like H_2SO_4 acid hydrolysis, ionic liquid salts, nanoparticles like nickel oxide, osmotic shock (NaCl), surfactants like dodecyl benzene sulfonate (SDBS) and biological disruption approach of enzymatic lysis using cellulase, lipase and protease, and algicidal treatments, which uses other microorganisms to lyze the microalgae cells, are also used for microalgae cell disruption, but they remained niche compared to mechanical approaches.

Most cell disruption methods are used as sole lipid extraction applications, or they assist the main lipid extraction method. These hybrid lipid extraction techniques, like sonication-assisted Bligh&Dyer, have promising lipid yields (Chhandama et al. 2021).

Lipids of pretreated microalgae samples are extracted through conventional solvent extraction methods and its modifications, as shown in Figure 2.11 (Sati et al., 2019). Most used conventional lipid extraction techniques from microalgae can be categorized into four classes: Bligh & Dyer (1959), Soxhlet (1879), Folch (1957) and Hara and Radin (1978).

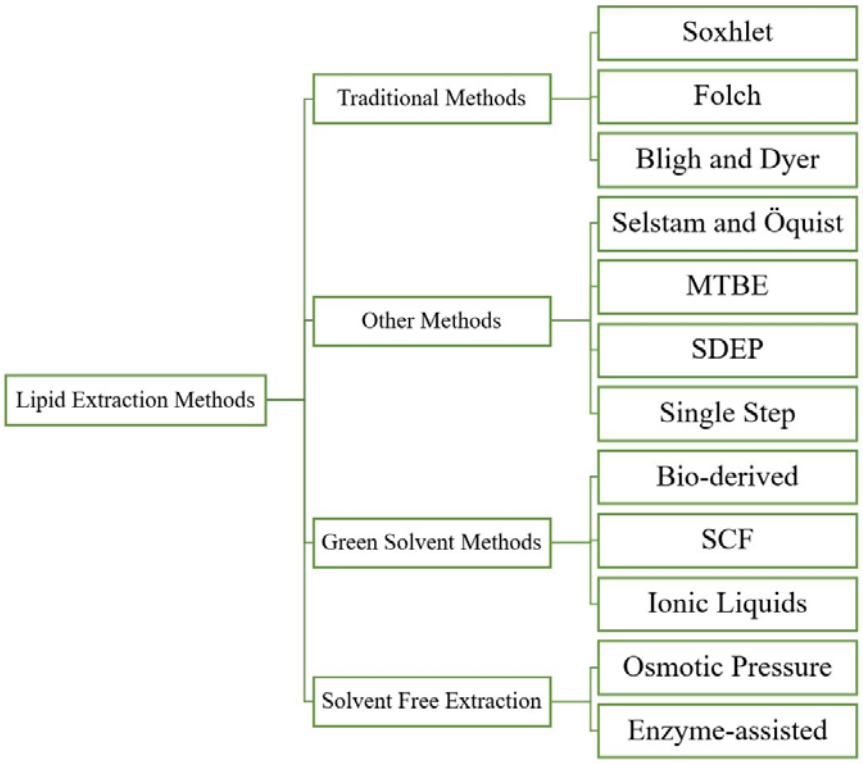

Figure 2.11. Categorization of lipid extraction methods from microalgae.

All methods aim to separate the metabolites (lipids, carbohydrates etc.) in microalgae according to their polarity in the presence of polar and nonpolar solvent, and to collect nonpolar extracts into nonpolar solvent (de Jesus et al., 2019). Both Bligh & Dyer and Folch methods use methanol as polar solvent, chloroform as the nonpolar solvent, and water as a phase separator.

Chloroform:methanol:water ratios are different in these methods, such as: 1:2:0.8 and 8:4:3 for Bligh & Dyer and Folch method, respectively (Iverson et al., 2001).

Results in lipid experiments with different polar-nonpolar solvent ratios also differ (Mustapha and Isa, 2020; Figure 2.12). In literature, 1:1 and 2:1 chloroform:methanol ratio was commonly used to extract microalgae lipids (Ren et al., 2021). In order to enhance phase separation of chloroform:methanol solution, salts (NaCl, $MgCl_2$) were added to lipid extract solutions (Kumar et al., 2018).

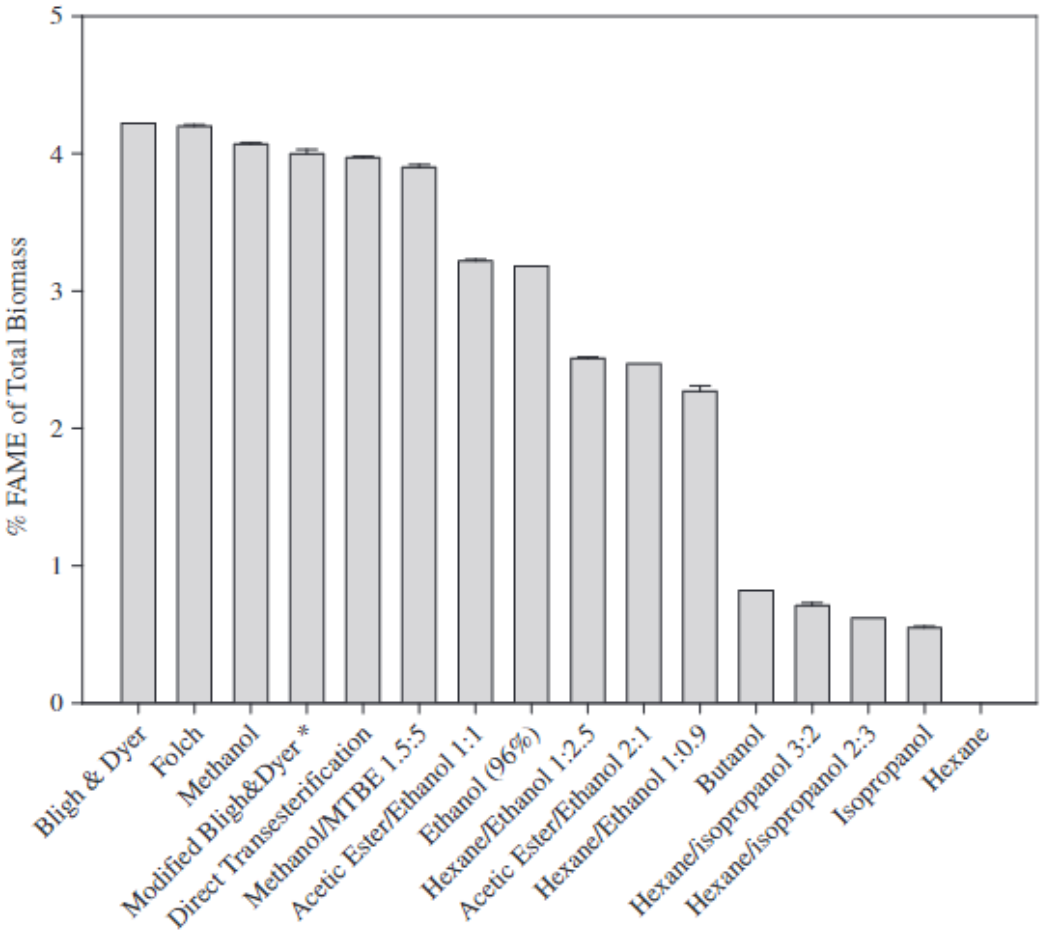

Figure 2.12. Total FAME percentage of *Synechocystis* PCC 6803 biomass using different methods (Sheng et al., 2011).

Soxhlet extraction system is the simplest, oldest, and longest (~8 h) lipid extraction method, by which sample is constantly extracted by refluxing solvent in Soxhlet apparatus (Lopez-Bascon and Castro, 2020). Preferred solvents for Soxhlet extraction are hexane and hexane-ethanol (Li et al. 2014). Soxhlet extraction event at its best was considered as time-intensive and less efficient lipid extraction for several microalgae species than conventional Bligh & Dyer method. Hexane Soxhlet

resulted in less lipid yield than conventional Bligh-Dyer method in the case of *C. gracilis* and *P. carterae* (Kanda et al., 2020). Cheung et al. observed that Soxhlet extraction has lower UFAs, which supports the fact that change in lipid extraction methods result in the FA profile of algal lipid (Cheung et al. 1998).

Lipid extraction using liquefied dimethyl ether (DME) requires more complex design, and less lipid yields than Soxhlet extraction (Bauer et al., 2020).

Methyl-butyl ether (MTBE) is a popular expensive alternative for nonpolar solvent in lipid extraction. Its density is lower than chloroform, which enables easier solvent collection and less dripping loss after separation (Matyash et al. 2009).

Eco-friendly and affordable solvents have been investigated for lipid extraction processes (Kumar et al. 2017). Because chloroform is toxic, bio-derived solvents have been used, for example D-limonene terpene from *Chlorella vulgaris*, and its performance was similar to hexane (Tanzi et al., 2012). Soybean oil methyl esters were used as bio-derived solvent (Spear et al., 2007). With more renewable solvent alternatives, lipid extraction processes will be more sustainable and affordable.

Supercritical fluid extraction (SCF) uses supercritical CO_2 as solvent at above 31.1°C and 7.38 MPa (Sehena et al., 2009). Supercritical fluid extraction offers high lipid recovery with short time and long chain PUFA protection. However capital-intensive and high lipid selective process combined with low solubility of polar lipids in supercritical CO_2 make SCF a better alternative for value-added lipid extraction like omega-3 (Cheng et al., 2011).

2.4. Transesterification and Fatty Acid Methyl Ester Analysis

Triacylglycerides (TAGs) from lipid extraction are required to be transesterified to liberate FAs. Transesterification can be defined as exchange between organic groups of esters and alcohol, as shown in Figure 2.13 (Otera, 1993). Transesterification process can be evaluated under two groups i.e. two-step and in situ transesterification (Figure 2.14). Difference between direct transesterification and two-step transesterification is the requirement of solvent extraction, which can offer higher lipid productivity but high operational cost and time-intensivity (Yoo et al., 2015). Direct transesterification is dominantly chosen against the two-step process.

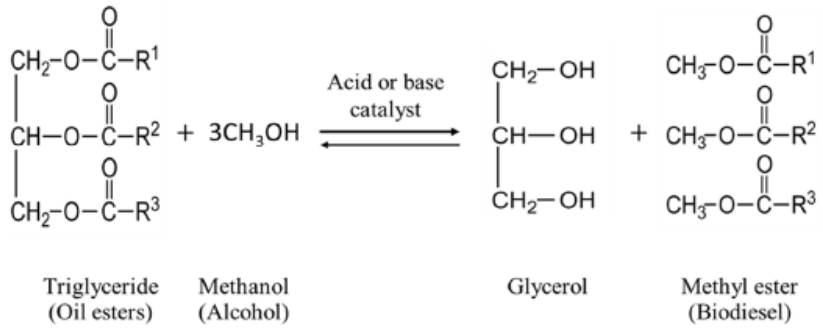

Figure 2.13. Transesterification reaction of microalgal lipids.

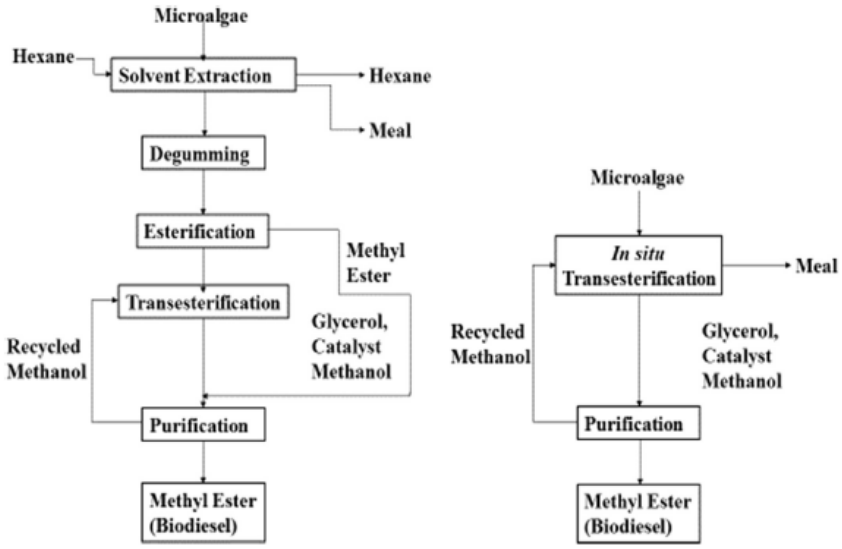

Figure 2.14. Flowchart of two-step transesterification (left) and in situ transesterification (right) (Salam et al., 2016).

Transesterification processes need a catalyst to be accelerated, and there are three types of catalyst which are homogeneous (acid and base), heterogeneous (acid/base + other catalysts) and biocatalyst (Taghavi et al., 2021). Homogeneous catalysts offer easy-to-apply, cheap solutions to catalyze transesterification. Base catalysts (NaOH, KOH) are more applicable and compatible to industrial scale. Additionally, base catalysts are less corrosive, and they do not need higher temperature as acid catalysts demand (Freedman et al., 1985). Acidic catalysts (H_2SO_4), on the other hand, have better lipid recovery rate and higher partitioning coefficient for lipids to dissolve in organic phase (Cavonius et al., 2014). It can be said that acid catalysts are suitable for analysis, as base catalysts are suitable for production.

Sivaramakrsihan and Incharoensakdi showed that at least 1.2% of catalyst is needed to transesterify the lipids to convert FAME efficiently (Sivaramakrsihan and Incharoensakdi, 2017). They also showed that methanol is the best candidate for organic group donors.

Heterogeneous catalysts are metal oxides, supported hydroxides/oxides and zeolites. They provide better usability and separation of catalysts, but they have smaller surface area to be active, and they are resistant to mass transfer (Akubude et al., 2019). FAMEs of *N. gaditana* were synthesized with ion-exchange resins and clay with montmorillonite, better than silica-alumina catalyst (Carrero et al., 2015).

Enzymatic transesterification becomes an interesting topic due to high efficiency and lack of soap byproducts during reaction. Immobilized lipase has been used as a biocatalyst, but it is very expensive for the scale-up process (Ranganathan et al., 2008).

After the transesterification step, the FAME profile of microalgal lipid needs to be analyzed in order to observe quality and quantity of FAs, which will be converted to hydrocarbons for bio-jet fuel. Most applicable method for FAME analysis is using gas chromatography (GC), either with flame ionization detector (-FID) or mass spectrometry (/MS) (Figure 2.15).

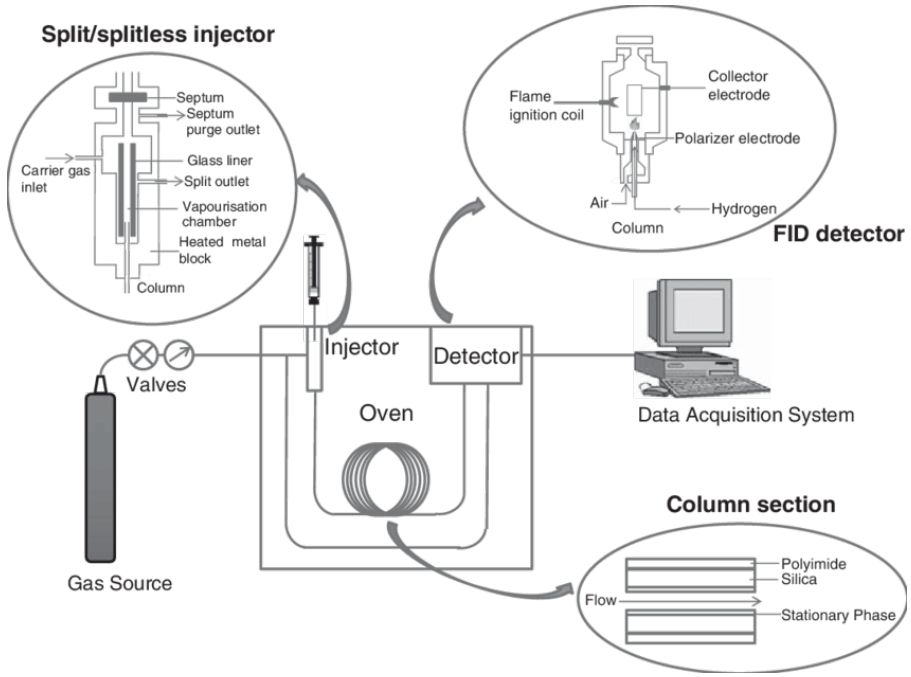

Figure 2.15. Overview of gas chromatography with flame ionization detector (Soria et al., 2014).

GC is an analytic method in which the mobile phase is gaseous form, and it separates volatile compounds according to their boiling point and polarity (Bartle and Myers et al., 2002). Flame

ionization detector ionizes the output gas from the column, ions create a current and the detector measures the change in current non-specifically (Soares et al., 2019). Mass spectrometry, on the other hand, ionizes the metabolite and analyzes their mass/charge ratios to specifically detect the compound (Cutignano et al., 2016). There are packed and capillary columns used in GC, where the former is far inexpensive, simple but less specific, and the letter has more resolution but is very specific and expensive (Mendiola et al., 2008). GC-FID with packed and capillary columns and GC/MS showed comparable results with higher divergence in GC/MS (Niemi et al. 2019). One significant advantage of GC/MS is that GC-FID can analyze only FAME or another class of lipids whereas GC/MS can detect most of lipid classes at the same time. Polarity of column, type and flow rate of mobile phase, injection method (split-splitless), temperature change can affect the retention time of FAs in column and peaks on chromatogram (Figure 2.15).

3. MATERIALS AND METHODS

In this section, preparation and analysis of algal lipids to be optimized for bio-jet fuel production were discussed. To facilitate traceability, the method section is divided into seven subsections: selection of algae strains, determination of algae growth conditions, algae harvesting and dewatering, lipid extraction from algae, lipid purification, transesterification, and FAME profiling.

3.1. Selection of Oleaginous Green Algae Strains

In this study, three different microalgae strains were selected as the species to be used to produce lipids for bio-jet fuel. These strains were *N. gaditana* CCMP 526, *Nannochloropsis sp*. CCAP 211/46, and *E. oleoabundans* UTEX 1185 (Figure 3.1). Strains with UTEX coded was obtained from University of Texas Culture Collection of Algae, CCMP coded from National Center for Marine Algae and Microbiota (USA), and CCAP from Culture Collection of Algae and Protozoa (U.K.). All the strains used in this study were maintained in İstanbul Microalgae Biotechnologies Research and Development Center (IMBIYOTAB) in Boğaziçi University.

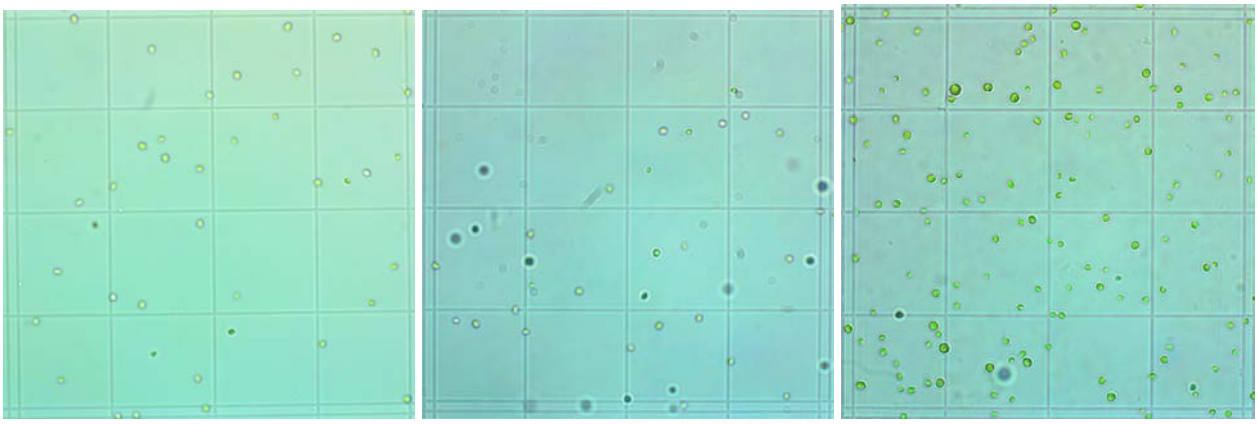

Figure 3.1. 40X Microscope images of *N. gaditana* CCMP 526 (left), *Nannochloropsis sp.* CCAP 211/46 (middle) and *E. oleoabundans* UTEX 1185 (right).

The main reason for selecting *Nannochloropsis* species is that it can show high lipid content and rapid growth at the same time, which is unlikely, in the literature (Matos et al., 2015). *Nannochloropsis* strains, known as a species resistant to external stresses, offer promising optimization options for lipid accumulation in outdoor open raceway ponds. As marine algae species, robust growth can be achieved without the need for freshwater use and minimal nutrient requirement.

With 2–3-micron cell radius and rigid cell walls, cell disruption of *Nannochloropsis* is still a challenge in the algal lipid research field.

The choice of *E. oleoabundans* species for lipid production is to extend jet fuel literature by adding algae species which have different features in this study. *E. oleoabundans* is a green alga that can grow both in fresh and saltwater, is versatile, and has a lipid content of up to 40% dry weight in the literature (Pruvost et al., 2009). Considering the technical expertise of the project team in working with this species, it was decided to observe the performance of *E. oleoabundans* in jet fuel studies.

3.2. Determination of Physicochemical Parameters for Microalgae Cultivation

As mentioned in the literature section 2.2, changes on extracellular parameters trigger lipid accumulation in microalgae cells. In this study, it was aimed to observe how total lipid and FAME concentrations of cultivated microalgae at the same scale would change by changing nutrient compositions, i.e., using different media. The responses to change in nitrogen concentration were observed by reducing the amount of nitrogen for all growth conditions. It was decided to select two promising growth conditions and to scale-up their cultivation volume in order to examine the growth and lipid accumulation behaviors of two conditions under outdoor large-scale cultivation. All technical details were explained under three headings in this subsection.

3.2.1. Different Nutrient Compositions in Small-scale Batches

In this subsection, small-scale PBR setup and the composition and preparation of four different media, in which microalgae were tested, were discussed.

3.2.1.1. Small scale PBR design. With 2L Erlenmeyer flask and a silicone stopper for each sample, an environment where sterility, light and air flow are suitable was prepared for small-scale algae cultivation. Working volume in the 2L Erlenmeyer flask was kept constant as 1650 mL media. Glass pipe was passed through the silicon stopper to ensure air flow. 0.45 μm filter was placed on the air inlet side of the pipe to prevent impurity from entering the reactor. Air diffuser was attached to a thin glass pipe outlet to distribute incoming air evenly in the reactor. S-shaped airlock is installed on the silicone stopper to ensure air outlet. Each reactor was constantly aerated with 0.5 L/min dry air flow. For the algae inside the reactor to not crash and grow efficiently, the reactors were stirred continuously using a magnetic stirrer. LED daylight sources and plug-in timer were used to ensure that each species provides the optimal light intensity and light-dark cycle for its cultivation. For *E.*

oleoabundans, 140 µmol m^{-2} s^{-1} light intensity and 14:10 h light:dark cycle were applied, while 200 µmol m^{-2} s^{-1} light intensity and 12:12 h light:dark cycle were applied for *N. gaditana* and *Nannochloropsis sp.* Optical density at 680 nm, pH, and temperature data of small scale PBRs were daily measured, cell count concentration was measured every two days. 5 mL of sample was taken from PBRs every day for data acquisition, and 5 mL of relevant media was added to each reactor in order not to change the working volume.

Figure 3.2. Small-scale PBR design in 2L Erlenmeyer flask.

3.2.1.2. Determining the types of media and nutrient compositions to be used for algae cultivation. For the cultivation of *E. oleoabundans*, Modified Bold 3N Medium (MB3N) medium prepared with fresh deionized water is used. It was decided to select 3 different media for *N. gaditana* and *Nannochloropsis sp*. in artificial seawater where marine conditions were provided. Considering the studies in the literature, these media were determined to be f/2 medium, Algal custom medium, and Mann&Myers (M&M) medium (Pedro et al., 2013). Component concentrations of the four media used are as shown in Table 3.1, Table 3.2 and Table 3.3 respectively.

Table 3.1. Concentration (g/L) of components in Algal, M&M, f/2, and MB3N media.

Component	Algal (g/L)	M&M (g/L)	f/2 (g/L)	MB3N (g/L)
NO_3^-	4.9×10^{-1}	7.3×10^{-1}	5.0×10^{-2}	5.5×10^{-1}
PO_4^{3-}	4.0×10^{-2}	5.0×10^{-2}	3.4×10^{-3}	1.6×10^{-1}
SO_4^{2-}	9.0×10^{-5}	4.7×10^{-1}	3.8×10^{-3}	6.2×10^{-2}
K^+	3.1×10^{-1}	2.0×10^{-2}	-	1.1×10^{-1}
Ca^{2+}	-	1.1×10^{-1}	-	6.8×10^{-3}
Mg^{2+}	-	1.2×10^{-1}	-	7.3×10^{-3}
Fe^{2+}	2.4×10^{-3}	4.0×10^{-4}	6.5×10^{-4}	1.2×10^{-4}
Cu^{2+}	6.0×10^{-5}	5.1×10^{-7}	2.5×10^{-6}	-
Co^{2+}	4.5×10^{-5}	1.4×10^{-6}	4.0×10^{-6}	3.0×10^{-6}
Zn^{2+}	3.0×10^{-4}	7.5×10^{-5}	5.0×10^{-6}	1.4×10^{-5}
Mn^{2+}	3.7×10^{-4}	6.1×10^{-4}	5.0×10^{-5}	6.9×10^{-5}
B^{3+}	-	1.1×10^{-3}	-	-
Mo^{6+}	5.4×10^{-4}	-	2.5×10^{-6}	9.8×10^{-6}
EDTA	9.4×10^{-3}	2.6×10^{-2}	3.5×10^{-3}	2.7×10^{-4}

Table 3.2. Freshwater medium MB3N recipe (UTEX, 2016).

		Freshwater Medium MB3N	
	Compound	**g/L**	**mM**
Macronutrients	$NaNO_3$	7.5×10^{-1}	8.82
	$CaCl_2.2H_2O$	2.5×10^{-2}	1.7×10^{-1}
	$MgSO_4.7H_2O$	7.39×10^{-2}	3.0×10^{-1}
	KH_2PO_4	5.9×10^{-2}	4.3×10^{-1}
	K_2HPO_4	2.25×10^{-1}	1.29
Micronutrients	$ZnCl_2$	3.03×10^{-5}	2.22×10^{-4}
	$Na_2MoO_4.2H_2O$	2.47×10^{-5}	1.02×10^{-4}
	$Na_2EDTA.2H_2O$	4.47×10^{-3}	1.20×10^{-2}
	$FeCl_3.6H_2O$	5.83×10^{-4}	2.15×10^{-3}
	$MnCl_2.4H_2O$	2.49×10^{-4}	1.26×10^{-3}
	$CoCl_2.6H_2O$	1.20×10^{-5}	5.04×10^{-6}
Vitamins	B12*	1.35×10^{-4}	9.96×10^{-5}
	Biotin*	2.5×10^{-5}	1.02×10^{-4}
	Thiamine*	3.0×10^{-6}	1.13×10^{-5}

In all small-scale bioreactors cultivating *N. gaditana* and *Nannochloropsis sp.*, marine salt was added to fresh water to reach a 25-30 ppt (or g/L) salinity to imitate marine environment before starting the media.

All media were prepared with aliquots from sterile stock solutions, and all media and PBR equipment were autoclaved at 121°C for 15 min before PBR preparation. After the media and PBR equipment were ready, it was important during algae inoculation to keep cell concentration of starting culture at day zero around 4 million cells/mL. All media conditions were studied as triplicates.

Table 3.3. Media recipe of marine media (modified version of Pedro et al., 2013).

	f/2		Algal		M&M	
Compound	**g/L**	**mM**	**g/L**	**mM**	**g/L**	**mM**
$NaNO_3$	7.5×10^{-2}	8.82×10^{-1}	6.71×10^{-1}	7.89	1	11.77
$Na_2HPO_4.H_2O$	5.0×10^{-3}	3.13×10^{-2}	5.88×10^{-2}	3.67×10^{-1}	7.35×10^{-2}	4.59×10^{-1}
KCl	-	-	6.0×10^{-1}	8.05	3.9×10^{-2}	5.23×10^{-1}
Na_2SO_4	-	-	-	-	6.71×10^{-1}	4.73
$CaCl_2.2H_2O$	-	-	-	-	4.03×10^{-1}	2.74
$MgCl_2.6H_2O$	-	-	-	-	1	4.92
Na_2SiO_3	2.04×10^{-2}	1.67×10^{-1}	1.22×10^{-2}	9.96×10^{-2}	1.29×10^{-2}	1.06×10^{-1}
$FeSO_4.7H_2O$	3.25×10^{-3}	1.17×10^{-2}	1.2×10^{-2}	4.32×10^{-2}	1.82×10^{-3}	6.55×10^{-3}
$CuSO_4.5H_2O$	9.8×10^{-6}	6.14×10^{-5}	2.4×10^{-4}	1.50×10^{-3}	2.01×10^{-6}	1.3×10^{-5}
$Co(NO_3)_2.6H_2O$	1.97×10^{-5}	6.78×10^{-5}	2.25×10^{-4}	7.73×10^{-4}	7.0×10^{-6}	2.4×10^{-5}
$ZnCl_2$	1.04×10^{-5}	7.63×10^{-5}	6.27×10^{-4}	4.60×10^{-3}	1.6×10^{-4}	1.17×10^{-3}
$MnSO_4.H_2O$	1.54×10^{-4}	9.1×10^{-4}	1.32×10^{-3}	7.81×10^{-3}	2.13×10^{-3}	1.26×10^{-2}
$Na_2MoO_4.2H_2O$	6.3×10^{-6}	2.6×10^{-5}	1.35×10^{-3}	5.58×10^{-3}	-	-
$Na_2EDTA.2H_2O$	4.48×10^{-3}	1.20×10^{-2}	1.21×10^{-2}	3.22×10^{-2}	3.3×10^{-2}	8.82×10^{-2}
H_3BO_3	-	-	-	-	6.28×10^{-3}	1.02×10^{-1}
B12*	1.35×10^{-4}	9.96×10^{-5}	1.35×10^{-4}	9.96×10^{-5}	1.35×10^{-4}	9.96×10^{-5}
Biotin*	2.5×10^{-5}	1.02×10^{-4}	2.5×10^{-5}	1.02×10^{-4}	2.5×10^{-5}	1.02×10^{-4}
Thiamine*	3.0×10^{-6}	1.13×10^{-5}	3.0×10^{-6}	1.13×10^{-5}	3.0×10^{-6}	1.13×10^{-5}

*: In large-scale cultivation, low purity vitamin complex was used to achieve related vitamin concentrations.

3.2.2. Nitrogen Deprivation in Small-scale Batches

Since the most used method to trigger lipid accumulation in microalgae is to create an extracellular stress factor by reducing the nitrate concentration in the media, it was decided to observe the growth conditions and lipid content of all media conditions planned to be tested in subsection 3.2.1.2, where only nitrate concentrations were reduced by one-tenth. Media prepared with nitrate concentrations reduced by one tenth were designated as N-deprived, N-deplete or simply N- whereas

normal media were designated as N-repletion, N-replete or simply N+. All equipment design, cleaning and media preparation procedures for N-replete growth conditions and other physicochemical conditions (light intensity, mixing speed, air flow rate etc.) are the same for N-deprived growth conditions (as shown in subsection 3.2.1.1 and 3.2.1.2). The only difference is tenfold difference in nitrate concentrations. Nitrate concentrations in N-replete and N-deprived conditions are given in Table 3.4. All remaining component concentrations of the media were held constant.

Table 3.4. Nitrate concentration in N-repleted and N-deprived media.

Nitrate concentration (NO_3^- g/L)	**Algal**	**M&M**	**f/2**	**MB3N**
N-repleted	4.9×10^{-1}	7.3×10^{-1}	5.0×10^{-2}	5.5×10^{-1}
N-deprived	4.9×10^{-2}	7.3×10^{-2}	5.0×10^{-3}	5.5×10^{-2}

3.2.3. Selection of Promising Conditions and Scale-up Process

Three species selected in subsection 3.1 were cultured with difference in media type and nitrate concentrations in subsection 3.2.2. Fourteen conditions tested on a small scale are in Table 3.5.

Table 3.5. Fourteen growth conditions tested in 2L PBRs.

Condition No	**Species Name**	**Media Name**	**Nitrate Condition**
1	*Nannochloropsis gaditana*	f/2	N+
2	*Nannochloropsis gaditana*	f/2	N-
3	*Nannochloropsis gaditana*	Algal	N+
4	*Nannochloropsis gaditana*	Algal	N-
5	*Nannochloropsis gaditana*	M&M	N+
6	*Nannochloropsis gaditana*	M&M	N-
7	*Nannochloropsis sp.*	f/2	N+
8	*Nannochloropsis sp.*	f/2	N-
9	*Nannochloropsis sp.*	Algal	N+
10	*Nannochloropsis sp.*	Algal	N-
11	*Nannochloropsis sp.*	M&M	N+
12	*Nannochloropsis sp.*	M&M	N-
13	*Ettlia oleoabundans*	MB3N	N+
14	*Ettlia oleoabundans*	MB3N	N-

As a result of the experiments, considering dry weight of biomass, growth performances, lipid to biomass ratio and FAME content, also to observe outdoor cultivation performance of different microalgae species, condition #3 (*N. gaditana*, Algal medium, N-replete) and condition #13 (*E. oleoabundans*, MB3N medium, N-replete) were selected to scale-up. In the next part of subsection, PBR designs used in the scale-up process and differences in small-scale and large-scale inoculation were discussed.

Figure 3.3. Scale-up process of microalgae cultivation (2L, 12L, 100L, 1000L and 15000L).

3.2.3.1. PBR and open raceway ponds used in scaling-up process. Microalgae grown in a 2 L Erlenmeyer flask as seed were inoculated into 12L indoor PBRs, and then outdoor 100L and 1000L open ponds, respectively. In order to decide on the next scaling stage in cultivation, it was waited for microalgae to reach mid-exponential growth period, and then inoculation was carried out. While scaling up from 2 to 12 L of cultivation volume, either a tubular PBR or glass carboy system was used. Growth and lipid differences between these two PBRs with same cultivation volume on one condition (condition #13) were also shown in the result section.

3.2.3.1.1. 12L tubular PBR design. Designed as 12L tubular PBR, Phyco-bubble (VariconAqua, UK) has an 11 cm outer radius and 1.5 meters length. They are made of Schott borosilicate glass and corrosion-resistant aluminum. Air inlet of the reactor is accompanied by an air diffuser from the bottom part. There are 4 air filter outlets of 0.45 microns for the air outlet on the top cover. Gro-lux broad spectrum fluorescent lighting (Slyvania, UK) is designed to boost algal growth and can reach 200 μmol m^{-2} s^{-1} light intensity. The day before using the PBR, it was filled with 12L of distilled water and sterilized overnight with 2 mL sodium hypochlorite addition while aeration occurs. In this tubular PBR system, all microalgae cultivation requirements in 2L were met.

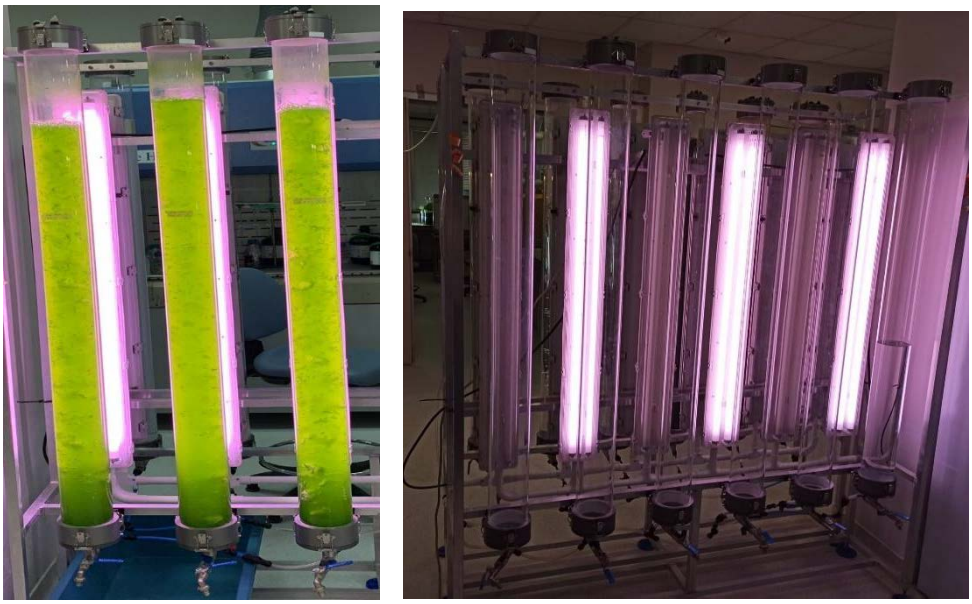

Figure 3.4. 12L tubular PBRs.

3.2.3.1.2. 15L glass carboy PBR design. Culture plug sponge made microalgae cultivation possible in 15-liter glass carboys. Inside of the reactor was aerated with an air hose with a 0.45μm filter inlet, which was dipped into the reactor by using elasticity of sponge. Each reactor was thus supplied with a 2L/min dry air flow. Unlike 2L PBRs, the air diffuser is not connected to the end of the hose that gave air to the reactors, and the media inside the carboy circulated with the bubble created by airflow itself. Light intensity and day-night cycle are provided as in 2L reactors. Glass carboys were autoclaved with media inside at 121°C for 15 min. and the inoculation process was carried out in a sterile environment. With the design installed in 15-liter glass carboys, microalgae seed was cultivated in large volume and under well-controlled conditions.

Figure 3.5. 15L glass carboy PBR.

3.2.3.1.3. 100L, 1000L and 15000L open raceway ponds. Large-scale microalgae cultivation in outdoor was operated in open raceway ponds in batch mode. All outdoor ponds were purchased from Microbio Engineering Inc. (CA, USA). Microalgae grown in 12L PBRs inside were first inoculated into 100L open ponds (RW0.5i). Tank parts are rotational-molded food-grade HDPE with UV stabilizer which enables the tank durability and lightweight. Pond uses magnetic mount 24V DC impeller mixers instead of paddle wheels, which are cheaper and safer. Impeller mixers rotate at approximately 4200 rpm to mix the microalgae culture. 100 L Open pond has 0.5 m^2 cultivation area per pond and 0.2 m max operating depth.

1000L open pond (RW 3.4) is similar to 100L open pond, except it has a stainless paddle wheel for mixing and aeration. Microalgae in this open pond has around 35 hertz rotational speed. the 1000L open pond has 3.4 m^2 cultivation area with 30 cm operating depth. Both 100L and 1000L ponds are elevating above ground by 20-30 cm.

The 15000L open pond (RW50) is prefabricated algae raceway including containment walls, NSF61 potable water grade liner and 316 stainless paddle wheels. Paddle wheels were run at 30-35 hertz rotational speed during microalgae cultivation.

Figure 3.6. 100L, 1000L and 15000L open raceway ponds, respectively.

Unlike indoor growing conditions, outdoor ponds were not supplemented with additional airflow, and light source. The light in microalgae cultivation in outdoor ponds comes entirely from the sun, and light intensity and daylight duration are directly related to the daily and seasonal conditions of the sun. Likewise, since algae are in direct contact in ambient air, they are vulnerable to contamination and affected by weather conditions such as rain and storm. These characteristics, which can create significant differences with indoor growing conditions, affect different growth and lipid content responses in the same species and in the same nutrient concentrations.

Difference between outdoor cultivation and indoor cultivation is as follows: Since there is no autoclave option for cleaning, open ponds were rinsed with tap water being used for cultivation and the dirt accumulated in ponds was drained. Then the entire surface was scrubbed with hydrogen peroxide diluted to a very low concentration, and all surfaces were again heavily rinsed with tap water to avoid any hydrogen peroxide residue. In media usage, chemical sacks containing 96-99% purity were purchased, and chemicals were poured into the ponds in solid form and the media was prepared in the pool. The use of industrial vitamins, which are used in 1-2% purity suitable for high-volume biomass production, was applied, rather than the high purity level used in indoor cultivation. For *E. oleoabundans*, soilwater solution was not used because of the volume needed in outdoor cultivation. Instead, an amount of nitrate and phosphate in soilwater was added to open ponds. For marine species, the marine salt used for indoor cultivation remained expensive and insufficient in volume, therefore artificial saltwater was prepared with chemical supplements for tap water in accordance with sea salt analysis for the preparation of artificial saltwater. Chemical recipe used for the artificial saltwater in open ponds is shown in Table 3.6.

Table 3.6. Chemical recipe of artificial saltwater for outdoor cultivation.

	Saltwater	
Compound	**g/L**	**mM**
NaCl	18	308.01
$CaCl_2.2H_2O$	5.6×10^{-1}	3.81
H_3BO_3	1.65×10^{-2}	0.27
$MgSO_4.7H_2O$	3.3	13.39
K_2SO_4	3.5×10^{-1}	2.01
$NaCO_3$	1.25×10^{-1}	1.18
$SrCO_3$	7.45×10^{-3}	0.05

3.3. Harvesting and Dewatering of Microalgae Photobioreactors using Centrifugation and Lyophilization

Harvesting process of microalgae cultures was initiated when the cultures were in stationary phase during their growth stages. For small-scale cultivation, harvesting was done by transferring microalgae in 50 mL falcon tubes using serological pipettes and the samples were centrifuged at 4500 rpm for 10 min (U-320 Centrifuge, Boeco, Germany) in a rotor suitable for 50 mL falcon tubes. For *N. gaditana* and *Nannochloropsis sp.*, extra centrifugation was performed if the supernatant appeared yellow-green. The supernatant was discarded, and microalgae pellets were kept at -20°C. Portion of the pellets was lyophilized at -110°C (HC4110, GYROZEN, Korea) for lipid extraction.

For medium-scale (100-1000L) cultivation, two options were used. Option #1 was centrifugation using a 12L ultracentrifuge which was efficient and labor-intensive. Option #2 was centrifugation using small-scale decanter (T10, Evodos, Netherlands) which had efficiency issues because it did not work with high volume samples (5000L+). Option #1 had only been used in some of 100L open ponds. Dewatering of medium-scale ponds was usually performed using a decanter. During harvesting, samples were sent from the pond to the decanter via hose connected to the small discharge pump (Figure 3.7). Paste-shaped biomass was packed and kept at -20 °C.

Figure 3.7. Centrifuge and decanter Evodos T10 used for harvesting and dewatering.

For large-scale cultivation (15000L), culture was collected in the 8 m^3 reservoir, taken into holding tanks and cleaned of sand and other impurities using hydrocyclones. The microalgae culture was concentrated in an industrial separator, then passed through the washing tank and sent to the high-pressure homogenizer (Ariete NS3015, GEA, Germany) where the cells were mechanically disrupted at a pressure of up to 1200 bar (Figure 3.8). The barrel with homogenized algae samples was stored in the +4°C room.

Figure 3.8. Hydrocyclane, separators (left) and homogenizer (right) for large-scale dewatering.

3.3.1. Dry Weight Calculation of Algal Biomass

For the dry weight determination of each algae growth condition, the dry weight calculation method from Zhu et al. was adapted to all samples (Zhu et al., 1997). The day before the experiment, for each sample, GF/A Whatman glass fiber filters (round, 47 mm, 1.6 µm pore size) were placed in an aluminum weighing dish and combusted at 450°C for 2 hr. Filters in dishes were stored in a desiccator overnight. Next day, empty filters and aluminum dishes were weighed. Filter system was assembled by placing filter on porous filter stone and vacuuming, as can be seen in Figure 3.9. Several mL of ultra-pure water (UPH_2O) was filtered before the sample for conditioning. 10 mL of liquid samples taken from algae culture were filtered under vacuum. For marine microalgae cultures, 20 mL of 0.5 M ammonium formate solution were added to filter to eliminate salts. Each filter was combusted in a drying oven at 105°C for 2 h. Filters were cooled down and kept in a desiccator for 30 min. Filters with dry biomass were weighed again.

Figure 3.9. Filtering unit for dry weight measurements.

Dry weight of algal sample (g/L) was calculated as shown in Equation 3.1:

$$M_{biomass} = (F_f - F_i) \times 100 \quad (3.1)$$

where;

$M_{biomass}$ = Dry weight of algae sample in culture

F_f = Final weight of filter after 105°C combustion and desiccation

F_i = Initial weight of filter before 105°C combustion and desiccation

For ash free dry weight calculation, dried filters which were used in dry weight determination were combusted into a muffle furnace at 450°C for 4 hours. After cooled down and kept in a desiccator for 30 min., filters were weighed. Ash content of dried algae biomass was calculated using the same equation above.

3.4. Total Lipid Extraction

In this section, the methods used to gravimetrically determine the total amount of lipid from both dried and wet microalgae and the purification process applied to the extracted oil were explained.

3.4.1. Lipid Extraction from Lyophilized Powder Microalgae

Modified Bligh & Dyer method with extensive cell disruption by Breuer et al. (Breuer et al., 2013) was applied to all microalgae samples to extract total lipids and quantify as percentage dry weight (%DW). First, polypropylene (PP) microtubes were prepared for bead beating by adding 300 mg of 0.1 mm and 100 mg of 0.5 mm diameter glass beads inside. Glass beads were kept overnight in 1 M strong acid, then rinsed with deionized water and dried in oven overnight (Daihan Scientific, South Korea) at 105 °C. 50 ± 1 mg lyophilized microalgae powder (sample) of each batch was added to PP microtubes with beads. As internal standard, known amount of pentadecanoic acid (C15:0) was added and mixed in chloroform:methanol 4:5 (v/v) solution to achieve a certain pentadecanoic acid concentration in solution, which is 50 mg/L. 1 mL chloroform:methanol 4:5 (v/v) solution containing pentadecanoic acid was added to each sample. Samples were bead beaten in tissue homogenizer (Miniliys' lyser, Bertin Technologies, France) 8 times at 4000 rpm for 60 sec, 2 min cooling down in between (24 min total). Homogenate and beads were transferred to a glass centrifuge tube with Teflon septum screw caps (Kimble Tubes). To ensure that all inside bead beating tubes were transferred, 1 ml chloroform: methanol 4:5 (v/v) solution with internal standard was added to the tubes, mixed and transferred to glass tubes three times (4 mL chloroform:methanol total). Glass tubes were vortexed 5 sec and sonicated in a sonication bath (Sonorex Super RK 102 H, Bandelin, Germany) for 10 min. 2.5 mL of distilled water which has 50 mM Tris and 1 M NaCl, and 7 pH using HCl was added to each sample to enhance the phase separation between chloroform and methanol. 5 sec vortex and 10 min sonication were applied to all samples. Samples were centrifuged at 1200 *g* for 5 min. Clean empty glass tubes for each sample were carefully weighed before any chloroform addition occurred. Chloroform phase between the methanol/water phase and beads were collected to clean the glass tube by glass Pasteur pipette. Samples were re-extracted at least once by adding 1 mL chloroform to *first glass tubes*. Same phase separation step was operated (5 sec vortex, 10 min sonication and 1200 *g*

centrifugation for 5 min). Bottom chloroform phase was pooled with the same chloroform in a clean glass tube. Collected chloroform was evaporated under inert (N_2) gas flushing. After all chloroform was evaporated, glass tubes with remaining extracts were weighed. Weight of remaining extract was gravimetrically found by subtracting empty glass tube from glass tube with extract inside.

Figure 3.10. Lyophilized microalgae powder (left), dried microalgae in chloroform:methanol solution in bead milling tube (middle), algal lipid extract samples (right).

Total lipid percentage of microalgae biomass was calculated by dividing the weight of remaining extract by amount of microalgae biomass added, which was shown in Equation 3.2. Extracts were stored in -20 °C for further processing.

$$\%_{lipid} = M_{extract} / M_{biomass} \times 100 \quad (3.2)$$

where;

$\%_{lipid}$ = Dry weight percentage of total lipid inside the microalgae biomass

$M_{extract}$ = Mass of remaining extract inside the glass tube after chloroform is evaporated

$M_{biomass}$ = Mass of weighed microalgae biomass (50 ± 1 mg)

3.4.2. Lipid Extraction from Wet Biomass

Among the seven different procedures suitable for extracting lipid from wet biomass without drying, modified Bligh & Dyer method of Gadora and Janda, which optimizes the use of solvents with ease of pretreatment and operation, was adopted (Garoma and Janda, 2016). Lipid extraction from wet biomass was applied to only large-scale microalgae cultivation, which were *N. gaditana* with Algal media in N-replete condition and *E. oleoabundans* in MB3N media in N-replete condition. 5 g wet biomass which their solid content was known were weighed in tubes. For pH pretreatment, samples of pH were adjusted to 3.2 using concentrated acetic acid. For ultrasonication as cell

disruption, 10 min. intervals of sonication ultrasonication (Sonopuls HD 4100 with TS 103 probe, Bandelin, Germany) were applied to all samples with 80% amplitude and 3s pulse-2 s off cycle. 10 min. 30 min and 50 min sonication pretreatments were applied to *N. gaditana* for cell disruption. In biomass:chloforom 1:10 ratio as default, 5 mL chloroform and 10 mL methanol were added for each gram of dried algae in wet biomass. Samples were vigorously shaken and vortexed for 3 min. 5 mL chloroform were added and samples were shaken and vortexed for 3 min. 5 mL distilled water (dH_2O) was added to each sample and samples were vortexed for 5 min (11 min. total vortex). Dry biomass:chloroform:methanol ratio was 1:10:10. Phase separation was achieved using centrifugation (U-320 Centrifuge, Boeco, Germany) at 3140 g for 20 min. Fresh empty tubes were weighed and the bottom chloroform phase of each sample was transferred to the weighted empty tube. Chloroform was evaporated using a nitrogen flushing unit. If the wet biomass amount is more than 15 mL for each sample, instead of nitrogen gas use, rotary evaporator (Rotavapor R-300, BUCHI, Germany) was used to evaporate chloroform at 60°C, 375 mbar and 150 rpm rotational speed. Extracts remaining on the tubes were weighed. Lipid percentage of the samples were calculated using the equation above.

While performing biomass:solvent ratio optimization experiments, the same method above was applied to samples, only dry biomass:chloroform:methanol ratio of 1:10:10 and 1:20:20 were tested.

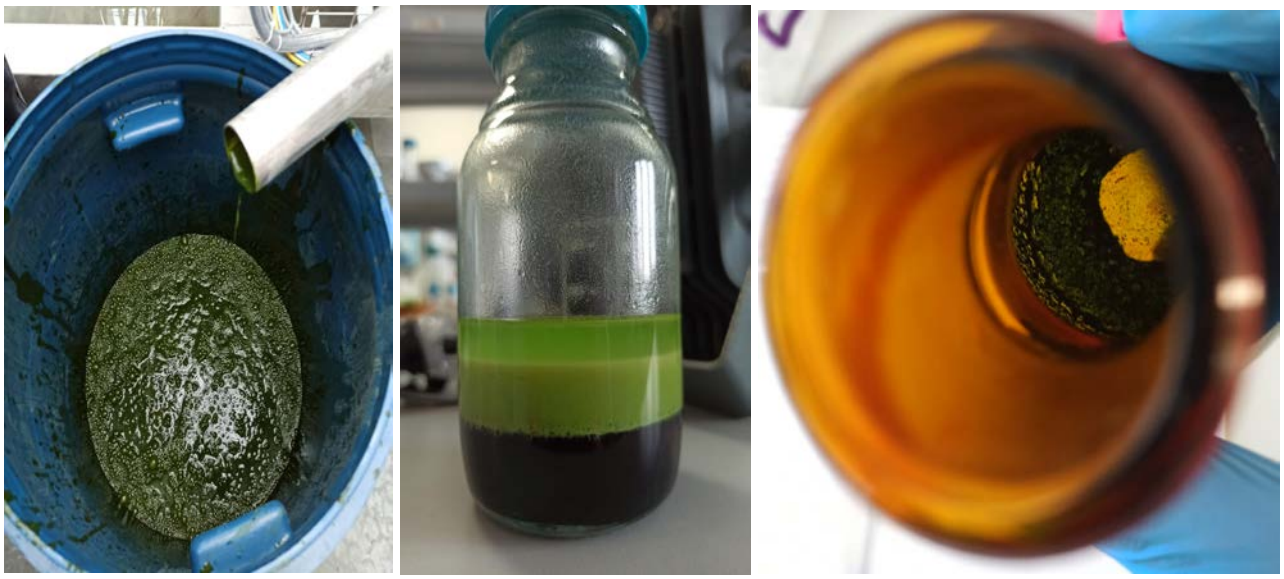

Figure 3.11. Homogenized *N. gaditana* in barrel (left), chloroform:methanol phase separation stage during lipid extraction (middle), lipid extracts after chloroform evaporation (right).

All the 15000-liter *N. gaditana* open ponds were treated with industrial high pressurize homogenizer with pressures from 400 bar to 1200 bar for several minutes at every 200 bars. Sample

were taken at 400, 600, 800, 1000 and 1200 bar homogenization step and the lipid extraction method described in this section was applied to the homogenized wet biomass. pH pretreatment and ultrasonication were not applied in wet biomass samples which industrial high pressurize homogenizer was used for cell disruption.

3.5. Algal Lipid Purification

In this section, lipid extracts of homogenized *N. gaditana* were aimed to be purified for bio-jet fuel conversion. In order to design robust and sustainable lipid extraction and purification stages, algal lipids were tested in four steps.

15 g homogenized wet biomass (5.7% solid content) was tested in 15 mL of acetonitrile and absolute ethanol to observe the performance of these solvent in biocrude extraction. 0.9 g $MgSO_4$, as water scavenger, and tubes were vigorously shaken for 5 sec. Samples were centrifuged at 4500 rpm at 4°C for 20 min. Four different activated carbon (AC) concentrations (3,8,30 and 50 mg AC/ml) were used to observe the performance of this pigment remover. Samples were vigorously shaken for 5 sec and mixed with a test tube rotator at 60 rpm for 1 hr. Samples were centrifuged 4500 rpm at 4°C for 20 min. 5mL of supernatant was transferred to the new tube and 5 mL chloroform ($CHCl_3$) was added. New samples were centrifuged at 4°C for 5 min. Bottom phase was transferred to the pre-weighed Kimble tube and solvents were evaporated using nitrogen flushing. FAME analysis of these samples was performed according to method 3.6 subsection.

Different modifications and scaling-ups of that design were tested, methods can be roughly divided in three types. Design of all experiments followed the pathway explained above. First, 150 g homogenized *N. gaditana* was tested with 150 mL methanol (MeOH) and 150 mL ethanol (EtOH) with 3 mg/mL AC. 400 mL of crude extract was transferred to 1L separatory funnel in this case, and 400 mL chloroform added. Bottom chloroform phase was collected after phase separation was achieved. Chloroform, methanol, and ethanol were evaporated by using a rotary evaporator at 50°C, 97mbar vacuum and 150 rpm rotational speed. Dissolved and non-dissolved parts were collected separately into pre-weighed Kimble tubes. Samples were weighed and transesterified according to method 3.6 subsection.

Second, 600 g homogenized *N. gaditana* was tested with 300 mL MeOH and EtOH with 3mg/mL AC. Samples were vigorously shaken for 5 sec. and centrifuged at 3300 rpm at 4°C for 30 min. Supernatant was collected in 1L separatory funnel, and 200 mL $CHCl_3$ was added. Bottom chloroform

phase was collected to 1L round bottom flask after phase separation was achieved. Chloroform was evaporated at 50°C, 332mbar vacuum and 150 rpm rotational speed. Samples were stored at -20°C until transesterification was applied as method 3.6. subsection follows. Third approach is the same as the second approach with one exception: the separator funnel was held at 4°C overnight.

After the assessment of performance of three approaches, the second approach was used as default to extract and purify the lipids. To ensure that activated carbon concentration was optimal for lipid purification, lipids of homogenized *N. gaditana* were extracted using second approach of lipid extraction and purification with 3 mg activated carbon (AC)/mL concentration to 9 mg AC/ml by increasing 1 mg AC/mL. Extracts were spectrophotometrically analyzed at 330, 440, 470 and 660 nm, and also their FAME profiles were analyzed using GC-FID in method 3.6 subsection.

Ultimately, a series of 150g homogenized *N. gaditana* was mixed according to wet biomass:MeOH:EtOH 1:1:1 ratio. 9g $MgSO_4$/each and 3 mg AC/mL were added, and samples were mixed with 110 rpm for 1 hr. Samples were centrifuged at 3300 rpm at 4°C for 30 min. 400 mL of crude extract were transferred to 1L separator funnel and either 400 mL $CHCl_3$ or 400 mL n-hexane was added. Bottom chloroform or upper n-hexane was collected, and solvents were evaporated at 50°C, 97mbar vacuum and 150 rpm. 5mL of dissolved and undissolved parts of evaporated samples were separately collected to pre-weighed Kimble tubes. Samples were transesterified and their FAME profiles were analyzed using method 3.6 subsection.

3.6. Transesterification of Algal Lipid Extracts for Fatty Acid Methyl Ester Profiling

Methanol with 5% sulfuric acid (v/v) was freshly prepared and 3 mL of methanol with 5% sulfuric acid (v/v) solution was added to dried lipid extract in glass tubes which were used to quantify the total lipid percentage. Screw caps with Teflon inserts were tightly closed, if necessary, caps were surrounded by Teflon tape to prevent leakage. Samples were incubated in a water bath (MaxTurdy-30, Daihan Scientific, Wonju, South Korea) at 70°C for 3 hr. During the incubation step, tubes were vortexed for 5 sec without opening the caps every 3 minutes. After acidic transesterification was completed, samples in tubes were cooled down to room temperature. 3 mL distilled water and 3 mL n-hexane were added to each sample. Samples were vortexed for 5 sec and slowly (~45 rpm) rotated to mix the solutions by using a test tube rotator (Wisemix RT-10, Witeg, Wertheim, Germany) for 15 min. Samples were centrifuged at 1200 *g* for 5 min. 2 mL of top hexane phase was collected to a fresh clean glass tube by using glass Pasteur pipette. Samples were refined at least once by adding 2 mL distilled water to collected hexane phase, vortexing for 5 sec and centrifuging at 1200 *g* for 5 min.

and collecting 2 mL of hexane phase to another clean glass tube (or GC vial). To analyze FAME in hexane, ~1 mL of refined hexane phase was filled to GC vials by syringing and filtering to eliminate impurities. Filled GC vials were sealed to prevent sample evaporation.

3.7. Quantification of Algal Fatty Acid Methyl Esters using Gas Chromatography

FAME quantification was analyzed by using gas chromatography (GC-2014, Shimadzu, Japan) with flame ionization detector (FID). GC-FID method used for quantification was adapted from an application report by Sigma-Aldrich (Buchanan et al., 2011). Samples in GC vials were placed in an auto-sampler (AOC-20i, Shimadzu, Japan) and samples were injected afterwards. Column used to analyze FAME was Supelco SLB®-IL111 capillary extremely polar GC column (length: 100 m, inner diameter: 0.25 mm, film thickness: 0.20 μm) (29647-U, Merck, Germany). Hydrogen was used as carrier gas, and its flow was set as 40 cm/s (linear velocity). With dry air and nitrogen gas use, total flow was adjusted to 214 mL/min and column flow to 2.05 mL/min. For analysis, temperature of injection block was set as 250°C and detector as 260°C. Initial oven temperature was set as 140°C in first 5 min, gradually increased to 180°C at 8°C/min rate, then to 260°C at 5°C/min rate. Analysis time was 26 min/sample. 1 μL of each sample in the GC vial was injected. Split injection was performed at 100:1 split ratio.

In order to quantify and qualify FAME profile in algal extracts, Supelco 37-component FAME mix (47885-U, Supelco, Germany) was used as external standard to construct calibration curve of each FAME component, with the method above. FAME mix was diluted in dichloromethane (DCM) to achieve different concentrations as can be seen in Table 3.7. Chromatogram of no #7 FAME mix standard was shown in Figure 3.12.

Table 3.7. FAME Mix dilutions in DCM to construct calibration curve.

No	1	2	3	4	5	6	7
FAME Mix (μL)	5	10	25	37,5	50	100	200
DCM (μL)	195	190	175	162,5	150	100	0
Total (μL)	200	200	200	200	200	200	200
Dilution factor	40X	20X	8X	5.33X	4X	2X	1X

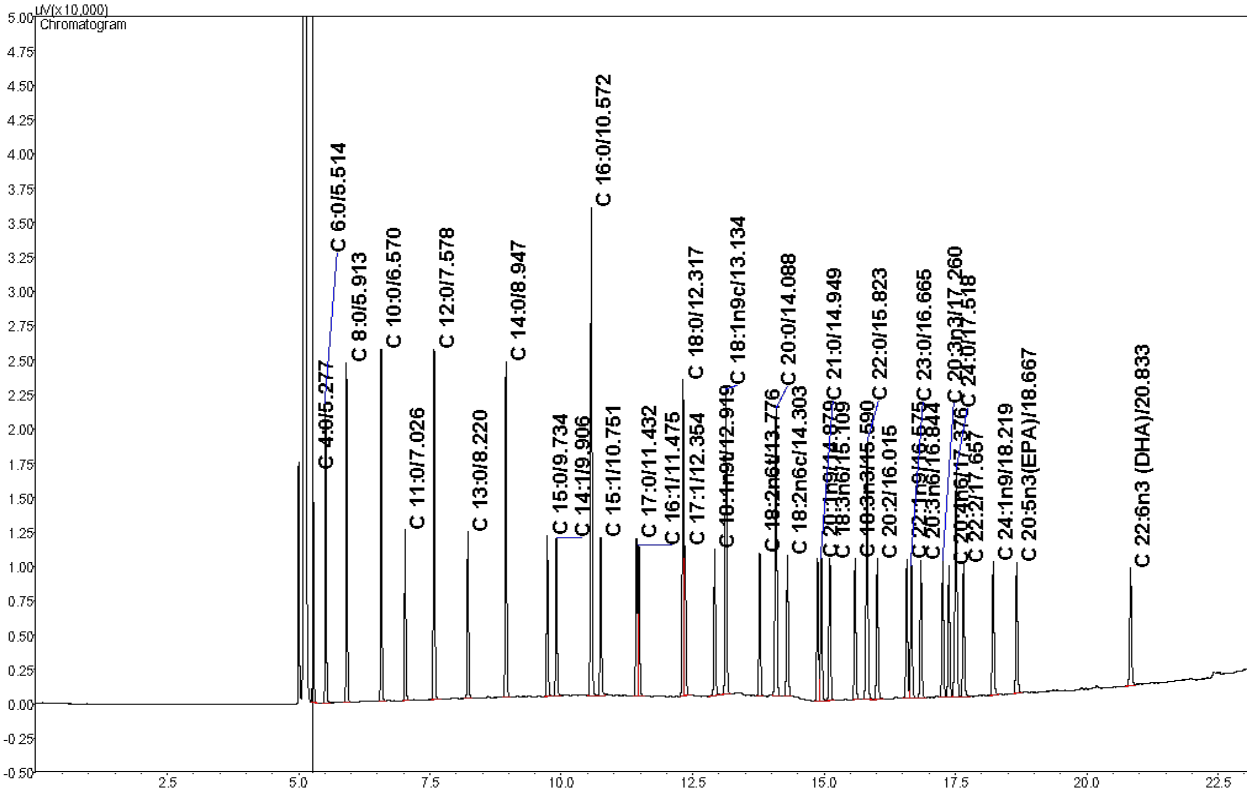

Figure 3.12. GC-FID chromatogram of FAME mix standard.

4. RESULTS

Result part is divided into six subsections in parallel with the course of the method. First, growth charts of small-scale microalgae cultivation were examined, then growth charts and other physicochemical parameters of scaling processes were investigated. After dry weight determination of all conditions, total lipid amounts are determined, and total lipids were compared between different growth conditions. Differences between several cell disruption and lipid extraction methods were addressed. The FAME profile of all conditions was compared to each other.

Growth conditions in Table 3.5 have been updated in Table 4.1 to cover scale-up performances. Condition numbering in Table 4.1 can be used in some figures and texts for ease of expression (like explaining the difference between condition #3 and condition #13 etc.).

Table 4.1. All growth conditions in this study.

Condition No	Species Name	Media Name	Nitrate Condition	Cultivation Volume (L)
1	*Nannochloropsis gaditana*	f/2	N+	2L
2	*Nannochloropsis gaditana*	f/2	N-	2L
3	*Nannochloropsis gaditana*	Algal	N+	2L
4	*Nannochloropsis gaditana*	Algal	N-	2L
5	*Nannochloropsis gaditana*	M&M	N+	2L
6	*Nannochloropsis gaditana*	M&M	N-	2L
7	*Nannochloropsis sp.*	f/2	N+	2L
8	*Nannochloropsis sp.*	f/2	N-	2L
9	*Nannochloropsis sp.*	Algal	N+	2L
10	*Nannochloropsis sp.*	Algal	N-	2L
11	*Nannochloropsis sp.*	M&M	N+	2L
12	*Nannochloropsis sp.*	M&M	N-	2L
13	*Ettlia oleoabundans*	MB3N	N+	2L
14	*Ettlia oleoabundans*	MB3N	N-	2L
15	*Nannochloropsis gaditana*	Algal	N+	12L
16	*Nannochloropsis gaditana*	Algal	N+	100L
17	*Nannochloropsis gaditana*	Algal	N+	1000L
18	*Nannochloropsis gaditana*	Algal	N+	15000L
19	*Nannochloropsis gaditana*	Algal	N-half stress	15000L
20	*Ettlia oleoabundans*	MB3N	N+	12L, Glass Bottle
21	*Ettlia oleoabundans*	MB3N	N+	12L, Tubular PBR
22	*Ettlia oleoabundans*	MB3N	N+	100L
23	*Ettlia oleoabundans*	MB3N	N+	1000L

4.1. Microalgae Growth

4.1.1. Growth Profile of Small-Scale Microalgae Cultivation and Change in Growth Profile under Nitrogen Deprivation

Marine microalgae *N. gaditana* and *Nannochloropsis sp.,* and freshwater microalgae *E. oleoabundans* were primarily grown in 2L Erlenmeyer flask with related PBR setup. Growth profile of both *Nannochloropsis* was observed on three different media, which are f/2, Algal and M&M media, while growth profile of *E. oleoabundans* was observed on MB3N medium.

N. gaditana reached 2.87 optical density (OD) at 680 nm under N-replete condition in f/2 media (Figure 4.1) This intensity, along with Algal N-replete condition, is one of the two (chlorophyll) intense conditions. In Algal medium N-replete condition, *N. gaditana* reached 2.75 optical density on the 16th cultivation day (Figure 4.3). Growth profile of *N. gaditana* on M&M medium was observed at 1.8 OD in 14 days (Figure 4.5). OD of *N. gaditana* in M&M N-replete condition was almost half of the other two media. Average optical density of *N. gaditana* is highest of all microalgae species. Relationship between biomass productivity and optical density in the conditions is consistent.

A decrease in OD of the culture was observed in all *N. gaditana* N-deplete conditions compared to N-replete conditions of the same media. *N. gaditana* reached 1.36 OD in 12 days on f/2 medium N-deplete condition (Figure 4.2). In Algal N-deplete condition, 1.16 OD was achieved on the 12th day (Figure 4.4), which is interestingly lower than f/2 N-deprived condition. 1.25 OD was reached during *N. gaditana* cultivation in M&M medium N-deprived condition (Figure 4.6) All *N. gaditana* N-deprived conditions showed similar growth trends gathered over optical density, with slightly better performance was shown in f/2 N-deprived profile. Change in nitrate concentration affected OD of *N. gaditana* the most in Algal medium.

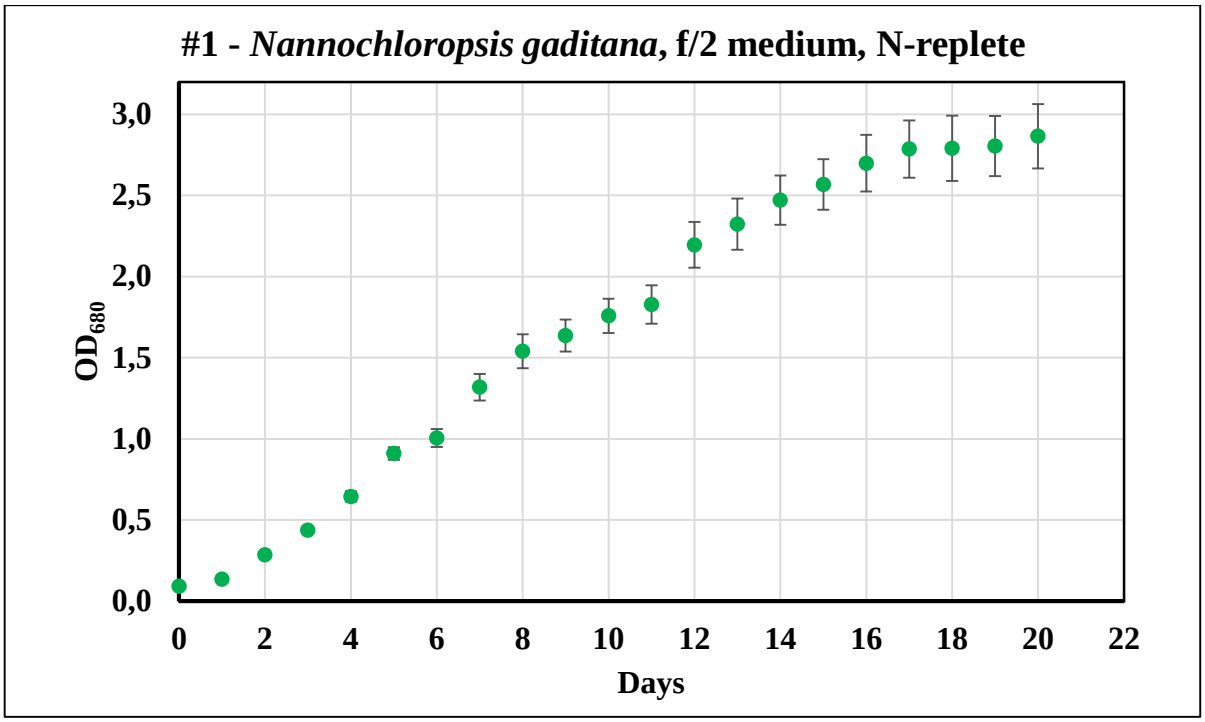

Figure 4.1. Growth profile of condition #1: *Nannochloropsis gaditana* in 2L f/2, N-replete.

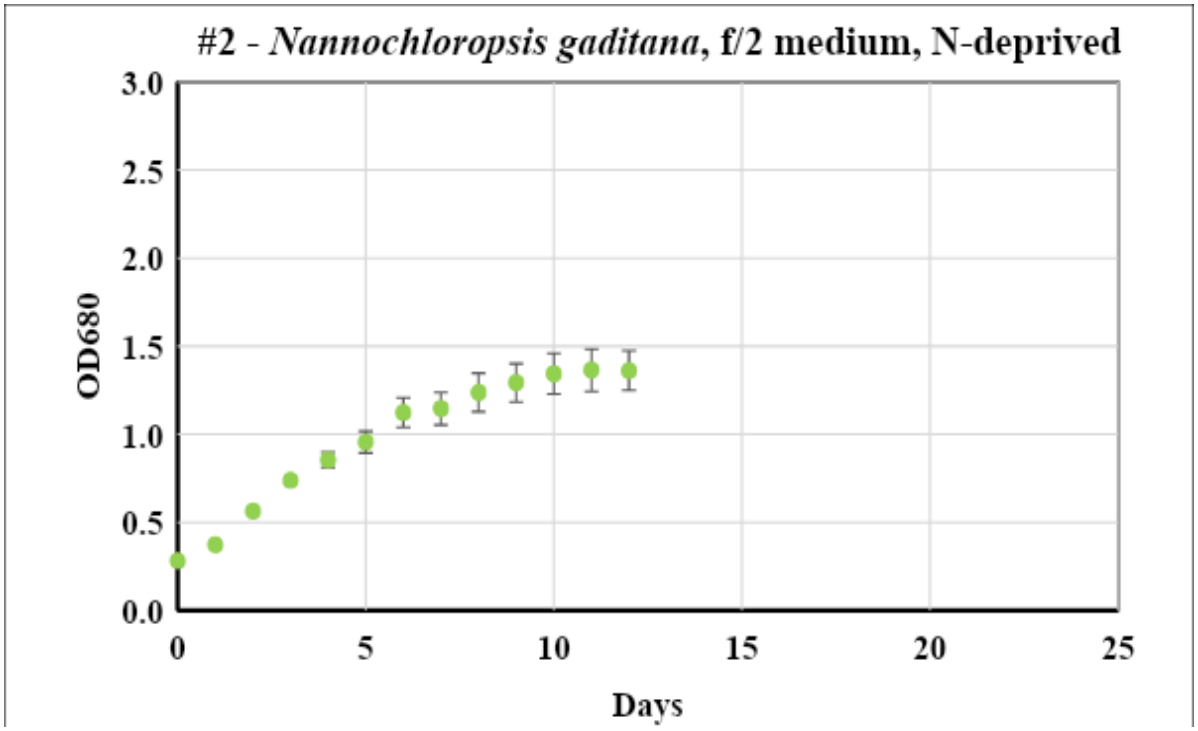

Figure 4.2. Growth profile of condition #2: *Nannochloropsis gaditana* in 2L f/2, N-deprived.

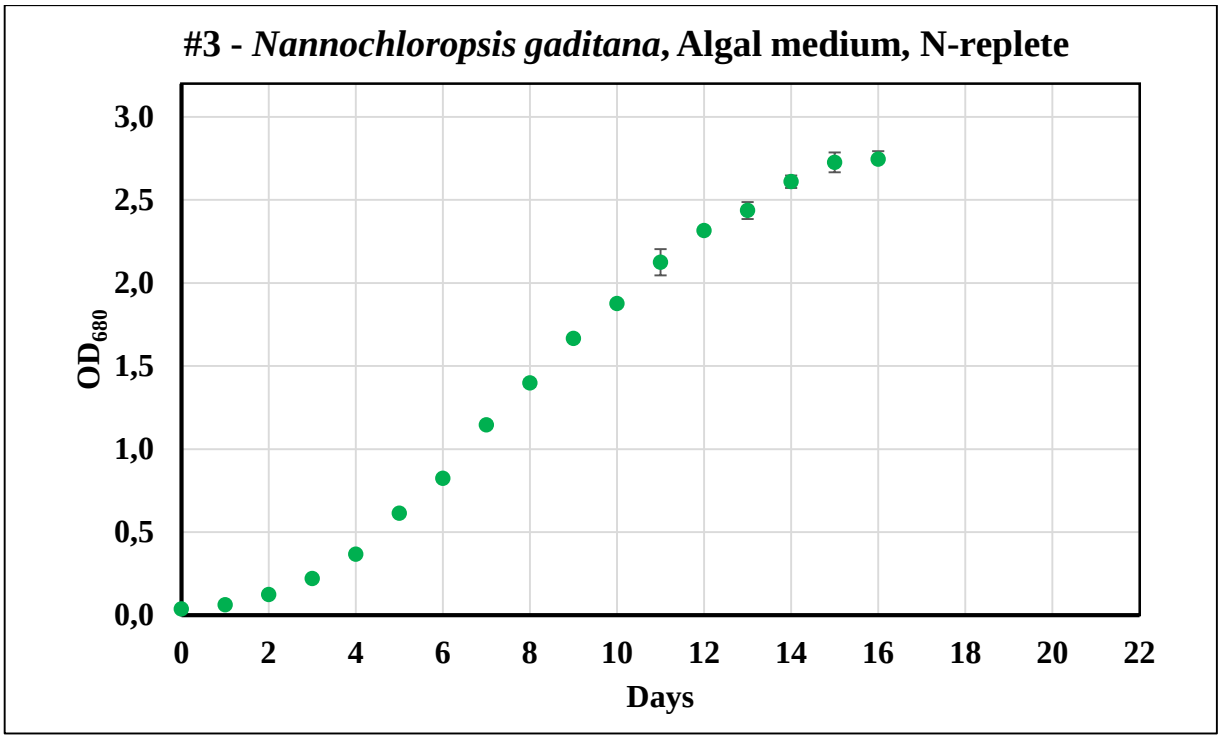

Figure 4.3. Growth profile of condition #3: *Nannochloropsis gaditana* in 2L Algal, N-replete.

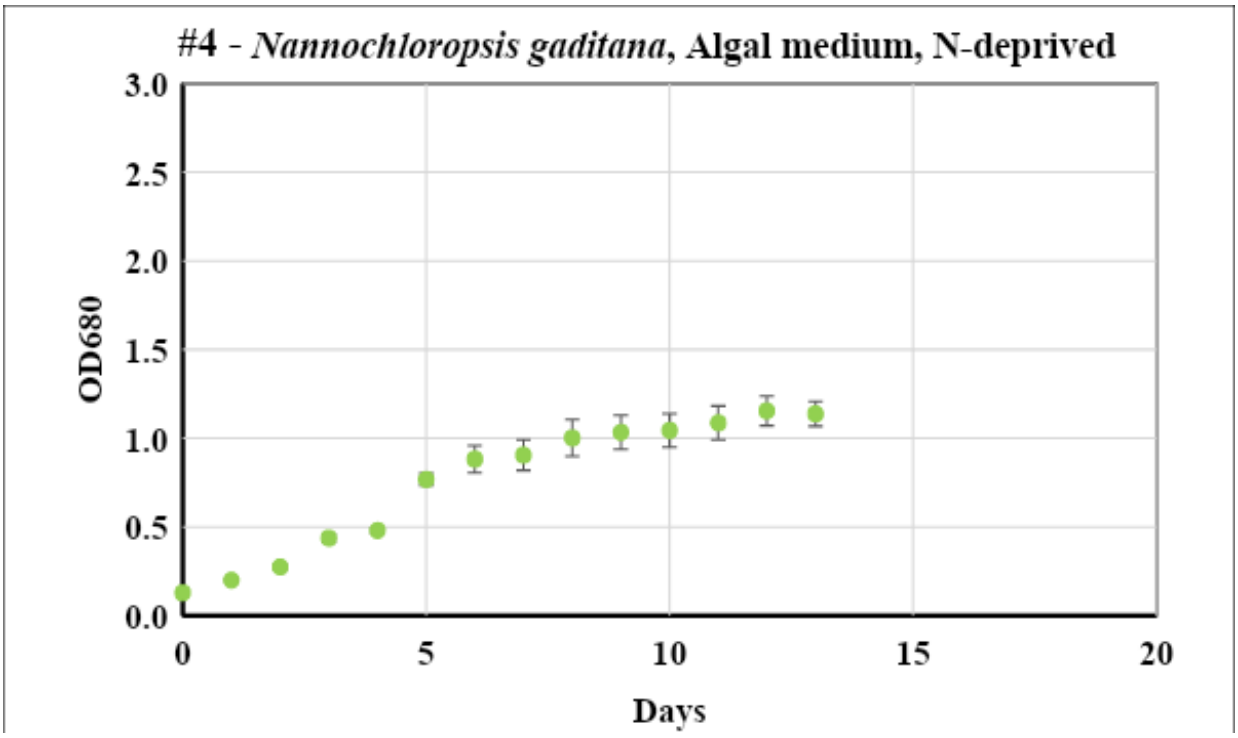

Figure 4.4. Growth profile of condition #4: *Nannochloropsis gaditana* in 2L Algal, N-deprived.

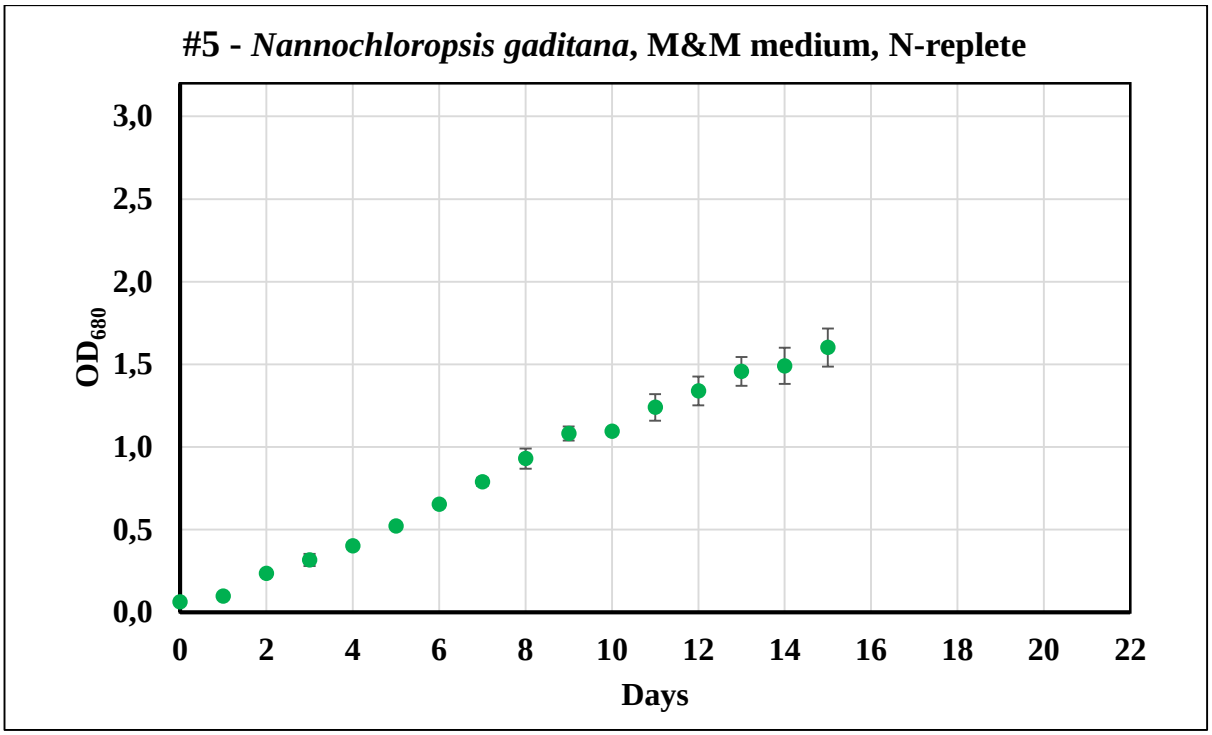

Figure 4.5. Growth profile of condition #5: *Nannochloropsis gaditana* in 2L M&M, N-replete.

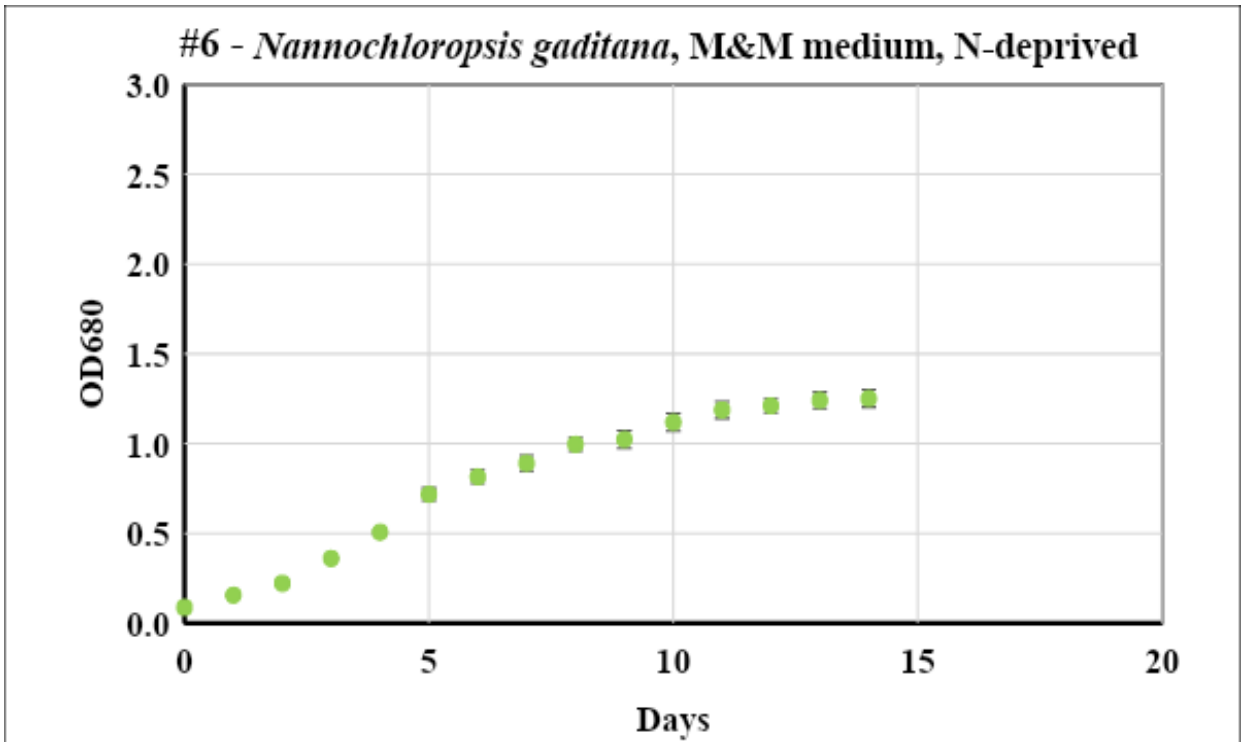

Figure 4.6. Growth profile of condition #6: *Nannochloropsis gaditana* in 2L M&M, N-deprived.

Growth profiles of *Nannochloropsis sp.* conditions in small-scale cultures were similar to growth profiles of *N. gaditana* cultures with several exceptions. *Nannochloropsis sp*. in f/2 medium reached 1.03 OD in 15 days (Figure 4.7). Same species in Algal medium under N-replete condition reached 2.36 OD in 21 days (Figure 4.9), which was the latest condition among small-scale cultivations to enter stationary phase. Lastly, *Nannochloropsis sp.* reached 1.8 OD in 14 days (Figure 4.11), which is relatively rapid growth. This species in f/2 N-replete medium rapidly arrived at the stationary phase on day 7, and no significant density increase was observed thereafter. Discrepancies were observed towards the late exponential phase in M&M media N-replete condition. Average OD of *Nannochloropsis sp.* were lower than average OD of *N. gaditana* under all conditions.

In *Nannochloropsis sp*. case, culture with f/2 N-deprived medium reached 1.39 OD in 16 days (Figure 4.8). Same species reached 0.99 OD on the 12th day in the Algal N-deprived medium (Figure 4.10) and 1.38 OD on the 13th day in the M & M medium (Figure 4.12). Unlike all other conditions, *Nannochloropsis sp.* grew in f/2 N-deprived medium more than f/2 N-replete condition. Nitrogen concentration of f/2 N-deprived condition is less than all media conditions. In all *Nannochloropsis sp*. N-deprived conditions, growth was decelerated after 5^{th} day. Slight increase in optical density was observed in the stationary phase for f/2 and M&M media. The only condition with an OD below 1 when the growth profile was completed was *Nannochloropsis sp.* in Algal medium N-deprived condition (Table 4.2).

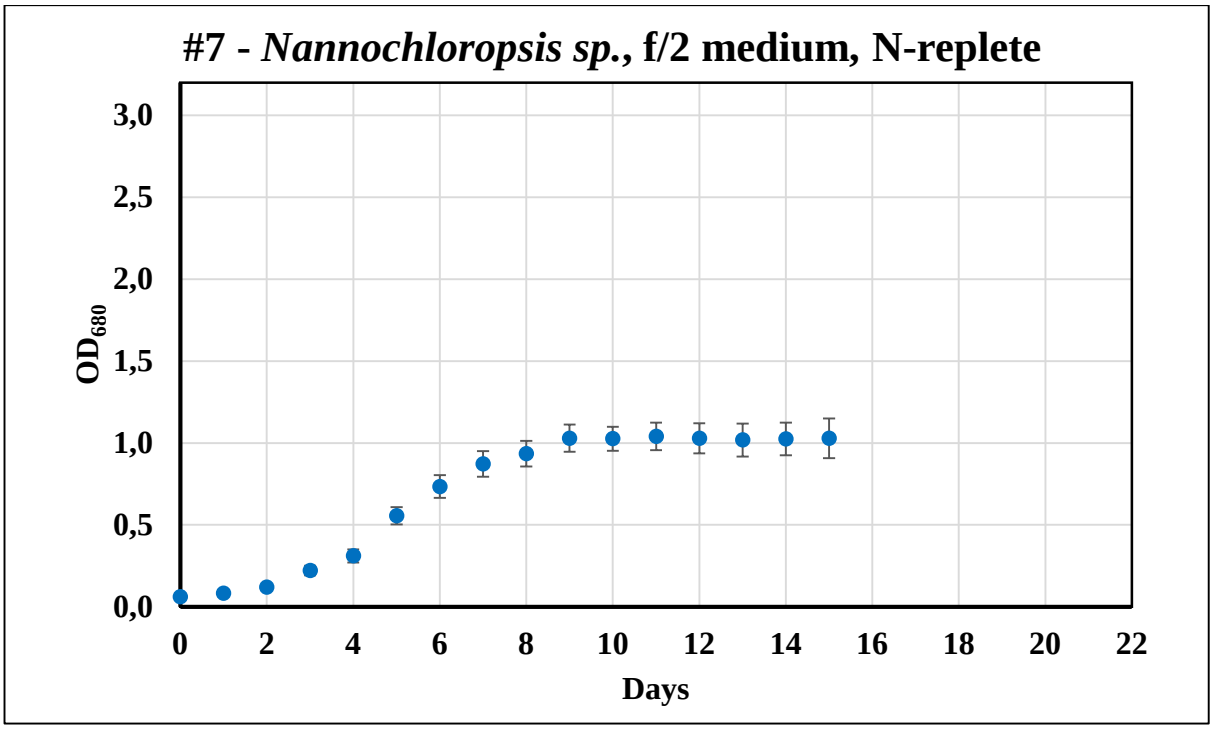

Figure 4.7. Growth profile of condition #7: *Nannochloropsis sp.* in 2L f/2 medium, N-replete.

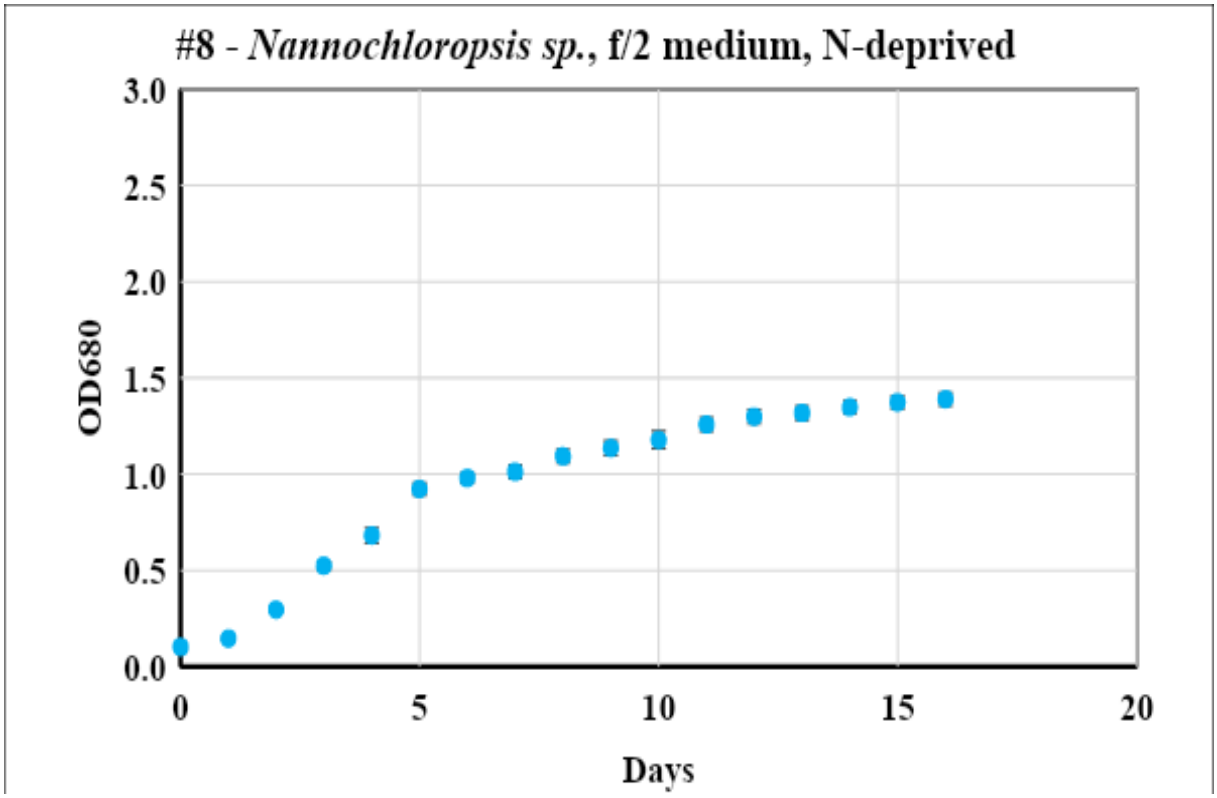

Figure 4.8. Growth profile of condition #8: *Nannochloropsis gaditana* in 2L f/2, N-deprived.

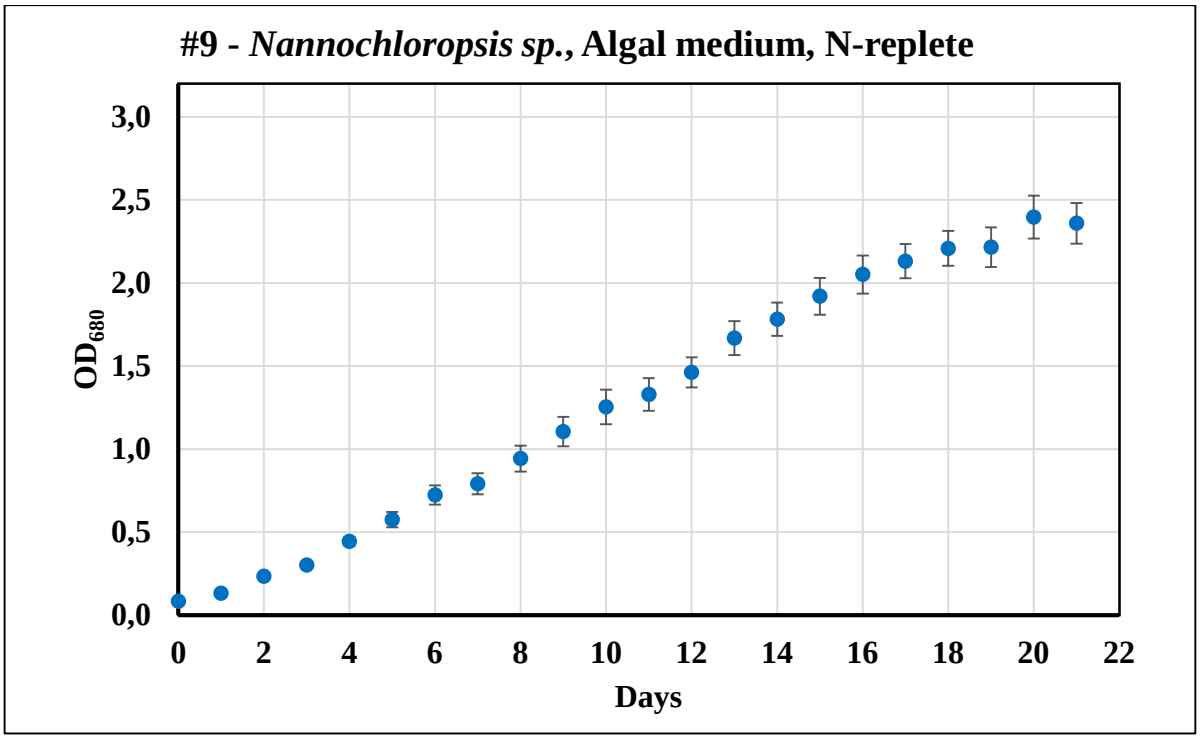

Figure 4.9. Growth profile of condition #9: *Nannochloropsis sp.* in 2L Algal medium, N-replete.

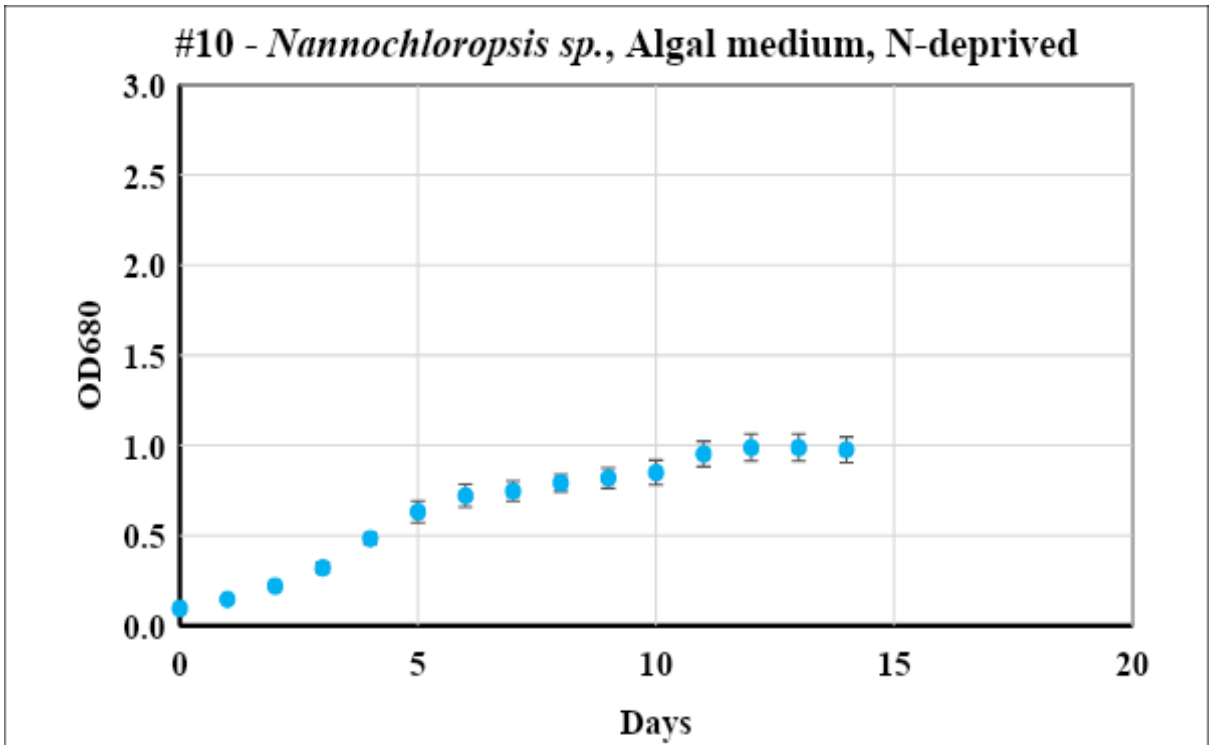

Figure 4.10. Growth profile of condition #10: *Nannochloropsis sp.* in 2L Algal, N-deprived.

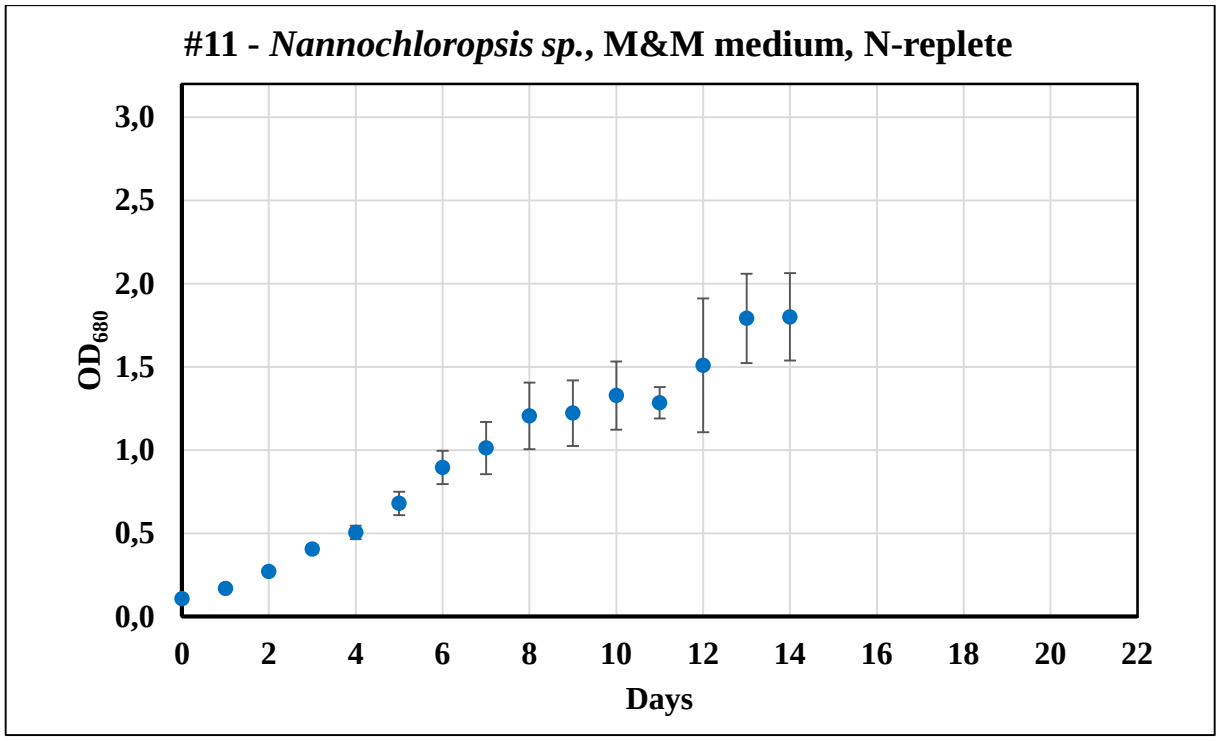

Figure 4.11. Growth profile of condition #11: *Nannochloropsis sp.* in 2L M&M medium, N-replete.

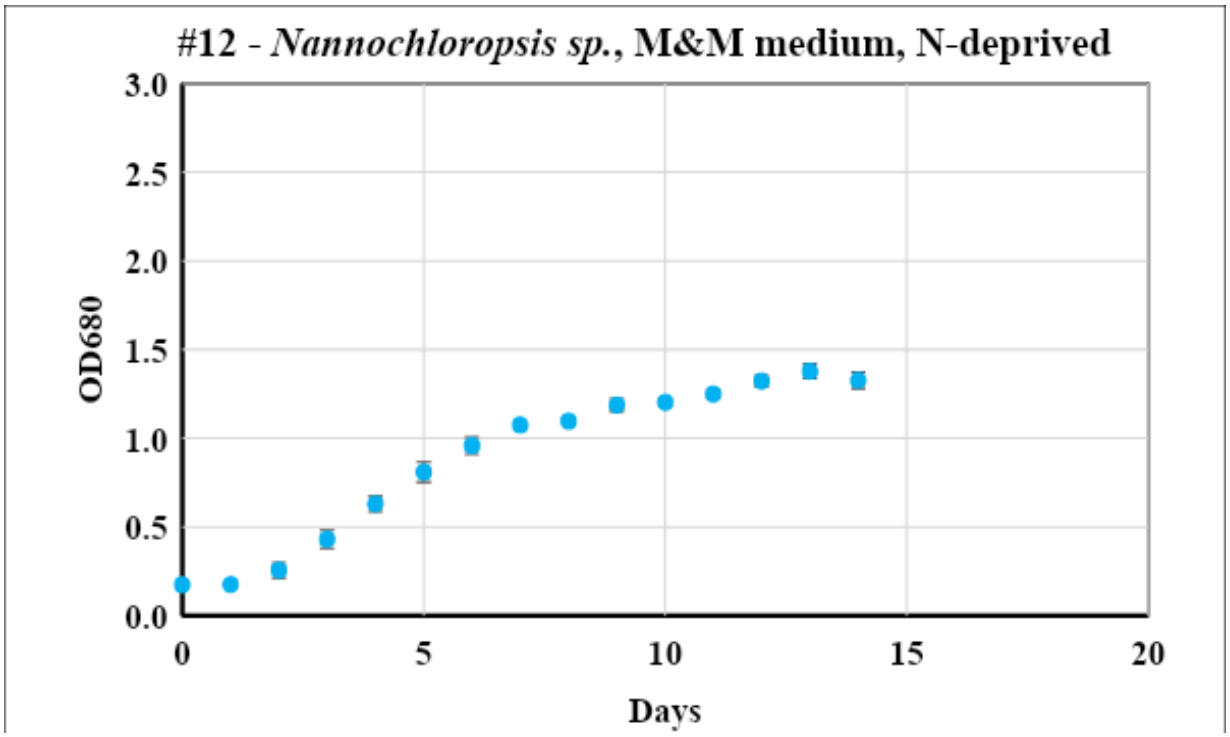

Figure 4.12. Growth profile of condition #12: *Nannochloropsis sp.* in 2L M&M, N-deprived.

E. oleoabundans reached 1.89 average OD in 14 days (Figure 4.13). *E. oleoabundans* underwent a rapid lag phase and exponentially grew early. Average OD of *E. oleoabundans* is similar to

Nannochloropsis sp. average OD and relatively stands behind in *N. gaditana* in terms of optical chlorophyll intensity.

E. oleoabundans in MB3N N-deprived condition reach 1.40 OD in 13 days (Figure 4.14). This species entered the exponential phase of growth profile more rapidly than other species, both in N-replete and N-deprived conditions. In order to be sure that *E. oleoabundans* entered the stationary phase under N-deprived condition, optical density was measured from following days despite the low growth rate.

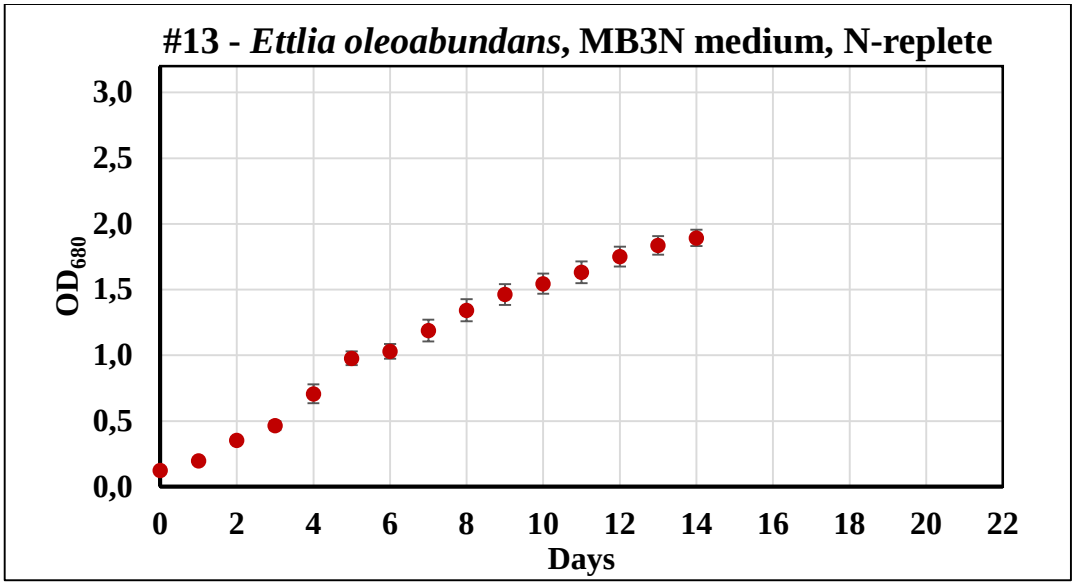

Figure 4.13. Growth profile of condition #13: *Ettlia oleoabundans.* in 2L MB3N medium, N-replete.

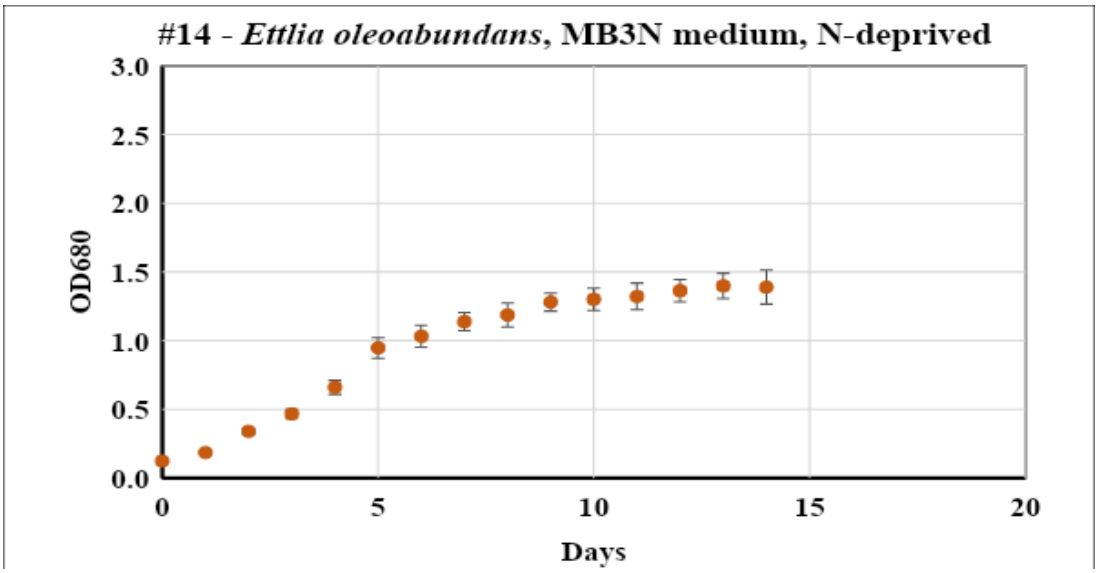

Figure 4.14. Growth profile of condition #14: *Ettlia oleoabundans* in 2L MB3N medium, N-deprived.

Growth profile performance for all three species in 2L cultivation under N-replete and N-deprived conditions are shown in Table 4.2. Considering dry weight and lipid productivity which were shown in following sections, it was decided to use condition #3 (*N. gaditana*, Algal medium N-replete) and condition #13 (*E. oleoabundans*, MB3N medium N-replete) in scale-up studies.

Table 4.2. Optical density changes of selected microalgae species using N-deprivation.

Condition No	Species Name	Media Name	Nitrate Condition	Max OD	OD Change in Nitrogen Stress
1	***Nannochloropsis gaditana***	f/2	N+	2.87	52.5% decrease
2			N-	1.36	
3		Algal	N+	2.75	58.5% decrease
4			N-	1.14	
5		M&M	N+	1.60	21.9% decrease
6			N-	1.25	
7	***Nannochloropsis sp.***	f/2	N+	1.03	35.1% increase
8			N-	1.39	
9		Algal	N+	2.36	58.7% decrease
10			N-	0.98	
11		M&M	N+	1.80	26.3% decrease
12			N-	1.33	
13	***Ettlia oleoabundans***	MB3N	N+	1.89	26.6% decrease
14			N-	1.39	

4.1.2. Growth Profile of Selected Microalgae Species in Scale-up Studies

Growth profiles of *N. gaditana* and *E. oleoabundans* cultivated in 12L PBRs and 100, 1000 and 15000L open ponds, as described in 3.2.3.1 method subsection, are examined in this subsection. Scaling-up conditions were shown in Table 4.1. All measurements in outdoor ponds were taken in autumn and winter, and data are susceptible to seasonal biases. 12L PBRs were performed in indoor conditions, and daily temperature of 12L reactors was always at 25 ± 2 °C. To facilitate comparison, growth profiles of the two conditions were shown as compared within themselves.

Firstly, cultivation designs using 12L glass carboys were used to scale-up *N. gaditana* from 2L to 12L. *N. gaditana* reached 2.40 optical density (OD) on the 26th day and its growth rate was stagnant

afterwards (Figure 4.15). At 16th day, when 2L *N. gaditana* culture reached OD peak, 12L *N. gaditana* culture continued its mid exponential growth, and OD of 12L *N. gaditana* culture on the 16th day was 42.9% less than of 2L culture (from 2.75 to 1.57). Maximum OD at the end of growth profiling of 2L and 12L cultures was slightly different (12.7% decrease in 12L) in each other. Compared to the 2L condition, more time was required to reach maximum OD for all scale-up cultures.

Growth profiles of outdoor open ponds did not ideally represent the phases (lag, log, stationary) which would theoretically be expected to occur. First inoculation from indoor to outdoor conditions was inoculating 100L open ponds, and even the initial OD of culture was high (0.61), expected growth phases were not observed. There was OD oscillation during all growth profiles, and maximum OD was observed at 19th day as 0.72. Optical density did not change more than 25% in 100-L *N. gaditana* open pond cultivation.

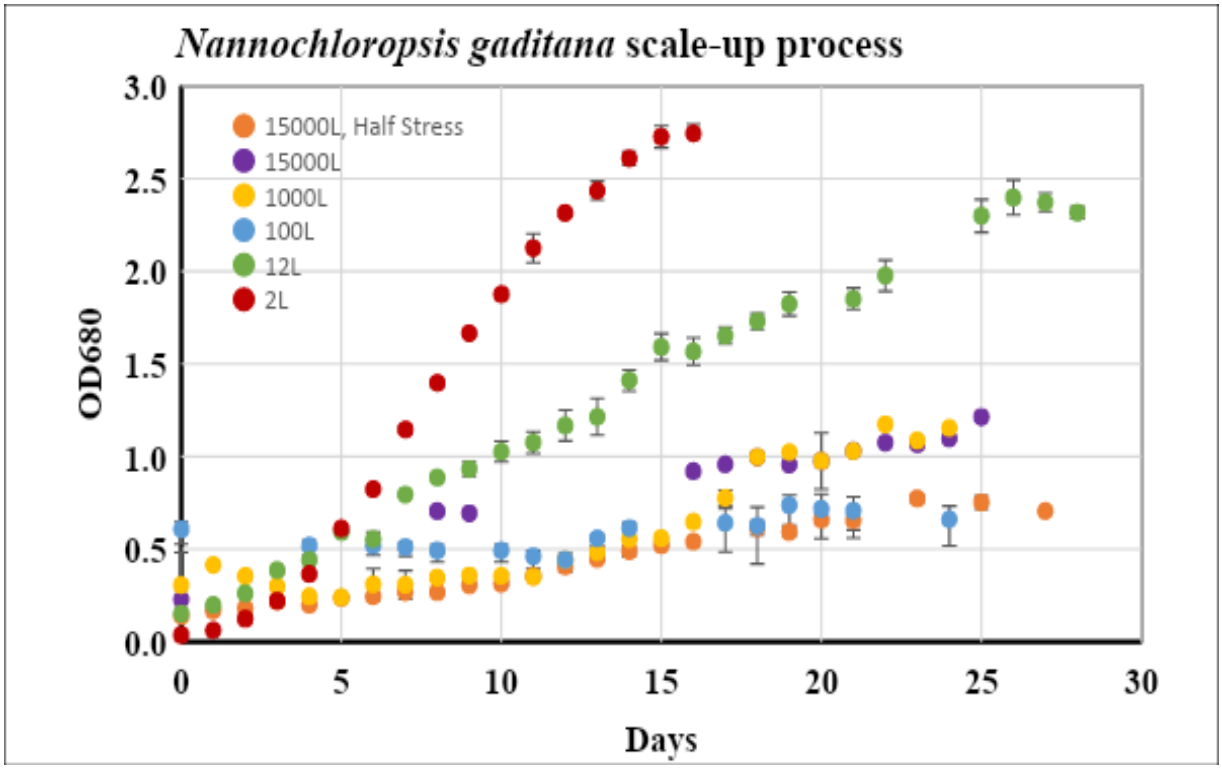

Figure 4.15. Growth profiles of *Nannochloropsis gaditana* in scale-up processes.

1000L *N. gaditana* cultivation showed the most successful growth performance among other open pond cultivations in cold weather. *N. gaditana* reached 1.17 OD on the 22nd day in the 1000L open pond, and with 1.21 OD on the 25th day in the 15000L open pond, the most optical intense conditions were achieved.

In 15000 L ponds, two conditions were tested which are the culture-as-usual nitrogen concentration and the culture with nitrogen concentration was half of the normal, called N-half stress. Increase in OD was observed in normal 15000L *N. gaditana* culture even on its harvest day. Maximum OD of 15000L *N. gaditana* culture was 1.21 OD on the 25th day. The culture was almost stagnant after the 16th day in terms of optical density. In the 15000L N-half stress case, the slowest growth profile was observed except 100-liter pond stasis (Figure 4.15). Compared to the same volume of culture, this condition showed in OD by almost half, especially after day 8. 0.75 OD was observed on day 25th in 15000-liter *N. gaditana* half N stress condition. OD comparison of all growth conditions was shown in Table 4.3.

Table 4.3. Comparison of *N. gaditana* cultivation parameters in scale-up process.

					OD comparison of scale-up culture (%)					
Condition No	**Condition Name**	**Cultivation Volume (L)**	**Max OD**	**Temperature range in that culture (°C)**	**2**	**12**	**100**	**1000**	**15000**	**15K, Half-N**
3	*Nannochloropsis gaditana* Algal medium N+	2	2.75	~ 20	0	14.4	371	234	226	354
15		12	2.40	22.1 - 24.8	12.6	0	325	204	198	309
16		100	0.74	2.7 - 17.3	73.2	69.2	0	37.1	39	0.47
17		1000	1.17	6.6 - 21.8	57.3	51.1	58.9	0	0.31	51.6
18		15000	1.21	10.9 - 19.6	55.9	59.6	64	0.32	0	56.3
19		15K, Half-N	0.77	2.7 - 13.8	71.8	67.7	0.49	34	36	0

In *E. oleoabundans* case, like in *N. gaditana*, an inverse correlation with growth rate and cultivation volume increased when the scale increased (Figure 4.16). Two different reactors were used for *E. oleoabundans* scale up to 12L. Growth profiles between two reactors significantly differed. Performance of one grown in tubular PBR has exceeded even the 2-liter small scale condition. Best optical density (OD) seen in *E. oleoabundans* with and 2.24 OD at 14th day was observed in 12L Phycobubble tubular PBRs (Blue dots in Figure 4.16). Growth rate of *E. oleoabundans* in 12L tubular PBR until 7th day was remarkable (0.22 OD increase/day). On the other hand, *E. oleoabundans* culture in glass carboy systems cultivated 27 days to reach the stationary phase and their maximum optical density, which was 1.65, was 26.5% less than that of tubular PBR system.

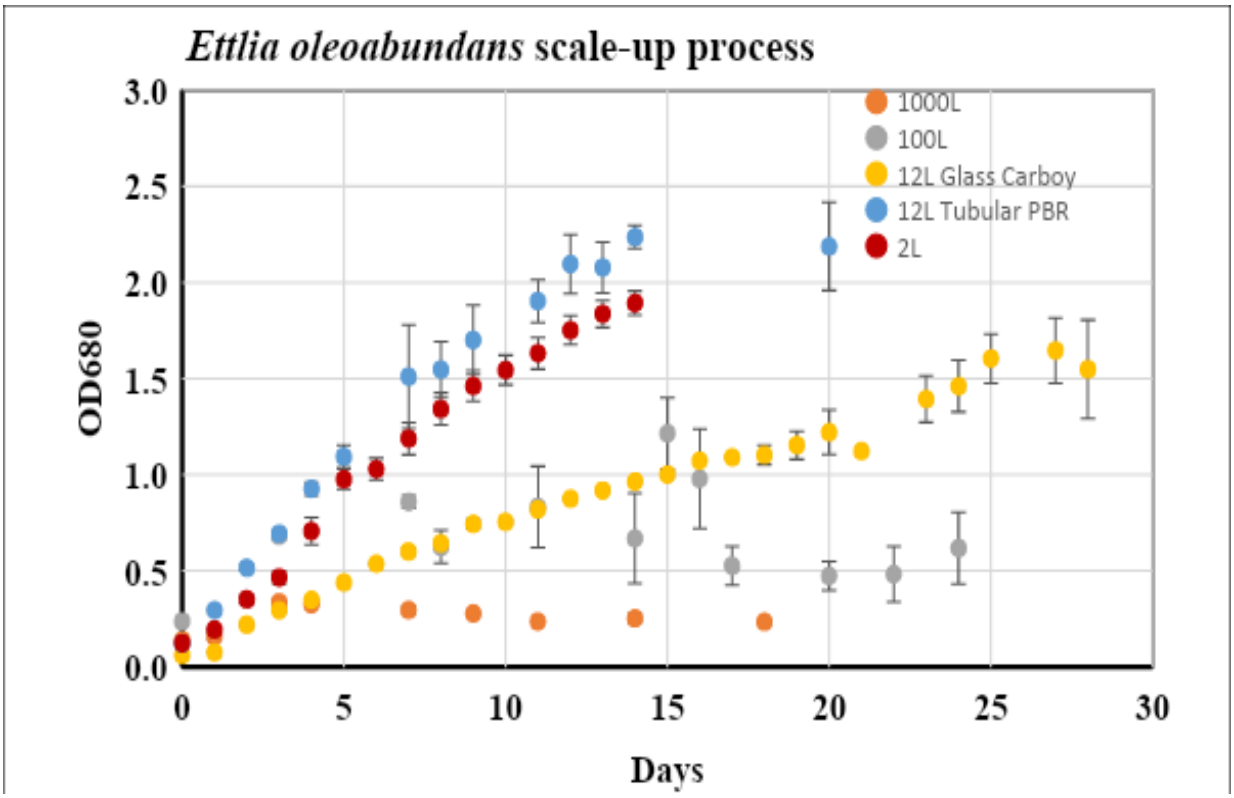

Figure 4.16. Growth profiles of *Ettlia oleoabundans* in scale-up processes.

In outdoor cultivation of *E. oleoabundans*, displaying a healthy growth profile was not achieved. 100-liter cultivation of *E. oleoabundans*, which is the smallest outdoor scale, showed an unstable growth profile. Average optical density of the culture with the same condition differed from each other, as error bars indicated in gray dots in Figure 4.16. In 100 liters condition, *E. oleoabundans* reach 1.22 OD at 15th day as its most optically dense point in outdoor cultivation in this study. In the 1000L case, *E. oleoabundans* showed no significant growth. 0.30 OD was the peak point of 1000L *E. oleoabundans* cultivation. It was decided to stop scaling-up of *E. oleoabundans* at 1000L and assess scaling up performance between 2L to 1000L conditions Table 4.4.

Table 4.4. Comparison of *E. oleoabundans* cultivation parameters in scale-up process.

Condition No	**Condition Name**	**Cultivation Volume (L)**	**Max OD**	**Temperature range in that culture (°C)**
13	*Ettlia oleoabundans* MB3N medium N+	2	1.89	~ 20
20		12, Glass Carboy	1.65	21.9 - 24.5
21		12, Tubular PBR	2.24	21.8 - 26.9
22		100	1.21	25.9 - 35.9
23		1000	0.34	17.7 - 24.1

4.2. Dry Weight Calculation of Algal Biomass

From this section on, harvesting and dewatering of microalgae cultures under 23 different conditions was performed in accordance with method 3.3. procedure, and downstream processes for lipid production was initiated. Dry biomass and ash content of all cultures were determined using the procedures in method 3.3.1. Dry weight measurements were made from liquid samples taken from cultures before harvesting. Dry weight determination of condition #23, which was *N. gaditana* Algal media 15000L Half-N stress condition was operated with the liquid sample taken from the culture on the 16th day.

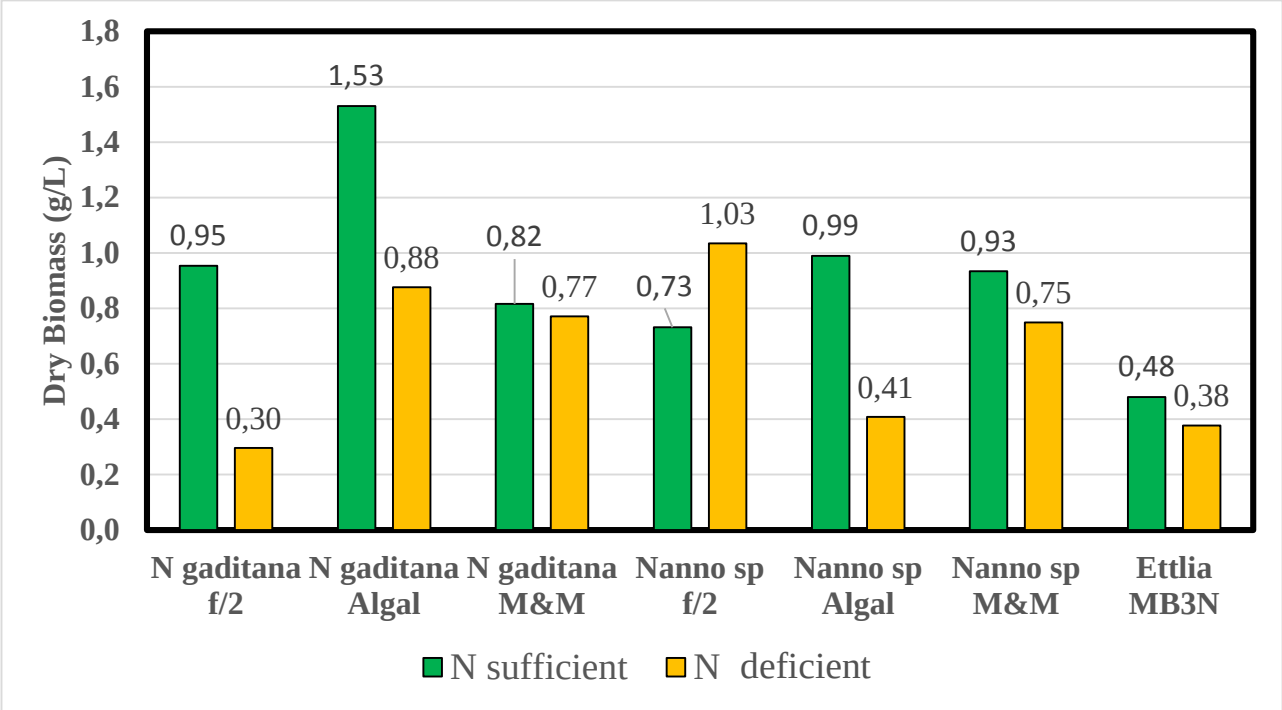

Figure 4.17. Biomass concentration of all 2L conditions (*Nanno sp*: *Nannochloropsis sp.*, *Ettlia*: *E. oleoabundans*).

Dry weight concentration of all 2L initial cultures were shown in Figure 4.17. Biomass productivity of *Nannochloropsis* genus was weighed as higher then *Ettlia* under media and PBR designs in this study. Biomass concentration of condition #3 (*N. gaditana*, Algal medium in N-replete condition) was calculated as 1.53 g/L, which is highest biomass productivity of all conditions. Biomass concentration of *N. gaditana* in f/2 and M&M N-replete condition was weighed as 0.95 and 0.82 g/L, respectively. As expected, *N. gaditana* culture in N-deprived conditions were less biomass concentration than N-replete ones. Biomass concentrations of *N. gaditana* at three different N-depleted conditions were 0.30 g/L for f/2 medium, 0.88 g/L for Algal medium, and 0.77 g/L for M&M medium. With nitrogen deprivation, biomass concentration loss changed the most in f/2 media,

affected the least in culture of M&M media. Relationship between optical densities and dry weight concentration is consistent.

Nannochloropsis sp. reached lower biomass concentrations than *N. gaditana*. Biomass concentrations of the related species in N-replete conditions were 0.73 g/L for f/2 medium, 0.99 g/L for Algal medium, and 0.93 g/L for M&M medium. *Nannochloropsis sp.* was cultivated in 2L N-deprived conditions as 1.03g/L for f/2 medium, 0.41g/L for Algal medium and 0.75g/L for M&M medium culture. In *Nannochloropsis sp.* in f/2 media conditions, N-deprived culture has a higher biomass concentration than N-replete cultures, which situation was only observed in this case. This discrepancy confirms discrepancy in same situation in optical density. There was an approximate 1.5-fold difference in biomass concentration between two *Nannochloropsis* species under Algal media growth conditions.

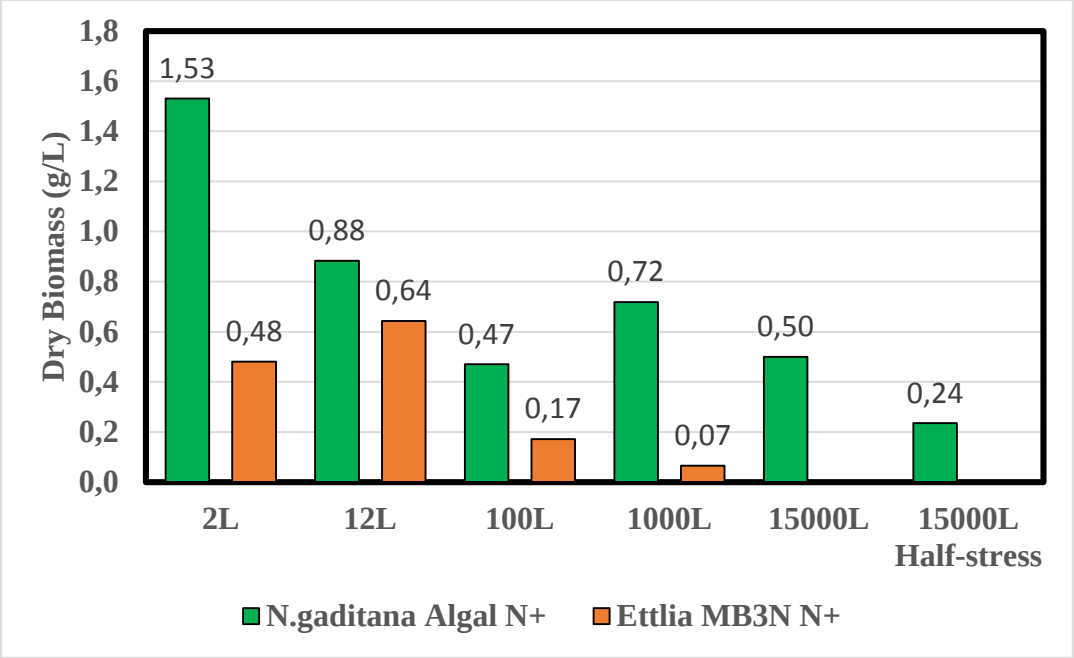

Figure 4.18. Biomass concentrations in selected microalgae species in scale-up process.

Biomass concentration of *E. oleoabundans* was weighed as 0.48g/L in N-replete condition, 0.38 g/L in N-deprived condition. Biomass concentration difference between conditions is consistent with the optical density data and is less than *Nannochloropsis* species.

Biomass concentrations of *N. gaditana* and *E. oleoabundans* during scale up from 2L to 15000L were shown in Figure 4.18. In both species, biomass concentration tended to decrease as the scale increased. 1000L *N. gaditana* cultivation was higher biomass concentration than 100L cultivation, and same exception is valid for 12L *E. oleoabundans* cultivation than 100L cultivation case. Biomass

concentration of *N. gaditana* cultivations were 0.88 g/L for 12L glass carboy, 0.47 g/L for 100L, 0.72 g/L for 1000L, 0.50 g/L for 15000L and 0.24 g/L for 15000L Half-N stress conditions, respectively. Biomass concentrations of *E. oleoabundans* cultures were 0.64 g/L for 12L glass carboy, 0.54 g/L for 12L tubular PBR (Table 4.5), 0.17 g/L for 100L and 0.07 g/L for 1000L conditions, respectively.

Ash and organic content of 23 conditions were shown in Table 4.5. Ash percentage of dry weights were between 5-43% of all dry weight. Organic content is the remaining of dry weight after removing ash part. The high ash content in 1000L *N. gaditana* open pond with relatively high biomass concentration indicated that the organic content in 100L and 1000L *N. gaditana* open ponds was at very close concentrations.

Table 4.5. Organic and ash content of all microalgae cultures.

No	Species Name	Conditions (Media, Nitrogen stress and cultivation volume)	Dry Weight ($g_{Biomass}/L$)	Ash content (%)	Organic content (g/L)
1		f/2, N+, 2L	0.95	18.80	0.78
2		f/2, N-, 2L	0.30	9.14	0.27
3	***Nannochloropsis gaditana***	**Algal, N+, 2L**	1.53	19.46	1.23
4		Algal, N-, 2L	0.88	12.92	0.76
5		M&M, N+, 2L	0.82	16.89	0.68
6		M&M, N-, 2L	0.77	13.46	0.67
7		f/2, N+, 2L	0.73	12.12	0.64
8		f/2, N-, 2L	1.04	5.00	0.98
9	***Nannochloropsis sp.***	Algal, N+, 2L	0.99	7.89	0.91
10		Algal, N-, 2L	0.41	5.24	0.39
11		M&M, N+, 2L	0.93	15.75	0.79
12		M&M, N-, 2L	0.75	9.84	0.68
13	***Ettlia oleoabundans***	**MB3N, N+, 2L**	0.48	23.97	0.37
14		MB3N, N-, 2L	0.38	20.03	0.30
15		Algal, N+, 12L	0.88	13.71	0.76
16	***Nannochloropsis gaditana***	Algal, N+, 100L	0.47	19.23	0.38
17		Algal, N+, 1000L	0.72	43.16	0.41
18		Algal, N+, 15000L	0.50	28.99	0.36
19		Algal, N-half, 15KL	0.24	15.09	0.20
20		MB3N, N+, 12L, G	0.64	7.72	0.59
21	***Ettlia oleoabundans***	MB3N, N+, 12L, PBR	0.54	6.52	0.51
22		MB3N, N+, 100L	0.17	17.08	0.14
23		MB3N, N+, 1000L	0.07	20.45	0.05

4.3. Total Lipid Extraction

4.3.1. Lipid Extraction from Lyophilized Powder Microalgae

Lipid percentage of *N. gaditana* in N-replete conditions were 26.6% ± 8.08% for f/2 medium, 46.87% ± 6.36% for Algal medium, and 27.23% ± 3.24% for M&M medium. Same species in N-deprived conditions performed 40.05% ± 7.88% lipid percentage for f/2 medium, 45.67% ± 1.33% for Algal medium, 57.44% ± 8.33% for M&M medium. *Nannochloropsis sp*. had 28.67% ± 1.55% total lipid in f/2 N-replete condition, 36.93% ± 7.43% for Algal N-replete, and 51.08% ± 2.68% for M&M N-replete conditions. It was measured that lipid percentage of *Nannochloropsis sp*. in N-deprived conditions were 51.87% ± 1.10% for f/2 medium, 47.71% ± 9.87% for Algal medium, and 51.08% ± 2.68% for M&M medium. *E. oleoabundans* in MB3N medium had 25.39% ± 4.15% for N-replete condition whereas 25.53 ± 5.73 for N-deprived condition. Lipid percentage comparison of 7 nitrogen deprivation was visualized in Figure 4.19.

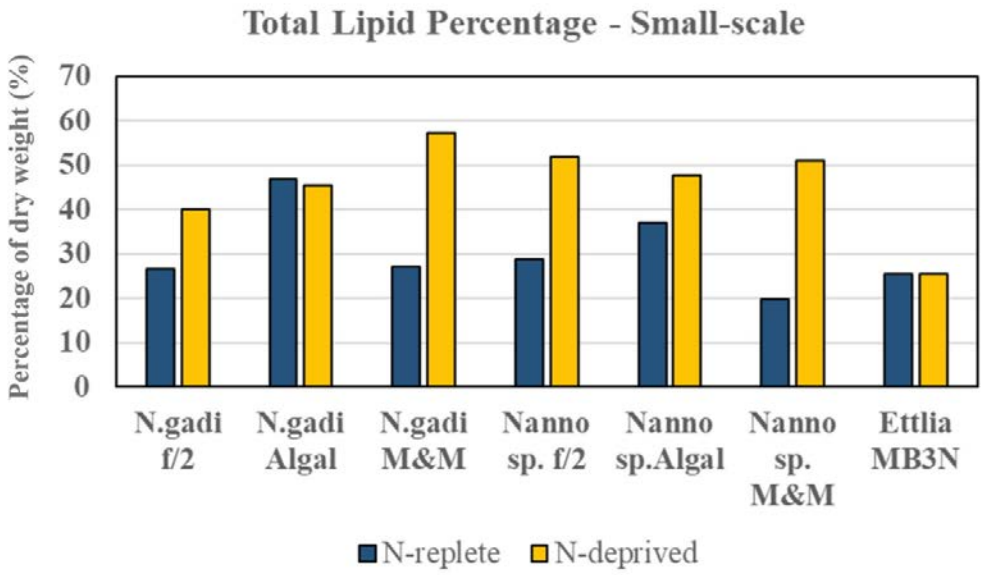

Figure 4.19. Total lipid percentage of 2L microalgae cultivation.

According to the measurements, lipid percentage of nearly all small-scale cultivation increased under nitrogen deprivation (Figure 4.19). One exception in *N. gaditana* cultivation in Algal medium (condition #3 and condition #4), which total lipid percentage of N-replete condition (46.8%) was similar to N-deprived condition (45.6%). Most lipid percent was gravimetrically measured as 57.44 % ± 8.33 % in *N. gaditana* cultivation in M&M medium under nitrogen deprivation. All N-deprived *Nannochloropsis sp*. cultures had at least 47% total lipid content. Condition #8 had higher biomass productivity and lipid content than condition #7, which was promising. Increase the lipid percentage

in nitrogen deprivation of both Nannochloropsis species in f/2 (+65% lipid increase) and M&M (+135% lipid increase) media was remarkable. There was no difference in total lipid percentage between N-deprived and N-replete *E. oleoabundans* cultures.

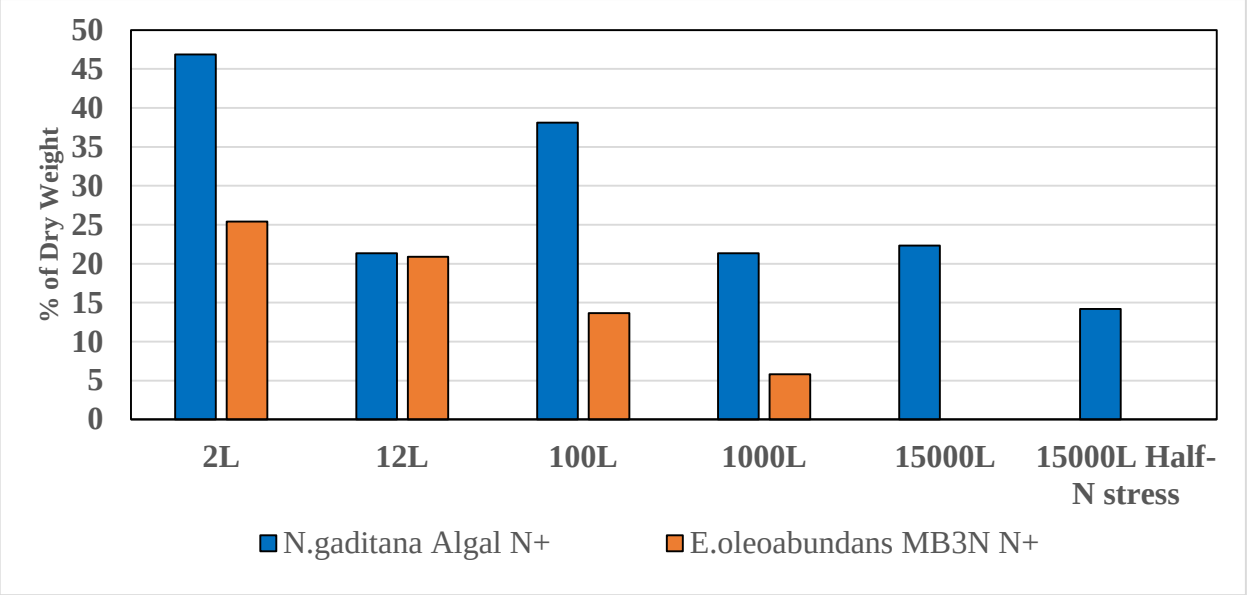

Figure 4.20. Total lipid percentage of scale-up process with selected microalgae conditions.

Lipid percentage of scaling up of condition #3 (*N. gaditana*, Algal medium in N-replete) and condition #13 (*E. oleoabundans*, MB3N medium in N-replete) were shown in Figure 4.20. Lipid percent of 2L cultures were added to compare the performances of scale-up. For *E. oleoabundans*, 12L lipid percentage was taken from 12L glass carboy cultures. Lipid percentage of *N. gaditana* was 22.60% ± 0.25% for 12L glass carboy, 38.11% ± 7.71% for 100L, 23.66% ± 0.91% for 1000L, 22.33% ± 2.10% for 15000L, and 14.21% ± 0.62% for 15000L in half-N stress. Lipid percentage of *E. oleoabundans* was 20.88% ± 6.31% for 12L glass carboy, 32.35% ± 3.18% for 12L tubular PBR, 13.66% ± 2.44% for 100L, 5.80% ± 0.94% for 1000L.

Lipid percentage of cultures were tended to decrease when cultivation volume increased. One exception was 100L *N. gaditana* cultivation, which was highest lipid productivity in outdoor open ponds. 12L, 1000L and 15000L *N. gaditana* cultures showed a similar lipid percentage. 15000 half-N stress pond had lower lipid percentage at its 16th day than 15000L N-replete condition.

E. oleoabundans had better maximum biomass concentration but less lipid productivity in 12L glass carboy than 12L tubular PBR. Lipid percentage of 12L *N. gaditana* and *E. oleoabundans* glass carboys were similar. Like small scale conditions, *Ettlia* showed less lipid productivity than *Nannochloropsis*.

4.3.2. Lipid Extraction from Wet Biomass

Lipids of 1000L *N. gaditana* wet biomass were extracted according to method 3.4.2 subsection. Figure 4.21 shows that there was no significant change between 1:10 and 1:20 dried biomass:chloroform ratio during lipid extraction from *N. gaditana* wet biomass. To avoid more waste and lower the operational cost and volume, 1:10 dried biomass:chloroform ratio was chosen to perform lipid extraction from wet biomass.

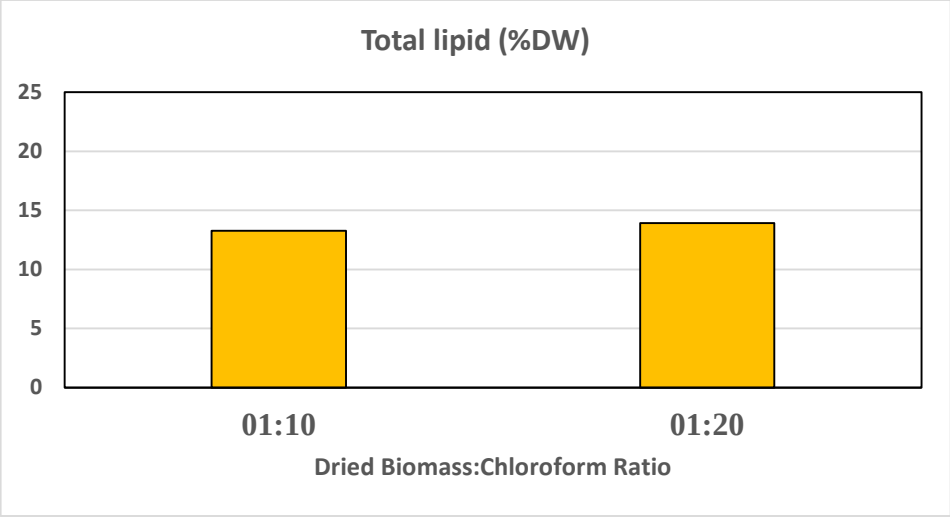

Figure 4.21. Biomass:chloroform ratio optimization of lipid extraction from wet biomass in acid treatment + ultrasonication 30 min.

Lipids of 15000L *N. gaditana* (condition #18) wet biomass were extracted with different pre-treatments. Method in subsection 3.4.2 was used with three different pre-treatments. Compared with bead milling and bath-type sonication pretreatment on dried microalgae method in subsection 3.4.1, which was called reference method, all of pretreatments on high volume (15L or above) wet biomass were measured as less efficient, as shown in Figure 4.22 (60% efficiency average). Lipid percentage of wet biomass with pH 3 treatment using acetic acid and ultrasonication for 30 min. was 15.70% and had highest percentage of the three. Only ultrasonication treatment for 50 min. had 10.03% lipid percent, which was significantly lower than others. Wet biomass pre-treated with industrial homogenizer and pH had 14.08%, which is close to pH+ ultrasonication for 30 min. Compared to reference method, bulk lipid extractions were not reached all lipids inside *N. gaditana* cells.

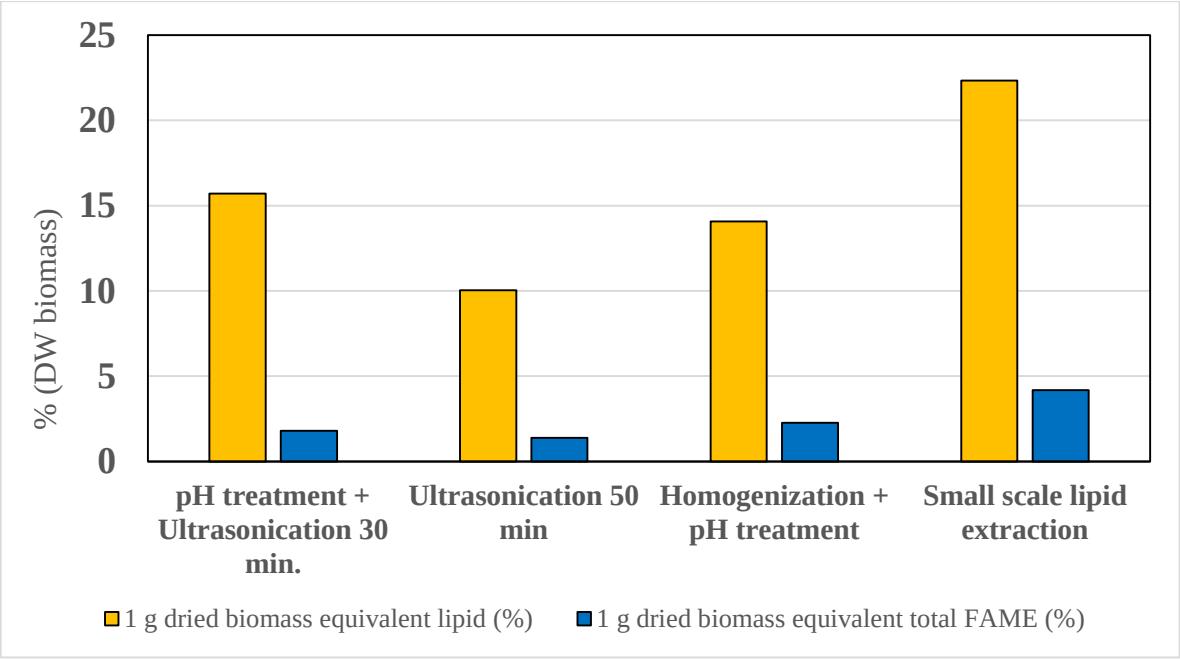

Figure 4.22. Comparison of lipid and FAME productivity of several lipid extraction approaches.

Same amount of *N. gaditana* wet biomass was homogenized in industrial high-pressure homogenizer from 400 bar to 1200 bar. Homogenization was applied for several minutes for each 200 bar intervals (Figure 4.23). Lipid percentage of homogenized *N. gaditana* wet biomass were 14.53% for 400 bar, 18.50% for 600 bar, 19.71% for 800 bar, 14.33% for 1000 bar and 16.63% for 1200 bar. Average lipid percentage of homogenization series was 16.1%. There was a slight increase in lipid yield from 400 bar to 800 bar homogenizations. Sudden decrease in lipid yield at 1000 bar was observed. Average lipid percentage of homogenization (16.1%) yielded 27.5% less than small lipid extraction method (22.2%) on the same biomass.

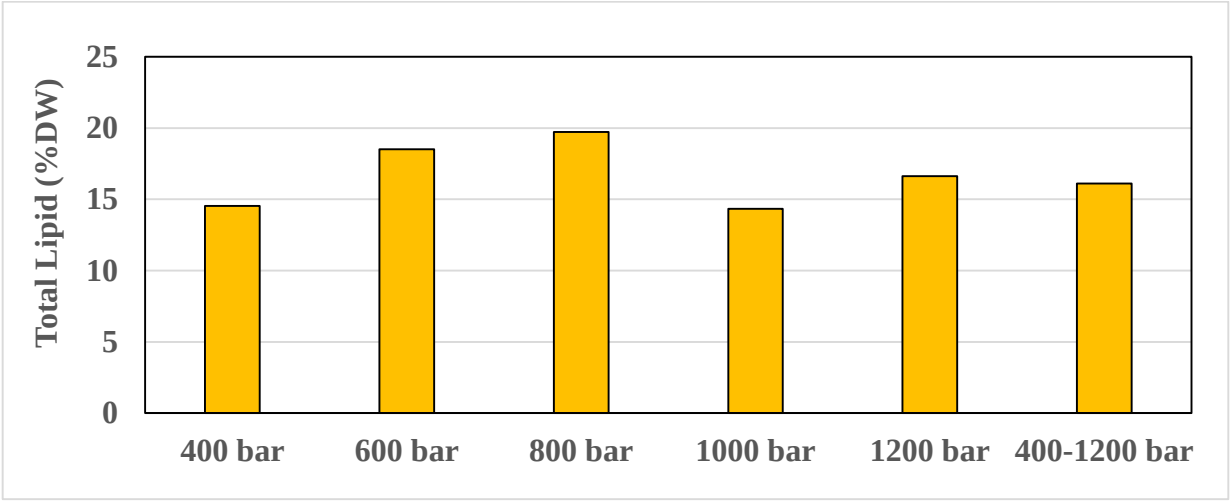

Figure 4.23. Comparison of lipid extraction efficiencies using homogenization at different pressures.

4.4. Transesterification and Fatty Acid Methyl Ester Profile of Algal Lipids using Gas Chromatography

In this section, FAME profiles extracted by reference lipid extraction method were explained (Method 3.4.1) from 23 different conditions (Table 4.1). 37 FA concentrations were analyzed at in each condition and analyzes resulted from significant data was explained in this section. GC-FID chromatograms were compared and analyzed like in Figure 4.24. All FA concentrations and percentages of the 23 conditions were added to the Appendix section.

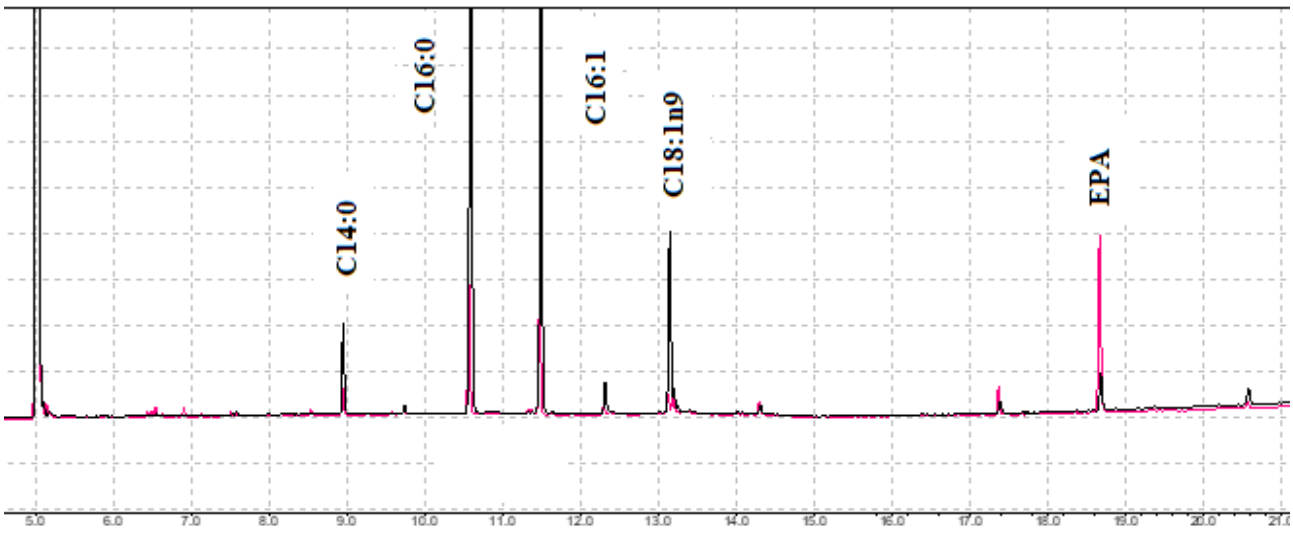

Figure 4.24. Comparison of FAME profile chromatograms of *N. gaditana* in 2L Algal medium under N-replete (purple peaks) and N-deprived (black peaks) conditions.

4.4.1. Fatty Acid Methyl Ester Concentration and Profile of Microalgae Cultivations

Among all small-scale cultures, total FAME concentration in biomass was increased under nitrogen deprivation. In *N. gaditana* cultures under N-replete conditions, total FAME concentrations were 99.40 $mg_{FAME}/g_{biomass}$ for f/2 medium, 78.65 $mg_{FAME}/g_{biomass}$ for Algal medium, and 61.74 $mg_{FAME}/g_{biomass}$ for M&M medium (Figure 4.25) *N. gaditana* on nitrogen deprivation performed 160.14 $mg_{FAME}/g_{biomass}$ for f/2 medium, 238.31 $mg_{FAME}/g_{biomass}$ for Algal medium, and 262.00 $mg_{FAME}/g_{biomass}$ for M&M medium (Figure 4.25). FAME concentrations were increased +61.09% for f/2 medium, +202.99% for Algal medium, and +324.38% for M&M medium under nitrogen deprivation on *N. gaditana*.

FAME profile of small-scale *N. gaditana* cultures depended on media type and nitrogen concentrations (Figure 4.26). More than 50% of FAMEs consisted of palmitic acid (C16:0) and palmitoleic acid (C16:1) in all *N. gaditana* small-scale conditions. All *N. gaditana* cultures had less C18 FAs, and high amount of EPA. N-replete conditions had higher EPA percentage and lower C16 FAs. In Algal medium N-replete condition, EPA production was 36.44% of all FA production in *N. gaditana*. Same condition had lowest C18 FA percentage in *N. gaditana* biomass. In M&M medium N-deprived condition, C16:0 and C16:1 FAs made up 20.28% of *N. gaditana* biomass.

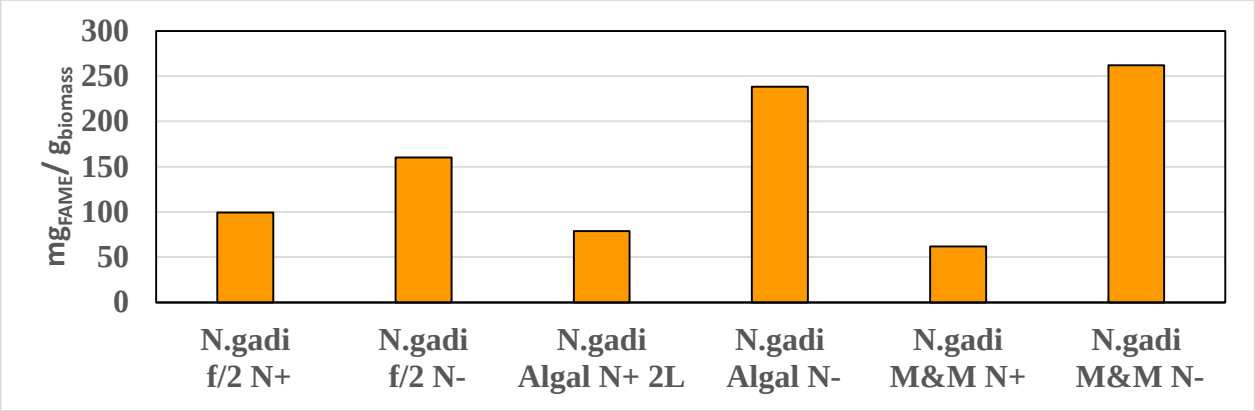

Figure 4.25. Total FAME concentration of *N. gaditana* in small scale.

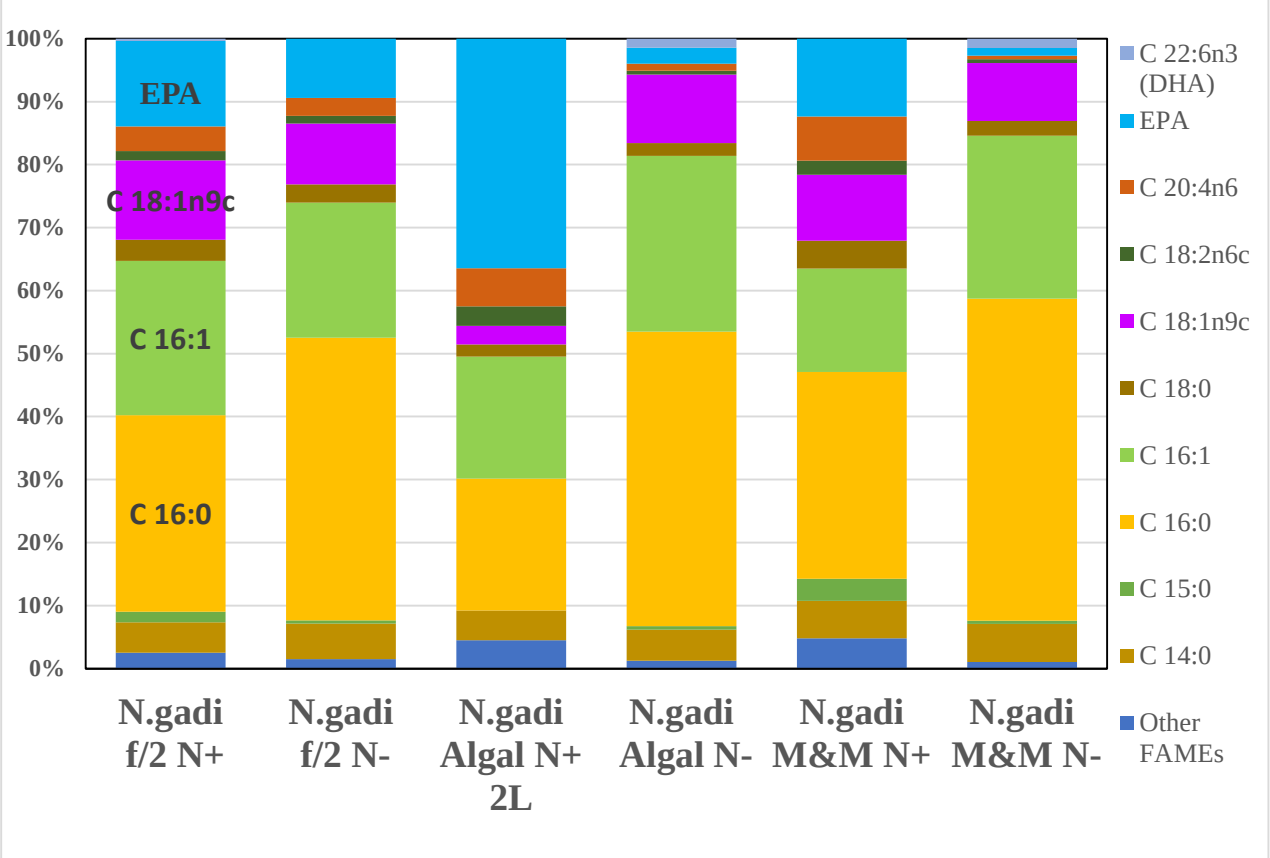

Figure 4.26. FAME profile of *N. gaditana* cultures in small-scale.

Nannochloropsis sp. performed similarly to *N. gaditana* in terms of FAME profile, with little differences in EPA and C18 FAs. *Nannochloropsis sp.* in N-replete conditions reached 73.97 $mg_{FAME}/g_{biomass}$ for f/2 medium, 54.32 $mg_{FAME}/g_{biomass}$ for Algal medium, 31.56 $mg_{FAME}/g_{biomass}$ for M&M medium (Figure 4.27). Condition #11 had the lowest FAME concentration in 2L *Nannochloropsis* cultures. Under nitrogen deprivation, FAME concentration of *Nannochloropsis sp.* cultures increased to 314.24 $mg_{FAME}/g_{biomass}$ for f/2 medium, 211.33 $mg_{FAME}/g_{biomass}$ for Algal medium, 199.45 $mg_{FAME}/g_{biomass}$ for M&M medium. FAME concentrations in *Nannochloropsis sp.* were increased +324.82% for f/2 medium, +289.05% for Algal medium, and +532.00% for M&M medium. Condition #11 and #12 had highest increase in FAME concentrations because of nitrogen deprivation, along with low base effect.

FAME profiles of *Nannochloropsis sp.* cultures were majorly consisted of C16 and C18 fatty acids (Figure 4.28). *Nannochloropsis sp.* cultures under nitrogen deprivation had more than 70% of C16:0 and C16:1 FAs in their FAME profiles. *Nannochloropsis sp.* in f/2 medium under N-deprivation had highest FAME concentration (31.42% of dry weight), along with highest C16 and C16:1 FA concentration which were 13.97% and 8.76% of dry weight, respectively. Small-scale *Nannochloropsis sp.* cultures had 56% less EPA production percentage than small-scale *N. gaditana* cultures, but *Nannochloropsis sp.* cultures had more average saturated fatty acid (SFA) concentration (87.78 $mg_{FAME}/g_{biomass}$) and average monounsaturated fatty acid (MUFA) concentration (60.36 $mg_{FAME}/g_{biomass}$) than small-scale *N. gaditana* cultures (SFA: 79.40 $mg_{FAME}/g_{biomass}$, MUFA: 51.31 $mg_{FAME}/g_{biomass}$). Significant amount (>3% of all FAME profile) of FAs shorter than C14:0 was not observed in all *Nannochloropsis* cultures.

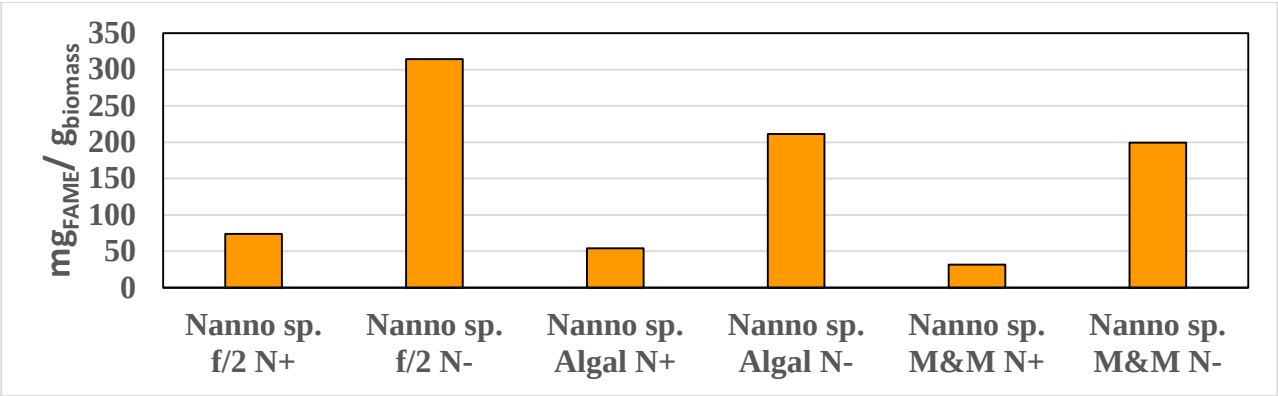

Figure 4.27. Total FAME concentration of *Nannochloropsis sp.* cultures in small-scale.

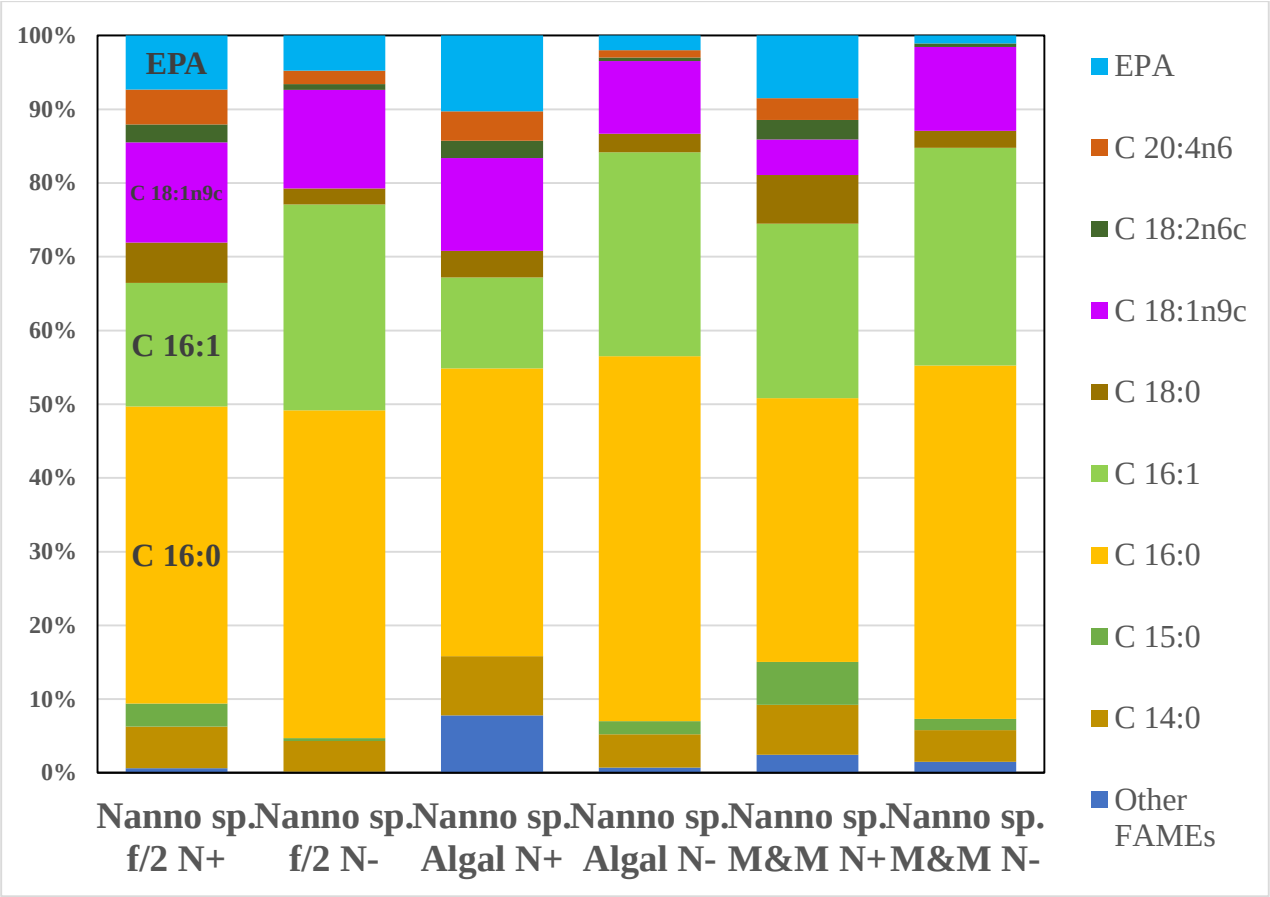

Figure 4.28. FAME profile of *Nannochloropsis sp.* cultures in small scale.

In scale-up process, there was a tendency to decrease FAME concentration in *N. gaditana* biomass (Figure 4.29). FAME concentration in *N. gaditana* cultures was 52.20 $mg_{FAME}/g_{biomass}$ for 12L, 57.46 $mg_{FAME}/g_{biomass}$ for 100L, 50.07 $mg_{FAME}/g_{biomass}$ for 1000L, 41.79 $mg_{FAME}/g_{biomass}$ for 15000L. FAME concentration in *N. gaditana* half-N stress at 16th day was 30.27 $mg_{FAME}/g_{biomass}$, 27.5% less than the N-replete culture. FAME concentrations of *N. gaditana* in scale-up process showed similar tendencies with lipid percentage in dry weight.

N. gaditana cultures in large-scale showed more EPA-productive profiles than small-scale *N. gaditana* cultures (Figure 4.30). Proportions of C16:0 and C16:1 FAs in their FAME profiles were reduced to 40% levels. Among large-scale cultures, 100L *N. gaditana* culture had highest MUFA proportion (30.66%) in FAME profile. On the other hand, 1000L *N. gaditana* culture had EPA as 42.77% of its total FAs, which was the highest ratio. Primary difference in 15000L *N. gaditana* cultures was MUFA proportion change, which was from 21.23% for N-replete, to 3.12% half-N stress culture. SFAs were tended to increase when nitrogen concentration was decreased. Arachidonic acid (C20:4n6) was produced in higher proportions in large-scale *N. gaditana* cultivation, 22.5% than the small-scale cultures. No C20:4n6 production was observed at condition #19.

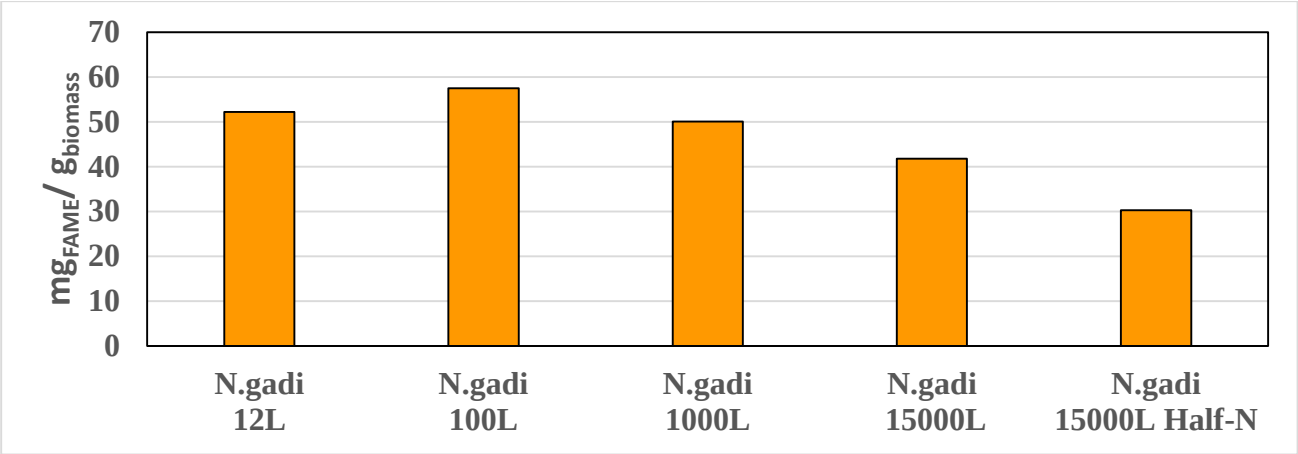

Figure 4.29. Total FAME concentration of *N. gaditana* culture in scale-up process.

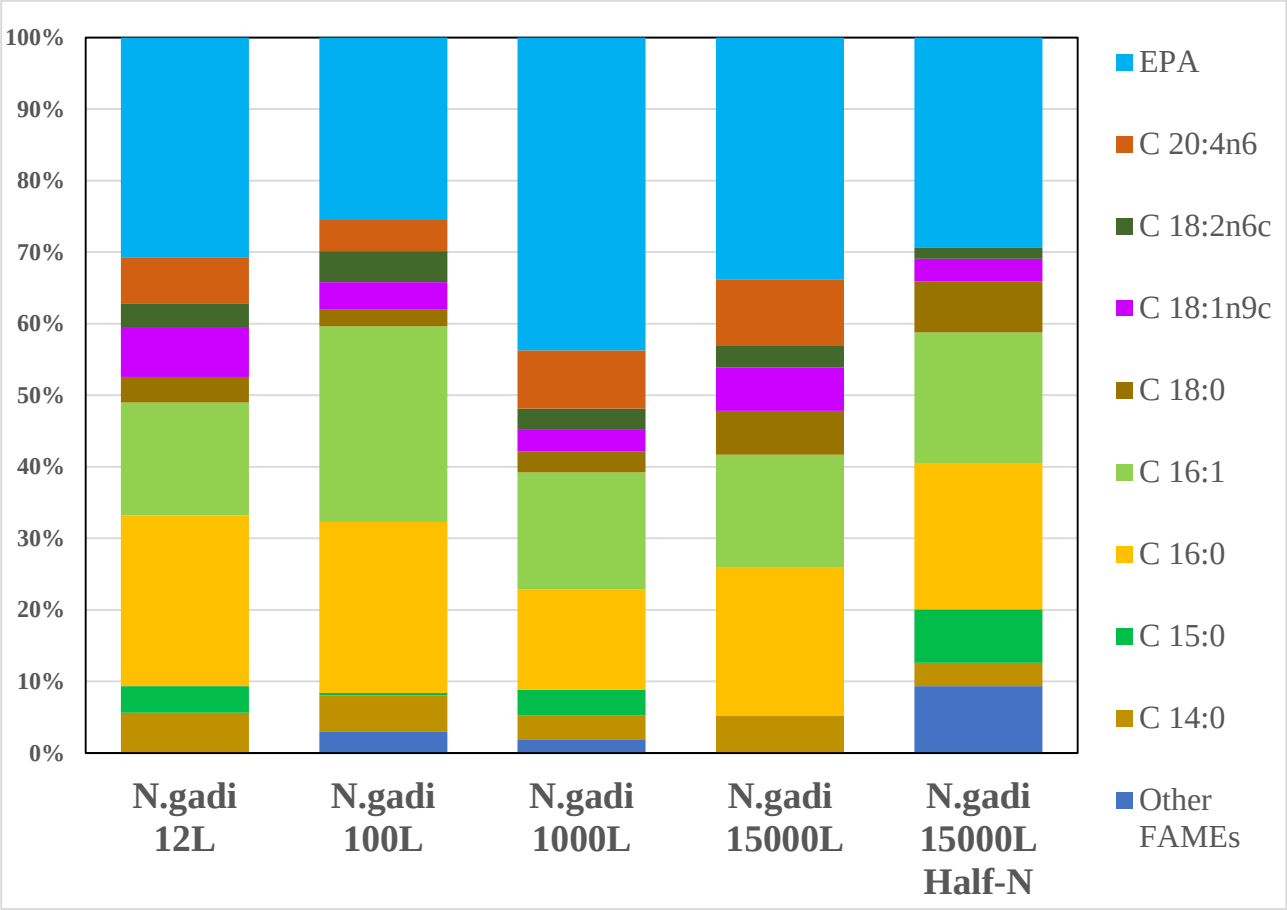

Figure 4.30. FAME profile of *N. gaditana* cultures in scale-up process.

In all *E. oleoabundans* conditions, FAME concentration depended on PBR design and nitrogen deprivation (Figure 4.31). Small-scale *E. oleoabundans* culture had 33.85 $mg_{FAME}/g_{biomass}$ in N-replete conditions, and 58.77 $mg_{FAME}/g_{biomass}$ in N-deprived conditions. FAME concentration in small *E. oleoabundans* culture increased even their lipid percentage did not change. In 12L working volume cultures, glass carboys had 28.69 $mg_{FAME}/g_{biomass}$ whereas tubular PBRs had 88.4 $mg_{FAME}/g_{biomass}$. There was +208.13% FAME concentration increase in *E. oleoabundans* dry biomass when same

microalgae cultivated in tubular PBRs. In *E. oleoabundans* outdoor ponds, lowest FAME concentrations were observed as 26.76 $mg_{FAME}/g_{biomass}$ for 100L, and 8.08 $mg_{FAME}/g_{biomass}$ for 1000L. Average FAME concentration of *E. oleoabundans* cultures (4.08%DW) was lower than average FAME concentrations of *N. gaditana* (15.03%DW) and *Nannochloropsis sp.* (14.74%DW).

C16 and C18 FA variants dominated the FAME profile of *E. oleoabundans* cultures (Figure 4.32). 5 variants of C18 FAs, which are C18:0 (Stearic acid), C18:1n9c (cis-9-octadecenoic acid / elaidate), C18:2n6c (cis-linoleic acid), C18:2n6t (trans-linoleic acid) and C18:3n3 (α-Linolenic acid), were detected in all *E. oleoabundans* cultures, except in 1000L *E. oleoabundans* culture. These variants helped to increase PUFA proportion of *Ettlia* lipids, up to 61.02% of all FAME in 2L N-replete condition. PUFA proportion decreased as cultivation volume increased or nitrogen deprivation were applied. C16 proportion in *E. oleoabundans* dry biomass was between 20-34% regardless of conditions. *E. oleoabundans* in 12L tubular PBR had 27.57 mg C16:0 production in 1g dry biomass, which was the highest singular FA production in any *E. oleoabundans* culture. Combining with vertical PBR advantage, *E. oleoabundans* in 12L PBR can reach 2180 mg_{FAME} $/m_2$/day productivity. Other areal and volumetric biomass, lipid and FAME productivity comparisons were shown in Figure 5.1.

C18:2n6 proportion were 37.71% in *E. oleoabundans* 2L N-replete condition and it was similar to other indoor *E. oleoabundans* conditions (29.8% for N-deprived, 37.2% for 12L glass carboy and 32.3% for 12L tubular PBR). However, outdoor conditions reduced C18:2n6 condition to 11.2% for 100L and 5.12% 1000L *E. oleoabundans* open ponds. It can be said that C18:2n6 proportion in FAME profile can be used for healthy growth indicator in *E. oleoabundans* cultures. Increase in C18:1n9 proportion was observed during nitrogen deprivation.

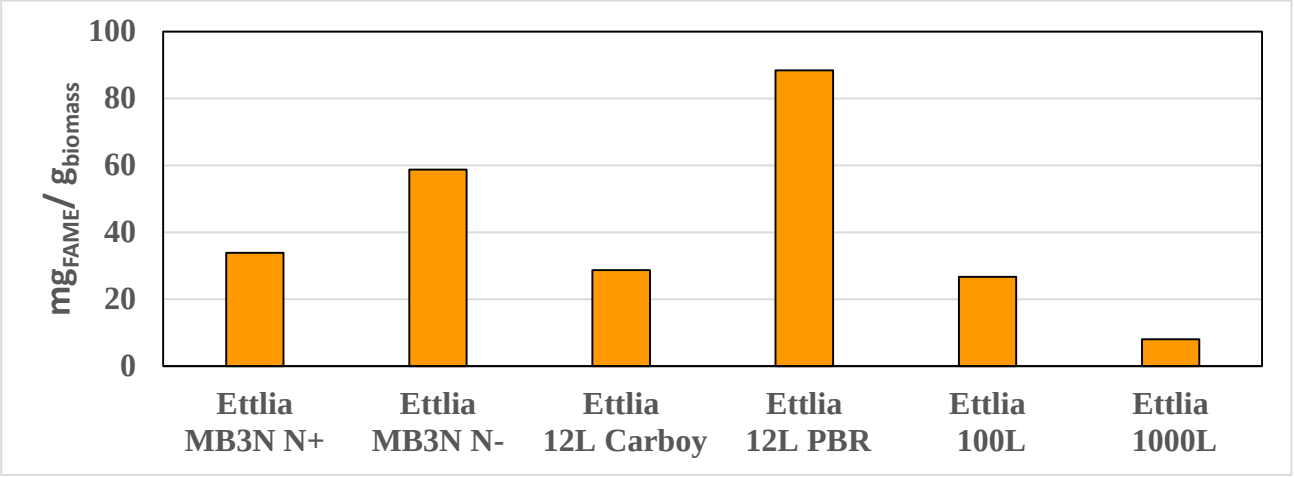

Figure 4.31. Total FAME concentration of all *E. oleoabundans* cultures.

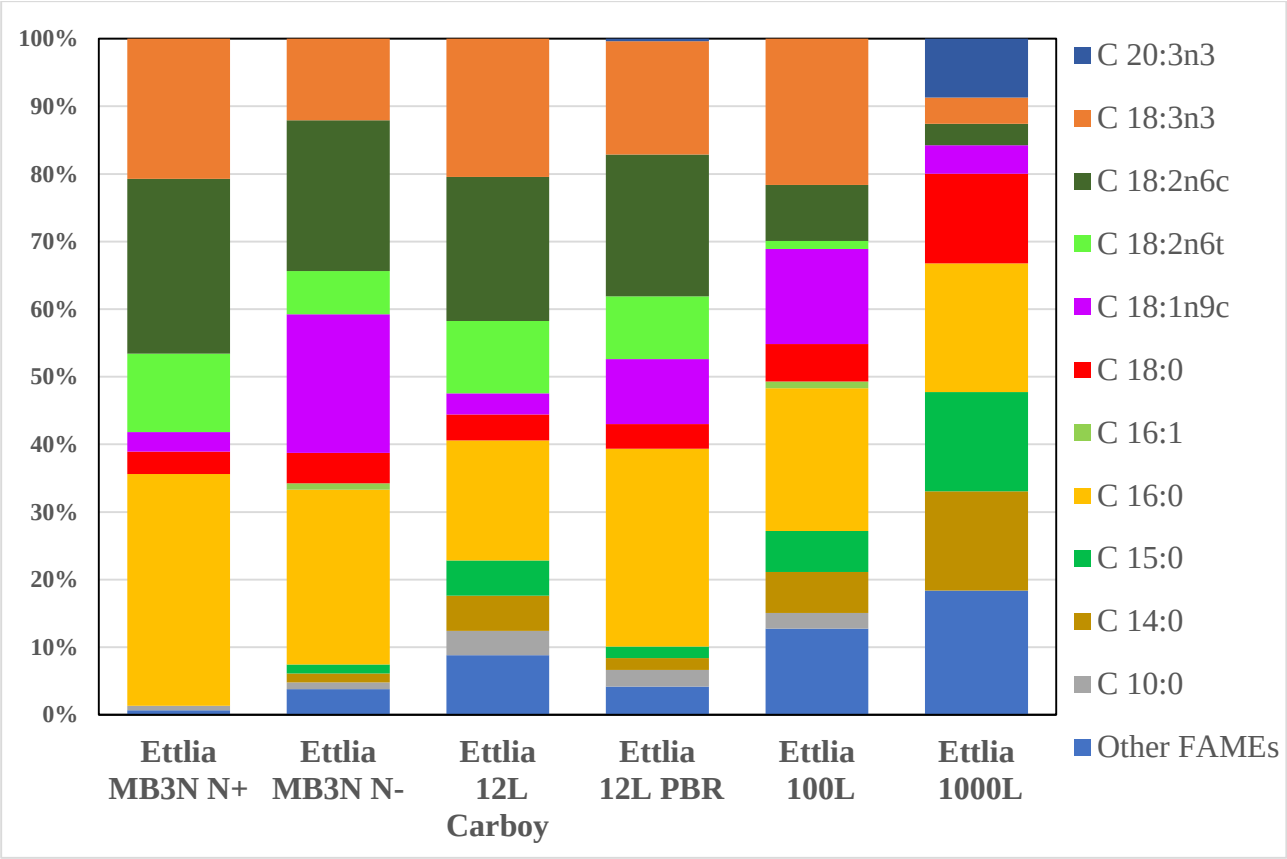

Figure 4.32. FAME profile of all *E. oleoabundans* cultures.

Among all of 23 conditions, total FAME concentration was highest at *Nannochloropsis sp.* biomass in 2L f/2 medium under N-deprived conditions, which was 31.4% of dry weight (Figure 4.33). *N. gaditana* had the second-best FAME yield in two different media (Algal and M&M) under nitrogen deprivation. The 8 conditions with the highest FAME concentration were *Nannochloropsis* cultures. Most concentrated FAME was found in *E. oleoabundans* at culture in 12L tubular PBR, as 8.84% of dry weight. Besides the amount of FAME in the biomass, biomass concentration in the culture is as much as important for FA productivity. This issue is also addressed in section of results overview.

High-value added FA production, like EPA and DHA, and conversion of these FA into a different product from the same raw material by separating them from FAs to be used in biofuel will help to achieve affordability of biofuels through multivalorization. *N. gaditana* produced 28.66 mg EPA per g biomass in Algal medium under N-replete conditions (Figure 4.34), which was the highest EPA yield of all conditions. Highest EPA yields were followed by *N. gaditana* in 1000L (21.42 mg) and 12L (15.73 mg) Algal medium N-replete. 7 of the best 8 conditions for EPA production were from *N. gaditana* cultures. EPA was not detected in *E. oleoabundans* cultures.

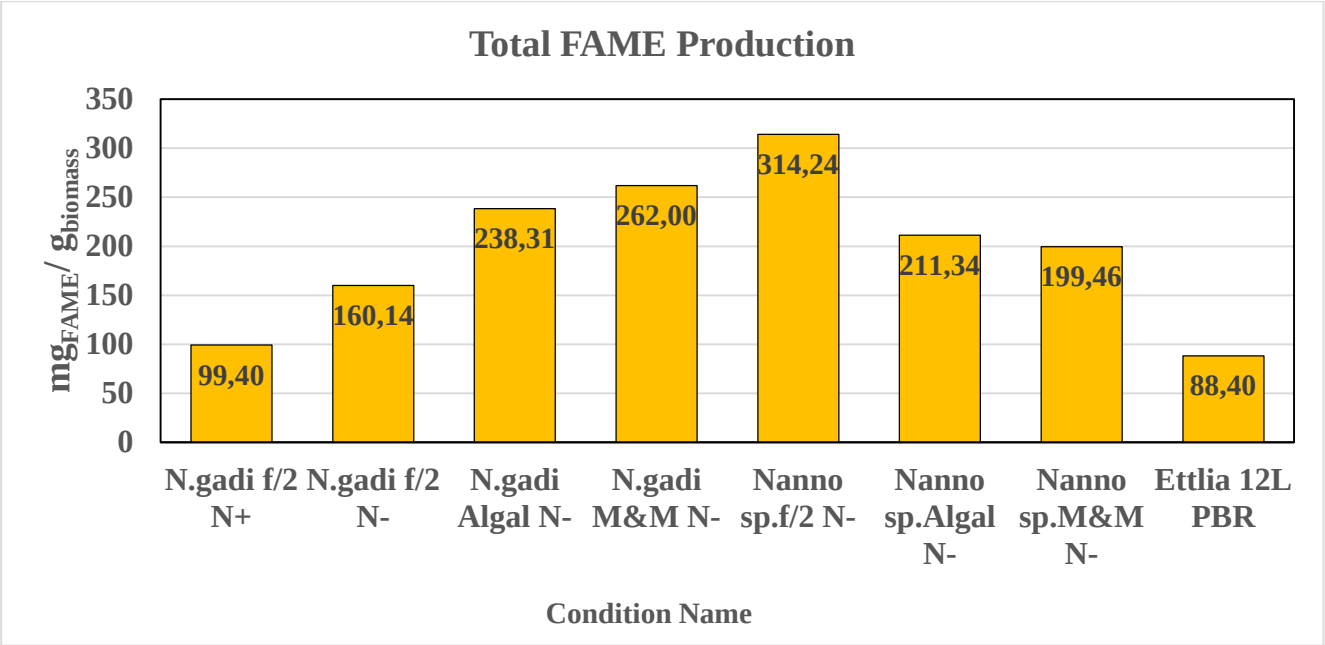

Figure 4.33. Highest total FAME concentrations of 23 microalgae cultivations.

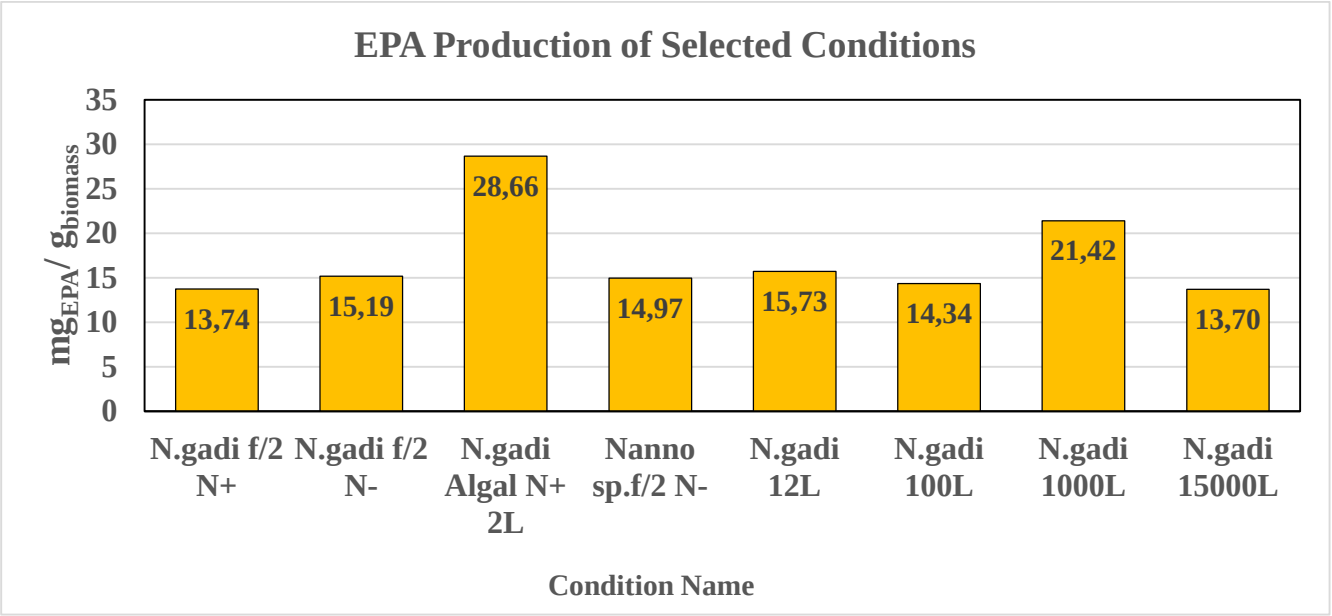

Figure 4.34. Highest EPA concentrations of 23 microalgae cultivations.

Table 4.6. Proportion of fatty acid saturation under N-replete and N-deprived conditions in small-scale microalgae cultivation. (SFA: saturated fatty acids, MUFA: monounsaturated fatty acids, PUFA: polyunsaturated fatty acids).

	2L N+	2L N-	Change
SFA %	47.55	53.12	111.72
MUFA%	25.01	35.47	141.85
PUFA%	27.44	11.40	41.558

Average saturation proportions of fatty acids from small-scale (2L) microalgae cultivation under N-replete and N-deprived conditions was shown in Table 4.6. Under nitrogen stress, PUFA concentrations were reduced up to 60%. It can be concluded that nitrogen deprivation can be applied mostly for saturated and monounsaturated fatty acid production.

4.4.2. Change in Fatty Acid Methyl Ester Profile Using Different Lipid Extraction Methods from Wet Microalgae Biomass

Change in FAME profile using different pretreatments for lipid extraction applied to same biomass was shown in Figure 4.35. It was observed that PUFA ratio was slightly reduced in the use ultrasonication for 50 min. and industrial homogenization. Small-scale lipid extraction method with bead milling extracted the most concentrated EPA from same biomass. C16:0 and C16:1 proportion were higher in ultrasonicated and homogenized samples than samples with bead milling pretreatment.

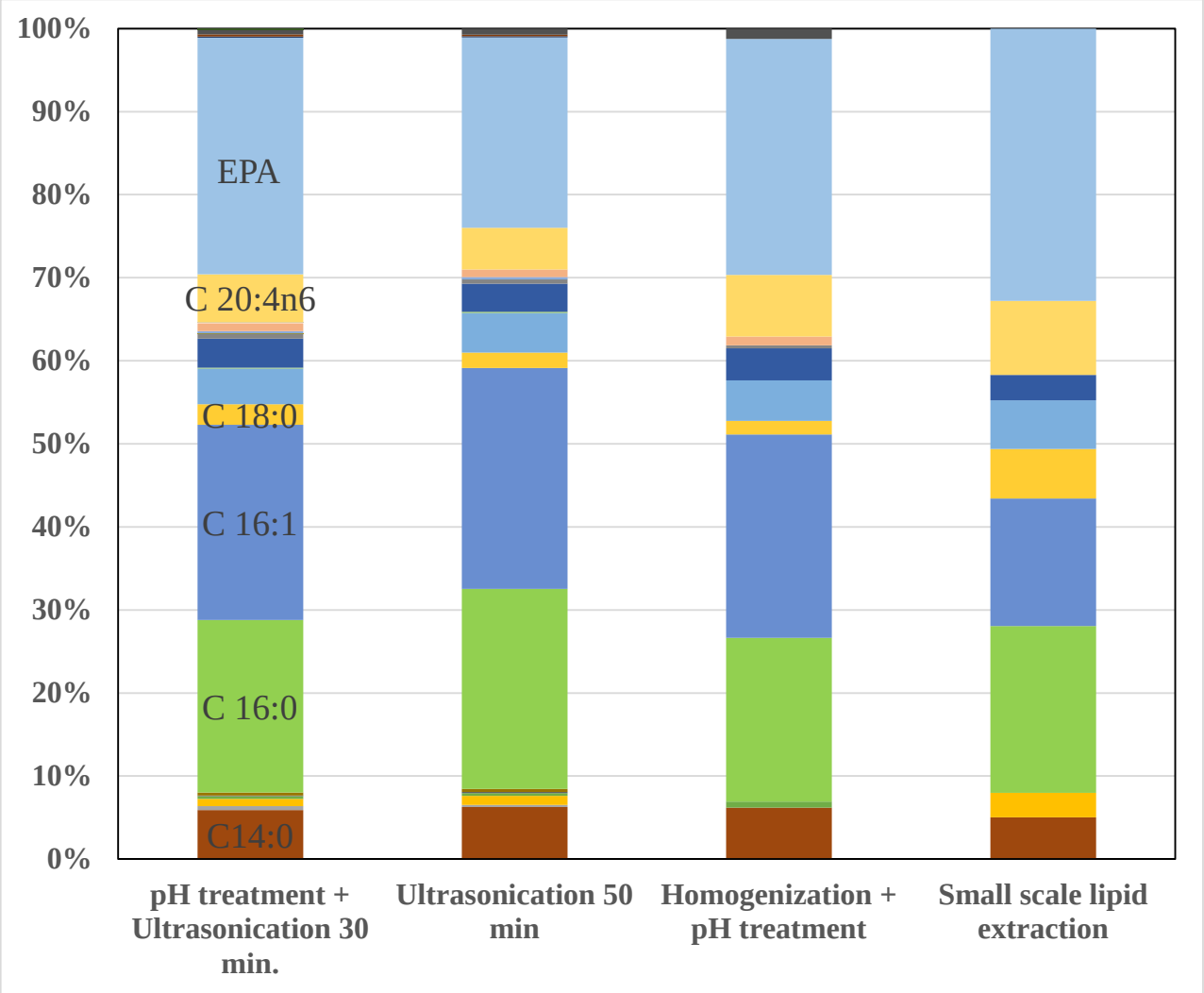

Figure 4.35. FAME profile comparison of several lipid extraction methods on same biomass.

4.5. Purification of Algal Lipid Extract

4.5.1. Selection of Primary Extraction Solvent for Lipid Purification

Acetonitrile and ethanol were tested as primary extraction solvent towards lipid purification according to method 3.5 subsection (Figure 4.36). Ethanol with 3 mg/mL activated carbon (AC) showed the best performance of lipid extraction and selectivity by far from the other conditions, shown in Figure 4.37. FAME was drastically lost after more than 3 mg/mL AC in solvent. Especially polar FAs were lost after excessive AC addition (data not shown). In acetonitrile solvent, there were two phases in 3 mg/mL AC condition, and their FAME concentrations were similar (161.52 µg FAME/mL for bottom phase, 203.47 µg FAME/mL for upper phase). Every FAME concentration of selected solvent in different AC concentrations was follow as µg/mL: In ethanol, 5238.2 µg/mL for 3 g/L AC, 31.27 µg/mL for 8 g/L AC, 19.45 µg/mL for 30g/L AC, 16.45 µg/mL for 80g/L AC. In acetonitrile, 364.92 µg/mL for 3g/L AC, 53.68 µg/mL for 8g/L AC, 23.66 µg/mL for 30g/L AC, 26.15 µg/mL for 80g/L AC.

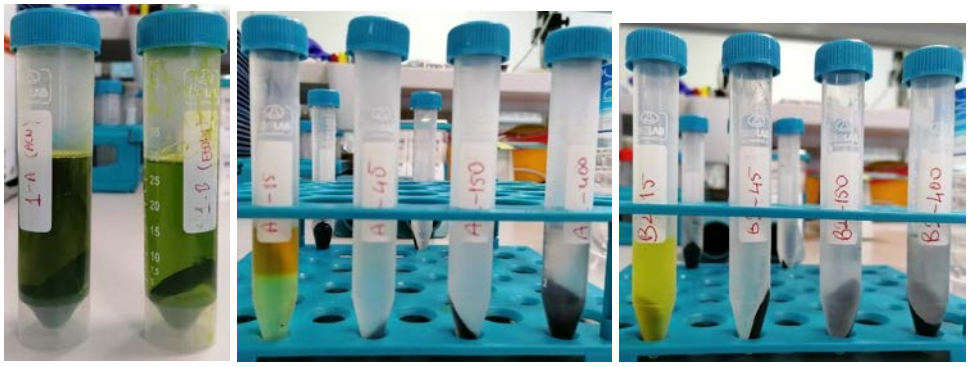

Figure 4.36. Crude extracts before chlorophyll removal (left), crude extracts in acetonitrile after chlorophyll removal (middle), crude extracts in ethanol after chlorophyll removal (right).

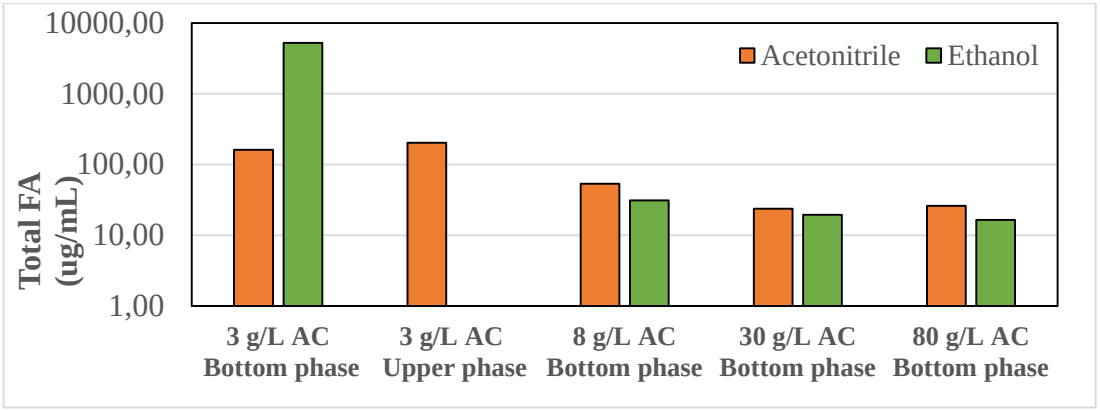

Figure 4.37. Total FA of crude extracts in selected primary extraction solvents in semi-logarithmic graph.

4.5.2. Comparison of Several Methodologic Differences for Lipid Purification

For lipid purification, three different approaches were used mentioned in method 3.5. subsection. 2 mL of the remained lipid part of each approach (Figure 4.38) was dried in glass tube and weighed. Dried extracts of each approach in 2 mL volume were 20.1 mg for first approach (EtOH-instant), 32.6 12.74 mg average for second approach (EtOH-MeOH instant), mg for third approach (EtOH-MeOH-overnight). FAME concentrations of different lipid extraction and purification methods were 136.1 µg FA/mg extract for first approach, 39.0 µg FA/mg extract for second approach and 47.3 µg FA/mg extract for third approach. FAME profiles of third approach were similar to each other, except in third approach, which was incubated at 4°C overnight, there was a slight increase in C16:1 FA and EPA and slight decrease in C16:0 FA proportions (data were not shown).

Figure 4.38. Different lipid extracts during lipid purification (leftmost: first approach, middle: third approach, remaining: second approach).

As a result of lipid and FAME concentration of different lipid extraction and lipid purification, it was concluded that high incubation time was not required for effective purification, and EtOH-MeOH was a useful candidate for biocrude extraction and lipid purification.

4.5.3. Fine Optimization of Activated Carbon Concentration

Concentration of activated carbon needs to be finely-optimized to ensure that impurities in lipids were adsorbed by activated carbon but there was not an empty activated carbon to adsorb the lipids of interest for bio-jet fuel studies. Supernatant of eight different AC concentration during lipid purification were spectrophotometrically measured and their FAME profile were analyzed using GC-FID. Eight AC concentrations were 0, 3, 4, 5, 6, 7, 8 and 9 mg AC/mL (Figure 4.39). Change in four wavelengths most absorbed, which were 330 nm, 440 nm, 470 nm and 660 nm, were measured while AC concentration increased.

Figure 4.39. Lipid extracts in ethanol with different activated carbon (AC) concentration (left: unprocessed, right: 9mg/mL AC, AC concentration increased from left to right).

660 nm absorbance, which gives indirect information about amount of chlorophyll, decreased by more than 80% from lowest activated carbon concentration (Figure 4.40). Absorbance at all four wavelengths also decreased by up to 95% as activated carbon increased. After AC concentration exceeded 5g/L and beyond, any significant absorbance could not be detected at highest four wavelengths.

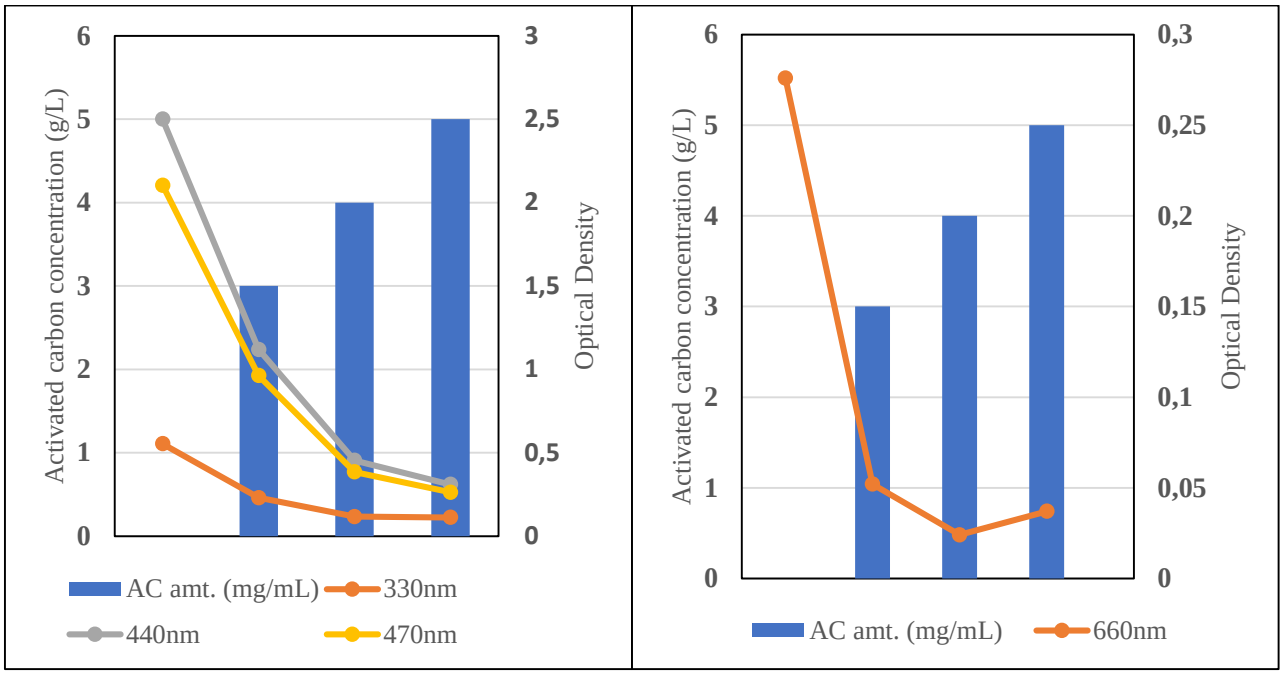

Figure 4.40. Change in four optical densities with different activated carbon concentrations.

Total fatty acid (FA) concentrations of samples with different activated carbon concentrations were (from 0 mg/ml to 9 mg/ml, respectively): 710.24, 367.89, 214.51, 184.59, 79.54, 44.84, 59.05, 48.88 µg FA/mL. FAME profile of samples treated by different activated carbon concentration was

shown in Figure 4.41. Most affected FA from AC treatment was EPA (C20:5). FA percentage in dried extract with different AC concentrations were (from 0 mg/ml to 9 mg/ml, respectively): 11.52%, 21.22%, 16.50%, 9.89%, 0.91%, 1.42%, 6.81%, 3.41%.

Based on the wavelength spectrum and FAME profile observations, it was decided to apply AC treatment as 3 mg/mL for lipid purification.

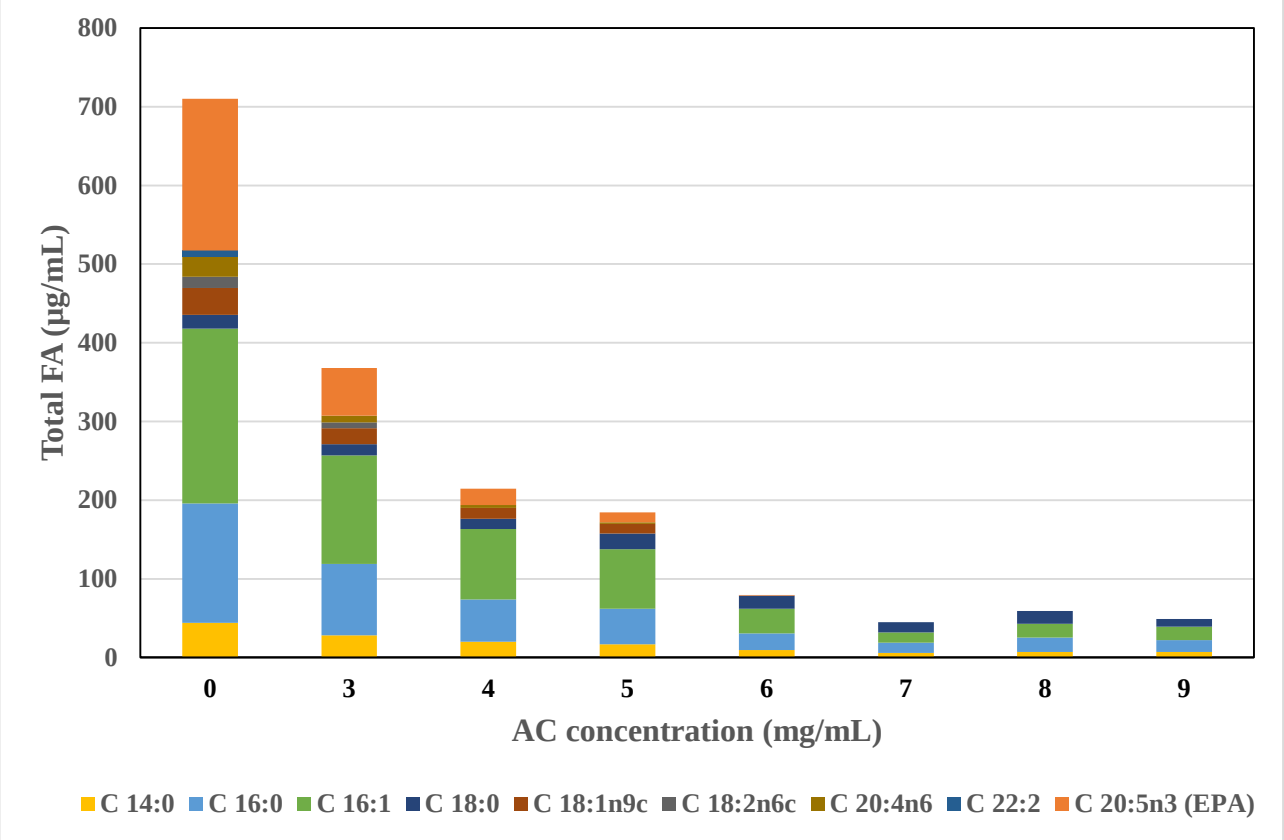

Figure 4.41. FAME profile of homogenized *N. gaditana* samples treated by different activated carbon (AC) concentration during lipid purification.

4.5.4. Recovered Chloroform Use and Biodiesel Production

In order to support sustainable production, a trial for biodiesel production was performed by using recovered chloroform and n-hexane in same lipid extraction and purification methods. n-hexane was also used in these experiments as a secondary (lipid) solvent extractor.

Figure 4.42. From left to right: crude extract before and after chlorophyll removal, chloroform extraction of crude extract, n-hexane extraction of crude extract and esterified algal lipids.

FA concentrations (also FA% in extract) of different lipid extraction and purification procedures were 0.13 mg_{FA}/ $mg_{extract}$ for hexane-1, 0.08 mg_{FA}/ $mg_{extract}$ for EtOH-1, and 0.16 mg_{FA}/ $mg_{extract}$ for hexane-2. FAME profile of each experiment was shown in Figure 4.43. FA concentrations of these experiments were low compared to other lipid extraction and purification methods. Ultimately, three extracts were mixed to form biodiesel.

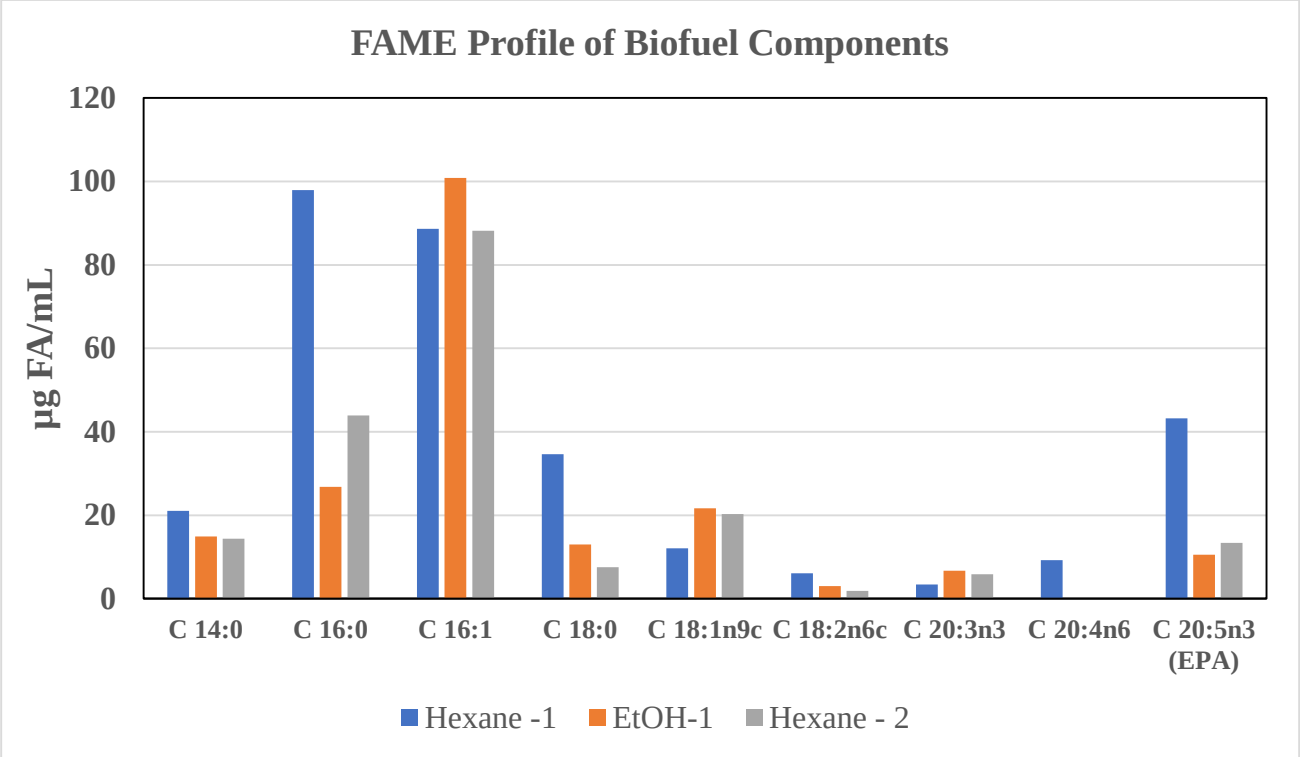

Figure 4.43. FAME profile of purified lipid extracts for biofuel.

4.6. Results Overview

23 different microalgae conditions were cultivated, and their growth profiles were spectrophotometrically analyzed. Organic and ash contents of each culture were measured. Total lipid percentage in dried biomass was gravimetrically calculated for each culture, and sample of their lipid extracts were transesterified and analyzed using GC-FID. Quantification of 37 fatty acids was performed using GC-FID. As a result, the connection between biomass, lipid and FAME productivity of all cultures was established (Figure 4.44)

In 3 microalgae species used in this study, *N. gaditana* in Algal medium under N-replete condition (condition #3) outperformed all small-scale conditions in terms of biomass and lipid productivity. However, transesterifiable lipids in this condition remained at low percentages (16.78% of all lipids were transesterifiable). The culture with the highest percentage of transesterifiable lipids, which was 67.7% of all lipid extract, was *Nannochloropsis sp.* in f/2 medium under nitrogen deprivation (condition #8). Thanks to high conversion rates, 363.2 mg_{FAME}/L medium was achieved in condition #8, whereas 120.4 mg_{FAME}/L medium was produced in condition #3. Biomass-lipid-FAME combined analysis provided the best eligible pathways to produce microalgae lipids to convert into jet-fuel hydrocarbons.

It was observed that lipid concentration and FAME profile obtained from same microalgae biomass were affected by PBR design and difference in physicochemical factors like light source and airflow, and also by different mechanical treatments (ultrasonication, bead milling and homogenization) for cell disruption. Bead milling in small scale ensured the most effective lipid and PUFA extraction without degradation. Optimization studies with industrial high-pressure homogenizer will positively affect the performance of large-scale lipid extraction.

In order to facilitate the conversion of lipid extract from microalgae to jet-fuel hydrocarbons, lipid purification studies were performed. Impurities in the extract have been significantly purified with crude extraction using ethanol:methanol 1:1 (v/v) solution and fully recoverable 3 mg/mL active carbon, and viscosity of algal lipid has been dramatically reduced.

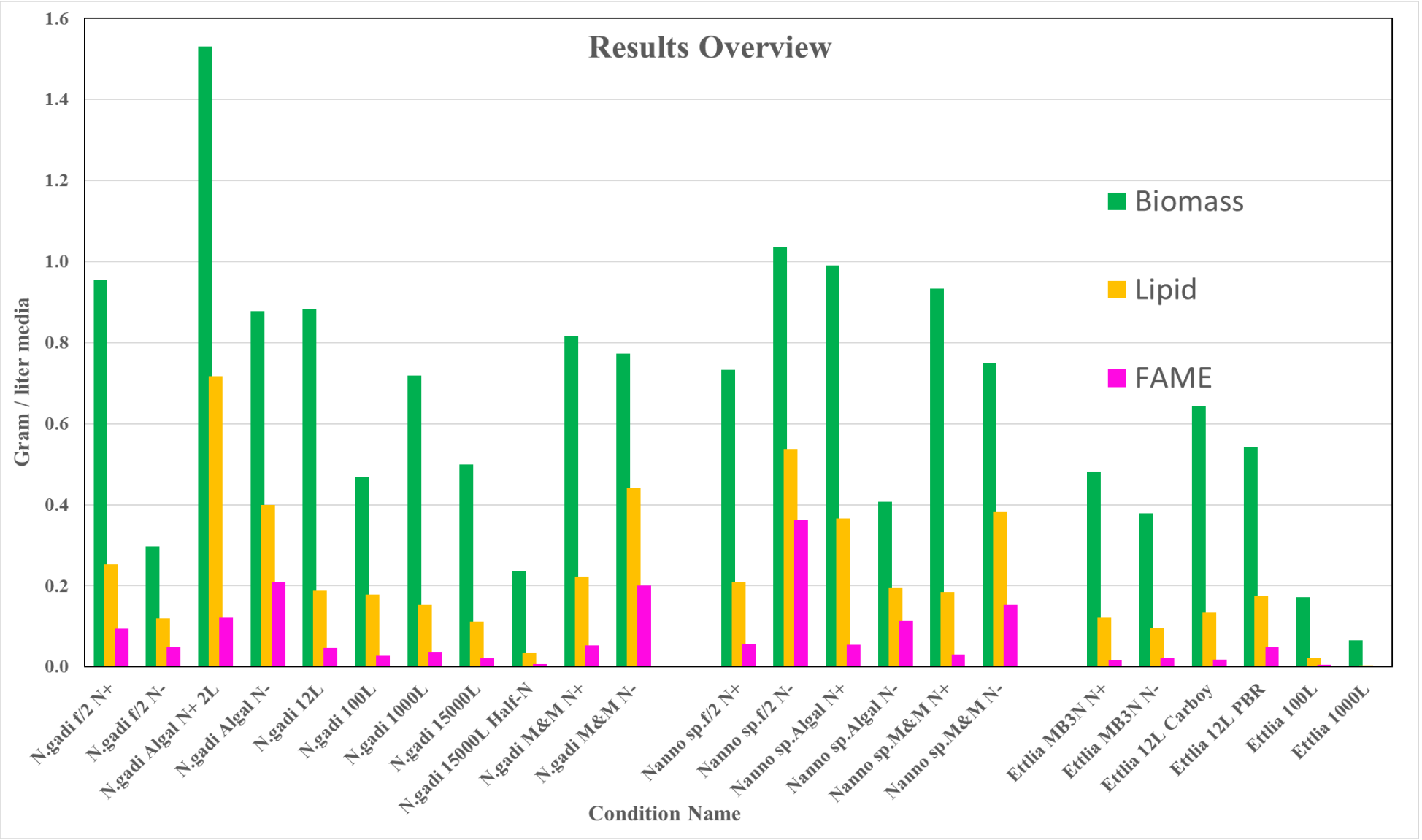

Figure 4.44. Biomass, lipid and FAME productivities of all microalgae cultures in this study.

5. DISCUSSION

In this study, microalgae lipid and FAME productivity under different upstream and downstream conditions were assessed. For bio-jet fuel production, it was aimed to produce highest FAME yield in unit area or volume (g_{FAME}/L/day). Performances of *E. oleoabundans* and *Nannochloropsis* species were analyzed in terms of biomass, lipid and 37 FAME productivities, mentioned in results section. Statistical review can be found in Table 5.1.

Table 5.1. Biomass, lipid, and FAME productivity of all studied microalgae cultures.

			Biomass			Lipid			FAME		
Condition No	Species Name	Conditions (Media, Nitrogen stress and cultivation volume)	g/L/day	g/m2	g/m2/day	g/L/day	g/m2	g/m2/day	mg/L/day	g/m2	g/m2/day
1	*Nannochloropsis gaditana*	f/2, N+, 2L	0.048	98.860	4.943	0.013	26.280	1.314	4.742	9.827	0.491
2		f/2, N-, 2L	0.025	30.777	2.565	0.010	12.318	1.026	4.059	5.048	0.421
3		Algal, N+,2L	0.096	158.653	9.916	0.045	74.355	4.647	7.526	12.478	0.780
4		Algal, N-, 2L	0.067	90.881	6.991	0.031	41.320	3.178	16.077	21.657	1.666
15		Algal, N+,12L	0.046	259.706	13.669	0.010	55.447	2.918	2.426	13.555	0.713
16		Algal, N+,100L	0.022	71.975	3.427	0.009	27.431	1.306	1.286	4.136	0.197
17		Algal, N+,1000L	0.034	205.790	9.800	0.007	43.936	2.092	1.712	10.304	0.491
18		Algal, N+,15000L	0.020	156.237	6.249	0.004	34.893	1.396	0.836	6.529	0.261
19		Algal, N-half, 15KL	0.017	73.431	5.245	0.002	10.435	0.745	0.508	2.223	0.159
5		M&M, N+,2L	0.054	84.560	5.637	0.015	23.026	1.535	3.563	5.538	0.369
6		M&M, N-,2L	0.055	80.000	5.714	0.032	45.879	3.277	14.358	20.830	1.488
7	*Nannochloropsis sp.*	f/2, N+, 2L	0.049	75.959	5.064	0.014	21.777	1.452	3.785	5.884	0.392
8		f/2, N-, 2L	0.065	107.254	6.703	0.034	55.629	3.477	22.702	37.640	2.353
9		Algal, N+,2L	0.047	102.591	4.885	0.017	37.890	1.804	2.583	5.620	0.268
10		Algal, N-, 2L	0.031	42.280	3.252	0.015	20.169	1.551	8.718	11.745	0.903
11		M&M, N+,2L	0.067	96.788	6.913	0.013	19.219	1.373	2.200	3.192	0.228
12		M&M, N-,2L	0.054	77.617	5.544	0.027	39.649	2.832	10.926	15.851	1.132
13	*Ettlia oleoabundans*	MB3N,N+, 2L	0.034	49.741	3.553	0.009	12.631	0.902	1.161	1.684	0.120
14		MB3N,N-, 2L	0.027	39.171	2.798	0.007	9.999	0.714	1.587	2.302	0.164
20		MB3N, N+,12L,G	0.023	189.118	6.754	0.005	39.481	1.410	0.659	5.426	0.194
21		MB3N, N+,12L,PBR	0.026	517.143	24.626	0.008	167.311	7.967	2.286	45.715	2.177
22		MB3N, N+,100L	0.007	26.340	1.054	0.001	3.593	0.144	0.184	0.705	0.028
23		MB3N, N+,1000L	0.004	18.917	1.051	0.000	1.098	0.061	0.030	0.153	0.008

E. oleoabundans cultures had rapid lag and exponential phase in their growth profiles in result 4.1. Even if the total biomass and lipid ratio of *E. oleoabundans* were lower than most of *Nannochloropsis* cultures, the ratio of two would be more comparable when time required for harvesting was added as a productivity factor. One advantage in *N. gaditana* cultures is that they were more resilient during the stationary phase and even after weeks had passed from first available time for harvesting, *N. gaditana* cultures did not rapidly crash and entered a long stationary stage in their growth profiles. However, *E. oleoabundans* cultures were vulnerable to wait after they reached the stationary phase without any crash. Resiliency of microalgae cultures against stress factors was one

of the most important parameters especially in outdoor cultivation. *Ettlia* needed to be harvested on time while *N. gaditana* endured and provided flexibility for other harvesting options.

Beside robustness of cultures, *Nannochloropsis* cultures had best g_{FAME}/L/day results. Most of *Ettlia* cultivation did not achieve the high FAME productivity performances. This can be resulted from the design of PBR and the decision of other physicochemical factors like light and airflow rate when microalgae were cultivated. One argument to support that idea is the difference of biomass and lipid percentage in two different 12L *E. oleoabundans* cultures, which are glass carboy and tubular PBR. Microalgae were grown in relatively different light intensity and light spectrum acquisition. Also, their airflow rate and mixing method were different and as a result, more biomass but less lipid rate were seen in 12L glass carboys than 12L tubular PBR. Optimization of light source and CO_2 uptake for microalgae cultivation are vital for lipid and FAME production.

Nitrogen deprivation of seven conditions were tested by reducing nitrate concentrations in one-tenth. However, four media had different nitrate concentration and assays of percentage decrease in nitrogen concentration (from 75% to 25% for example) for each media were not tested. Nitrogen deprivation affected lipid percentage in algal cells in 5 of 7 conditions, did not affect the lipid percentage of the 2 conditions. Fine optimization to apply nitrogen deprivation was addressed in these microalgae cultures. Beside the nitrogen concentration, other stress factors like nutrient deprivation and light intensity manipulation should be tested in order to achieve higher FAME productivity in all microalgae cultures for production of bio-jet fuel precursor.

Lipid percentage of dried microalgae cell does not directly give information about change in lipid profile of microalgae cells. There are many different lipid classes (fatty acids, steroids, terpenoids, glycerides, carotenoids, sphingosine etc.) inside the microalgae cell and change in lipid percentage did not proportionally affect fatty acid concentrations. Change in lipid profile (beside the FAME profile) needs to be analyzed using more specific instruments like GC/MS (Gas chromatography with mass spectrometry) and LC/MS (Liquid chromatography with mass spectrometry). In N-replete and N-deprived example of *N. gaditana* 2L cultures in Algal medium, lipid percentages were 46.87% and 45.47%, respectively. However, in their FAME profiles, EPA production in N-replete condition was four times higher than N-deprived condition whereas C16:0 and C16:1 were produced in N-deprived condition at least six times higher than N-replete condition (Figure 4.26). Conversion of other lipid metabolites under N-deprivation needs to be investigated even significant shifts occur in only FAME profile.

Connecting the biomass-lipid-FAME productivity pathway is a necessity for reliable microalgae lipid production. Lipid and biomass productivity are inversely proportional, in general. Total FAME concentrations increase in lipid percentage, in general. However, actual data on biomass-lipid-FAME productivity need to be analyzed because change in any factor (PBR design, light, media, species, harvesting day, cell disruption method etc.) result in different shift in biomass-lipid-FAME productivity. It was decided to use *N. gaditana* culture in Algal medium (condition #3) for scale-up by testing its high biomass and lipid productivity. However, transesterifiable lipids in *N. gaditana* in Algal medium were low percentage (16.8% of all lipids). On the other hand, *Nannochloropsis sp.* in f/2 medium under nitrogen deprivation had lower biomass and lipid productivity than condition #3 but much higher transesterifiable lipids (FAME) percentage, which was 67.7% of all lipids. As a result, *Nannochloropsis sp.* in N-deprived f/2 medium provided FAME productivity three times higher than promising *N. gaditana* in Algal medium case (Figure 4.33). Biomass-lipid-FAME productivity of all conditions must be analyzed and microalgae lipid production as a raw material of bio-jet fuel needs to be designed according to this analysis.

Non-transesterifiable lipid crude needs to be purified for jet-fuel production in with standards. In this study, activated carbon and filtration were used to eliminate the impurities inside the microalgal lipid. Activated carbon was fully recyclable and can be recovered after each experiment. Other purification techniques, like silica gel column chromatography, can be used and changes in different lipid purification results can be compared to optimize.

Organic content and ash content in same microalgae species changed with different cultivation conditions. Even more than 40% ash content was seen in *N. gaditana* culture. Organic and inorganic content of the biomass must be known before analyzing lipid and FAME concentrations of the cultures. Additionally, in dry weight and total lipid determination, change in very small masses (several milligrams) and high dilution rates was monitored. Change in several milligrams affect the lipid percentage up to 10% in performance of lipid experiment in this study. Especially chloroform evaporation stages were performed with intensive care to ensure that there was no liquid inside the tubes to manipulate the weight of dried lipid extracts. Simple and high-volume lipid and dry weight experiments may not be affected by fine weigh changes.

There is a tendency in the results of in this study between biomass productivity and increase in lipid productivity. In order to ensure that lipid percentage of dry cell was not affected from high biomass concentration as false positive, a microalga which is known as high biomass productivity, but very low lipid percentage needs to be studied in this study as well.

Daily and seasonal changes affect the performance of outdoor microalgae cultivation. Open ponds are open system, and any adverse weather event and contamination may lower the biomass-lipid-FAME productivity of open ponds. Most of the open pond cultures in this study were operated in autumn and winter seasons, which daily temperatures and daytime were lower than spring and summer. Additionally, open ponds in these studies were vulnerable to harsh wind and wild vegetation in this geography. Due to time shortage, change in growth profile of open pond cultivation according to seasons could not be evaluated. In literature, outdoor open pond cultivation has better biomass productivity on sunny and hot seasons (March to September in North Hemisphere).

Ultimately, lipid extraction protocols need to be scaled up to align with volume availability for bio-jet fuel production. In result section, it was showed that lipid percentage and FAME profile of same biomass was changed according to pre-treatment and cell disruption methods. Proper modifications of lipid extraction design may be needed for large-scale lipid extraction from microalgae biomass. In this study and mostly in literature, chloroform was used as nonpolar solvent for lipid extraction. Chloroform is toxic solvent and high working volume of chloroform is dangerous to be applied in lipid extraction. Alternative, green solvents need to be investigated for large-scale lipid production.

In biorefinery approach, fractionation and multivalorization of products from same biomass are essential. Microalgal lipids need to be fractionated into the high-value added fatty acids (mainly PUFAs) and other fatty acids for bio-jet fuel production. Remaining biomass after lipid extraction is rich in carbohydrates and lipids, and it can be utilized as feed or fertilizer supplement etc. This approach can help the algal fuels to compete with conventional fuel prices.

6. CONCLUSION

Oleaginous green microalgae biomass is promising feedstock for biofuel production. Growth profile of *N. gaditana, Nannochloropsis sp*. and *E. oleoabundans* were discovered under 23 different cultivations in total. *E. oleoabundans* attracted attention with its rapid growth in a short time. The effect of nitrogen deprivation on lipid and biomass production was observed in 7 different conditions. N-deprived conditions are prominent cultures for bio-jet fuel production with high lipid and FAME productivity despite the decrease in biomass production. PBR design affected biomass and lipid productivity of *E. oleoabundans,* as 12L tubular PBR produce less biomass but more lipid and FAME.

Biomass, lipid, and FAME productivity of 23 different microalgae cultivation were analyzed. Highest biomass productivity was observed in *N. gaditana* in N-replete Algal medium as 1.53 g/L and 0.10g/L/day. Highest lipid productivity was observed in same condition as 0.72 g/L and 0.05 g/L/day. Highest FAME productivity was achieved as 363.2 mg/L and 22.7 mg/L/day in *Nannochloropsis sp.* culture with N-deprived f/2 medium. *N. gaditana* in N-replete Algal medium produced 28.66 $mg_{EPA}/ g_{biomass}$, a high-value added fatty acid which can be used in pharmaceutical industry. Algal medium induced EPA production in green algae. 5 of 6 *Nannochloropsis* conditions under nitrogen deprivation had more than 20% FAME of their dry weight. 90% of their FAME profile was saturated and monounsaturated fatty acids.

For large scale lipid extraction, it was observed that different pretreatment resulted in FAME profile change. Homogenization and ultrasonication at large scale have less lipid extraction efficiency than bead milling at small scale. EtOH:MetOH solution is a promising crude extraction solvent for lipid extraction at large scale. Algal lipids need to be purified for bio-jet fuel use, and fully recoverable activated carbon adsorbed pigments and impurities inside algal lipids. Ideal activated carbon dosage was optimized as 3 mg/mL for lipid purification, and additional activated carbon rapidly decreased lipids of interest in solution. High throughput lipid extraction from microalgae for bio-jet fuel production has high development potential and promising alternatives in terms of cell disruption methods, extraction solvents and lipid purification.

REFERENCES

Abd El Baky, H. H., El-Baroty, G. S., Bouaid, A., Martinez, M., Aracil, J., 2012. Enhancement of lipid accumulation in *Scenedesmus obliquus* by Optimizing CO2 and Fe3+ levels for biodiesel production. Bioresource Technology, 119, 429–432.

Adams, C., Godfrey, V., Wahlen, B., Seefeldt, L., Bugbee, B., 2013. Understanding precision nitrogen stress to optimize the growth and lipid content tradeoff in oleaginous green microalgae. Bioresource Technology, 131, 188–194.

Adenan, N. S., Yusoff, F. M., Medipally, S. R., Shariff, M., 2016. Enhancement of Lipid Production in two Marine Microalgae under Different Levels of Nitrogen and Phosphorus Deficiency. Journal of Environmental Biology, 37.

Air Transport Action Group., 2020. Aviation: Benefits Beyond Borders 2020. Blueprint for a Green Recovery.

Akubude, V., Nwaigwe, K., Dintwa, E., 2019. Production of biodiesel from microalgae via nanocatalyzed transesterification process: A review. Materials Science for Energy Technologies, 2(2), 216–225.

Alfieri, A., Imperlini, E., Nigro, E., Vitucci, D., Orrù, S., Daniele, A., Buono, P., Mancini, A., 2017. Effects of Plant Oil Interesterified Triacylglycerols on Lipemia and Human Health. International Journal of Molecular Sciences, 19(1), 104.

Algaebase: Listing the World's Algae. AlgaeBase. https://www.algaebase.org/. Date accessed 6 January 2022.

Alishah Aratboni, H., Rafiei, N., Garcia-Granados, R., Alemzadeh, A., Morones-Ramírez, J. R., 2019. Biomass and lipid induction strategies in microalgae for biofuel production and other applications. Microbial Cell Factories, 18(1).

Asiedu, A., Davis, R., Kumar, S., 2020. Catalytic transfer hydrogenation and characterization of flash hydrolyzed microalgae into hydrocarbon fuels production (jet fuel). Fuel, 261, 116440.

Asquith, J., 2020, April 6. If Aviation Was A Country It Would Be The World's 20th Largest By GDP. Forbes. https://www.forbes.com/sites/jamesasquith/2020/04/06/if-aviation-was-a-country-it-would-be-the-worlds-20th-largest-by-gdp/?sh=14ab1b65e5b5. Date accessed 6 January 2022.

Bartle, K. D., Myers, P., 2002. History of Gas Chromatography. Trends in Analytical Chemistry, 21, 547.

Bauen, A., Bitossi, N., German, L., Harris, A., Leow, K., 2020. Sustainable Aviation Fuels. Johnson Matthey Technology Review, 64 (3), 263.

Bauer, M. C., Konnerth, P., Kruse, A., 2020. Extraction of common microalgae by liquefied dimethyl ether: influence of species and pretreatment on oil yields and composition. Biomass Conversion and Biorefinery.

Behera, B., Unpaprom, Y., Ramaraj, R., Maniam, G. P., Govindan, N., Paramasivan, B., 2021. Integrated biomolecular and bioprocess engineering strategies for enhancing the lipid yield from microalgae. Renewable and Sustainable Energy Reviews, 148, 111270.

Benvenuti, G., Bosma, R., Ji, F., Lamers, P., Barbosa, M. J., Wijffels, R. H., 2016. Batch and semi-continuous microalgal TAG production in lab-scale and outdoor photobioreactors. Journal of Applied Phycology, 28(6), 3167–3177.

Bernaerts, T. M., Gheysen, L., Foubert, I., Hendrickx, M. E., van Loey, A. M., 2019. Evaluating microalgal cell disruption upon ultra high pressure homogenization. Algal Research, 42, 101616.

Bošnjaković, M., Sinaga, N., 2020. The Perspective of Large-Scale Production of Algae Biodiesel. Applied Sciences, 10(22), 8181.

BP., 2020. Statistical Review of World Energy 2020 (No. 69).

Brindhadevi, K., Anto, S., Rene, E. R., Sekar, M., Mathimani, T., Thuy Lan Chi, N., Pugazhendhi, A., 2021. Effect of reaction temperature on the conversion of algal biomass to bio-oil and biochar through pyrolysis and hydrothermal liquefaction. Fuel, 285, 119106.

Bwapwa, J. K., Anandraj, A., Trois, C., 2017. Possibilities for conversion of microalgae oil into aviation fuel: A review. Renewable and Sustainable Energy Reviews, 80, 1345–1354.

Byreddy, A. R., Gupta, A., Barrow, C. J., Puri, M., 2016. A quick colorimetric method for total lipid quantification in microalgae. Journal of Microbiological Methods, 125, 28–32.

Cancela, A., Pérez, L., Febrero, A., Sánchez, A., Salgueiro, J., Ortiz, L., 2019. Exploitation of *Nannochloropsis gaditana* biomass for biodiesel and pellet production. Renewable Energy, 133, 725–730.

Capaz, R. S., Guida, E., Seabra, J. E. A., Osseweijer, P., Posada, J. A., 2020. Mitigating carbon emissions through sustainable aviation fuels: costs and potential. Biofuels, Bioproducts and Biorefining, 15(2), 502–524.

Carrero, A., Vicente, G., Rodríguez, R., Peso, G. L. D., Santos, C., 2015. Synthesis of fatty acids methyl esters (FAMEs) from *Nannochloropsis gaditana* microalga using heterogeneous acid catalysts. Biochemical Engineering Journal, 97, 119–124.

Cavonius, L. R., Carlsson, N. G., Undeland, I., 2014. Quantification of total fatty acids in microalgae: comparison of extraction and transesterification methods. Analytical and Bioanalytical Chemistry, 406(28), 7313–7322.

Chalima, A., Oliver, L., Fernández De Castro, L., Karnaouri, A., Dietrich, T., Topakas, E., 2017. Utilization of Volatile Fatty Acids from Microalgae for the Production of High Added Value Compounds. Fermentation, 3(4), 54.

Chang, J. S., Show, P. L., Ling, T. C., Chen, C. Y., Ho, S. H., Tan, C. H., Nagarajan, D., Phong, W. N., 2017. Photobioreactors. In Current Developments in Biotechnology and Bioengineering: Bioprocesses, Bioreactors and Controls, 313-352, Elsevier Inc., U.S.A.

Chapman, K. D., Ohlrogge, J. B., 2012. Compartmentation of Triacylglycerol Accumulation in Plants. Journal of Biological Chemistry, 287(4), 2288–2294.

Chemical and Physical Information. In JP-5, JP-8, and Jet A Fuels (p. 145).

Chen, M., Tang, H., Ma, H., Holland, T. C., Ng, K. S., Salley, S. O., 2011. Effect of nutrients on growth and lipid accumulation in the green algae *Dunaliella tertiolecta*. Bioresource Technology, 102(2), 1649–1655.

Cheng, C. H., Du, T. B., Pi, H. C., Jang, S. M., Lin, Y. H., Lee, H. T., 2011. Comparative study of lipid extraction from microalgae by organic solvent and supercritical CO2. Bioresource Technology, 102(21), 10151–10153.

Chhandama, M. V. L., Satyan, K. B., Changmai, B., Vanlalveni, C., Rokhum, S. L., 2021. Microalgae as a feedstock for the production of biodiesel: A review. Bioresource Technology Reports, 15, 100771.

Chiaramonti, D., 2019. Sustainable Aviation Fuels: the challenge of decarbonization. Energy Procedia, 158, 1202–1207.

Chiaramonti, D., Prussi, M., Buffi, M., Rizzo, A. M., Pari, L., 2017. Review and experimental study on pyrolysis and hydrothermal liquefaction of microalgae for biofuel production. Applied Energy, 185, 963–972.

Chiranjeevi, P., Venkata Mohan, S., 2016. Optimizing the Critical Factors for Lipid Productivity during Stress Phased Heterotrophic Microalgae Cultivation. Frontiers in Energy Research, 4.

Chiu, S. Y., Kao, C. Y., Tsai, M. T., Ong, S. C., Chen, C. H., Lin, C. S., 2009. Lipid accumulation and CO2 utilization of *Nannochloropsis oculata* in response to CO2 aeration. Bioresource Technology, 100(2), 833–838.

Choi, S. P., Nguyen, M. T., Sim, S. J., 2010. Enzymatic pretreatment of *Chlamydomonas reinhardtii* biomass for ethanol production. Bioresource Technology, 101(14), 5330–5336.

Converti, A., Casazza, A. A., Ortiz, E. Y., Perego, P., del Borghi, M., 2009. Effect of temperature and nitrogen concentration on the growth and lipid content of *Nannochloropsis oculata* and *Chlorella vulgaris* for biodiesel production. Chemical Engineering and Processing: Process Intensification, 48(6), 1146–1151.

Cupo, A., Landi, S., Morra, S., Nuzzo, G., Gallo, C., Manzo, E., Fontana, A., D'Ippolito, G., 2021. Autotrophic vs. Heterotrophic Cultivation of the Marine Diatom *Cyclotella cryptica* for EPA Production. Marine Drugs, 19(7), 355.

Cutignano, A., Luongo, E., Nuzzo, G., Pagano, D., Manzo, E., Sardo, A., Fontana, A., 2016. Profiling of complex lipids in marine microalgae by UHPLC/tandem mass spectrometry. Algal Research, 17, 348–358.

Das, P., Lei, W., Aziz, S. S., Obbard, J. P., 2011. Enhanced algae growth in both phototrophic and mixotrophic culture under blue light. Bioresource Technology, 102(4), 3883–3887.

de Jesus, S. S., Ferreira, G. F., Moreira, L. S., Wolf Maciel, M. R., Maciel Filho, R., 2019. Comparison of several methods for effective lipid extraction from wet microalgae using green solvents. Renewable Energy, 143, 130–141.

de Jong, S., Hoefnagels, R., Faaij, A., Slade, R., Mawhood, R., Junginger, M., 2015. The feasibility of short-term production strategies for renewable jet fuels - a comprehensive techno-economic comparison. Biofuels, Bioproducts and Biorefining, 9(6), 778–800.

Deane, P., Gallachòir, B. Ò., Shea, R. O., 2017. Biofuels for Aviation: Policy Goals and Costs. In Europe's Energy Transition (p. 79). Elsevier.

Dejoye Tanzi, C., Abert Vian, M., Ginies, C., Elmaataoui, M., Chemat, F., 2012. Terpenes as Green Solvents for Extraction of Oil from Microalgae. Molecules, 17(7), 8196–8205.

del Campo, J. A., Rodrìguez, H., Moreno, J., Vargas, M., Rivas, J., Guerrero, M. G., 2004. Accumulation of astaxanthin and lutein in *Chlorella zofingiensis* (Chlorophyta). Applied Microbiology and Biotechnology, 64(6), 848–854.

Diederichs, G. W., Ali Mandegari, M., Farzad, S., Görgens, J. F., 2016. Techno-economic comparison of bio-jet fuel production from lignocellulose, vegetable oil and sugar cane juice. Bioresource Technology, 216, 331–339.

Doliente, S. S., Narayan, A., Tapia, J. F. D., Samsatli, N. J., Zhao, Y., Samsatli, S., 2020. Bio-aviation Fuel: A Comprehensive Review and Analysis of the Supply Chain Components. Frontiers in Energy Research, 8.

Duman, G., Uddin, M. A., Yanik, J., 2014. Hydrogen production from algal biomass via steam gasification. Bioresource Technology, 166, 24–30.

Elmoraghy, M., 2013. Production of bio-jet fuel from microalgae. University of New Hampshire, Durham.

The White House, 2021. FACT SHEET: Biden Administration Advances the Future of Sustainable Fuels in American Aviation., 2021, September 10. https://www.whitehouse.gov/briefing-room/statements-releases/2021/09/09/fact-sheet-biden-administration-advances-the-future-of-sustainable-fuels-in-american-aviation/. Date accessed 6 January 2022.

Fonseca, N., Oliveira, V., Fréty, R., Sales, E., 2021. Thermal and Catalytic Fast Pyrolysis of Oily Extracts of Microalgae: Production of Biokerosene. Journal of the Brazilian Chemical Society.

Fox, J. M., Zimba, P. V., 2018. Minerals and Trace Elements in Microalgae. In Levine I., Fleurence J. (Eds.), Microalgae in Health and Disease Prevention, 177-193, Elsevier Inc., U.S.A.

Freedman, B., Butterfield, R. O., Pryde, E. H., 1986. Transesterification kinetics of soybean oil. Journal of the American Oil Chemists' Society, 63(10), 1375–1380.

Frey, W., Gusbeth, C., Schwartz, T., 2013. Inactivation of *Pseudomonas putida* by Pulsed Electric Field Treatment: A Study on the Correlation of Treatment Parameters and Inactivation Efficiency in the Short-Pulse Range. The Journal of Membrane Biology, 246(10), 769–781.

Furuhashi, T., Weckwerth, W., 2013. Introduction to Lipid (FAME) Analysis in Algae Using Gas Chromatography–Mass Spectrometry. Weckwerth, W., Kahl, G. (Eds.), The Handbook of Plant Metabolomics (1st ed., p. 215). Wiley.

Gardner, R., Peters, P., Peyton, B., Cooksey, K. E., 2010. Medium pH and nitrate concentration effects on accumulation of triacylglycerol in two members of the *Chlorophyta*. Journal of Applied Phycology, 23(6), 1005–1016.

Gerken, H. G., Donohoe, B., Knoshaug, E. P., 2012. Enzymatic cell wall degradation of *Chlorella vulgaris* and other microalgae for biofuels production. Planta, 237(1), 239–253.

Ghedini, E., Taghavi, S., Menegazzo, F., Signoretto, M., 2021. A Review on the Efficient Catalysts for Algae Transesterification to Biodiesel. Sustainability, 13(18), 10479.

Global Monitoring Laboratory - Carbon Cycle Greenhouse Gases. Global Monitoring Laboratory Earth System Research Laboratories. https://gml.noaa.gov/ccgg/trends/graph.html. Date accessed 6 January 2022.

Goettel, M., Eing, C., Gusbeth, C., Straessner, R., Frey, W., 2013. Pulsed electric field assisted extraction of intracellular valuables from microalgae. Algal Research, 2(4), 401–408.

Gómez-De La Cruz, A., Romero-Izquierdo, A., Gutiérrez-Antonio, C., Gómez-Castro, F., Hernández, S., 2017. Modelling of the hydrotreating process to produce renewable aviation fuel from micro-algae oil. Computer Aided Chemical Engineering, 655–660.

Gorain, P. C., Bagchi, S. K., Mallick, N., 2013. Effects of calcium, magnesium and sodium chloride in enhancing lipid accumulation in two green microalgae. Environmental Technology, 34(13–14), 1887–1894.

Graver, B., Zhang, K., Rutherford, D., 2019. CO2 emissions from commercial aviation, 2018. The International Council on Clean Transportation.

Griffiths, M. J., van Hille, R. P., Harrison, S. T. L., 2010. Selection of Direct Transesterification as the Preferred Method for Assay of Fatty Acid Content of Microalgae. Lipids, 45(11), 1053–1060.

Guiry, M. D., 2012. How Many Species of Algae Are There? Journal of Phycology, 48(5), 1057–1063.

Gustafsson, I. B., Boberg, M., 1992. Fatty Acid Content and Chemical Composition of Freshwater Microalgae. Journal of Phycology, 28.

Hall, W. K., Kokes, R. J., Emmett, P. H., 1957. Mechanism Studies of the Fischer-Tropsch Synthesis. The Addition of Radioactive Methanol, Carbon Dioxide and Gaseous Formaldehyde. Journal of the American Chemical Society, 79(12), 2983–2989.

Han, F., Pei, H., Hu, W., Han, L., Zhang, S., Ma, G., 2016. Effect of high-temperature stress on microalgae at the end of the logarithmic phase for the efficient production of lipid. Environmental Technology, 37(20), 2649–2657.

Hawrot-Paw, M., Ratomski, P., Koniuszy, A., Golimowski, W., Teleszko, M., Grygier, A., 2021. Fatty Acid Profile of Microalgal Oils as a Criterion for Selection of the Best Feedstock for Biodiesel Production. Energies, 14(21), 7334.

Heimann, K., Huerlimann, R., 2015. Microalgal Classification: Major Classes and Genera of Commercial Microalgal Species. In Kim Se-Kwon (Ed.), Handbook of Marine Microalgae, 25-41, Elsevier In. U.S.A.

Hirano, A., Hon-Nami, K., Kunito, S., Hada, M., Ogushi, Y., 1998. Temperature effect on continuous gasification of microalgal biomass: theoretical yield of methanol production and its energy balance. Catalysis Today, 45(1–4), 399–404.

Ho, S. H., Chen, C. Y., Chang, J. S., 2012. Effect of light intensity and nitrogen starvation on CO2 fixation and lipid/carbohydrate production of an indigenous microalga *Scenedesmus obliquus* CNW-N. Bioresource Technology, 113, 244–252.

Ho, S. H., Nakanishi, A., Kato, Y., Yamasaki, H., Chang, J. S., Misawa, N., Hirose, Y., Minagawa, J., Hasunuma, T., Kondo, A., 2017. Dynamic metabolic profiling together with transcription analysis reveals salinity-induced starch-to-lipid biosynthesis in alga *Chlamydomonas sp.* JSC4. Scientific Reports, 7(1).

Hossain, N., Mahlia, T. M. I., 2019. Progress in physicochemical parameters of microalgae cultivation for biofuel production. Critical Reviews in Biotechnology, 39(6), 835–859.

IATA., 2020. Fact Sheet 2: Sustainable Aviation Fuel: Technical Certification. Canada.

IATA., 2021a. Net zero carbon 2050 resolution. Canada.

IATA., 2021b. Tourism Economics Air Passenger Forecasts. Canada.

ICAO., 2022. Effects of Novel Coronavirus (COVID-19) on Civil Aviation: Economic Impact Analysis. Canada.

Iverson, S. J., Lang, S. L. C., Cooper, M. H., 2001. Comparison of the bligh and dyer and folch methods for total lipid determination in a broad range of marine tissue. Lipids, 36(11), 1283–1287.

Jareonsin, S., Pumas, C., 2021. Advantages of Heterotrophic Microalgae as a Host for Phytochemicals Production. Frontiers in Bioengineering and Biotechnology, 9.

Kanda, H., Hoshino, R., Murakami, K., Wahyudiono, Zheng, Q., Goto, M., 2020. Lipid extraction from microalgae covered with biomineralized cell walls using liquefied dimethyl ether. Fuel, 262, 116590.

Karl, D. M., 2000. Phosphorus, the staff of life. Nature, 406(6791), 31–33.

Khan, M. A. H., Bonifacio, S., Clowes, J., Foulds, A., Holland, R., Matthews, J. C., Percival, C. J., Shallcross, D. E., 2021. Investigation of Biofuel as a Potential Renewable Energy Source. Atmosphere, 12(10), 1289.

Khozin-Goldberg, I., 2016. Lipid Metabolism in Microalgae. In M. A. Borowitzka Et Al. (Ed.), The Physiology of Microalgae, Developments in Applied Phycology (6th ed., p. 413). Springer.

Kolosz, B. W., Luo, Y., Xu, B., Maroto-Valer, M. M., Andresen, J. M., 2020. Life cycle environmental analysis of ‘drop in’ alternative aviation fuels: a review. Sustainable Energy & Fuels, 4(7), 3229–3263.

Kumar, V., Arora, N., Nanda, M., Pruthi, V., 2019. Different Cell Disruption and Lipid Extraction Methods from Microalgae for Biodiesel Production. M. A. Alam, Z. Wang (Eds.), Microalgae Biotechnology for Development of Biofuel and Wastewater Treatment (p. 265). Springer.

Kwon, S., Kang, N. K., Koh, H. G., Shin, S. E., Lee, B., Jeong, B. R., Chang, Y. K., 2017. Enhancement of biomass and lipid productivity by overexpression of a bZIP transcription factor in *Nannochloropsis salina*. Biotechnology and Bioengineering, 115(2), 331–340.

le Quéré, C., Jackson, R. B., Jones, M. W., Smith, A. J. P., Abernethy, S., Andrew, R. M., De-Gol, A. J., Willis, D. R., Shan, Y., Canadell, J. G., Friedlingstein, P., Creutzig, F., Peters, G. P., 2020. Temporary reduction in daily global CO_2 emissions during the COVID-19 forced confinement. Nature Climate Change, 10(7), 647–653.

Lee, D., Fahey, D., Skowron, A., Allen, M., Burkhardt, U., Chen, Q., Doherty, S., Freeman, S., Forster, P., Fuglestvedt, J., Gettelman, A., de León, R., Lim, L., Lund, M., Millar, R., Owen, B., Penner, J., Pitari, G., Prather, M., Sausen, R., Wilcox, L., 2021. The contribution of global aviation to anthropogenic climate forcing for 2000 to 2018. Atmospheric Environment, 244, 117834.

Lee, E., Jalalizadeh, M., Zhang, Q., 2015. Growth kinetic models for microalgae cultivation: A review. Algal Research, 12, 497–512.

Lee, S. Y., Cho, J. M., Chang, Y. K., Oh, Y. K., 2017. Cell disruption and lipid extraction for microalgal biorefineries: A review. Bioresource Technology, 244, 1317–1328.

Lee, S. Y., Khoiroh, I., Vo, D. V. N., Senthil Kumar, P., Show, P. L., 2020. Techniques of lipid extraction from microalgae for biofuel production: a review. Environmental Chemistry Letters, 19(1), 231–251.

Li, J., Fang, X., Bian, J., Guo, Y., Li, C., 2018. Microalgae hydrothermal liquefaction and derived biocrude upgrading with modified SBA-15 catalysts. Bioresource Technology, 266, 541–547.

Li, Y., Ghasemi Naghdi, F., Garg, S., Adarme-Vega, T., Thurecht, K. J., Ghafor, W., Tannock, S., Schenk, P. M., 2014. A comparative study: the impact of different lipid extraction methods on current microalgal lipid research. Microbial Cell Factories, 13(1), 14.

Liang, K., Zhang, Q., Gu, M., Cong, W., 2012. Effect of phosphorus on lipid accumulation in freshwater microalga *Chlorella sp*. Journal of Applied Phycology, 25(1), 311–318.

Lim, J. H. K., Gan, Y. Y., Ong, H. C., Lau, B. F., Chen, W. H., Chong, C. T., Ling, T. C., Klemeš, J. J., 2021. Utilization of microalgae for bio-jet fuel production in the aviation sector: Challenges and perspective. Renewable and Sustainable Energy Reviews, 149, 111396.

Liu, Y., Murata, K., Inaba, M., 2019. Hydrocracking of algae oil to aviation fuel-ranged hydrocarbons over NiMo-supported catalysts. Catalysis Today, 332, 115–121.

Lokesh, K., Sethi, V., Nikolaidis, T., Goodger, E., Nalianda, D., 2015. Life cycle greenhouse gas analysis of bio-jet fuels with a technical investigation into their impact on jet engine performance. Biomass and Bioenergy, 77, 26–44.

Lòpez Bascòn, M. A., de Castro, L., 2020. Soxhlet Extraction. In Liquid-Phase Extraction (p. 327). Elsevier.

Masson-Delmotte, V., Zhai, P., Pörtner, H.-O., Roberts, D., Skea, J., Shukla, P.R., Pirani, A., Moufouma-Okia, W., Péan, C., Pidcock, R., Connors, S., Matthews, J.B.R., Chen, Y., Zhou, X., Gomis, M.I., Lonnoy, E., Maycock, T., Tignor, M., Waterfield, T. (Eds.)., 2018. Summary for Policymakers. In: Global Warming of 1.5°C. An IPCC Special Report on the impacts of global warming of 1.5°C above pre-industrial levels and related global greenhouse gas emission pathways, in the context of strengthening the global response to the threat of climate change, sustainable development, and efforts to eradicate poverty. IPCC.

Matos, N. P., Feller, R., Moecke, E. H. S., Sant'Anna, E. S., 2015. Biomass, lipid productivities and fatty acids composition of marine *Nannochloropsis gaditana* cultured in desalination concentrate. Bioresource Technology, 197, 48–55.

Matyash, V., Liebisch, G., Kurzchalia, T. V., Shevchenko, A., Schwudke, D., 2008. Lipid extraction by methyl-tert-butyl ether for high-throughput lipidomics. Journal of Lipid Research, 49(5), 1137–1146.

Mawhood, R., Gazis, E., de Jong, S., Hoefnagels, R., Slade, R., 2016. Production pathways for renewable jet fuel: a review of commercialization status and future prospects. Biofuels, Bioproducts and Biorefining, 10(4), 462–484.

McMillan, J. R., Watson, I. A., Ali, M., Jaafar, W., 2013. Evaluation and comparison of algal cell disruption methods: Microwave, waterbath, blender, ultrasonic and laser treatment. Applied Energy, 103, 128–134.

Mendiola, J. A., Rodrìguez-Meizoso, I., Señoràns, F. J., Reglero, G., Cifuentes, A., Inàñez, E., 2008. Antioxidants in Plant Foods and Microalgae Extracted Using Compressed Fluids. Electronic Journal of Environmental, Agricultural and Food Chemistry, 7(8).

Menten, F., Chèze, B., Patouillard, L., Bouvart, F., 2013. A review of LCA greenhouse gas emissions results for advanced biofuels: The use of meta-regression analysis. Renewable and Sustainable Energy Reviews, 26, 108–134.

Merlo, S., Gabarrell Durany, X., Pedroso Tonon, A., Rossi, S., 2021. Marine Microalgae Contribution to Sustainable Development. Water, 13(10), 1373.

Murata, K., Liu, Y., Watanabe, M. M., Inaba, M., Takahara, I., 2014. Hydrocracking of Algae Oil into Aviation Fuel-Range Hydrocarbons Using a Pt–Re Catalyst. Energy & Fuels, 28(11), 6999–7006.

Mustapha, S. I., Isa, Y. M., 2020. Utilization of quaternary solvent mixtures for extraction of lipids from *Scenedesmus obliquus* microalgae. Cogent Engineering, 7(1), 1788877.

Nagappan, S., Devendran, S., Tsai, P. C., Dahms, H. U., Ponnusamy, V. K., 2019. Potential of two-stage cultivation in microalgae biofuel production. Fuel, 252, 339–349.

Nagappan, S., Devendran, S., Tsai, P. C., Jayaraman, H., Alagarsamy, V., Pugazhendhi, A., Ponnusamy, V. K., 2020. Metabolomics integrated with transcriptomics and proteomics: Evaluation of systems reaction to nitrogen deficiency stress in microalgae. Process Biochemistry, 91, 1–14.

Nanda, S., Rana, R., Sarangi, P. K., Dalai, A. K., Kozinski, J. A., 2018. A Broad Introduction to First-, Second-, and Third-Generation Biofuels. Recent Advancements in Biofuels and Bioenergy Utilization, 1–25.

National Renewable Energy Laboratory, Wang, W., Tao, L., Markham, J., Zhang, Y., Tan, E., Batan, L., Warner, E., Biddy, M., 2016, July. Review of Biojet Fuel Conversion Technologies. U. S. Department of Energy.

Neagu, O., Teodoru, M., 2019. The Relationship between Economic Complexity, Energy Consumption Structure and Greenhouse Gas Emission: Heterogeneous Panel Evidence from the EU Countries. Sustainability, 11(2), 497.

Nemer, G., Louka, N., Vorobiev, E., Salameh, D., Nicaud, J. M., Maroun, R. G., Koubaa, M., 2021. Mechanical Cell Disruption Technologies for the Extraction of Dyes and Pigments from Microorganisms: A Review. Fermentation, 7(1), 36.

Neto, J. M., Komesu, A., da Silva Martins, L. H., Gonçalves, V. O. O., de Oliveira, J. A. R., Rai, M., 2019. Third Generation Biofuels: an Overview. In Sustainable Bioenergy (p. 283).

Ng, K. S., Farooq, D., Yang, A., 2021. Global biorenewable development strategies for sustainable aviation fuel production. Renewable and Sustainable Energy Reviews, 150, 111502.

Niemi, C., Lage, S., Gentili, F. G., 2019. Comparisons of analysis of fatty acid methyl ester (FAME) of microalgae by chromatographic techniques. Algal Research, 39, 101449.

Niu, Y. F., Zhang, M. H., Li, D. W., Yang, W. D., Liu, J. S., Bai, W. B., Li, H. Y., 2013. Improvement of Neutral Lipid and Polyunsaturated Fatty Acid Biosynthesis by Overexpressing a Type 2 Diacylglycerol Acyltransferase in Marine Diatom *Phaeodactylum tricornutum*. Marine Drugs, 11(11), 4558–4569.

Novelli, P., 2011, April. Sustainable Way for Alternative Fuels and Energy in Aviation.

Olaizola, M., Grewe, C., 2019. Commercial Microalgal Cultivation Systems. Hallmann, A., Rampelotto, P. H. (Eds.), Grand Challenges in Algae Biotechnology (p. 3). Springer.

O'Malley, J., Pavlenko, N., Searle, S., 2021. Estimating sustainable aviation fuel feedstock availability to meet growing European Union demand. International Council on Clean Transportation.

Osorio, H., Jara, C., Fuenzalida, K., Rey-Jurado, E., Vásquez, M., 2019. High-efficiency nuclear transformation of the microalgae *Nannochloropsis oceanica* using Tn5 Transposome for the generation of altered lipid accumulation phenotypes. Biotechnology for Biofuels, 12(1).

Otera, J., 1993. Transesterification. Chemical Reviews, 93, 1449.

Ozcelik, D., Sakarya, F. K., Erdinçler, B., Yılmaz, A., Avcı, S., Borhan, E., Haznedaroğlu, B. Z., 2021. Recent Advancements in Algal Biorefineries. Shekh, A., Sarada, R. (Eds.), Microalgal Biotechnology: Recent Advances, Market Potential, and Sustainability (p. 77). the Royal Society of Chemistry.

Pacific Northwest National Laboratory, Bioenergy Technologies Office., 2020, November. Hydrothermal Liquefaction: Path to Sustainable Aviation Fuel. U.S. Department of Energy.

Pancha, I., Chokshi, K., Mishra, S., 2015. Enhanced biofuel production potential with nutritional stress amelioration through optimization of carbon source and light intensity in *Scenedesmus sp*. CCNM 1077. Bioresource Technology, 179, 565–572.

Park, J., Seo, J., Kwon, E. E., 2012. Microalgae Production Using Wastewater: Effect of Light-Emitting Diode Wavelength on Microalgal Growth. Environmental Engineering Science, 29(11), 995–1001.

Park, J. Y., Park, M. S., Lee, Y. C., Yang, J. W., 2015. Advances in direct transesterification of algal oils from wet biomass. Bioresource Technology, 184, 267–275.

Peng, K. T., Zheng, C. N., Xue, J., Chen, X. Y., Yang, W. D., Liu, J. S., Bai, W., Li, H. Y., 2014. Delta 5 Fatty Acid Desaturase Upregulates the Synthesis of Polyunsaturated Fatty Acids in the Marine Diatom *Phaeodactylum tricornutum*. Journal of Agricultural and Food Chemistry, 62(35), 8773–8776.

Peng, X., Meng, F., Wang, Y., Yi, X., Cui, H., 2020. Effect of pH, Temperature, and CO2 Concentration on Growth and Lipid Accumulation of *Nannochloropsis sp*. MASCC 11. Journal of Ocean University of China, 19(5), 1183–1192.

Pires, A. P. P., Han, Y., Kramlich, J., Garcia-Perez, M., 2018. Chemical Composition and Fuel Properties of Alternative Jet Fuels. BioResources, 13(2).

Poddar, M., Anand, M., Farooqui, S., Martin, G., Maurya, M., Sinha, A., 2018. Hydroprocessing of lipids extracted from marine microalgae *Nannochloropsis sp*. over sulfided CoMoP/Al2O3 catalyst. Biomass and Bioenergy, 119, 31–36.

Poh, Z. L., Amalina Kadir, W. N., Lam, M. K., Uemura, Y., Suparmaniam, U., Lim, J. W., Show, P. L., Lee, K. T., 2020. The effect of stress environment towards lipid accumulation in microalgae after harvesting. Renewable Energy, 154, 1083–1091.

Praveenkumar, R., Shameera, K., Mahalakshmi, G., Akbarsha, M. A., Thajuddin, N., 2012. Influence of nutrient deprivations on lipid accumulation in a dominant indigenous microalga *Chlorella sp*., BUM11008: Evaluation for biodiesel production. Biomass and Bioenergy, 37, 60–66.

Prussi, M., Weindorf, W., Buffi, M., Sánchez López, J., Scarlat, N., 2021. Are algae ready to take off? GHG emission savings of algae-to-kerosene production. Applied Energy, 304, 117817.

Pruvost, J., van Vooren, G., Cogne, G., Legrand, J., 2009. Investigation of biomass and lipids production with *Neochloris oleoabundans* in photobioreactor. Bioresource Technology, 100(23), 5988–5995.

Quigg, A., 2016. Micronutrients. Borowitzka, M.A., et al. (Eds.), The Physiology of Microalgae (6th ed., p. 211). Springer.

Ranganathan, S. V., Narasimhan, S. L., Muthukumar, K., 2008. An overview of enzymatic production of biodiesel. Bioresource Technology, 99(10), 3975–3981.

Ranjith Kumar, R., Hanumantha Rao, P., Arumugam, M., 2015. Lipid Extraction Methods from Microalgae: A Comprehensive Review. Frontiers in Energy Research, 2.

Reza, A. M., Tavakoli, J., Zhou, Y., Qin, J., Tang, Y., 2020. Synthetic fluorescent probes to apprehend calcium signaling in lipid droplet accumulation in microalgae—an updated review. Science China Chemistry, 63(3), 308–324.

Robota, H. J., Alger, J. C., Shafer, L., 2013. Converting Algal Triglycerides to Diesel and HEFA Jet Fuel Fractions. Energy & Fuels, 27(2), 985–996.

Rodolfi, L., Chini Zittelli, G., Bassi, N., Padovani, G., Biondi, N., Bonini, G., Tredici, M. R., 2009. Microalgae for oil: Strain selection, induction of lipid synthesis and outdoor mass cultivation in a low-cost photobioreactor. Biotechnology and Bioengineering, 102(1), 100–112.

Ruangsomboon, S., 2012. Effect of light, nutrient, cultivation time and salinity on lipid production of newly isolated strain of the green microalga, *Botryococcus braunii* KMITL 2. Bioresource Technology, 109, 261–265.

Rye, L., Blakey, S., Wilson, C. W., 2010. Sustainability of supply or the planet: a review of potential drop-in alternative aviation fuels. Energy Environ. Sci., 3(1), 17–27.

Sahena, F., Zaidul, I., Jinap, S., Karim, A., Abbas, K., Norulaini, N., Omar, A., 2009. Application of supercritical CO2 in lipid extraction – A review. Journal of Food Engineering, 95(2), 240–253.

Sahoo, A., Saini, K., Jindal, M., Bhaskar, T., Pant, K. K., 2021. Co-Hydrothermal Liquefaction of algal and lignocellulosic biomass: Status and perspectives. Bioresource Technology, 342, 125948.

Sajjadi, B., Chen, W. Y., Raman, A. A. A., Ibrahim, S., 2018. Microalgae lipid and biomass for biofuel production: A comprehensive review on lipid enhancement strategies and their effects on fatty acid composition. Renewable and Sustainable Energy Reviews, 97, 200–232.

Salam, K. A., Velasquez-Orta, S. B., Harvey, A. P., 2016. A sustainable integrated in situ transesterification of microalgae for biodiesel production and associated co-product-a review. Renewable and Sustainable Energy Reviews, 65, 1179–1198.

Salama, E. S., Kim, H. C., Abou-Shanab, R. A. I., Ji, M. K., Oh, Y. K., Kim, S. H., Jeon, B. H., 2013. Biomass, lipid content, and fatty acid composition of freshwater *Chlamydomonas mexicana* and *Scenedesmus obliquus* grown under salt stress. Bioprocess and Biosystems Engineering, 36(6), 827–833.

Santelices, B., 2007. The discovery of kelp forests in deep-water habitats of tropical regions. Proceedings of the National Academy of Sciences, 104(49), 19163–19164.

Santos, A., Janssen, M., Lamers, P., Evers, W., Wijffels, R., 2012. Growth of oil accumulating microalga *Neochloris oleoabundans* under alkaline–saline conditions. Bioresource Technology, 104, 593–599.

Santos, F. M., Gonçalves, A. L., Pires, J. C. M., 2019. Negative Emission Technologies. In Pires, J. C. M.; Gonçalves, A. L. (Eds.). Bioenergy with Carbon Capture and Storage, 1-13. Elsevier, Netherland.

Sati, H., Mitra, M., Mishra, S., Baredar, P., 2019. Microalgal lipid extraction strategies for biodiesel production: A review. Algal Research, 38, 101413.

Schenk, P. M., Thomas-Hall, S. R., Stephens, E., Marx, U. C., Mussgnug, J. H., Posten, C., Kruse, O., Hankamer, B., 2008. Second Generation Biofuels: High-Efficiency Microalgae for Biodiesel Production. BioEnergy Research, 1(1), 20–43.

Scholz, M. J., Weiss, T. L., Jinkerson, R. E., Jing, J., Roth, R., Goodenough, U., Posewitz, M. C., Gerken, H. G., 2014. Ultrastructure and Composition of the *Nannochloropsis gaditana* Cell Wall. Eukaryotic Cell, 13(11), 1450–1464.

Sharma, Y. C., Singh, V., 2017. Microalgal biodiesel: A possible solution for India's energy security. Renewable and Sustainable Energy Reviews, 67, 72–88.

Shene, C., Monsalve, M. T., Vergara, D., Lienqueo, M. E., Rubilar, M., 2015. High pressure homogenization of *Nannochloropsis oculata* for the extraction of intracellular components: Effect of process conditions and culture age. European Journal of Lipid Science and Technology, 118(4), 631–639.

Sheng, J., Vannela, R., Rittmann, B. E., 2011. Evaluation of methods to extract and quantify lipids from *Synechocystis* PCC 6803. Bioresource Technology, 102(2), 1697–1703.

Shokravi, Z., Shokravi, H., Aziz, M. A., Shokravi, H., 2019. The Fourth-Generation Biofuel: A Systematic Review on Nearly Two Decades of Research from 2008 to 2019. In Fossil Free Fuels Trends in Renewable Energy (p. 214).

Shokravi, Z., Shokravi, H., Chyuan, O. H., Lau, W. J., Koloor, S. S. R., Petrů, M., Ismail, A. F., 2020. Improving 'Lipid Productivity' in Microalgae by Bilateral Enhancement of Biomass and Lipid Contents: A Review. Sustainability, 12(21), 9083.

Singh, D., Sharma, D., Soni, S., Sharma, S., Kumar Sharma, P., Jhalani, A., 2020. A review on feedstocks, production processes, and yield for different generations of biodiesel. Fuel, 262, 116553.

Singh, P., Kumari, S., Guldhe, A., Misra, R., Rawat, I., Bux, F., 2016. Trends and novel strategies for enhancing lipid accumulation and quality in microalgae. Renewable and Sustainable Energy Reviews, 55, 1–16.

Sivaramakrishnan, R., Incharoensakdi, A., 2016. Production of methyl ester from two microalgae by two-step transesterification and direct transesterification. Environmental Science and Pollution Research, 24(5), 4950–4963.

Soares, A. T., da Costa, D. C., Silva, B. F., Lopes, R. G., Derner, R. B., Antoniosi Filho, N. R., 2014. Comparative Analysis of the Fatty Acid Composition of Microalgae Obtained by Different Oil Extraction Methods and Direct Biomass Transesterification. BioEnergy Research, 7(3), 1035–1044.

Soares, A. T., da Costa, D. C., Vieira, A. A. H., Antoniosi Filho, N. R., 2019. Analysis of major carotenoids and fatty acid composition of freshwater microalgae. Heliyon, 5(4), e01529.

Soria, A. C., Rodrìguez-Sànchez, S., Sanz, J., Martìnez-Castro, I., 2014. Gas Chromatographic Analysis of Food Bioactive Oligosaccharides. Moreno, F. J., Sanz, M. L. (Eds.), Food Oligosaccharides: Production, Analysis and Bioactivity (1st ed., p. 370). Wiley.

Suganya, T., Varman, M., Masjuki, H., Renganathan, S., 2016. Macroalgae and microalgae as a potential source for commercial applications along with biofuels production: A biorefinery approach. Renewable and Sustainable Energy Reviews, 55, 909–941.

Sun, X. M., Ren, L. J., Zhao, Q. Y., Ji, X. J., Huang, H., 2018. Microalgae for the production of lipid and carotenoids: a review with focus on stress regulation and adaptation. Biotechnology for Biofuels, 11(1).

Sun, X. M., Ren, L. J., Zhao, Q. Y., Ji, X. J., Huang, H., 2019. Enhancement of lipid accumulation in microalgae by metabolic engineering. Biochimica et Biophysica Acta (BBA) - Molecular and Cell Biology of Lipids, 1864(4), 552–566.

Sundararaj, R. H., Kumar, R. D., Raut, A. K., Sekar, T. C., Pandey, V., Kushari, A., Puri, S., 2019. Combustion and emission characteristics from biojet fuel blends in a gas turbine combustor. Energy, 182, 689–705.

Takeda, H., 1991. Sugar Composition of the Cell Wall and The Taxonomy of *Chlorella (Chlorophyceae)* 1. Journal of Phycology, 27(2), 224–232.

Tatsuzawa, H., Takizawa, E., Wada, M., Yamamoto, Y., 1996. Fatty Acid and Lipid Composition of the Acidophilic Green Alga *Chlamydomonas SP*.1. Journal of Phycology, 32(4), 598–601.

Taylor, J. D., Jenni, M. M., Peters, M. W., 2010. Dehydration of Fermented Isobutanol for the Production of Renewable Chemicals and Fuels. Topics in Catalysis, 53(15–18), 1224–1230.
Thompson, P., 2012. The Agricultural Ethics of Biofuels: The Food vs. Fuel Debate. Agriculture, 2(4), 339–358.

Topare, N. S., Raut, S. J., Renge, V. C., Khedkar, S. V., Chavan, Y. P., Bhagat, S. L., 2011. Extraction of Oil from Algae by Solvent Extraction and Oil Expeller Method. International Journal of Chemical Sciences, 9(4).

TÜİK., 2021, November. Dış Ticaret İstatistikleri, Ekim 2021. TÜİK Kurumsal. https://data.tuik.gov.tr/Bulten/Index?p=Dis-Ticaret-Istatistikleri-Ekim-2021-37422. Date accessed 6 January 2022.

Tüpraş., 2018. Product Specification Kerosine Type Jet Fuel (Jet A-1) (*) 300.

United Nations Environment Programme., 2021. Emissions Gap Report 2021: The Heat Is On – A World of Climate Promises Not Yet Delivered – Executive Summary. Nairobi.

Vasistha, S., Khanra, A., Clifford, M., Rai, M., 2021. Current advances in microalgae harvesting and lipid extraction processes for improved biodiesel production: A review. Renewable and Sustainable Energy Reviews, 137, 110498.

Venkata Subhash, G., Rohit, M., Devi, M. P., Swamy, Y., Venkata Mohan, S., 2014. Temperature induced stress influence on biodiesel productivity during mixotrophic microalgae cultivation with wastewater. Bioresource Technology, 169, 789–793.

Vuppaladadiyam, A. K., Prinsen, P., Raheem, A., Luque, R., Zhao, M., 2018. Microalgae cultivation and metabolites production: a comprehensive review. Biofuels, Bioproducts and Biorefining, 12(2), 304–324.

Waghmare, A., Nagula, K., Pandit, A., Arya, S., 2019. Hydrodynamic cavitation for energy efficient and scalable process of microalgae cell disruption. Algal Research, 40, 101496.

Wahidin, S., Idris, A., Shaleh, S. R. M., 2013. The influence of light intensity and photoperiod on the growth and lipid content of microalgae *Nannochloropsis sp*. Bioresource Technology, 129, 7–11.

Wan, L., Han, J., Sang, M., Li, A., Wu, H., Yin, S., Zhang, C., 2012. De Novo Transcriptomic Analysis of an Oleaginous Microalga: Pathway Description and Gene Discovery for Production of Next-Generation Biofuels. PLoS ONE, 7(4), e35142.

Wang, C., Lan, C. Q., 2018. Effects of shear stress on microalgae – A review. Biotechnology Advances, 36(4), 986–1002.

Wang, S. K., Stiles, A. R., Guo, C., Liu, C. Z., 2014. Microalgae cultivation in photobioreactors: An overview of light characteristics. Engineering in Life Sciences, 14(6), 550–559.

Wang, W. C., Tao, L., 2016. Bio-jet fuel conversion technologies. Renewable and Sustainable Energy Reviews, 53, 801–822.

Weber, K., Burow, M., 2017. Nitrogen – essential macronutrient and signal controlling flowering time. Physiologia Plantarum, 162(2), 251–260.

Wei, H., Liu, W., Chen, X., Yang, Q., Li, J., Chen, H., 2019. Renewable bio-jet fuel production for aviation: A review. Fuel, 254, 115599.

Wei, H., Shi, Y., Ma, X., Pan, Y., Hu, H., Li, Y., Luo, M., Gerken, H., Liu, J., 2017. A type-I diacylglycerol acyltransferase modulates triacylglycerol biosynthesis and fatty acid composition in the oleaginous microalga, *Nannochloropsis oceanica*. Biotechnology for Biofuels, 10(1).

Wu, J. Y., Lay, C. H., Chen, C. C., Wu, S. Y., 2017. Lipid accumulating microalgae cultivation in textile wastewater: Environmental parameters optimization. Journal of the Taiwan Institute of Chemical Engineers, 79, 1–6.

Yaakob, Z., Kamarudin, K. F., Rajkumar, R., Takriff, M. S., Badar, S. N., 2014. The Current Methods for the Biomass Production of the Microalgae from Wastewaters: An Overview. World Applied Sciences Journal, 31(10).

Yang, X., Guo, F., Xue, S., Wang, X., 2016. Carbon distribution of algae-based alternative aviation fuel obtained by different pathways. Renewable and Sustainable Energy Reviews, 54, 1129–1147.

Yang, Z., Cheng, J., Ye, Q., Liu, J., Zhou, J., Cen, K., 2016. Decrease in light/dark cycle of microalgal cells with computational fluid dynamics simulation to improve microalgal growth in a raceway pond. Bioresource Technology, 220, 352–359.

Yeesang, C., Cheirsilp, B., 2011. Effect of nitrogen, salt, and iron content in the growth medium and light intensity on lipid production by microalgae isolated from freshwater sources in Thailand. Bioresource Technology, 102(3), 3034–3040.

Yilmaz, N., Atmanli, A., 2017. Sustainable alternative fuels in aviation. Energy, 140, 1378–1386.

Yoo, G., Park, M. S., Yang, J. W., 2015. Chemical Pretreatment of Algal Biomass. In Pretreatment of Biomass, 227-258. Elsevier Inc, U.S.A.

Zhang, R., Grimi, N., Marchal, L., Lebovka, N., Vorobiev, E., 2019. Effect of ultrasonication, high pressure homogenization and their combination on efficiency of extraction of biomolecules from microalgae *Parachlorella kessleri*. Algal Research, 40, 101524.

Zhu, L., 2015. Biorefinery as a promising approach to promote microalgae industry: An innovative framework. Renewable and Sustainable Energy Reviews, 41, 1376–1384.

Zhuang, L. L., Yu, D., Zhang, J., Liu, F. F., Wu, Y. H., Zhang, T. Y., Dao, G. H., Hu, H. Y, 2018. The characteristics and influencing factors of the attached microalgae cultivation: A review. Renewable and Sustainable Energy Reviews, 94, 1110–1119.

APPENDIX A: RELATIVE OD AND FATTY ACID METHYL ESTER COMPARISON IN SMALL-SCALE MICROALGAE CULTIVATION

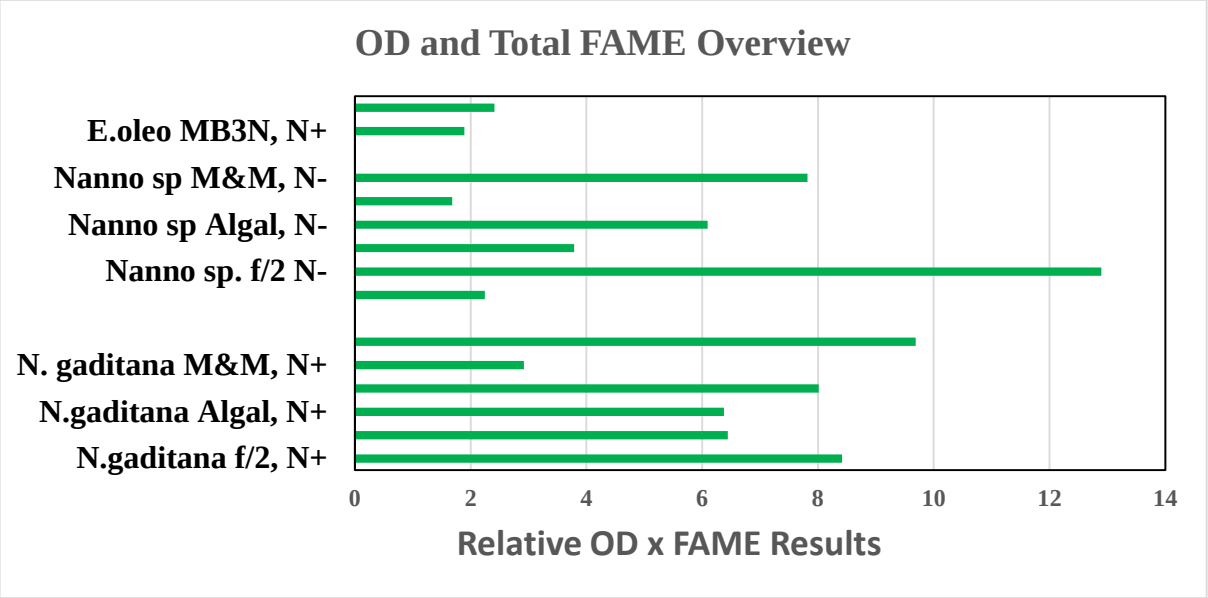

Figure A. 1. Max OD-FAME assessment of small scale microalgae cultivation.

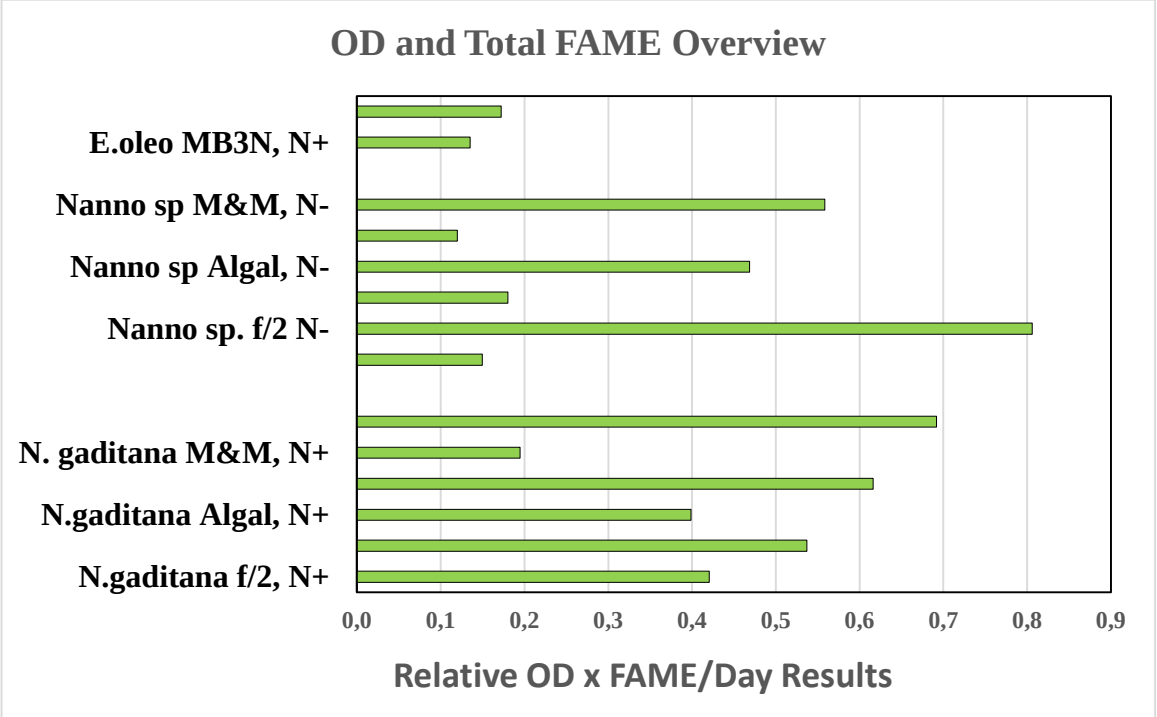

Figure A. 2. OD-FAME in unit time assessment of small scale microalgae cultivation.

APPENDIX B: FATTY ACID METHYL ESTER CALIBRATION CURVES

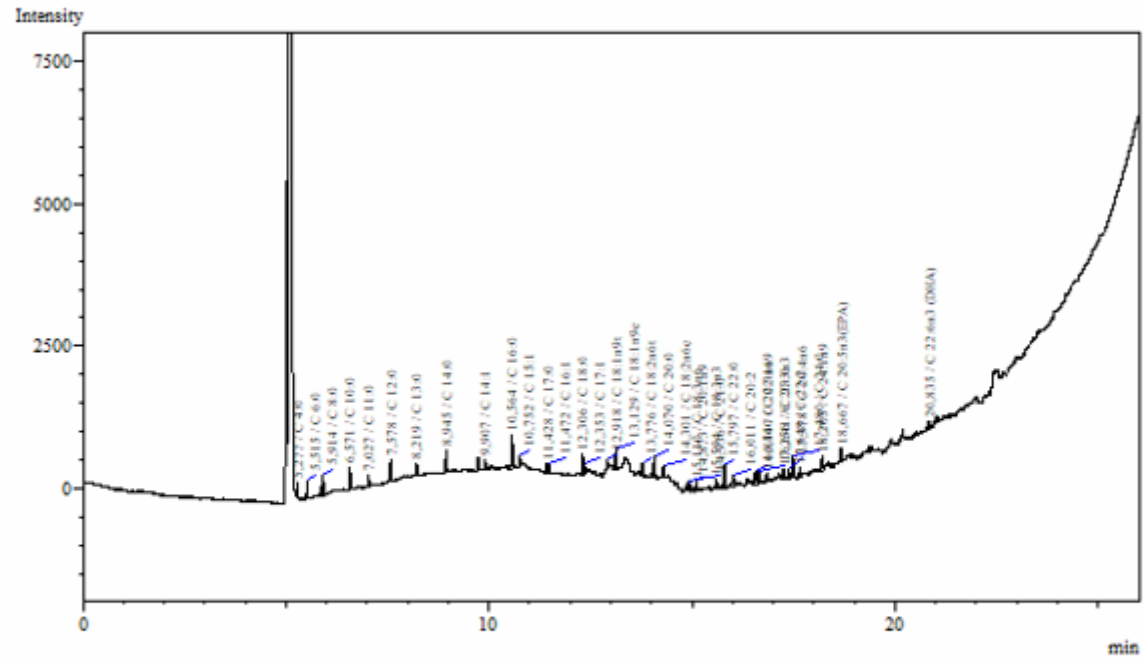

Peak#	Ret.Time	Area	Height	Conc.	Unit	Mark	ID#	Cmpd Name
1	5,277	308	234	12,329	ug/ml		1	C 4:0
2	5,515	463	313	13,262	ug/ml		2	C 6:0
3	5,914	548	348	12,416	ug/ml		3	C 8:0
4	6,571	649	392	12,573	ug/ml		4	C 10:0
5	7,027	292	185	5,824	ug/ml		5	C 11:0
6	7,578	701	384	12,520	ug/ml		6	C 12:0
7	8,219	422	200	6,467	ug/ml		7	C 13:0
8	8,945	809	386	12,283	ug/ml		8	C 14:0
9	9,907	329	175	5,740	ug/ml		9	C 14:1
10	10,564	1310	574	17,633	ug/ml		12	C 16:0
11	10,752	430	184	5,041	ug/ml		11	C 15:1
12	11,428	315	166	5,808	ug/ml		14	C 17:0
13	11,472	337	165	5,209	ug/ml	V	13	C 16:1
14	12,306	776	367	11,982	ug/ml		16	C 18:0
15	12,353	384	186	6,302	ug/ml		15	C 17:1
16	12,918	302	148	5,649	ug/ml		18	C 18:1n9t
17	13,129	831	381	11,713	ug/ml		17	C 18:1n9c
18	13,776	518	202	6,323	ug/ml		20	C 18:2n6t
19	14,070	901	377	11,197	ug/ml	V	23	C 20:0
20	14,301	438	194	5,494	ug/ml		19	C 18:2n6c
21	14,873	257	134	7,062	ug/ml		24	C 20:1n9
22	14,936	399	188	7,713	ug/ml	V	30	C 21:0
23	15,110	515	204	5,669	ug/ml		21	C 18:3n6
24	15,594	406	175	4,444	ug/ml		22	C 18:3n3
25	15,797	853	384	11,222	ug/ml	V	31	C 22:0
26	16,011	526	216	5,864	ug/ml	V	25	C 20:2
27	16,560	701	235	8,146	ug/ml	V	32	C 22:1n9
28	16,641	526	207	6,655	ug/ml	V	35	C 23:0
29	16,844	505	174	5,818	ug/ml	V	26	C 20:3n6
30	17,256	653	195	6,802	ug/ml	V	27	C 20:3n3
31	17,378	352	151	5,155	ug/ml		28	C 20:4n6
32	17,480	916	391	11,812	ug/ml		36	C 24:0
33	17,648	356	170	5,667	ug/ml		33	C 22:2
34	18,205	671	261	5,546	ug/ml	V	37	C 24:1n9
35	18,667	528	214	5,520	ug/ml	V	29	C 20:5n3(EPA)
36	20,835	264	138	4,932	ug/ml		34	C 22:6n3 (DHA)
Total		19491	8998					

Figure B.1. Chromatogram of FAME Mix Dilution #1.

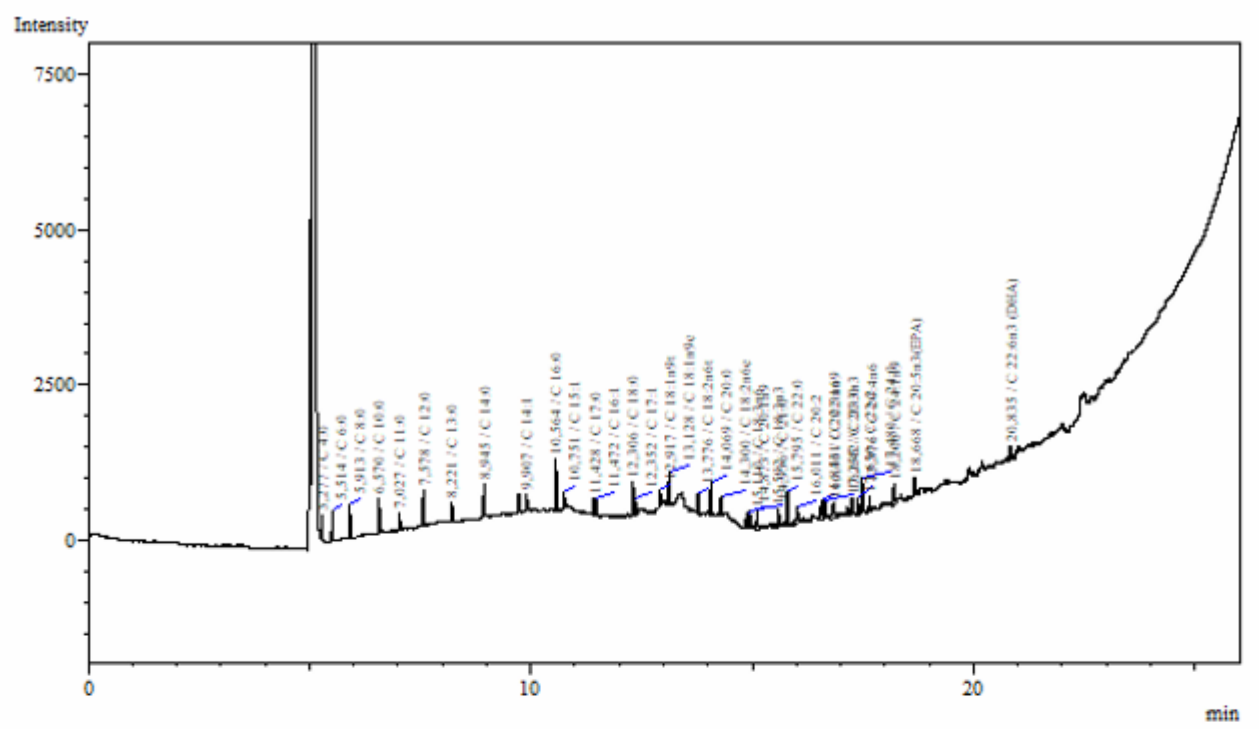

Peak#	Ret.Time	Area	Height	Conc.	Unit	Mark	ID#	Cmpd Name
1	5,277	521	372	16,470	ug/ml		1	C 4:0
2	5,514	678	475	16,549	ug/ml		2	C 6:0
3	5,913	797	524	15,742	ug/ml		3	C 8:0
4	6,570	897	552	15,600	ug/ml		4	C 10:0
5	7,027	480	276	8,008	ug/ml		5	C 11:0
6	7,578	972	560	15,602	ug/ml		6	C 12:0
7	8,221	516	278	7,519	ug/ml		7	C 13:0
8	8,945	988	540	14,273	ug/ml		8	C 14:0
9	9,907	466	247	7,255	ug/ml		9	C 14:1
10	10,564	1685	830	21,685	ug/ml		12	C 16:0
11	10,751	661	288	7,557	ug/ml		11	C 15:1
12	11,428	504	252	7,928	ug/ml		14	C 17:0
13	11,472	521	259	7,208	ug/ml	V	13	C 16:1
14	12,306	1144	545	15,844	ug/ml		16	C 18:0
15	12,352	545	274	8,173	ug/ml	V	15	C 17:1
16	12,917	543	255	8,144	ug/ml		18	C 18:1n9t
17	13,128	1130	530	14,956	ug/ml		17	C 18:1n9c
18	13,776	671	296	8,070	ug/ml		20	C 18:2n6t
19	14,069	1225	553	14,746	ug/ml	V	23	C 20:0
20	14,300	661	287	7,908	ug/ml		19	C 18:2n6c
21	14,873	523	249	9,975	ug/ml		24	C 20:1n9
22	14,936	636	280	10,270	ug/ml	V	30	C 21:0
23	15,110	714	295	7,976	ug/ml		21	C 18:3n6
24	15,592	733	283	8,164	ug/ml	V	22	C 18:3n3
25	15,795	1177	545	14,798	ug/ml	V	31	C 22:0
26	16,011	738	283	8,214	ug/ml		25	C 20:2
27	16,561	774	296	8,892	ug/ml		32	C 22:1n9
28	16,642	654	280	8,040	ug/ml	V	35	C 23:0
29	16,843	872	253	9,865	ug/ml		26	C 20:3n6
30	17,255	724	261	7,625	ug/ml	V	27	C 20:3n3
31	17,376	644	249	8,512	ug/ml		28	C 20:4n6
32	17,480	1352	569	16,656	ug/ml	V	36	C 24:0
33	17,650	592	265	8,281	ug/ml		33	C 22:2
34	18,206	846	337	7,556	ug/ml		37	C 24:1n9
35	18,668	849	309	9,064	ug/ml		29	C 20:5n3(EPA)
36	20,835	502	224	7,869	ug/ml	V	34	C 22:6n3 (DHA)
Total		27935	13171					

Figure B.2. Chromatogram of FAME Mix Dilution #2.

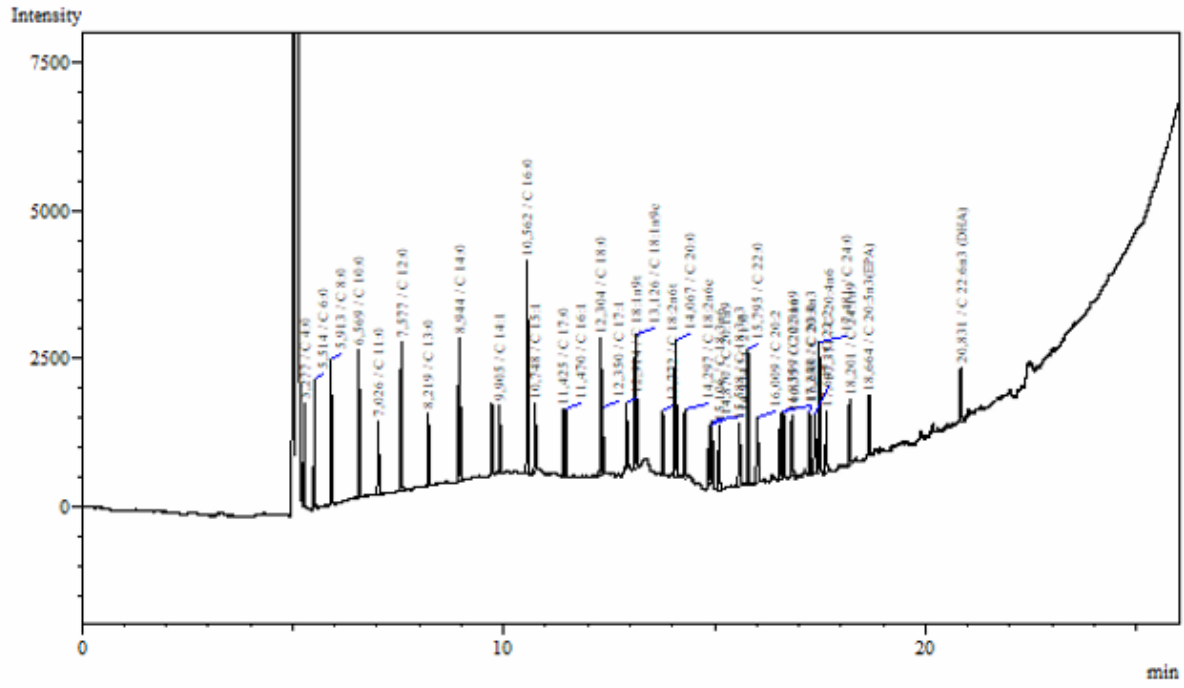

Peak#	Ret.Time	Area	Height	Conc.	Unit	Mark	ID#	Cmpd Name
1	5,277	2408	1712	53,156	ug/ml		1	C 4:0
2	5,514	3033	2129	52,504	ug/ml		2	C 6:0
3	5,913	3675	2397	54,262	ug/ml		3	C 8:0
4	6,569	4037	2479	53,990	ug/ml		4	C 10:0
5	7,026	2132	1241	27,221	ug/ml		5	C 11:0
6	7,577	4344	2482	54,048	ug/ml		6	C 12:0
7	8,219	2223	1188	26,581	ug/ml		7	C 13:0
8	8,944	4583	2400	54,180	ug/ml		8	C 14:0
9	9,905	2237	1148	26,869	ug/ml		9	C 14:1
10	10,562	7184	3555	81,107	ug/ml		12	C 16:0
11	10,748	2374	1149	26,246	ug/ml		11	C 15:1
12	11,425	2212	1123	27,100	ug/ml		14	C 17:0
13	11,470	2367	1131	27,307	ug/ml	V	13	C 16:1
14	12,304	4792	2287	54,155	ug/ml		16	C 18:0
15	12,350	2123	1113	26,436	ug/ml	V	15	C 17:1
16	12,914	2181	1064	25,085	ug/ml		18	C 18:1n9t
17	13,126	4876	2282	55,517	ug/ml		17	C 18:1n9c
18	13,772	2326	1055	27,048	ug/ml		20	C 18:2n6t
19	14,067	4962	2289	55,729	ug/ml	V	23	C 20:0
20	14,297	2484	1134	27,619	ug/ml		19	C 18:2n6c
21	14,870	1850	979	24,528	ug/ml		24	C 20:1n9
22	14,934	1918	986	24,100	ug/ml		30	C 21:0
23	15,106	2346	1071	26,891	ug/ml		21	C 18:3n6
24	15,588	2420	1068	27,324	ug/ml	V	22	C 18:3n3
25	15,795	4819	2273	55,004	ug/ml		31	C 22:0
26	16,009	2434	1083	27,007	ug/ml		25	C 20:2
27	16,559	2443	1105	25,878	ug/ml		32	C 22:1n9
28	16,640	2388	1117	26,739	ug/ml	V	35	C 23:0
29	16,839	2296	1020	25,552	ug/ml		26	C 20:3n6
30	17,253	2314	1011	25,953	ug/ml		27	C 20:3n3
31	17,371	2224	978	26,690	ug/ml		28	C 20:4n6
32	17,481	4737	2203	54,261	ug/ml	V	36	C 24:0
33	17,647	2269	1039	26,824	ug/ml		33	C 22:2
34	18,201	2481	1103	26,412	ug/ml		37	C 24:1n9
35	18,664	2314	1008	25,266	ug/ml		29	C 20:5n3(EPA)
36	20,831	2124	908	27,906	ug/ml		34	C 22:6n3 (DHA)
Total		107930	54310					

Figure B.3. Chromatogram of FAME Mix Dilution #3.

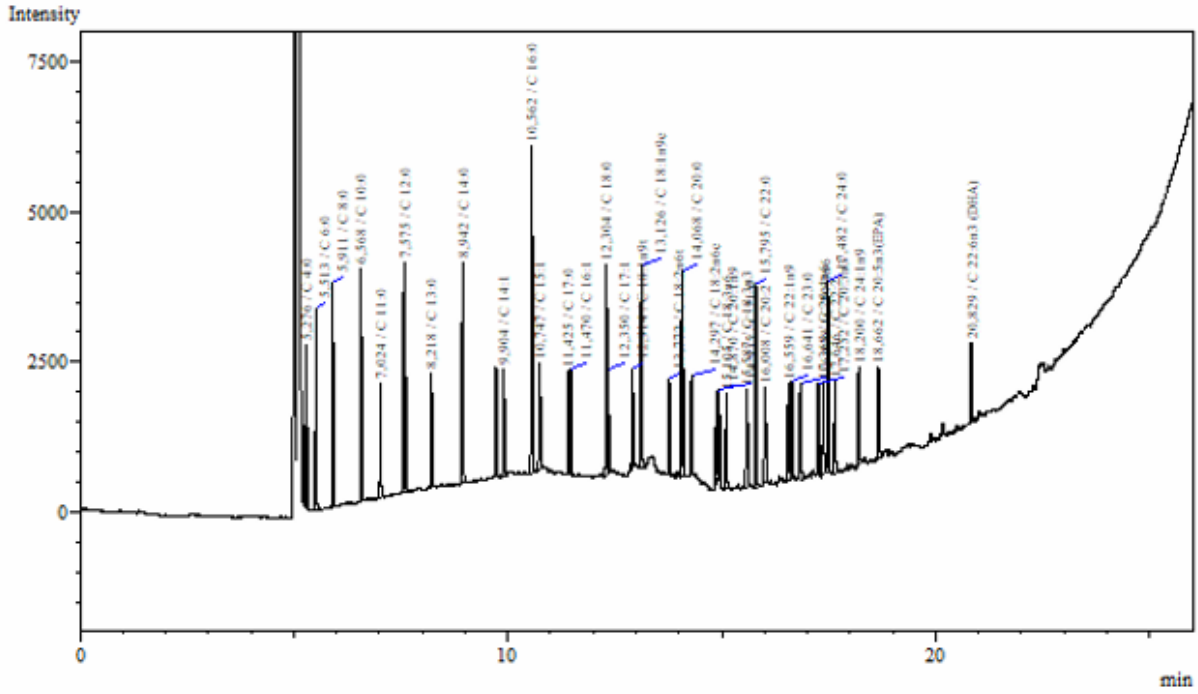

Peak#	Ret.Time	Area	Height	Conc.	Unit	Mark	ID#	Cmpd Name
1	5,276	3868	2659	81,537	ug/ml		1	C 4:0
2	5,513	4864	3249	80,467	ug/ml		2	C 6:0
3	5,911	5693	3722	81,257	ug/ml		3	C 8:0
4	6,568	6238	3831	80,892	ug/ml		4	C 10:0
5	7,024	3249	1872	40,210	ug/ml		5	C 11:0
6	7,575	6637	3767	80,183	ug/ml		6	C 12:0
7	8,218	3469	1868	40,496	ug/ml	V	7	C 13:0
8	8,942	6903	3620	79,940	ug/ml		8	C 14:0
9	9,904	3515	1770	41,030	ug/ml		9	C 14:1
10	10,562	11011	5392	122,470	ug/ml		12	C 16:0
11	10,747	3630	1769	39,947	ug/ml		11	C 15:1
12	11,425	3385	1705	40,273	ug/ml		14	C 17:0
13	11,470	3616	1740	40,909	ug/ml	V	13	C 16:1
14	12,304	7332	3504	80,827	ug/ml		16	C 18:0
15	12,350	3257	1722	39,570	ug/ml	V	15	C 17:1
16	12,914	3462	1629	38,347	ug/ml		18	C 18:1n9t
17	13,126	7088	3359	79,462	ug/ml		17	C 18:1n9c
18	13,772	3348	1558	38,767	ug/ml		20	C 18:2n6t
19	14,068	7188	3415	80,135	ug/ml	V	23	C 20:0
20	14,297	3504	1651	38,640	ug/ml		19	C 18:2n6c
21	14,870	2826	1475	35,228	ug/ml		24	C 20:1n9
22	14,935	2803	1470	33,642	ug/ml		30	C 21:0
23	15,105	3471	1612	39,936	ug/ml		21	C 18:3n6
24	15,587	3676	1627	41,596	ug/ml	V	22	C 18:3n3
25	15,795	7279	3377	82,160	ug/ml	V	31	C 22:0
26	16,008	3469	1566	38,482	ug/ml		25	C 20:2
27	16,559	3640	1611	38,060	ug/ml		32	C 22:1n9
28	16,641	3477	1612	38,487	ug/ml	V	35	C 23:0
29	16,838	3515	1539	38,987	ug/ml		26	C 20:3n6
30	17,252	3381	1515	38,246	ug/ml		27	C 20:3n3
31	17,369	3332	1511	39,446	ug/ml		28	C 20:4n6
32	17,482	6845	3108	77,684	ug/ml		36	C 24:0
33	17,646	3440	1505	39,778	ug/ml		33	C 22:2
34	18,200	3685	1628	40,297	ug/ml		37	C 24:1n9
35	18,662	3651	1498	40,042	ug/ml		29	C 20:5n3(EPA)
36	20,829	2945	1300	38,044	ug/ml		34	C 22:6n3 (DHA)
Total		162692	81756					

Figure B.4. Chromatogram of FAME Mix Dilution #4.

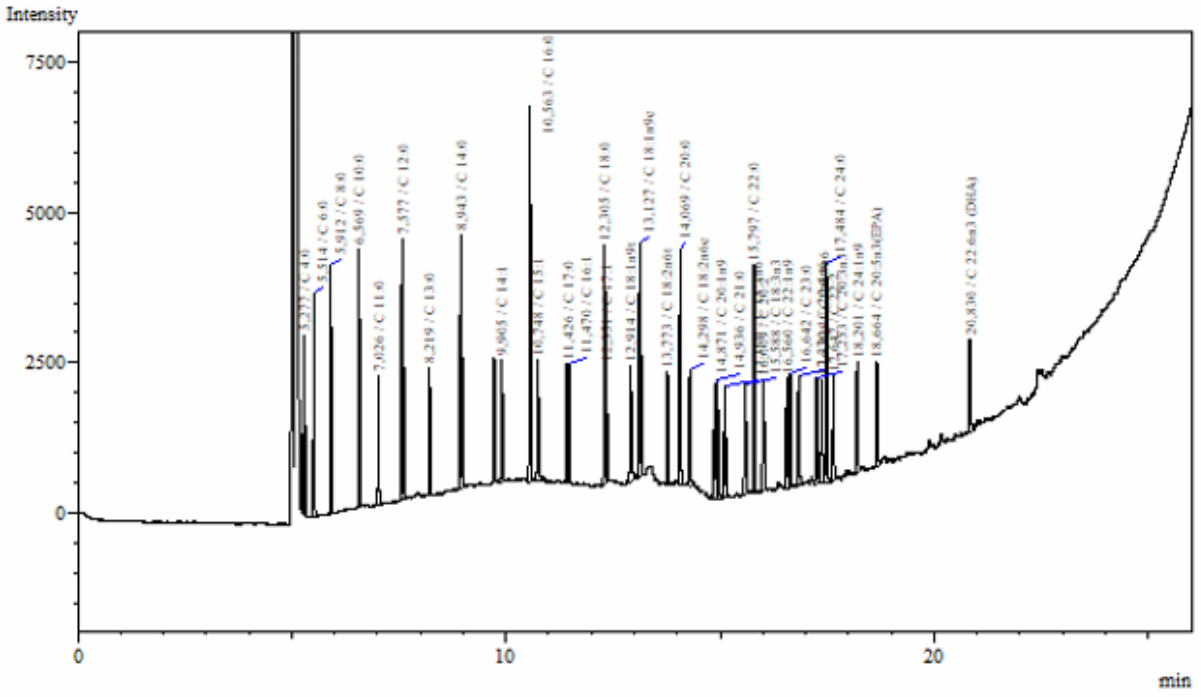

Peak#	Ret.Time	Area	Height	Conc.	Unit	Mark	ID#	Cmpd Name
1	5,277	4253	2935	89,023	ug/ml		1	C 4:0
2	5,514	5451	3657	89,423	ug/ml		2	C 6:0
3	5,912	6261	4096	88,860	ug/ml		3	C 8:0
4	6,569	6957	4275	89,682	ug/ml		4	C 10:0
5	7,026	3631	2116	44,644	ug/ml		5	C 11:0
6	7,577	7549	4306	90,578	ug/ml		6	C 12:0
7	8,219	3863	2064	44,901	ug/ml		7	C 13:0
8	8,943	8127	4175	93,526	ug/ml		8	C 14:0
9	9,905	3933	2007	45,654	ug/ml		9	C 14:1
10	10,563	12419	6223	137,683	ug/ml		12	C 16:0
11	10,748	4436	1990	48,739	ug/ml		11	C 15:1
12	11,426	3799	1963	44,921	ug/ml		14	C 17:0
13	11,470	4106	1964	46,243	ug/ml	V	13	C 16:1
14	12,305	8224	3955	90,199	ug/ml		16	C 18:0
15	12,351	3763	1941	45,422	ug/ml	V	15	C 17:1
16	12,914	4616	1912	50,283	ug/ml		18	C 18:1n9t
17	13,127	8243	3875	91,972	ug/ml	V	17	C 18:1n9c
18	13,773	3949	1840	45,661	ug/ml		20	C 18:2n6t
19	14,069	8286	3914	92,170	ug/ml	V	23	C 20:0
20	14,298	4261	1927	46,832	ug/ml		19	C 18:2n6c
21	14,871	4088	1890	49,067	ug/ml	V	24	C 20:1n9
22	14,936	4314	1959	49,941	ug/ml	V	30	C 21:0
23	15,106	3980	1837	45,835	ug/ml		21	C 18:3n6
24	15,588	3983	1826	45,085	ug/ml		22	C 18:3n3
25	15,797	8042	3745	90,586	ug/ml	V	31	C 22:0
26	16,009	4210	1834	46,696	ug/ml		25	C 20:2
27	16,560	4161	1836	43,364	ug/ml	V	32	C 22:1n9
28	16,642	4164	1858	45,901	ug/ml	V	35	C 23:0
29	16,839	4094	1807	45,357	ug/ml	V	26	C 20:3n6
30	17,253	4214	1742	47,852	ug/ml	V	27	C 20:3n3
31	17,370	3969	1707	46,768	ug/ml	V	28	C 20:4n6
32	17,484	8209	3623	92,830	ug/ml	V	36	C 24:0
33	17,647	3966	1740	45,590	ug/ml		33	C 22:2
34	18,201	4274	1846	47,091	ug/ml		37	C 24:1n9
35	18,664	4232	1735	46,465	ug/ml		29	C 20:5n3(EPA)
36	20,830	3775	1530	48,290	ug/ml	V	34	C 22:6n3 (DHA)
Total		189802	93650					

Figure B.5. Chromatogram of FAME Mix Dilution #5.

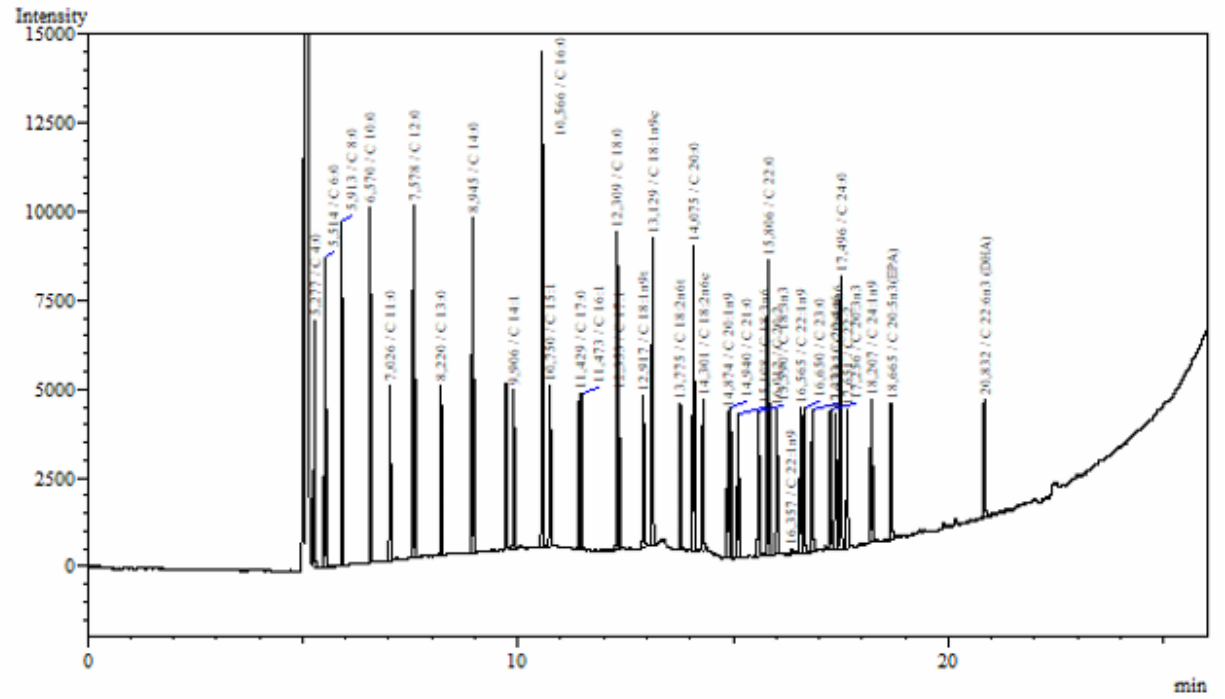

Peak#	Ret.Time	Area	Height	Conc.	Unit	Mark	ID#	Cmpd Name
1	5,277	10088	6861	202,485	ug/ml		1	C 4:0
2	5,514	12876	8636	202,794	ug/ml		2	C 6:0
3	5,913	14751	9419	202,463	ug/ml		3	C 8:0
4	6,570	16167	9864	202,263	ug/ml		4	C 10:0
5	7,026	8485	4904	101,093	ug/ml		5	C 11:0
6	7,578	17329	9835	202,070	ug/ml		6	C 12:0
7	8,220	8888	4755	101,035	ug/ml		7	C 13:0
8	8,945	17789	9394	200,798	ug/ml		8	C 14:0
9	9,906	8880	4487	100,452	ug/ml		9	C 14:1
10	10,566	27571	13760	301,423	ug/ml		12	C 16:0
11	10,750	9088	4499	99,471	ug/ml		11	C 15:1
12	11,429	8793	4355	100,971	ug/ml		14	C 17:0
13	11,473	9056	4389	100,124	ug/ml	V	13	C 16:1
14	12,309	18869	8938	201,993	ug/ml		16	C 18:0
15	12,353	8572	4325	101,096	ug/ml	V	15	C 17:1
16	12,917	9372	4251	99,492	ug/ml		18	C 18:1n9t
17	13,129	18348	8642	201,381	ug/ml	V	17	C 18:1n9c
18	13,775	8786	4080	101,130	ug/ml		20	C 18:2n6t
19	14,075	18214	8450	201,023	ug/ml	V	23	C 20:0
20	14,301	9226	4220	100,507	ug/ml		19	C 18:2n6c
21	14,874	8837	4039	101,140	ug/ml		24	C 20:1n9
22	14,940	9078	4226	101,334	ug/ml	V	30	C 21:0
23	15,108	8712	4012	100,692	ug/ml		21	C 18:3n6
24	15,590	8850	4072	100,388	ug/ml	V	22	C 18:3n3
25	15,806	18065	8232	201,230	ug/ml		31	C 22:0
26	16,012	9086	4032	100,738	ug/ml		25	C 20:2
27	16,357	801	126	9,166	ug/ml		32	C 22:1n9
28	16,565	9186	4073	94,504	ug/ml	V	32	C 22:1n9
29	16,650	9289	4103	101,178	ug/ml	V	35	C 23:0
30	16,842	9182	3992	101,421	ug/ml		26	C 20:3n6
31	17,256	8783	3889	100,522	ug/ml		27	C 20:3n3
32	17,373	8633	3816	100,430	ug/ml	V	28	C 20:4n6
33	17,496	18014	7547	201,757	ug/ml	V	36	C 24:0
34	17,651	8963	3867	100,860	ug/ml		33	C 22:2
35	18,207	8870	4013	100,099	ug/ml		37	C 24:1n9
36	18,665	9133	3842	100,643	ug/ml	V	29	C 20:5n3(EPA)
37	20,832	7958	3339	99,958	ug/ml	V	34	C 22:6n3 (DHA)
Total		422588	209284					

Figure B.6. Chromatogram of FAME Mix Dilution #6.

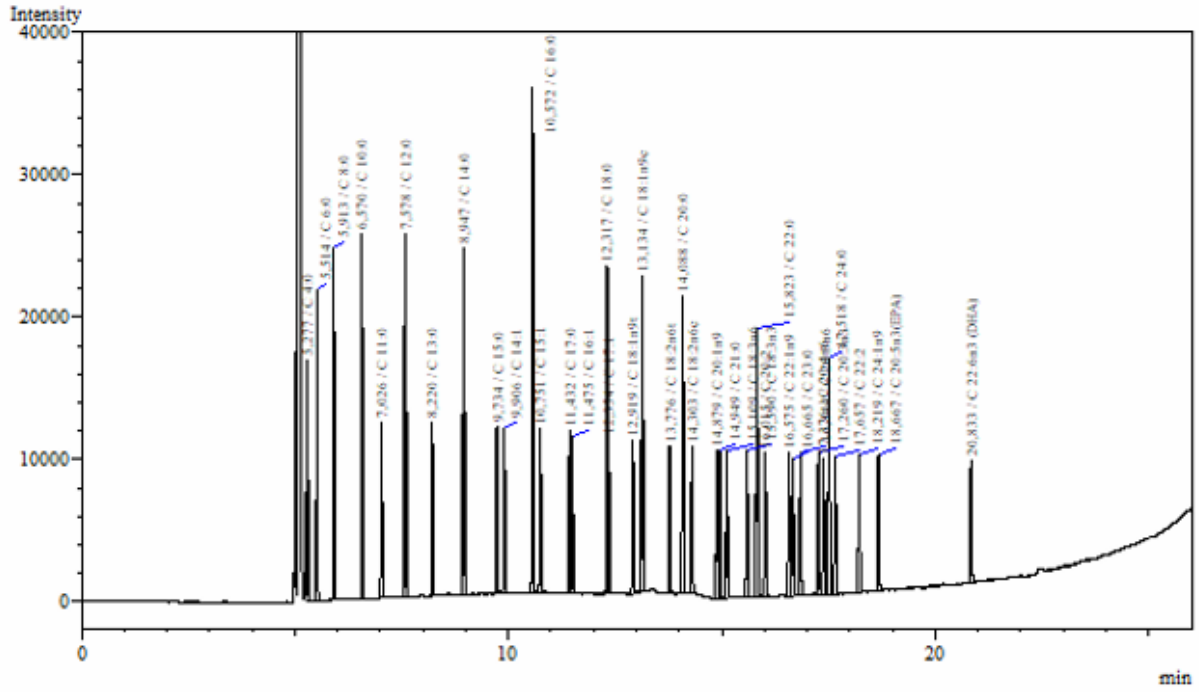

Peak#	Ret.Time	Area	Height	Conc.	Unit	Mark	ID#	Cmpd Name
1	5,277	24353	16720	479,875	ug/ml		1	C 4:0
2	5,514	31696	21444	490,145	ug/ml		2	C 6:0
3	5,913	36966	24147	499,730	ug/ml		3	C 8:0
4	6,570	40877	25280	504,335	ug/ml		4	C 10:0
5	7,026	20728	12305	245,699	ug/ml		5	C 11:0
6	7,578	44132	25223	507,622	ug/ml		6	C 12:0
7	8,220	21940	11962	246,822	ug/ml		7	C 13:0
8	8,947	45185	23870	504,947	ug/ml		8	C 14:0
9	9,734	22649	11650	248,881	ug/ml		10	C 15:0
10	9,906	22300	11474	246,763	ug/ml		9	C 14:1
11	10,572	70990	35025	770,634	ug/ml		12	C 16:0
12	10,751	23172	11451	253,087	ug/ml	V	11	C 15:1
13	11,432	21855	11392	247,595	ug/ml		14	C 17:0
14	11,475	23243	10905	254,584	ug/ml	V	13	C 16:1
15	12,317	49313	22738	521,713	ug/ml		16	C 18:0
16	12,354	19898	10825	234,258	ug/ml	V	15	C 17:1
17	12,919	23359	10543	244,220	ug/ml		18	C 18:1n9t
18	13,134	46869	21942	510,208	ug/ml	V	17	C 18:1n9c
19	13,776	22000	10296	252,645	ug/ml		20	C 18:2n6t
20	14,088	46789	20765	514,339	ug/ml	V	23	C 20:0
21	14,303	22906	10200	248,424	ug/ml		19	C 18:2n6c
22	14,879	22399	10272	249,841	ug/ml		24	C 20:1n9
23	14,949	22736	10279	248,651	ug/ml	V	30	C 21:0
24	15,109	22141	10262	256,371	ug/ml		21	C 18:3n6
25	15,590	22386	10247	254,188	ug/ml	V	22	C 18:3n3
26	15,823	45838	18745	507,844	ug/ml		31	C 22:0
27	16,015	23095	10187	256,003	ug/ml		25	C 20:2
28	16,575	22438	10076	229,390	ug/ml		32	C 22:1n9
29	16,665	22880	9514	247,783	ug/ml	V	35	C 23:0
30	16,844	22634	9933	249,643	ug/ml		26	C 20:3n6
31	17,260	22161	9893	254,723	ug/ml	V	27	C 20:3n3
32	17,376	21579	9515	249,391	ug/ml	V	28	C 20:4n6
33	17,518	44626	16427	497,407	ug/ml	V	36	C 24:0
34	17,657	21831	9648	243,172	ug/ml	V	33	C 22:2
35	18,219	22717	9557	259,791	ug/ml		37	C 24:1n9
36	18,667	21841	9441	241,131	ug/ml		29	C 20:5n3(EPA)
37	20,833	20402	8449	253,646	ug/ml	V	34	C 22:6n3 (DHA)
Total		1082924	532602					

Figure B.7. Chromatogram of FAME Mix Dilution #7.

APPENDIX C: FATTY ACID METHYL ESTER PROFILES OF MICROALGAE CULTURES

Table C.1. FAME Profile of All Microalgae Cultivations as mg_{FAME} / $g_{biomass}$ (Conditions are sorted by their condition numbers)

	For mg FAME/g biomass																						
	N.gadi	N.gadi	N.gadi	N.gadi	N.gadi	N.gadi	Nanno	Nanno	Nanno	Nanno	Nanno	Nanno	Ettlia	Ettlia	N.gadi	N.gadi	N.gadi	N.gadi	N.gadi	Ettlia	Ettlia	Ettlia	Ettlia
Condition No	1	2	3	4	5	6	7	8	9	10	11	12	13	14	15	16	17	18	19	20	21	22	23
C 4:0	0.00	0.00	0.00	0.00	0.00	0.00	0.00	0.00	0.00	0.00	0.00	0.00	0.00	0.00	0.00	0.00	0.00	0.00	0.00	0.00	0.00	0.00	0.00
C 6:0	0.42	0.00	0.00	0.00	0.00	0.00	0.00	0.00	0.00	0.00	0.00	0.00	0.00	0.00	0.00	0.00	0.00	0.00	0.00	0.00	0.00	0.00	0.00
C 8:0	0.00	0.00	0.75	0.00	0.00	0.14	0.00	0.00	0.28	0.00	0.00	0.00	0.00	0.00	0.00	0.00	0.00	0.00	0.00	0.00	0.00	0.00	0.00
C 10:0	0.23	0.53	1.51	0.61	0.81	0.00	0.00	0.00	1.20	0.00	0.78	0.00	0.23	0.63	1.15	0.93	1.11	1.24	0.40	1.20	2.32	0.74	0.00
C 11:0	0.00	0.00	0.00	0.00	0.00	0.00	0.00	0.00	0.00	0.00	0.00	0.00	0.00	0.00	0.00	0.00	0.00	0.00	0.00	0.00	0.00	0.00	0.00
C 12:0	0.00	0.70	0.77	0.46	0.00	0.73	0.46	0.00	0.56	0.41	0.00	0.53	0.00	0.00	0.00	0.00	0.00	0.00	0.00	0.00	0.00	0.00	0.00
C 13:0	0.00	0.00	0.00	0.00	0.00	0.00	0.00	0.00	0.00	0.00	0.00	0.00	0.00	0.00	0.00	0.00	0.00	0.00	0.00	0.00	0.00	0.00	0.00
C 14:0	4.85	9.08	3.68	11.86	3.80	15.91	4.18	12.99	4.35	9.53	2.13	8.56	0.00	0.49	2.87	2.83	1.66	2.10	0.98	0.00	0.00	0.11	0.00
C 14:1	0.00	0.00	0.00	0.00	0.00	0.00	0.00	0.00	0.00	0.00	0.00	0.00	0.00	0.00	0.00	0.00	0.00	0.00	0.00	0.00	0.00	0.00	0.00
C 15:0	1.70	0.80	0.00	1.29	2.26	1.34	2.31	1.28	0.00	3.84	1.83	3.03	0.00	0.80	1.90	0.22	1.77	0.00	2.23	1.74	1.63	1.92	1.91
C 15:1	0.00	0.00	0.00	0.00	0.00	0.00	0.00	0.00	0.00	0.00	0.00	0.00	0.00	0.00	0.00	0.00	0.00	0.00	0.00	0.00	0.00	0.00	0.00
C 16:0	31.53	72.23	16.49	111.98	21.02	134.61	29.82	139.75	21.22	104.54	11.29	95.67	11.67	15.79	12.20	13.50	6.87	8.39	6.11	5.92	27.57	6.68	2.49
C 16:1	24.77	34.54	15.22	66.94	10.48	68.21	12.41	87.76	6.71	58.49	7.47	58.89	0.00	0.59	8.04	15.44	8.01	6.42	0.00	0.00	0.00	0.30	0.00
C 17:0	0.21	0.00	0.00	0.00	0.00	0.00	0.00	0.00	0.24	0.00	0.00	0.00	0.00	0.00	0.00	0.00	0.00	0.00	5.46	0.00	0.00	0.00	0.28
C 17:1	0.00	0.00	0.00	0.00	0.00	0.00	0.00	0.00	0.00	0.00	0.00	0.00	0.00	0.00	0.00	0.00	0.00	0.00	0.00	0.00	0.00	0.00	0.00
C 18:0	3.42	4.63	1.51	4.87	2.83	6.09	4.02	6.76	1.95	5.34	2.09	4.53	1.13	2.74	1.83	1.33	1.44	2.49	2.13	1.29	3.45	1.75	1.73
C 18:1n9c	12.74	15.57	2.32	26.08	6.71	24.31	10.07	42.09	6.85	20.77	1.51	22.72	0.98	12.52	3.48	2.18	1.52	2.45	0.95	1.03	9.06	4.46	0.55
C 18:1n9t	0.00	0.00	0.00	0.00	0.00	0.00	0.00	0.00	0.00	0.00	0.00	0.00	0.00	0.00	0.00	0.00	0.00	0.00	0.00	0.00	0.00	0.00	0.00
C 18:2n6c	1.48	1.93	2.43	1.37	1.43	1.57	1.78	2.37	1.25	1.02	0.84	0.93	8.81	13.62	1.77	2.44	1.40	1.27	0.46	7.10	19.79	2.62	0.41
C 18:2n6t	0.00	0.00	0.00	0.00	0.00	0.00	0.00	0.00	0.00	0.00	0.00	0.00	3.95	3.91	0.00	0.00	0.00	0.00	0.00	3.58	8.78	0.38	0.00
C 18:3n6	0.00	0.17	0.52	0.28	0.00	0.00	0.00	0.25	0.00	0.00	0.00	0.00	0.00	0.00	0.00	0.14	0.00	0.00	0.00	0.00	0.00	0.09	0.00
C 18:3n3	0.00	0.00	0.00	0.00	0.00	0.00	0.00	0.00	0.00	0.00	0.00	0.00	7.07	7.38	0.00	0.47	0.17	0.00	0.00	6.83	15.79	6.84	0.51
C 20:0	0.00	0.00	0.00	0.34	0.00	0.42	0.00	0.00	0.00	0.24	0.00	0.25	0.00	0.00	0.00	0.00	0.00	0.00	0.00	0.00	0.00	0.00	0.00
C 20:1n9	0.00	0.00	0.00	0.00	0.00	0.00	0.00	0.00	0.00	0.00	0.00	0.76	0.00	0.00	0.00	0.00	0.00	0.00	0.00	0.00	0.00	0.00	0.00
C 20:2	0.00	0.00	0.00	0.00	0.00	0.00	0.00	0.00	0.00	0.00	0.00	0.00	0.00	0.00	0.00	0.00	0.00	0.00	0.00	0.00	0.00	0.00	0.00
C 20:3n6	0.00	0.22	0.00	0.00	0.00	0.12	0.00	0.28	0.00	0.27	0.00	0.30	0.00	0.00	0.00	0.49	0.73	0.00	0.69	0.00	0.00	0.00	0.00
C 20:3n3	0.00	0.00	0.00	0.00	0.00	0.00	0.00	0.00	0.00	0.36	0.00	1.13	0.00	0.00	0.00	0.00	0.00	0.00	2.09	0.00	0.00	0.00	0.00
C 20:4n6	3.94	4.55	4.77	2.71	4.50	1.48	3.51	5.76	2.17	2.15	0.94	0.00	0.00	0.00	3.23	2.54	3.98	3.73	0.00	0.00	0.00	0.18	0.00
C 20:5n3(EPA)	13.74	15.19	28.66	6.09	7.90	3.11	5.42	14.97	5.59	4.18	2.68	2.17	0.00	0.29	15.73	14.34	21.42	13.70	8.78	0.00	0.00	0.00	0.00
C 21:0	0.00	0.00	0.00	0.00	0.00	0.00	0.00	0.00	0.90	0.00	0.00	0.00	0.00	0.00	0.00	0.00	0.00	0.00	0.00	0.00	0.00	0.00	0.00
C 22:0	0.00	0.00	0.00	0.00	0.00	0.00	0.00	0.00	0.00	0.00	0.00	0.00	0.00	0.00	0.00	0.00	0.00	0.00	0.00	0.00	0.00	0.00	0.00
C 22:1n9	0.00	0.00	0.00	0.00	0.00	0.00	0.00	0.00	0.24	0.20	0.00	0.00	0.00	0.00	0.00	0.00	0.00	0.00	0.00	0.00	0.00	0.69	0.21
C 22:2	0.00	0.00	0.00	0.00	0.00	0.00	0.00	0.00	0.00	0.00	0.00	0.00	0.00	0.00	0.00	0.60	0.00	0.00	0.00	0.00	0.00	0.00	0.00
C 22:6n3 (DHA	0.36	0.00	0.00	3.43	0.00	3.97	0.00	0.00	0.00	0.00	0.00	0.00	0.00	0.00	0.00	0.00	0.00	0.00	0.00	0.00	0.00	0.00	0.00
C 23:0	0.00	0.00	0.00	0.00	0.00	0.00	0.00	0.00	0.83	0.00	0.00	0.00	0.00	0.00	0.00	0.00	0.00	0.00	0.00	0.00	0.00	0.00	0.00
C 24:0	0.00	0.00	0.00	0.00	0.00	0.00	0.00	0.00	0.00	0.00	0.00	0.00	0.00	0.00	0.00	0.00	0.00	0.00	0.00	0.00	0.00	0.00	0.00
C 24:1n9	0.00	0.00	0.00	0.00	0.00	0.00	0.00	0.00	0.00	0.00	0.00	0.00	0.00	0.00	0.00	0.00	0.00	0.00	0.00	0.00	0.00	0.00	0.00
TOTAL (mgFA	99.40	160.14	78.65	238.31	61.74	262.00	73.97	314.24	54.32	211.34	31.56	199.46	33.85	58.78	52.19	57.46	50.07	41.79	30.27	28.69	88.40	26.76	8.08
SFA	42.36	87.98	24.72	131.41	30.71	159.23	40.78	160.77	31.51	123.86	18.12	112.56	13.03	20.46	19.95	18.81	12.85	14.22	17.31	10.15	34.98	11.20	6.41
MUFA	37.52	50.10	17.55	93.02	17.19	92.52	22.47	129.85	13.80	79.75	8.98	82.37	0.98	13.12	11.52	17.62	9.54	8.87	0.95	1.03	9.06	5.45	0.76
PUFA	19.52	22.06	36.38	13.88	13.83	10.25	10.71	23.62	9.01	7.72	4.45	4.52	19.83	25.20	20.73	21.04	27.69	18.70	12.02	17.51	44.36	10.12	0.92
SFA %	42.62	54.94	31.43	55.14	49.74	60.78	55.13	51.16	58.01	58.61	57.43	56.43	38.51	34.80	38.22	32.73	25.66	34.03	57.18	35.38	39.57	41.85	79.25
MUFA%	37.74	31.29	22.31	39.03	27.85	35.31	30.38	41.32	25.40	37.74	28.46	41.30	2.90	22.32	22.07	30.66	19.05	21.23	3.12	3.60	10.25	20.35	9.34
PUFA%	19.64	13.78	46.26	5.83	22.41	3.91	14.48	7.52	16.59	3.65	14.11	2.27	58.59	42.88	39.71	36.61	55.29	44.75	39.70	61.02	50.18	37.80	11.40